

**BINDING AND TRANSPORT OF CALCIUM BY  
SYNTHETIC ANALOGUES OF IONOMYCIN**

By

**Thomas Qiuxiong Hu**

**B.Sc., South China Institute of Technology, 1985**

**M.Sc., University of British Columbia, 1988**

**A THESIS SUBMITTED IN PARTIAL FULFILLMENT OF  
THE REQUIREMENTS FOR THE DEGREE OF  
DOCTOR OF PHILOSOPHY**

in

**THE FACULTY OF GRADUATE STUDIES**

**Department of Chemistry**

**We accept this thesis as conforming  
to the required standard**

---

**THE UNIVERSITY OF BRITISH COLUMBIA**

**December 1992**

**© Thomas Qiuxiong Hu, 1992**

In presenting this thesis in partial fulfilment of the requirements for an advanced degree at the University of British Columbia, I agree that the Library shall make it freely available for reference and study. I further agree that permission for extensive copying of this thesis for scholarly purposes may be granted by the head of my department or by his or her representatives. It is understood that copying or publication of this thesis for financial gain shall not be allowed without my written permission.

(Signature)

Department of CHEMISTRY

The University of British Columbia  
Vancouver, Canada

Date JAN. 12, 1993

## ABSTRACT

The syntheses of simple analogues of ionomycin (**3**), namely a series of  $\beta$ -diketo  $\omega$ -carboxylic acids **4-6**, **28-30** and **33-35**, were achieved by consecutive alkylation of the dianion of 2,4-pentanedione (**7**) with appropriate bromides and subsequent oxidation of the  $\beta$ -diketo  $\omega$ -alcohols.

The transport of calcium across an organic barrier by these synthetic analogues of ionomycin was determined in a cylindrical glass cell using chloroform as the artificial membrane. The presence of the  $\beta$ -diketone and carboxyl groups within the same molecule and a sufficient lipid solubility of the compounds were shown to be necessary and sufficient conditions for calcium transport. Small and no transport of calcium was found for analogue **4** and **6** respectively due to the low lipid solubility of these compounds. The relative calcium transport rates for analogues **28** and **33-35** were  $28 > 33 > 35 > 34$ , which demonstrated that optimum calcium transport was achieved when the  $\beta$ -diketone group was separated from the carboxyl group by seven methylene units identical to the backbone found in ionomycin. Analogues **28-30** were comparable to ionomycin and calcimycin in terms of calcium transport. The transport of calcium by synthetic analogues of ionomycin was found to be a saturable process which obeyed Michaelis-Menten kinetics. It was dependent of the pH in the aqueous source phase and independent of the pH in the receiving phase. Both the carboxyl and the  $\beta$ -diketone groups were ionized in the transport of calcium, indicating the stoichiometry of calcium complex in transport was 1:1. Analogues **29** and **33** were found to cause transient calcium mobilization in cultured human leukemic cells.

The  $pK_a$  of the  $\beta$ -diketone group of the analogues was determined to be in the range of 10.90 to 11.16 in 80% MeOH-H<sub>2</sub>O by UV spectrophotometric titration. The  $pK_a$  values were

directly related to the lipid solubility of the compounds and the hydrocarbon chain length between the  $\beta$ -diketone and the carboxyl groups.

The binding constants of the analogues with calcium and magnesium in 80% MeOH-H<sub>2</sub>O were determined to be in the order of  $10^2 \text{ M}^{-1}$  and  $10^3 \text{ M}^{-1}$  respectively using the  $\text{pK}_a$  method. The binding constants of the analogues with magnesium were also determined by the mole ratio method which established the 1:1 stoichiometry in the magnesium complex. The selectivity in binding was the same as the selectivity in transport, which was  $\text{Mg}^{2+} > \text{Ca}^{2+} \gg \text{Na}^+, \text{K}^+$ .

Dimethylation of the  $\beta$ -diketone **42** proceeded with high diastereoselectivity. The major diastereomer (**43b**) had the two methyl groups *trans* to each other. The characterization of the calcium salt of analogue **28** showed that the stoichiometry of the calcium complex in the solid state was 1:1.

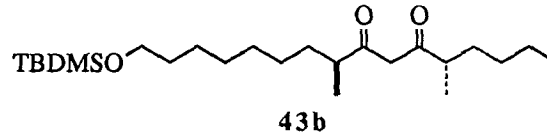
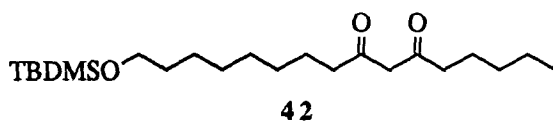
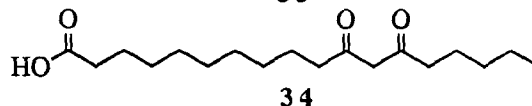
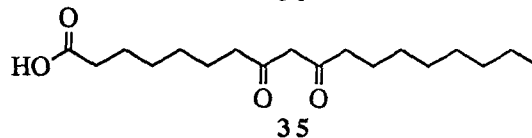
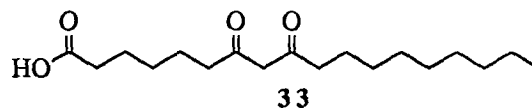
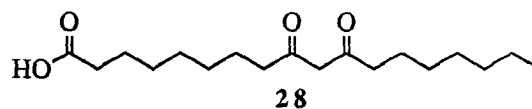
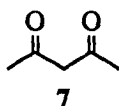
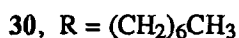
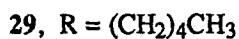
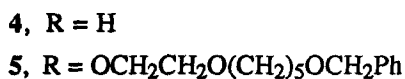
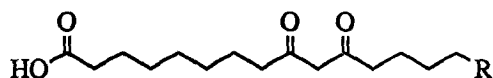
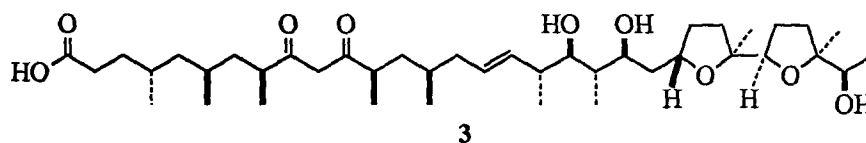




## TABLE OF CONTENTS

	Page
Abstract.....	ii
Table of Contents .....	iv
List of Tables .....	vii
List of Figures .....	viii
List of Abbreviations.....	x
Acknowledgements .....	xii
Dedication .....	xiii
 CHAPTER ONE Introduction.....	 1
1.1 Calcium in Biological Systems .....	2
1.2 Calcium as a Cellular Messenger.....	4
1.3 Manipulation of Intracellular Calcium.....	8
1.4 Polyether Calcium Ionophores and Calcium Transport.....	9
1.5 Ionomycin and Its Unique Structure and Function .....	14
1.6 Calcium Ionophores Based on Ionomycin.....	18
 CHAPTER TWO Results and Discussion .....	 19
2.1 Design and Synthesis of Ionomycin Analogues.....	19
2.2 Transport of Calcium across a Chloroform Liquid Membrane.....	29
2.3 Effect of Carrier Lipophilicity on Calcium Transport.....	33
2.4 Effect of Distance between the $\beta$ -Diketone and Carboxyl Groups on Calcium Transport.....	38
2.5 Comparison of Ionomycin Analogues to Calcimycin and Ionomycin.....	42
2.6 Cation Selectivity in Transport.....	44
2.7 Calcium Transport in Cultured Human Leukemic Cells .....	46

2.8	Effect of Substrate Concentration on Calcium Transport .....	50
2.9	Effect of pH on Calcium Transport.....	53
2.10	Characterization of Calcium Complex of Analogue 28.....	57
2.11	Binding of Ionomycin Analogues with Calcium Ions.....	62
2.12	Determination of $pK_a$ of $\beta$ -Diketone by Ultraviolet Spectrophotometric Titration.....	67
2.13	Binding of Calcium and Other Metal Ions by Ionomycin Analogues.....	71
2.14	Incorporation of Rigid Elements into Ionomycin Analogues.....	80
2.15	Conclusions and Future Consideration.....	83
CHAPTER THREE Experimental.....		87
3.1	General.....	87
3.2	Synthesis of 9,11-Dioxopentadecanoic Acid (4).....	94
3.3	Synthesis of 15-[2-(5-Benzoyloxy)-pentyloxy]-ethoxy-9,11-dioxopentadecanoic Acid (5).....	100
3.4	Synthesis of 15-Methoxymethoxy-9,11-dioxopentadecanoic Acid (6).....	109
3.5	Synthesis of 9,11-Dioxododecanoic Acid (27).....	113
3.6	Synthesis of 9,11-Dioxooctadecanoic Acid (28).....	115
3.7	Synthesis of 9,11-Dioxoeicosanoic Acid (29).....	118
3.8	Synthesis of 9,11-Dioxodoeicosanoic Acid (30).....	121
3.9	Synthesis of 8,10-Octadecanedione (31).....	124
3.10	Synthesis of 7,9-Dioxooctadecanoic Acid (33) .....	126
3.11	Synthesis of 11,13-Dioxooctadecanoic Acid (34) .....	132
3.12	Synthesis of 8,10-Dioxooctadecanoic Acid (35).....	138
3.13	Synthesis of Calcium Salt of 9,11-Dioxooctadecanoic Acid (36).....	144
3.14	Synthesis of 8,12-Dimethyl-9,11-dioxohexadecanoic Acid (41) .....	145
3.15	Transport of Calcium and Other Metal Ions by Synthetic Analogues of Ionomycin .	149
3.16	$pK_a$ of the $\beta$ -Diketone Groups of Synthetic Analogues of Ionomycin.....	162

3.17 Binding of Calcium and Other Metal Ions by Synthetic Analogues of Ionomycin...	167
References.....	185
Appendix 1 (Spectra).....	191
Appendix 2 (Preparation of Various Buffers) .....	248

## LIST OF TABLES

	Page
Table I.	Amount of Calcium in the Receiving Phase at Different Times.....30
Table II.	Calcium Transport Rates (J) for Compounds 4, 5 and 6.....32
Table III.	Calcium Transport Rates for Analogues 4 and 27-30 .....33
Table IV.	Fragmental Constants for Various Fragments in Chloroform-Water System.....36
Table V.	Calculated and Measured log P for Simple $\beta$ -Diketones and Carboxylic Acids ...36
Table VI.	Calcium Transport Rates (J) and Calculated log P Values for Compounds 4 and 27-30.....37
Table VII.	Number of Methylene Units (n) between the Two Functional Groups and Calcium Transport Rates (J) of Compounds 33, 35, 28 and 34.....39
Table VIII.	Calcium Transport Rates for Calcimycin, Ionomycin and Compounds 28-30....42
Table IX	Calcium, Magnesium, Sodium and Potassium Transport Rates for Analogue 28.....44
Table X.	Calcium Transport Rates (J) at Various Calcium Concentrations in the Source Phase .....51
Table XI.	Calcium Transport Rates (J) at Various pH in the Receiving Phase.....53
Table XII.	Calcium Transport Rates (J) at Various pH in the Source Phase.....54
Table XIII.	$pK_a$ of the $\beta$ -Diketone Group of Ionomycin and of Analogues.....69
Table XIV.	Binding Constants of Ionomycin and Analogues with Calcium and Magnesium..72
Table XV.	Binding Constants of Analogues with Potassium and Sodium.....73
Table XVI.	Total Concentrations of Analogue 33 and Magnesium, Absorbance, Concentrations of the Complex, Analogue and Magnesium at Each Titration Point and Binding Constants Based on 1:1 Stoichiometry.....76
Table XVII.	Binding Constants of Analogues with Magnesium Using the $pK_a$ and $pK_a'$ Method and the Mole Ratio Method.....78
Table XVIII.	Binding Constants of Various Stereoisomers of Lasalocid A with Barium Ions ..80

## LIST OF FIGURES

	Page
Figure 1. Crystal structure of the barium salt of lasalocid A .....	10
Figure 2. Mechanism of calcium transport across a phospholipid membrane by calcium ionophores .....	11
Figure 3. Cross sections of the U-tube and the cylindrical glass cell for the studies of calcium transport.....	13
Figure 4. Crystal structure of the calcium salt of ionomycin.....	15
Figure 5. The enolization and ionization of a $\beta$ -diketone.....	16
Figure 6. Binding of the carboxylate and enolate of $\beta$ -diketone in the calcium salt of ionomycin.....	20
Figure 7. Construction of a $\beta$ -diketone by aldol condensation and oxidation.....	22
Figure 8. Construction of a $\beta$ -diketone by dithiane alkylation, oxidation and hydrolysis.....	22
Figure 9. Construction of a $\beta$ -diketone by dianion alkylation of 2,4-pentanedione (7).....	22
Figure 10. Retrosynthetic analysis of analogues 4, 5 and 6.....	23
Figure 11. Cross section and top view of the cylindrical glass cell for the studies of calcium transport across a chloroform liquid membrane.....	29
Figure 12. Plot of the amount of calcium in the receiving phase versus time.....	31
Figure 13. Graph of calcium transport rate versus the number of methylene units separating the $\beta$ -diketone and carboxyl groups .....	40
Figure 14. $[Ca^{2+}]_i$ in THP-1 cell stimulated by calcimycin bromide and analogue 6.....	46
Figure 15. $[Ca^{2+}]_i$ in THP-1 cell stimulated by ionomycin and analogue 27.....	47
Figure 16. $[Ca^{2+}]_i$ in THP-1 cell stimulated by calcimycin bromide and analogue 28.....	47
Figure 17. $[Ca^{2+}]_i$ in THP-1 cell stimulated by ionomycin and analogue 29.....	48
Figure 18. $[Ca^{2+}]_i$ in THP-1 cell stimulated by calcimycin bromide and analogue 33.....	48
Figure 19. The Michaelis-Menten expression for enzymatic catalysis.....	50

Figure 20. The Michaelis-Menten expression for ionophore-catalyzed calcium transport.....	51
Figure 21. Curve of the dependence of transport rates on calcium concentration of the source phase.....	52
Figure 22. Plot of log J as a function of pH in the source phase.....	55
Figure 23. Plot of the dependence of transport rates on pH of the source phase.....	56
Figure 24. Equilibrium between the calcium complex and the free ions in MeOH-d <sub>4</sub> .....	60
Figure 25. Representative mole ratio plots of complexes of various stabilities.....	63
Figure 26. Continuous variation curves plotted for hypothetical systems with a stoichiometry of 1:1 and binding constant.....	64
Figure 27. UV spectrophotometric absorption spectra of analogue 33 as the pH of the solution increased from 5.80 to 13.00.....	67
Figure 28. Plot of absorbance at 298 nm versus pH for analogue 33.....	68
Figure 29. UV spectrophotometric absorption spectra of analogue 33 as the concentration of MgCl <sub>2</sub> increased from 0.00 to $1.34 \times 10^{-3}$ M at pH = 9.10.....	75
Figure 30. Plot of the number of moles of magnesium bound per mole of analogue 33 versus concentration of magnesium.....	77
Figure 31. UV spectrophotometric absorption spectra of analogue 33 as the pH of the solution increased from 5.40 to 11.46 in the presence of CaCl <sub>2</sub> .....	167
Figure 32. Plot of the UV absorbance at 298 nm versus pH for analogue 33 in the presence of CaCl <sub>2</sub> .....	168
Figure 33. UV spectrophotometric absorption spectra of analogue 33 as the pH of the solution increased from 5.61 to 9.51 in the presence of MgCl <sub>2</sub> .....	171
Figure 34. Plot of the UV absorbance at 298 nm versus pH for analogue 33 in the presence of MgCl <sub>2</sub> .....	172
Figure 35. UV spectrophotometric absorption spectra of analogue 33 as the pH of the solution increased from 5.84 to 12.70 in the presence of NaCl.....	174
Figure 36. Plot of the UV absorbance at 298 nm versus pH for analogue 33 in the presence of NaCl.....	175
Figure 37. UV spectrophotometric absorption spectra of analogue 33 as the pH of the solution increased from 5.84 to 12.70 in the presence of KCl.....	178
Figure 38. Plot of the UV absorbance at 298 nm versus pH for analogue 33 in the presence of KCl.....	179

## LIST OF ABBREVIATIONS

A	absorbance
Å	angstrom
ATP	adenosine triphosphate
cAMP	cyclic adenosine monophosphate
CAPS	3-(cyclohexylamino)-propanesulfonic acid
CHES	2-(cyclohexylamino)-ethanesulfonic acid
calcd	calculated
d	doublet
dd	double doublet
dt	double triplet
DCC	1,3-dicyclohexylcarbodiimide
DMAP	4-dimethylaminopyridine
DMSO	dimethylsulfoxide
Elem. Anal.	elemental analysis
ether	diethyl ether
eV	electron volts
FAB-MS	fast atom bombardment mass spectrometry
GC	gas chromatography
h	hour(s)
HEPPS	N-2-hydroxyethylpiperazine-N'-3-propanesulfonic acid
HOAc	acetic acid
HPLC	high performance liquid chromatography
HRMS	high resolution mass spectrometry
IR	infrared
J	transport rate

LDA	lithium diisopropylamide
LRMS	low resolution mass spectrometry
m	multiplet
M <sup>+</sup>	molecular ion
MES	2-(N-morpholino)-ethanesulfonic acid
min	minute(s)
MOPS	3-(N-morpholino)-propanesulfonic acid
mp	melting point
m/z	mass to charge ratio
NMR	nuclear magnetic resonance
PPTs	pyridinium p-toluenesulphonate
R <sub>f</sub>	the ratio of the distance a solute travels to the distance the solvent front travels
r.p.m.	round per minute
R <sub>T</sub>	retention time
s	singlet
t	triplet
TEA	triethylamine
THF	tetrahydrofuran
THP	tetrahydropyran
TLC	thin layer chromatography
TBDMS	tert-butyldimethylsilyl
UV	ultraviolet



## ACKNOWLEDGEMENTS

I wish to express my sincere gratitude to my supervisor, Dr. Larry Weiler, for his guidance and encouragement during the course of this work, and for his advice and assistance during the preparation of this thesis.

I am indebted to Dr. Robert Young of Merck Frosst Canada for his valuable discussions concerning the progress of this research and to Dr. Edward Neeland of Okanagan College for proof reading this thesis. I am grateful to members of the Weiler Research Group, both past and present, for providing a pleasant work place.

Thanks are also due to Dean Clyne, Ellay Harshenin, Nova Lee, Sulia Lo, Ross Lonergan, Margot Purdon, Annie Wong, Jackson Wu and Gerald Yeung whose friendships have made the past four years a time to remember.

In addition, financial assistance in the form of graduate fellowships from the University of British Columbia and the efficient cooperation of the staff of the NMR, elemental analysis and mass spectrometry service are gratefully acknowledged.

Finally and most importantly, I would like to thank my parents for their encouragement, patience and support throughout the course of my education. My gratitude to them is beyond mere words.

## DEDICATION

This thesis is dedicated to my parents.

## CHAPTER ONE

### INTRODUCTION

The earth is replete with animals and plants in which calcium plays a vital part in their skeletal structures and biochemistry. In the human body, calcium is the fifth most abundant element and is mainly bound in bones and tooth enamel as calcium phosphate. Geologists have used the calcareous remains of extinct organisms to study the fossil record and understand the course of evolution since the middle of the 19<sup>th</sup> century.

Although the importance of calcium in the skeletal structures of living organisms has been recognized for more than a century, only recently have other biological roles for calcium, particularly its role as an intracellular messenger, drawn the attention of scientists from many disciplines. A minute flow of calcium ions across cell membranes has been found to trigger such diverse processes as the regulation of muscle contraction, the secretion of hormones, the transport of salt and water across the intestinal lining and the control of glycogen metabolism in the liver.<sup>1</sup>

While biologists continue to elucidate calcium-induced cellular events, chemists have been called upon to develop natural and synthetic compounds that will specifically bind to calcium ions and transport them across cell membranes. The development of such compounds would open the possibility of regulating intracellular calcium levels and thus pharmacologically controlling a large number of physiological processes.

### 1.1 Calcium in Biological Systems

The discovery of calcium dates back to the early 19<sup>th</sup> century when Humphry Davy at the Royal Institution in London isolated the metal and named it after the Latin word 'calx' meaning lime.<sup>2</sup> Following its discovery, biologists found that calcium carbonate and phosphate were the major constituents of shell, bone and teeth in both living and extinct organisms.

The first description of calcium as an important ion for the normal function and growth of organisms was provided by the English physician and physiologist Sydney Ringer in 1883.<sup>3</sup> Ringer was studying the effect of inorganic compounds on frog heart muscle contraction. He found that the muscle tissue failed to contract in a tissue culture medium made with distilled water, but it did contract in a medium made with tap water. The missing element was soon shown to be calcium. Further experiments by Ringer revealed that calcium was required for the development of fertilized eggs and for the adhesion of cells to each other.<sup>4</sup>

Subsequently Locke demonstrated that motor nerves exposed to a sodium chloride solution lost their stimulant effect on muscle contractility. However, it could be restored by adding the proper proportions of calcium.<sup>5</sup> At the turn of the century others, such as Loeb, Mines and Loewi, were able to show the involvement of calcium in the morphology and physiology of cells, and in the action of cell stimuli by adrenaline and by drugs such as digitalis.<sup>6</sup>

Having established the universal requirement of calcium in living organisms, physiologists and biologists started to investigate the sources of calcium and to define its biological role. In 1937 Heilbrunn and Wilbur proposed that following various cell stimuli calcium ions could come from both external and internal pools of bound calcium.<sup>7a</sup> Ten years later, Heilbrunn and Wiercinski confirmed the regulatory role of intracellular calcium by an experiment in which muscle contraction was stimulated by an intracellular injection of calcium into cardiac cells.<sup>7b</sup>

By the middle of the 1960s four major roles of calcium ions in biological systems had been demonstrated.<sup>8</sup> In addition to providing rigidity to organisms as a major constituent of the skeletal structures, calcium carries charge across biological membranes of excitable cells and influences excitability by affecting the kinetics of sodium and potassium permeability. Calcium also functions as a cofactor for extracellular enzymes and proteins. Finally, calcium serves as an intracellular messenger, conveying signals received at the cell surface to the inside of the cell and triggering a range of cellular events such as muscle contraction and hormone secretion.

Although the intracellular messenger role of calcium was recognized as early as the 1920s and was demonstrated by Heilbrunn and Wiercinski in 1947, the idea was slow to gain universal acceptance. There were three particular problems. Firstly, it was not generally realized that the concentration of free calcium in the living cells was very low. Secondly, it was difficult to imagine how calcium ions, at low concentrations, could provide the energy for processes such as muscle contraction. Thirdly, some so-called calcium-activated cells were found to work perfectly well without external calcium. The role of calcium as an intracellular messenger was finally accepted universally by the middle of the 1960s with the development of techniques for the direct measurement of intracellular calcium concentration, with the discovery and isolation of calcium binding cellular proteins such as calmodulin and troponin C, and with the identification of mechanisms responsible for the regulation of intracellular calcium.<sup>9</sup>

## 1.2 Calcium as a Cellular Messenger

In a multicellular organism where each cell must perform a very specific function, it is essential that those cells performing the same function act in concert. This coordination is achieved by the use of chemical signals or messengers. One family of intercellular chemical messengers are the hormones.

Hormones regulate the harmonious interplay of different tissues and organs in the body. They control metabolism and many other cellular functions such as cell growth, blood pressure and kidney function. Usually one organ will produce the hormone and secrete it into the blood stream which will carry it to specific receptor sites on the cells of the target tissue.

These intercellular messengers (primary messengers) arrive at a receptor site on the target cell where they are detected and translated into internal signals. These signals are then carried across the cell membrane by a limited number of intracellular messengers (secondary messengers) to the specific cellular structure or enzyme that is the ultimate target of the hormone.

Two pathways involved in the transmission of signals across the cell membranes by intracellular messengers have been identified.<sup>1</sup> One involves the activation of membrane-bound adenylate cyclase to convert adenosine triphosphate (ATP) to cyclic adenosine monophosphate (cAMP) which then serves to regulate enzymes within the cell.<sup>10</sup> The other pathway utilizes several messengers such as inositol triphosphate, diacylglycerol and calcium ions.<sup>1,10</sup> These intracellular messengers bind directly to a cellular protein or activate an enzyme which then phosphorylates a cellular protein. Both actions trigger a conformation change in the target protein and lead to an appropriate physiological response.

There are several other common ions besides calcium in the biological environment; they include the doubly charged magnesium ion and singly charged sodium, potassium and chloride ions. The selection of calcium over these other common ions as an intracellular messenger is an

example of the remarkable ability of cells to differentiate and evolve in response to the organism's need. For a substance to act as an intracellular messenger, a target protein must be able to bind it tightly and with high specificity. It is also necessary that the messenger substance undergo a large increase in concentration. A tenfold increase in concentration may be needed to change an enzyme from the "off" to the "on" state.

Calcium is far better suited to tight and specific binding with proteins than other common ions are. The negatively charged oxygens found on the side chains of aspartate and glutamate residues as well as uncharged oxygens from the carbonyls of the protein backbone bind to calcium with high affinity. Potassium and chloride ions have relatively large radii (1.33 Å and 1.81 Å respectively).<sup>9</sup> Hence, they do not fit into the compact binding sites on proteins. The sodium ion has a smaller radius (0.95 Å), about the same as that of calcium ion (0.99 Å), but because it bears only a single charge, sodium binds to proteins weakly. Although magnesium ion is capable of strong binding with proteins, its requirement for tetrahedral coordination and its smaller size (0.65 Å) make it difficult for a protein to adopt the binding conformation to accommodate it.<sup>9</sup>

To detect calcium signals, cells have evolved an elaborate system of proteins that bind calcium with high selectivity at physiological concentrations ( $10^{-7}$  to  $10^{-5}$  M). Two examples of such calcium-binding proteins are the regulatory proteins, calmodulin and troponin C of the skeletal muscle. These calcium-dependent regulatory molecules have binding sites that wrap around a calcium ion, thereby modifying their molecular conformations. This structural change is then translated into an alteration in the activity of the regulated molecules such as myosin light-chain kinase or troponin I, to which the calcium-dependent regulatory molecules are bound.<sup>11</sup>

Not only does the cell have the ability to detect the calcium signal, but it is also capable of removing calcium and terminating the signal quickly. The regulation of intracellular calcium is usually achieved by intracellular organelles such as the mitochondria and endoplasmic reticulum.

The endoplasmic reticulum in various cell types (muscle, nerve, liver, etc.) has been found to be able to buffer and sequester free calcium.<sup>12</sup>

The resting intracellular concentration of free calcium is very low, on the order of  $10^{-7}$  M in virtually all animal cells.<sup>13</sup> Kretsinger has suggested that this low calcium concentration may have resulted from early cells avoiding the formation of insoluble calcium phosphate in the cytosol, so that they could utilize ATP as the energy carrier.<sup>14</sup> However, even if the secondary messenger role of calcium was only an evolutionary afterthought, the low intracellular calcium concentration has been utilized to an advantage in cells. A low intracellular calcium concentration makes the use of this ion as an intracellular messenger energetically inexpensive. The very low calcium concentration means that relatively few ions need to be moved, with a relatively small expenditure of energy, to raise the intracellular calcium concentration by a factor of 10 for the regulation of an enzyme. The intracellular concentrations of magnesium, potassium and sodium are all too high to allow a large increase in concentration. Hence, these ions would be much less effective than calcium as intracellular messengers.

In contrast to the low intracellular calcium concentration, free calcium concentration in the extracellular medium is high, on the order of  $10^{-3}$  M in vertebrates and higher in marine invertebrates. This calcium concentration gradient, together with a membrane potential of -40 to -90 mV, allows for a rapid entry of calcium into the cell upon the activation of calcium-selective channels by appropriate electrical or chemical signals.<sup>15</sup> Alternatively, the sources of calcium may come from intracellular storage sites where calcium is bound to the cytoplasmic surface of the plasma membrane, or sequestered in mitochondria or the endoplasmic reticulum.<sup>16</sup>

The intricacies of calcium regulation are only now being unraveled. Digitalis, a drug which has been used for thousands of years, exemplifies the clinical importance of controlling intracellular calcium concentration. The ability of digitalis to strengthen the heartbeat was recognized long ago. Today it is known that digitalis and other related drugs work by raising the



level of intracellular calcium in the heart by affecting the sodium-potassium pump in the membrane. For many heart patients the result of raising the level of intracellular calcium in the heart is a longer and more secure life.

### 1.3 Manipulation of Intracellular Calcium

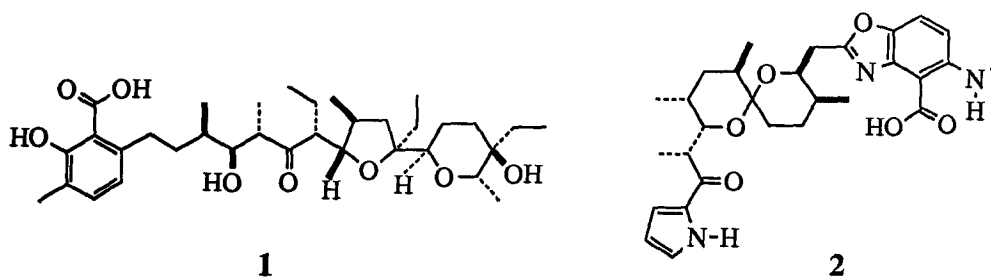
Because of the extensive role of calcium in the cell, it is essential to regulate intracellular calcium level to be able to effectively control cellular processes. Two typical ways of altering intracellular calcium concentrations are to inject calcium or a calcium chelating agent such as ethylenediaminetetraacetic acid (EDTA) into the cell or to add a substance to the extracellular fluid which will increase or decrease the concentration of intracellular calcium.

The first approach was adopted by Heilbrunn and Wiercinski who showed that the injection of calcium into frog muscle stimulated contraction.<sup>7b</sup> Simple as this approach might seem, it is fraught with several difficulties. Firstly, the micropipette can cause irreversible damage to the electrical and biochemical response of the cell. Secondly, the quantity of calcium that must be injected to significantly raise the concentration of calcium in the cytoplasm, and yet not to be too high to cause damage, is often unknown. Finally, since calcium-buffering systems exist inside cells, an elevated free calcium concentration in the cytoplasm for more than a few seconds is difficult to maintain by the injection method.

An alternative approach is to introduce a substance which affects either the calcium permeability of the cell membrane or intracellular calcium stores. Since the extracellular calcium concentration is  $10^3$  to  $10^6$  higher than the intracellular calcium concentration, calcium may be transported across the cell membrane down its concentration gradient by lipophilic compounds known as calcium "ionophores" (phore from the Greek *pherein* to bear). The term ionophore is used in a biophysical context to mean a compound which facilitates the transport of an ion through a natural or artificial lipid membrane from one aqueous medium to another.<sup>17</sup> The search for naturally-occurring and synthetic calcium ionophores, particularly the polyether calcium ionophores, has attracted the attention of biologists and chemists since the early 1970s.

#### 1.4 Polyether Calcium Ionophores and Calcium Transport

In 1951, the first polyether calcium ionophore, lasalocid A (**1**) (formerly known as X-537A) was extracted from *Streptomyces lasaliensis*.<sup>18</sup> More than twenty years elapsed before the second polyether calcium ionophore, calcimycin (**2**) (formerly known as A23187) was isolated from *Streptomyces chartreusensis*.<sup>19</sup> The molecular structures of lasalocid A and calcimycin were established in 1970 and in 1974 respectively by spectroscopic methods and a crystal structure analysis of the free acids.<sup>20</sup> The common structural characteristics of lasalocid A and calcimycin are the presence of a carboxyl group and a number of tetrahydrofuran and tetrahydropyran rings, the latter results in the term "polyether".



Both lasalocid A and calcimycin are very soluble in organic solvents. When their organic solutions were exposed to aqueous alkali or alkaline base, there was no extraction of the ionophore anion into the aqueous phase. In fact, cations of the base were extracted into the organic phase!<sup>18,19</sup> This led to the investigation of the ability of these two compounds to transport divalent cations across an organic barrier and to the widespread use of these two compounds, particularly calcimycin, in the elucidation of calcium-induced cellular events.

The extraction of divalent cations from an aqueous phase into an organic phase by lasalocid A or calcimycin is due to the ability of these compounds to form a lipid soluble ionophore-cation complex.<sup>21</sup> The crystal structure of the 2:1 barium salt of lasalocid A was determined by Johnson and co-workers (Figure 1).<sup>22</sup>

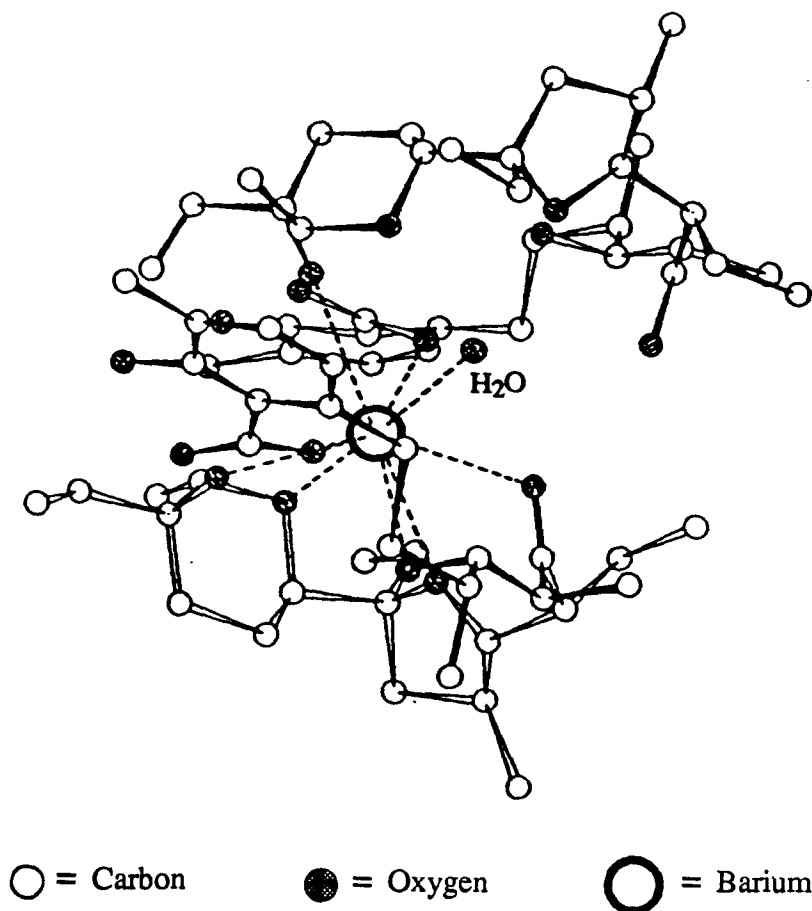


Figure 1. Crystal structure of the barium salt of lasalocid A.<sup>22</sup>

Oxygens from the carboxylate, the tetrahydrofuran and tetrahydropyran, the ketone and the two hydroxyls of one ionophore molecule, together with the carboxylate oxygen and one hydroxyl oxygen from the second ionophore molecule, chelate the barium ion to form a 2:1 ionophore-barium complex. The surface of the complex is composed largely of nonpolar hydrocarbon chains and the aromatic residues, which provide a lipophilic shield for the polar chelating portion of the complex, thereby rendering it soluble in organic solvents. The crystal structure of the calcium salt of calcimycin was found to be almost identical to its solution structure.<sup>23</sup> Calcimycin forms a lipid soluble 2:1 complex with calcium similar to the barium salt of lasalocid A.<sup>23</sup>

The nonchelating substituents of the ionophores and their stereochemistry are believed to be important in preorganizing the conformations of the molecules for ion complexation.<sup>24</sup> Still and co-workers proposed that particular arrays of the nonchelating substituents could destabilize undesired rotomers and reduce the available conformations of the ionophores to those suitable for metal ion binding.<sup>24</sup>

Both lasalocid A and calcimycin can act as mobile carriers to transport calcium across an organic barrier such as a phospholipid membrane (Figure 2).<sup>25</sup> At physiological pH, the carboxyl group of the ionophore (HL) is likely to be ionized with the carboxylate group in the aqueous medium, and the lipid soluble part of the molecule, inside the membrane. The extracellular calcium ion approaches the ionophore and loses its water of solvation as successive chelating oxygen and/or nitrogen atoms of the ionophore bind to it, forming the neutral, lipid soluble 2:1 calcium complex ( $\text{CaL}_2$ ). Although this complex formation is undoubtedly a multistage reaction it can be given a single composite rate constant,  $k_f$ . Once the complex is formed it diffuses across the membrane at a rate  $k_{\text{diff}}$ . At the inside surface, the reverse process occurs. This is also a multistep reaction which can be assigned the composite rate constant  $k_d$  in which the calcium complex releases calcium into the cell interior with the regeneration of the neutral ionophore. The released calcium ion is then available to stimulate the action of the cell concerned. The mechanism (Figure 2) involves the neutral ionophore diffusing back to the outside surface. In actual cells this species may be another metal complex.

In general, the direction and extent of such calcium transport are governed by the calcium concentration gradients across the membrane. The transport of calcium across cell membranes will be more efficient if certain kinetic criteria are fulfilled, such as a facile complexation reaction ( $k_f \gg k_d$ ) on the outside of the membrane, and a facile decomplexation reaction ( $k_d \gg k_f$ ) on the inside of the membrane.<sup>26</sup>

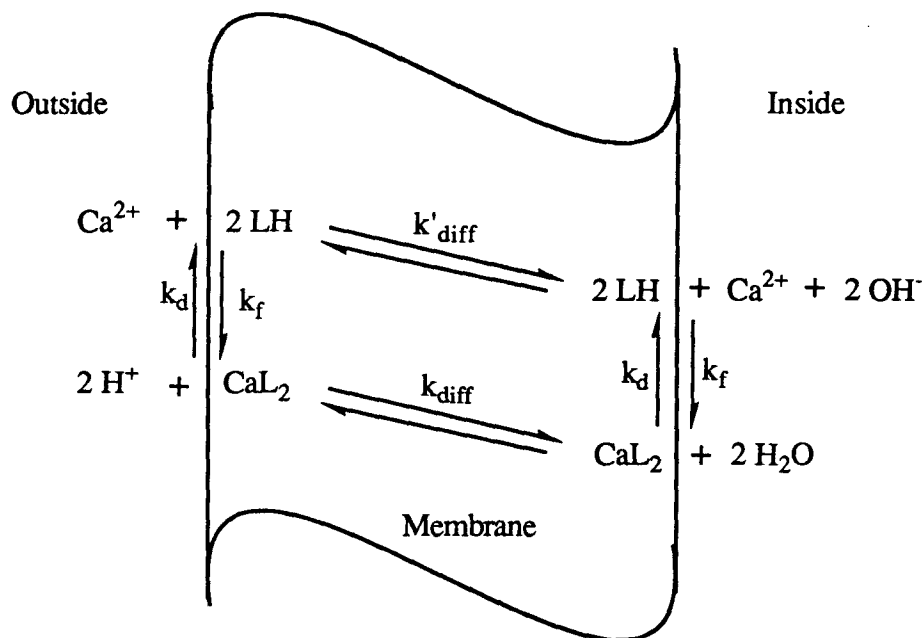


Figure 2. Mechanism of calcium transport across a phospholipid membrane by calcium ionophores.

Efforts to develop synthetic calcium ionophores based on consideration of the structures of lasalocid A and calcimycin, and the desirable characteristics (e.g., ion selectivity, favorable binding constant and calcium on/off kinetics) of an ideal calcium ionophore have been met with certain success.<sup>27a,b</sup> Two diglycolamic acids prepared by Umen and Scarpa were shown to transport calcium across an artificial membrane comparable to lasalocid A and calcimycin.<sup>27a</sup> The use of lipophilic acyclic polyether dicarboxylic acids as mobile carriers to transport calcium, magnesium and barium across an artificial membrane was reported by Hiratani and co-workers.<sup>27b</sup>

An artificial membrane such as a bulk liquid membrane was used by the above authors and others as a simple way to study ionophore-catalyzed calcium transport.<sup>27</sup> In this experiment two aqueous compartments in a U-tube (Figure 3a)<sup>27g</sup> or a cylindrical glass cell (Figure 3b)<sup>27f</sup> are separated by a gently stirred solution of the ionophore in chloroform. One aqueous compartment is filled with solution containing calcium ions. The other compartment is filled with aqueous

solution without calcium ions. The appearance of calcium ions in this later compartment can be followed by using a number of techniques including calcium atomic spectrophotometry or calcium specific electrodes.

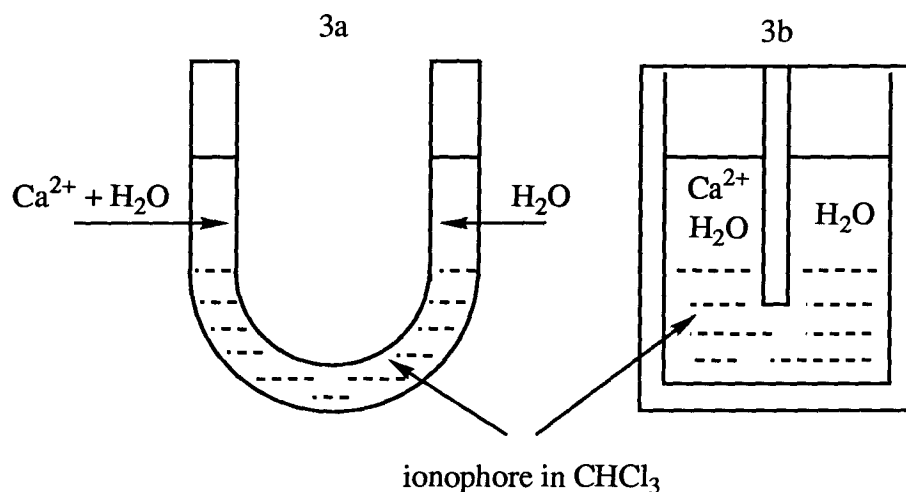


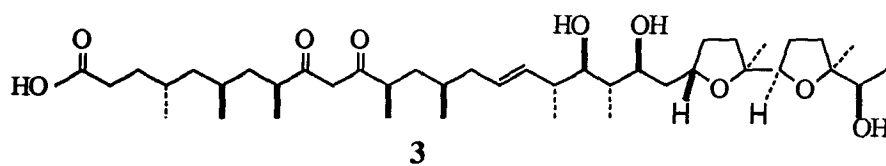
Figure 3. Cross sections of the U-tube and the cylindrical glass cell for the studies of calcium transport.

The U-tube or the cylindrical glass cell experiment can be used to determine the relative calcium transport efficiency of different ionophores. It can also be used to determine the cation selectivity of an ionophore by placing competing cations in the source phase and following their concentrations in the receiving phase. Chloroform is usually employed in these transport studies because its dielectric constant ( $\epsilon = 4.8$ ) is similar to the dielectric constant of the interior of a phospholipid membrane ( $\epsilon = 2 - 4$ ).<sup>28</sup>

The U-tube or the cylindrical glass cell experiment is a very crude approximation of calcium transport across biological membranes in terms of the membrane size, membrane composition and the transport time scale. However, it can serve as a model of transport behavior. Many factors which control the transport of calcium across biological membranes, such as the lipophilicity of an ionophore, can be studied in this simple system.

### 1.5 Ionomycin and Its Unique Structure and Function

In 1975, a novel polyether calcium ionophore ionomycin (**3**) was isolated by Meyers, et al. as a fermentation product of *Streptomyces globatus*.<sup>29</sup> Its molecular structure was determined by Toeplitz et al. using <sup>1</sup>H NMR spectroscopy, mass spectrometry, and X-ray crystallographic analysis of three crystalline forms of its cadmium and calcium salts.<sup>30</sup>



Like other polyether calcium ionophores, ionomycin has been found to be a potent antimicrobial agent. It is active against Gram-positive bacteria with no demonstrable effect against Gram-negative bacteria. However, ionomycin was found to have very unusual physical, chemical, and biological properties. It possesses a  $\beta$ -diketone group which, together with the carboxyl group, confers the dibasic character to the ionophore. It has a very high affinity for calcium and other divalent cations. In fact, the calcium salt of ionomycin was extracted from an aqueous solution of pH 12 which had been made alkaline with sodium hydroxide.<sup>29</sup>

Ionomycin is unique among polyether ionophores in that it forms a 1:1 calcium complex. As shown in the crystal structure of the calcium salt of ionomycin (Figure 4), the carboxylate group, the enolate of the  $\beta$ -diketone, two hydroxyl groups and a tetrahydrofuran oxygen form an octahedral complex around the calcium ion. The ligand wraps around the calcium ion with the oxygen atoms directed towards the inside of the sphere. The alkyl groups, on the other hand, protrude from the shell, providing the calcium complex with its lipophilic properties.



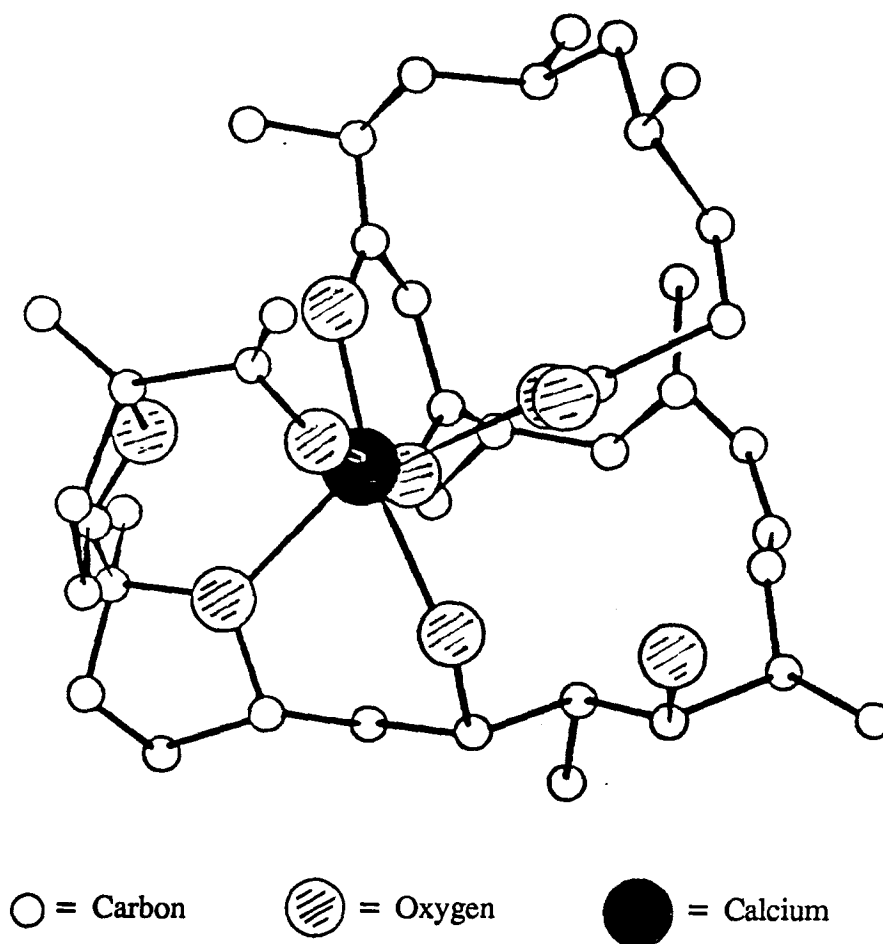


Figure 4. Crystal structure of the calcium salt of ionomycin.<sup>30</sup>

The structural characteristic which distinguishes ionomycin from other polyether ionophores is the presence of a  $\beta$ -diketone group. The  $\beta$ -diketone exists as an equilibrium mixture of tautomeric keto and enol forms, the latter absorbs at 276 nm.<sup>31</sup> Ionization of the  $\beta$ -diketone shifts the UV absorption to 300 nm (Figure 5). This permits the study of protonation and cation binding equilibria of ionomycin by UV spectrophotometric titration. The  $pK_a$  of the  $\beta$ -diketone group in ionomycin was determined to be  $11.94 \pm 0.02$  in 80% MeOH-H<sub>2</sub>O using this technique.<sup>32</sup>

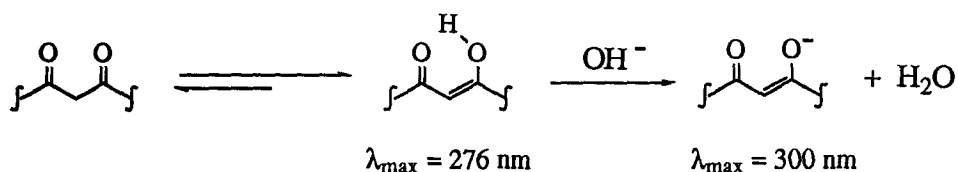


Figure 5. The enolization and ionization of a  $\beta$ -diketone.

Liu and Hermann studied the extraction of calcium ions from an aqueous phase into an organic phase and the transport of calcium across an organic barrier by ionomycin.<sup>33</sup> They found that the extraction of calcium by ionomycin was strongly dependent on the pH of the aqueous phase. Essentially no complexing of calcium occurred below pH 7.0 and complexation reached a maximum at about pH 9.5. In contrast, the extraction of calcium by calcimycin was observed down to pH 5.0 and reached a maximum near pH 7.5. Under the same experimental conditions, ionomycin bound twice as much calcium as calcimycin and it had a greater selectivity for calcium over magnesium than calcimycin.<sup>33</sup> The selectivity of ionomycin for divalent cations was shown to be  $\text{Ca}^{2+} > \text{Mg}^{2+} \gg \text{Sr}^{2+} = \text{Ba}^{2+}$ . No complexation with monovalent cations could be detected.<sup>34</sup>

*In vivo* studies also revealed that ionomycin was more effective than calcimycin as a mobile calcium carrier. In studies of rat liver mitochondria, it was shown that ionomycin efficiently catalyzed the exchange of two protons for one calcium ion across the cell membrane.<sup>34</sup> The turnover numbers for calcium transport by ionomycin were 3- to 5-fold greater than those by calcimycin.<sup>35</sup> Ionomycin has been found to stimulate the release of histamine from mast cells and catecholamine from pheochromocytoma cells by transporting calcium across the cell membranes.<sup>36</sup> It has also been linked to the activation of human blood platelets by facilitating transport of calcium across the membrane and mobilizing calcium stored in organelles.<sup>37</sup>

Currently, ionomycin is being used to study the biochemical basis of asthma. Mast cells located in airway walls release histamine and leukotriene C. Leukotriene C is believed to be a mediator in asthma as a potent muscle contractant that constricts small airways in the lung. It is a

metabolite of arachidonic acid whose synthesis is shown to be stimulated by ionomycin mediated calcium transport.<sup>38</sup>

Since its discovery in 1976 ionomycin has been used in place of calcimycin and lasalocid A as a superior calcium ionophore. It has been shown to mimic, at least qualitatively, the effects of many physiological cell stimuli. However, the scarcity of ionomycin limits its applications as an ionophore in biological studies, and its toxicity prevents its uses in the treatment of calcium related diseases.

### 1.6 Calcium Ionophores Based on Ionomycin

Although the partial and total synthesis of ionomycin has been achieved,<sup>39</sup> the difficulties associated with the stereoselective introduction of the numerous asymmetric centers on the molecule have been significant. Provision of ionomycin through total synthesis is not an economical choice.

Little is known about the structural features of ionomycin which control its calcium specificity in transport. One objective of this project is to design and synthesize simple ionomycin analogues to analyze the role of the functional groups of ionomycin in calcium binding and transport and to study the effect of other structural features, such as lipophilicity and oxygen coordination, on calcium transport. It is also our objective to improve the calcium transport efficiency of these simple molecules based on structure-activity relationships and to finally provide new calcium ionophores based on ionomycin both as biological tools and potential therapeutic agents.

## CHAPTER TWO

### RESULTS AND DISCUSSION

#### 2.1 Design and Synthesis of Ionomycin Analogues

The first stage of this project involved the design of ionomycin analogues based on the information gathered about the mode of action of ionomycin itself. The molecules would contain those functional groups thought to be vital to the function of ionomycin while maintaining the potential membrane (lipid) solubility. The numerous stereochemical centers found along the carbon backbone of ionomycin were omitted to simplify the preparation of the model compounds.

The chemical and physical data on ionomycin suggest that the  $\beta$ -diketone and carboxyl groups are crucial to its ionophoric properties. The crystal structure of the calcium salt of ionomycin (Figure 4) shows that both these groups are ionized and coordinated to the metal cation in the formation of the neutral 1:1 calcium complex. It was deemed important that these two functional groups be retained in the model compounds.

In the natural product, there is a seven-carbon chain separating the  $\beta$ -diketone and the carboxyl groups. The presence of this seven-carbon chain could certainly contribute to the high lipid solubility of the ionophore-calcium complex. The distance between these two functional groups is such that a 12-membered chelate ring is formed on chelation of a calcium ion by the carboxylate oxygen and the first oxygen of the  $\beta$ -diketone enolate (Figure 6).

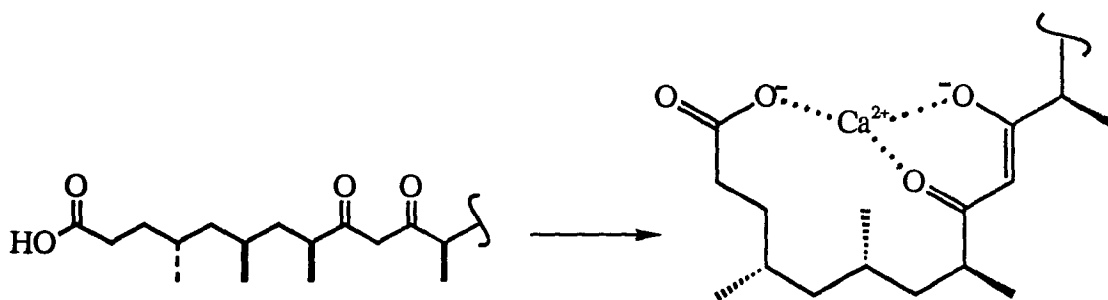
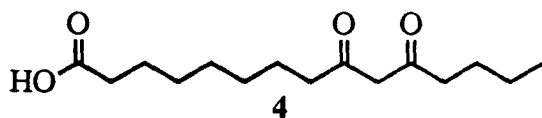


Figure 6. Binding of the carboxylate and enolate of  $\beta$ -diketone in the calcium salt of ionomycin.

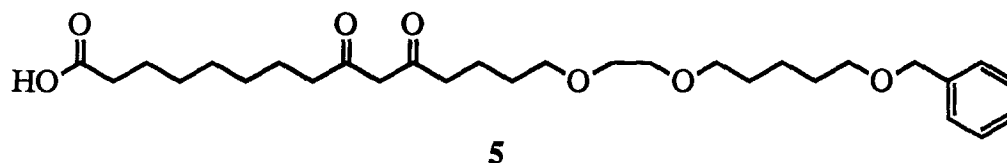
The formation of a 12-membered chelate ring would have less entropy to overcome than that of a larger chelate ring. On the other hand, the complex formed could be expected to have more favorable enthalpy than a smaller chelate ring. The interplay of entropy and enthalpy effects may be optimized for efficient calcium transport when a seven-carbon chain separates the two functional groups. Thus, a seven methylene unit was chosen as the linkage of these two functional groups in the model compounds.

To maintain the membrane solubility, high lipophilicity of the compounds may be needed. The simplest analogue fulfilling the above requirements would be a 9,11-dioxocarboxylic acid such as 9,11-dioxopentadecanoic acid (**4**) which was chosen as the first target molecule.

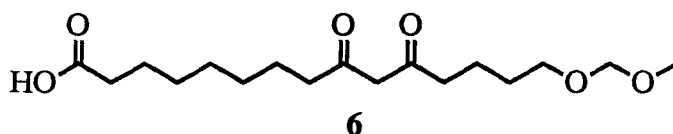


Since two hydroxyl and one tetrahydrofuranyl oxygen of the natural product are involved in coordination to the calcium ion (Figure 4), we suspected it would be necessary to incorporate a side-chain which contained appropriately placed oxygen atoms to retain the six calcium binding sites found in ionomycin. A side-chain that contains an ethylene glycol and an ether function five methylene units away was chosen to mimic the calcium coordination sites in ionomycin. An ether function, such as a benzyl ether, could compensate for the decrease of lipophilicity produced by the introduction of three oxygen atoms in such a molecule. Therefore, a

benzyloxypentyloxyethoxyl unit was incorporated into analogue 4 to give the second molecule 15-[2-(5-benzyloxy)-pentyloxy]-ethoxy-9,11-dioxopentadecanoic acid (5).



The presence of six oxygen coordination sites may not be necessary for the binding and transport of calcium. A molecule of water from the aqueous medium could occupy a calcium coordination site as is often observed in the binding of calcium with proteins.<sup>40</sup> The crystal structure of the barium salt of lasalocid A shows one molecule of water in the ionophore-barium complex (Figure 1). The water molecule not only occupies a barium coordination site, but it also holds the two ionophore molecules together through the formation of hydrogen bonds. Thus, it may be sufficient to incorporate a side chain which contains only one or two oxygen atoms as potential calcium coordination sites. With this in mind we incorporated a methoxymethoxyl unit in analogue 4 to give a further target molecule 15-methoxymethoxy-9,11-dioxopentadecanoic acid (6).



The second stage of the project was to develop a synthetic route to each of the proposed analogues. The carboxyl function of the compounds could be made by oxidation of a hydroxyl group.<sup>41</sup> The etheral units in analogues 5 and 6 could be prepared using known chemistry.<sup>42</sup> The crucial part in the synthesis of the analogues appeared to be the introduction of the  $\beta$ -diketone and the construction of the carbon backbone.

A  $\beta$ -diketone could be prepared by oxidation of a  $\beta$ -hydroxyl ketone which in turn could be generated by an aldol condensation between a methyl ketone and an aldehyde. This route was used in the synthesis of ionomycin by Hanessian's group<sup>39a</sup> and by Evan's group.<sup>39b</sup> (Figure 7)

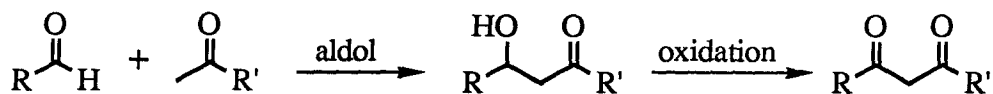


Figure 7. Construction of a  $\beta$ -diketone by aldol condensation and oxidation.

Alternatively, the  $\beta$ -diketone could be prepared by alkylation of the anion of a dithiane with an epoxide, followed by oxidation of the hydroxyl group and hydrolysis of the dithiane (Figure 8). This method was employed in the synthesis of an ionomycin fragment by Weiler and Shelly.<sup>39c</sup>

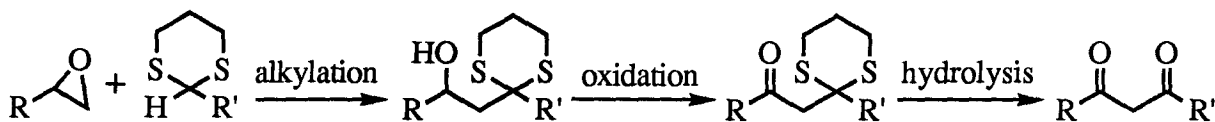


Figure 8. Construction of a  $\beta$ -diketone by dithiane alkylation, oxidation and hydrolysis.

These two methods could be applied to the synthesis of our proposed analogues of ionomycin. However, neither route appeared to be very efficient. The former method converted a carbonyl to an alcohol and later back to the carbonyl, and the latter had one more synthetic manipulation than the former. A logical precursor of a  $\beta$ -diketone appeared to be the simplest  $\beta$ -diketone, the commercially available 2,4-pentanedione (7). Consecutive alkylation of 2,4-pentanedione at the methyl carbons could be achieved using the dianion chemistry (Figure 9).

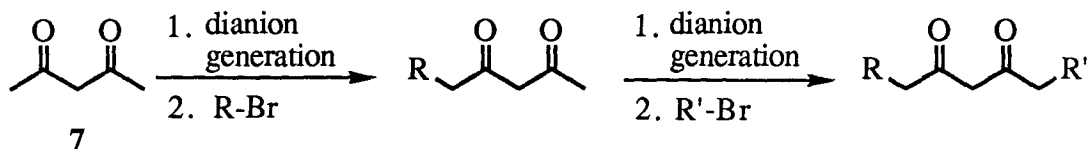


Figure 9. Construction of a  $\beta$ -diketone by dianion alkylation of 2,4-pentanedione (7).



Using this method, the synthesis of analogues **4**, **5** and **6** was reduced to the preparation of bromides **8-11** (Figure 10).

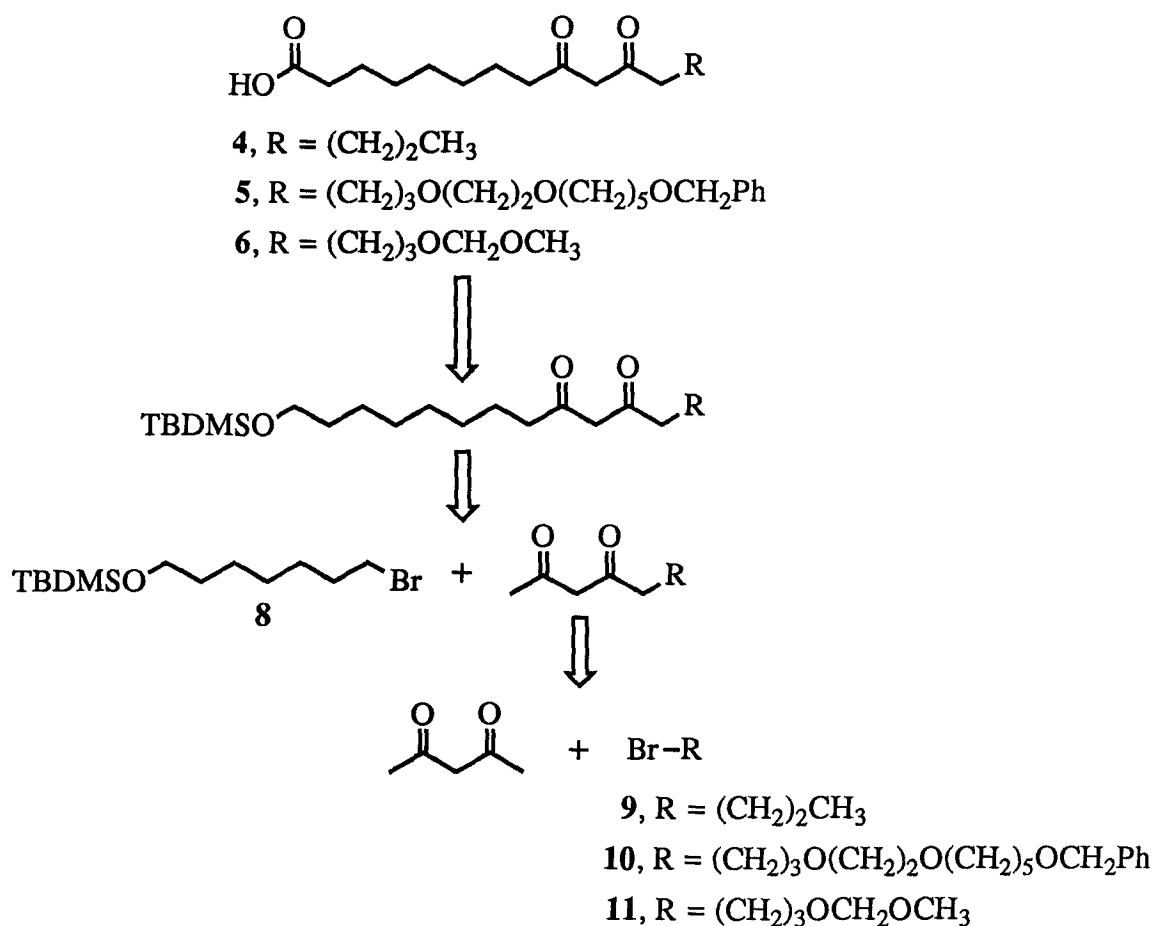
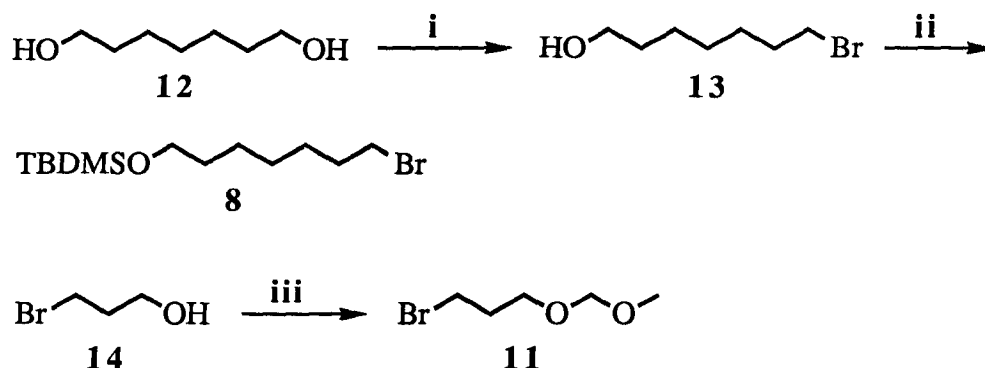


Figure 10. Retrosynthetic analysis of analogues **4**, **5** and **6**.

Bromide **9** is commercially available. Our synthesis of bromide **8**, a common intermediate in the preparation of the analogues, and bromide **11** is illustrated in Scheme I.

Scheme I.



i. HBr, 72%; ii. TEA, DMAP, TBDMSCl, 82%; iii. P<sub>2</sub>O<sub>5</sub>, CH<sub>2</sub>(OCH<sub>3</sub>)<sub>2</sub>, 91%

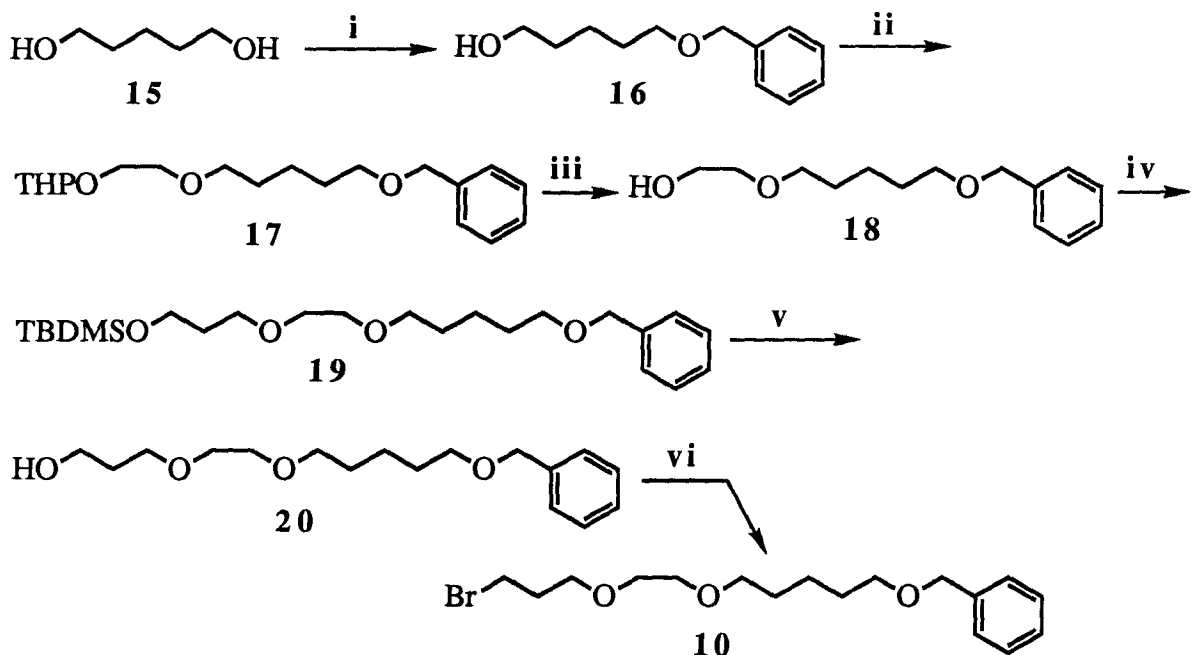
---

Monobromination of 1,7-heptanediol (**12**) was achieved by continuously extracting a mixture of diol **12** and aqueous hydrobromic acid with heptane.<sup>44</sup> The hydroxyl group of bromide **13** was protected as its tert-butyldimethylsilyl ether<sup>45</sup> to give bromide **8**. Bromide **11** was prepared by treatment of 3-bromo-1-propanol (**14**) with phosphorus pentoxide and dimethoxymethane.<sup>46</sup>

Our synthesis of bromide **10** is outlined in Scheme II. It was initiated with the monobenzoylation of 1,5-pentanediol (**15**).<sup>47</sup> Treatment of diol **15** with two equivalents of sodium hydride and one equivalent of benzyl bromide gave the monobenzylated alcohol **16** in 54% yield, together with a small amount of dibenzylated product.

The alcohol **16** was subjected to the modified Williamson ether synthesis procedure.<sup>48</sup> This involved the vigorous mixing of a two-phase system containing the alcohol, 1-bromo-2-tetrahydropyranyloxylethane and aqueous sodium hydroxide in the presence of a phase transfer catalyst tetrabutylammonium hydrogen sulfate. The reaction gave the desired ether **17** in 83% yield. Only a small amount of alcohol **16** could be converted to ether **17** when the reaction was carried out using sodium hydride as a base in polar aprotic solvents such as dimethylformamide.

Scheme II.

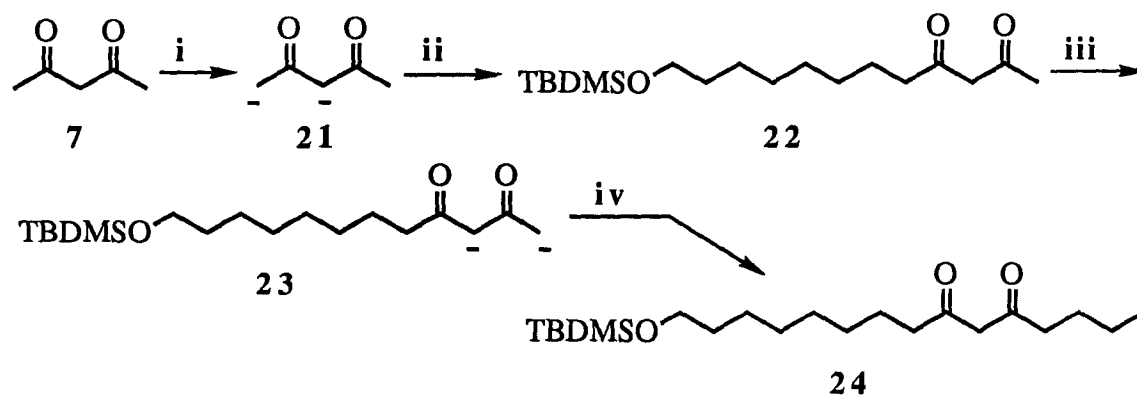


*i*. NaH, BrCH<sub>2</sub>Ph, 54%; *ii*. NaOH, Bu<sub>4</sub>NHSO<sub>4</sub>, THPO(CH<sub>2</sub>)<sub>2</sub>Br, 83%; *iii*. PPTs, 83%;  
*iv*. NaOH, Bu<sub>4</sub>NHSO<sub>4</sub>, TBDMSO(CH<sub>2</sub>)<sub>3</sub>Br, 83%; *v*. Bu<sub>4</sub>NF, 89%; *vi*. Ph<sub>3</sub>P, CBr<sub>4</sub>, 91%

The tetrahydropyranyl ether protecting group in **17** was cleaved with pyridium *p*-toluenesulfonate to give alcohol **18** in 83% yield.<sup>49</sup> The alcohol **18** was subjected to the modified Williamson ether synthesis procedure using 1-bromo-3-tert-butyldimethylsilyloxypropane to give the ether **19** in 83% yield. Deprotection of the TBDMS ether with tetrabutylammonium fluoride<sup>50</sup> gave alcohol **20** which was converted to bromide **10** by treatment with triphenylphosphine and carbon tetrabromide.<sup>51</sup>

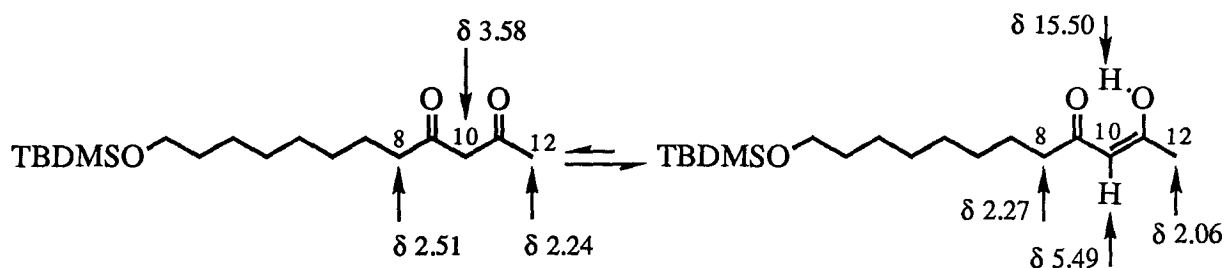
With bromides **8**, **9**, **10** and **11** in hand, we were ready to perform the dianion alkylation reactions on 2,4-pentanedione (**7**). The use of the dianion alkylation reactions in the synthesis of analogue **4** is shown in Scheme III. Treatment of 2,4-pentanedione (**7**) with one equivalent of sodium hydride and one equivalent of *n*-butyllithium generated the dianion **21** which reacted with bromide **8** to give the monoalkylated  $\beta$ -diketone **22** in 81% yield.<sup>43a</sup>

Scheme III.



i. NaH, n-BuLi; ii. TBDMSO(CH<sub>2</sub>)<sub>7</sub>Br, 81%; iii. 2.0 LDA; iv. Br(CH<sub>2</sub>)<sub>2</sub>CH<sub>3</sub>, 81%

The structure of the monoalkylated β-diketone **22** was confirmed by <sup>1</sup>H NMR spectroscopy. The spectrum of compound **22** exhibited a triplet at δ 2.51 which integrated to 0.4 proton and a triplet at δ 2.27 which integrated to 1.6 protons ascribable to the methylene protons at C-8 of the keto and enol forms of the β-diketone respectively. A 0.6-proton singlet at δ 2.24 and a 2.4-proton singlet at δ 2.06 were assigned to the methyl protons at C-12 of the keto and enol forms respectively. A 0.8-proton singlet at δ 15.50, a 0.8-proton singlet at δ 5.49 and a 0.4-proton singlet at δ 3.58 were assigned to the enol hydroxyl proton, the vinyl proton and the methylene proton at C-10 respectively as shown below.

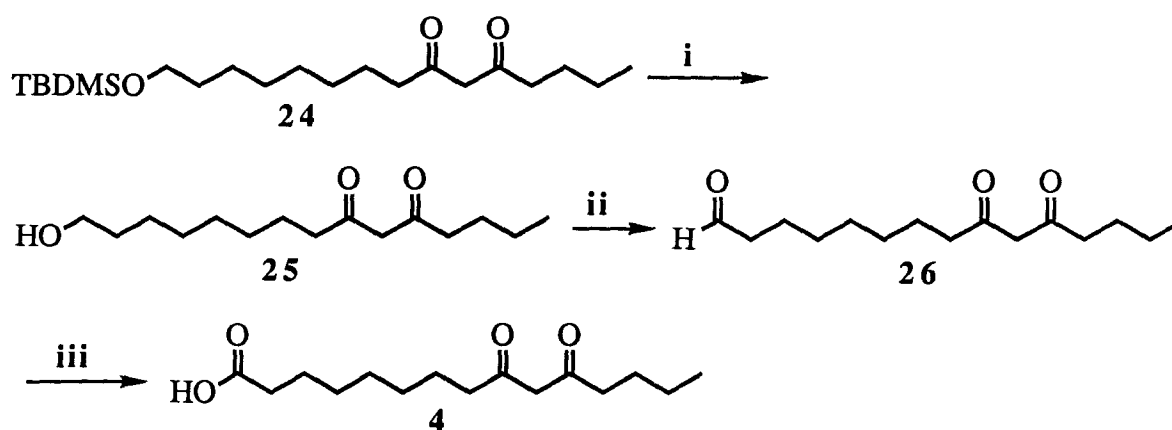


The second dianion alkylation reaction was achieved by treating the β-diketone **22** with two equivalents of lithium diisopropylamide (LDA) and subsequently with one equivalent of

1-bromopropane (**9**). The sterically hindered base LDA was used to regioselectively generate dianion **23**.<sup>43b</sup> Reaction of dianion **23** with bromide **9** produced the  $\beta$ -diketone **24** in 81% yield. The regioselective alkylation was also confirmed by  $^1\text{H}$  NMR spectroscopy. The spectrum of compound **24** showed two triplets at  $\delta$  2.53 - 2.24 integrating to a total of four protons ascribable to the methylene protons at C-8 and C-12. In addition, three singlets at  $\delta$  15.51, 5.48 and 3.54 integrating to a total of two protons ascribable to the enol hydroxyl proton, the vinyl proton and the methylene proton at C-10 were present in the spectrum.

To complete the synthesis of analogue **4**, the silyl ether protecting group of compound **24** was cleaved with tetrabutylammonium fluoride to give alcohol **25** in 91% yield (Scheme IV). The alcohol **25** was oxidized to aldehyde **26** with dimethylsulfoxide and dicyclohexylcarbodiimide in the presence of dichloroacetic acid.<sup>52</sup> Treatment of the aldehyde with silver nitrate and sodium hydroxide<sup>53</sup> produced the  $\beta$ -diketone carboxylic acid **4** in 69% yield. Oxidation of alcohol **25** using Jones oxidation<sup>54</sup> gave a complex mixture of products which were difficult to purify. No further effort was made to convert the alcohol **25** to the acid **4** in one step using Jones oxidation.

Scheme IV.

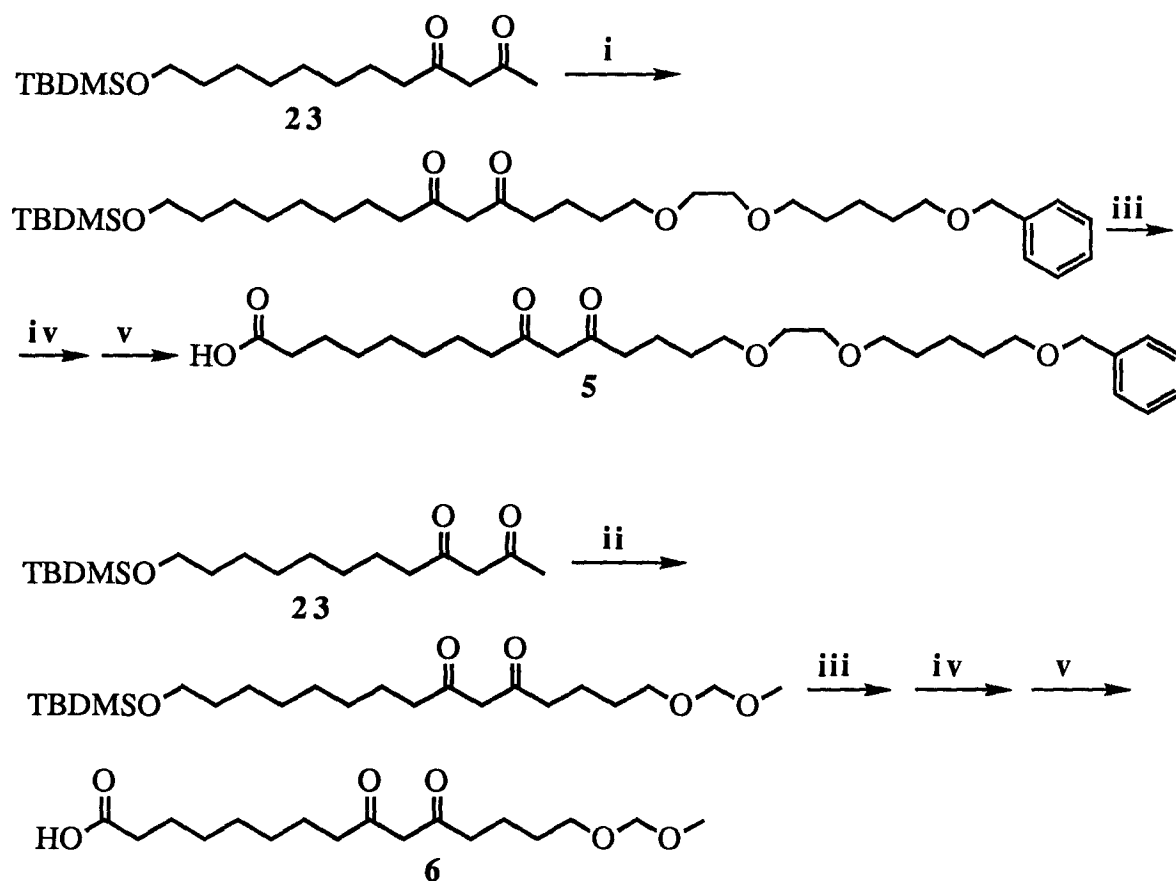


i.  $\text{Bu}_4\text{NF}$ , 91%; ii. DMSO, DCC,  $\text{Cl}_2\text{CHCO}_2\text{H}$ ; iii.  $\text{AgNO}_3$ ,  $\text{NaOH}$ , 69%

---

To synthesize analogues **5** and **6**, we used the  $\beta$ -diketone **23** as the starting material. Regioselective dianion alkylation of **23** with bromide **10** and **11** respectively, subsequent deprotection of the TBDMS ethers and oxidation of the alcohols furnished analogues **5** and **6** in yields similar to those of analogue **4** (Scheme V).

Scheme V.



**i.** 2.0 LDA, Br(CH<sub>2</sub>)<sub>3</sub>O(CH<sub>2</sub>)<sub>2</sub>O(CH<sub>2</sub>)<sub>5</sub>OCH<sub>2</sub>Ph; **ii.** 2.0 LDA, Br(CH<sub>2</sub>)<sub>3</sub>OCH<sub>2</sub>OCH<sub>3</sub>;  
**iii.** Bu<sub>4</sub>NF; **iv.** DMSO, DCC, Cl<sub>2</sub>CHCO<sub>2</sub>H; **v.** AgNO<sub>3</sub>, NaOH

## 2.2 Transport of Calcium across a Chloroform Liquid Membrane

With ample quantities of analogues 4, 5 and 6 in hand, we proceeded to evaluate the ability of these molecules to transport calcium across an organic barrier in a cylindrical glass cell (Figure 11).<sup>27d</sup>

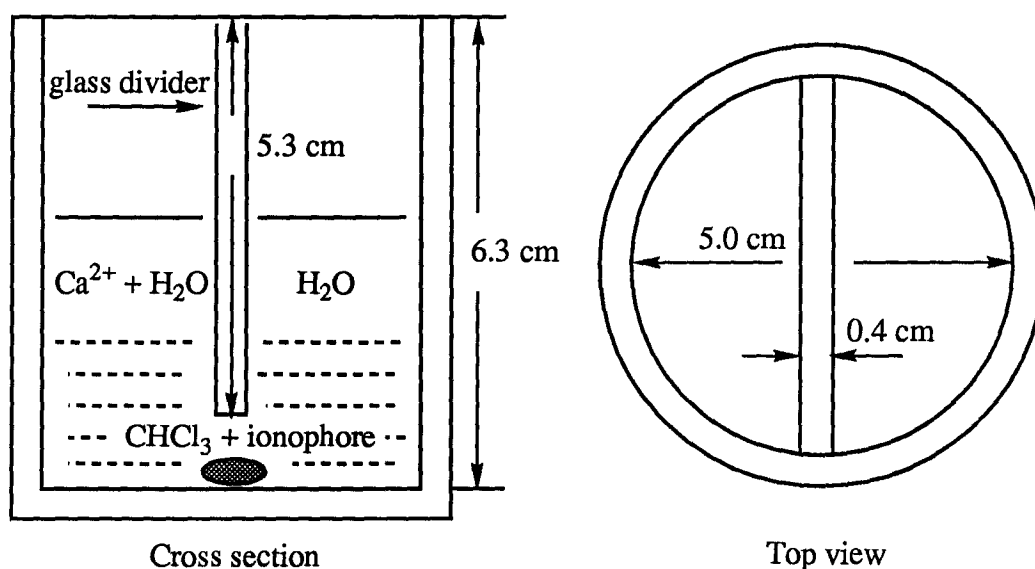
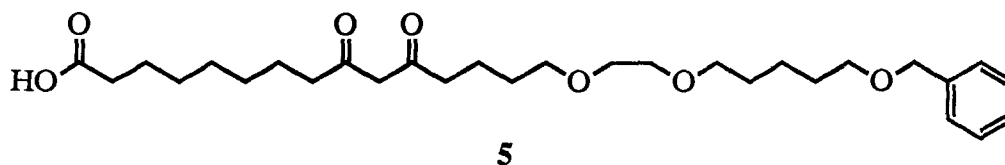


Figure 11. Cross section and top view of the cylindrical glass cell for the studies of calcium transport across a chloroform liquid membrane.

A solution of analogue 5 (200  $\mu\text{M}$ ) in chloroform (40 mL) was placed at the bottom of the transport vessel. The volume of the chloroform solution was such that two separate compartments were created above the organic solution (Figure 11). An aqueous solution (10 mL) of calcium chloride (500 mM) and CHES/ $\text{Me}_4\text{NOH}$  buffer (40 mM, pH = 9.5) was placed atop of the chloroform solution on one side of the transport vessel as the source phase. A solution of deionized distilled water (10 mL) containing MOPS/ $\text{Me}_4\text{NOH}$  buffer (40 mM, pH = 7.0) was placed on the other side of the transport vessel as the receiving phase. The chloroform solution was stirred continuously and samples (0.2 mL) were withdrawn from the receiving phase at

different times. The organic phase remained clear during the experiment and subsequent studies showed that the concentration of ionophore was below the critical micelle concentration.



Analogue **5** was chosen as the ionophore in our first transport experiment since this compound possessed more oxygen donor sites than analogues **4** and **6** and might mimic the ionophoric properties of ionomycin better. The aqueous source phase was buffered at a higher pH and the receiving phase at a lower pH to possibly facilitate the transport process.

To our satisfaction, calcium atomic absorption spectrophotometric analysis of the samples withdrawn from the receiving phase at different times showed a steady increase of calcium. The results are given in Table I. Each value in the Table is the average of three independent experiments with a standard error of approximately  $\pm 10\%$ .

Table I. Amount of Calcium in the Receiving Phase at Different Times.

Time (h)	0	12	16	20	24	36	42	48	60
Ca <sup>2+</sup> ( $\mu$ mol)	0	5.8	7.8	10	12	17	19	22	25

To determine if the above calcium transport was due to the leakage of calcium across the chloroform layer (blank transport of calcium), we carried out the transport experiment without the addition of compound **5** in the chloroform layer. Analysis of the samples withdrawn from the receiving phase using calcium atomic absorption spectrophotometry showed no detectable presence of calcium. The ability of analogue **5** to function as a carrier for the transport of calcium across an organic barrier was thus established.



The data in Table I shows that the amount of calcium in the receiving phase increases linearly with time when the amount of calcium transported is small (less than 0.5% of calcium from the aqueous source phase). A plot of the amount of calcium transported versus time within this linear range is given in Figure 12. The slope of the straight line is 0.50 and the area between the organic and the receiving phase is  $6.8 \text{ cm}^2$ , thus the initial transport rate,  $J$ , expressed as the moles of calcium transported per square centimeter of the chloroform per hour was calculated to be  $(7.3 \pm 0.7) \times 10^{-8} \text{ mole cm}^{-2} \text{ h}^{-1}$ .

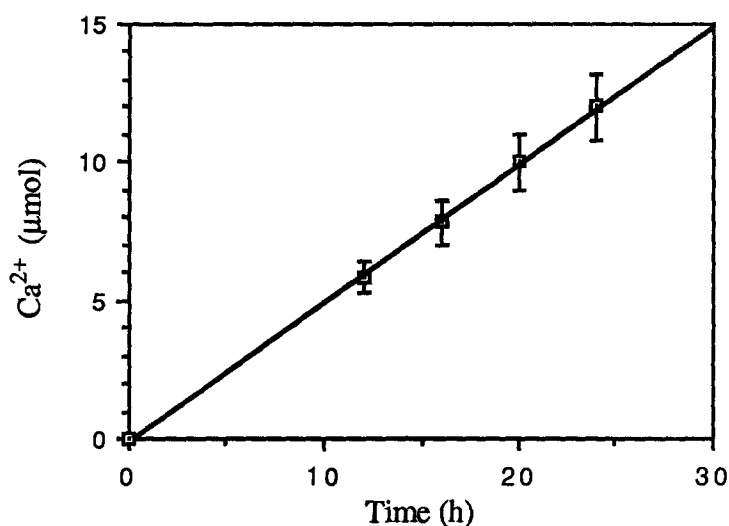
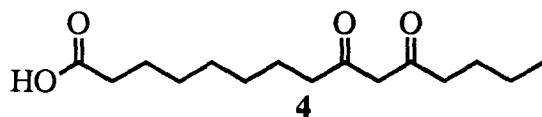
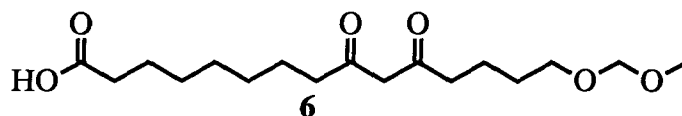


Figure 12. Plot of the amount of calcium in the receiving phase versus time. The points represent the average of three experimental values.

This linear relationship between initial transport and time was observed in all our subsequent transport experiments. These transport results will be given as the transport rate  $J$  with its upper and lower limit.

Next, we carried out the transport experiments on compounds **4** and **6** to examine the effect of minor structural changes on calcium transport. The results are summarized in Table II.



Table II. Calcium Transport Rates (J) for Compounds **4**, **5** and **6**.

Compound	<b>4</b>	<b>5</b>	<b>6</b>
J ( $10^{-8}$ mole $\text{cm}^{-2}$ $\text{h}^{-1}$ )	$0.3 \pm 0.1$	$7.3 \pm 0.7$	0

Compound **5** was found to be the most efficient carrier for the transport of calcium. Presumably this was due to the effect of coordination of calcium by the three oxygen atoms on the side chain of the molecule. Surprisingly no detectable transport of calcium was observed for compound **6** which had two additional oxygen donor atoms compared to compound **4**. This contradicted what was anticipated from the possible contribution of coordination of calcium by additional oxygen atoms to the transport of calcium. In fact, it appeared that additional oxygen atoms on the side chain of compound **6** were detrimental to the transport of calcium.

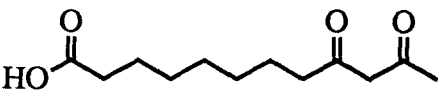
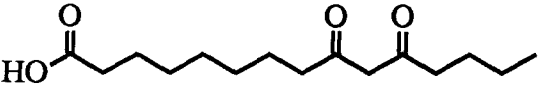
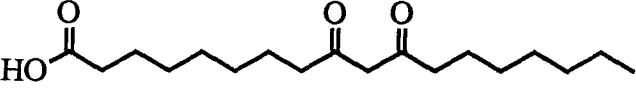
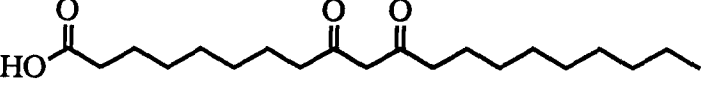
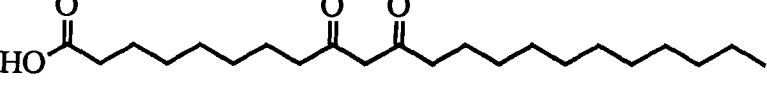
Besides providing potential coordination sites for calcium, additional oxygen atoms on the side chain of compounds **5** and **6** could change the lipophilicity of the molecules, which may affect the calcium transport ability of the compounds. Although the lipid solubility of the compounds was not determined, it is very likely that they follow the order **5** > **4** > **6** based on the ratio of the numbers of carbon and hydrogen atoms to oxygen atoms. This is the same order as the calcium transport rate of the compounds.

The hypothesis that the lipophilicity of the compounds may control calcium transport could be tested by varying the lipid solubility of the molecules in a predictable manner and study the transport behavior of such molecules. To this end, compounds **27**, **28**, **29** and **30** which had various alkyl side chains were prepared. The synthesis of these compounds was very similar to that of analogue **4**. Therefore, it will not be discussed here.

### 2.3 Effect of Carrier Lipophilicity on Calcium Transport

The transport experiments were carried out on compounds **27-30** to probe the effect of lipophilicity on calcium transport. The results are given in Table III.

Table III. Calcium Transport Rates (J) for Compounds **4** and **27-30**.

Compound	J ( $10^{-8}$ mole $\text{cm}^{-2}$ $\text{h}^{-1}$ )
 <b>27</b>	0
 <b>4</b>	$0.3 \pm 0.1$
 <b>28</b>	$15 \pm 2$
 <b>29</b>	$15 \pm 2$
 <b>30</b>	$13 \pm 1$

As seen from Table III, the lipophilicity of the compounds appears to play an important role in the transport of calcium. Compound **27** with no methylene units on the hydrocarbon side chain did not transport calcium across the chloroform phase. Compound **4** had three methylene units on the side chain and was able to transport calcium. The addition of more methylene units

resulted in a significant increase of calcium transport rate for compounds **28**, **29** and **30**. In fact, compounds **28-30** are more efficient calcium carriers than compound **5**. It appears that additional oxygen binding sites on the side chain of analogue **5** may not coordinate with calcium.

Interestingly, the transport rate of compound **30** was comparable to compounds **28** and **29** even though it had more methylene units on the side chain. This may be due to the low solubility of compound **30** in the high dielectric constant interface of the chloroform and aqueous source phase where calcium transport is initiated. Compounds **28** and **29** appears to have optimal lipid solubility for calcium transport.

Additional evidence pointing to the importance of lipid solubility in calcium transport was obtained when the concentration of the carrier in the chloroform phase was monitored during the transport experiments. A small volume (1 mL) of the chloroform solution was withdrawn at different times, the solvent was evaporated and the residue was dissolved in methanol. The magnitude of the UV absorption at 276 nm of the methanol solution was used to determine the carrier concentration. We found that the concentration of compounds **28**, **29** and **30** in the chloroform phase remained constant throughout the transport experiments. In contrast, the concentration of compound **27** in the chloroform phase steadily decreased. Using UV spectroscopy the lost compound was found to be in the aqueous source phase. Thus, compounds **28**, **29** and **30** were efficient carriers for the transport of calcium because these compounds and their calcium complexes had sufficient lipid solubility to remain in the chloroform phase. Compound **27** did not transport calcium across the chloroform layer because it was extracted into the aqueous source phase due to its higher hydrophilicity.

The results illustrate the importance of lipophilicity in calcium transport and suggest that other compounds possessing the  $\beta$ -diketone and carboxyl groups with different carbon backbones may also be efficient calcium carriers if their lipophilicity is similar to compounds **28-30**. The

results with compound **27** illustrate the need to consider the partitioning of the carrier between the organic and the aqueous phase.

The partition coefficient (*P*) of a substance between an organic phase and an aqueous phase is defined as the ratio of equilibrium concentration of the substance in the organic phase to that in the aqueous phase.<sup>55</sup> The partition coefficient, or its logarithm has been correlated to the velocity with which a compound penetrates cells, and thus to the biological activity of the compound.<sup>55</sup> Much effort has been made to develop methods to estimate the partition coefficient of a substance based on its structure. Among them Rekker's hydrophobic fragmental constant method (*f* method) is considered to be the most reliable.<sup>56</sup> In this method, log *P* of a substance is an additive property of the substance and can be calculated using Equation 1, where *f<sub>i</sub>* represents the hydrophobic fragmental constant of the various fragments in the molecule and *a<sub>i</sub>* is the frequency of a given fragment in the molecule.

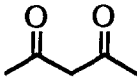
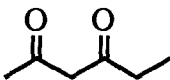
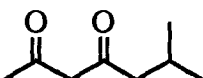
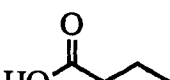

$$\log P = a_1f_1 + a_2f_2 + \dots\dots\dots + a_nf_n \quad (1)$$

Fragmental constants have been derived from the partition coefficients of a large number of compounds for which reliable experimental data are available. Some fragments and their *f* values in CHCl<sub>3</sub>-H<sub>2</sub>O calculated by Rekker<sup>56</sup> are given in Table IV. The calculated values of log *P* for a number of simple β-diketones and carboxylic acids, together with their experimental values<sup>56</sup>, are given in Table V. These results demonstrate the utility of the *f* method.

Table IV. Fragmental Constants for Various Fragments in the Chloroform-Water System.<sup>56</sup>

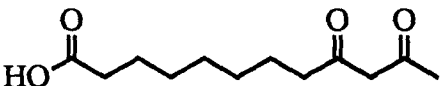
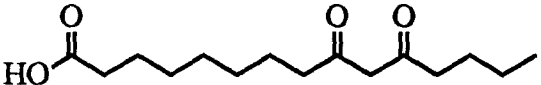
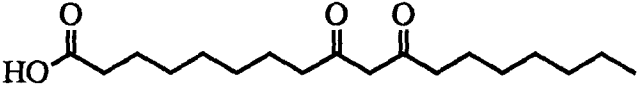
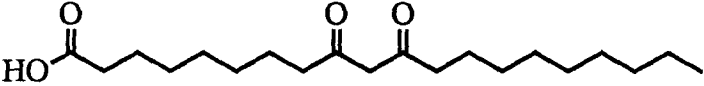
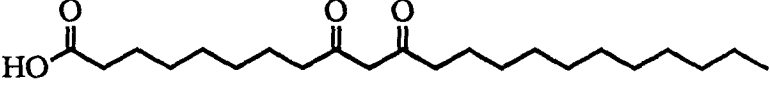
Fragment	-CH <sub>3</sub>	-CH <sub>2</sub> -	-COOH	-CH <sub>2</sub> COCH <sub>2</sub> COCH <sub>3</sub>	-CH <sub>2</sub> COCH <sub>2</sub> COCH <sub>2</sub> -
f <sub>i</sub>	0.965	0.628	-2.485	0.90	0.56

Table V. Calculated and Measured log P for Simple β-Diketones and Carboxylic Acids.<sup>56</sup>

Compound	log P (calculated)	log P (found) <sup>56</sup>
	1.24	1.40
	1.87	1.75
	3.00	2.97
	-0.26	-0.27
	0.36	0.34

Using the f method, we calculated log P values for compounds **27-30** and **4** (Table VI). The calcium transport rates (J) by these compounds are also listed. Log P values for compounds **5** and **6** were not calculated because the f values of their fragments are not available.

Table VI. Calcium Transport Rates (J) and Calculated log P Values for Compounds 4 and 27-30.

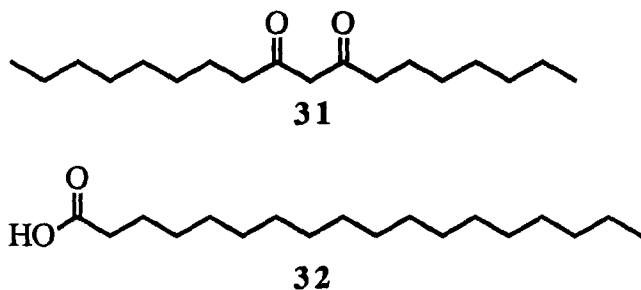
Compound	J ( $10^{-8}$ mole $\text{cm}^{-2}$ $\text{h}^{-1}$ )	log P
 27	0	2.18
 4	$0.3 \pm 0.1$	4.06
 28	$15 \pm 2$	5.95
 29	$15 \pm 2$	7.20
 30	$13 \pm 1$	8.45

The data in Table VI suggests that the minimum value of log P for calcium transport is about 4 and the optimal value of log P for calcium transport is in the range of 6-8. The future design of simple analogues based on ionomycin should have a value of log P in this range.

#### 2.4 Effect of Distance between the $\beta$ -Diketone and Carboxyl Groups on Calcium Transport

The studies of analogues with various alkyl side chains produced three simple compounds **28**, **29** and **30** as efficient calcium carriers. As a result, our efforts to further probe the structural features controlling the calcium transport of ionomycin and its simple analogues focussed on these compounds. The role of the  $\beta$ -diketone and carboxyl groups was investigated first.

Compound **31** was prepared using the same synthetic procedures as before. This compound and the commercially available octadecanoic acid (**32**) were subjected to the transport experiments separately. No detectable transport of calcium was observed even though the lipid solubility of these two compounds was sufficiently high compared to compounds **28-30**. This indicates that both the  $\beta$ -diketone and carboxyl groups are required for the transport of calcium.



To determine if the presence of the two functional groups within the same molecule is required, we performed a transport experiment with both compounds in the chloroform phase. Again no transport of calcium was detected. Therefore, the presence of the  $\beta$ -diketone and carboxyl groups within the same molecule is a necessary condition for the transport of calcium.

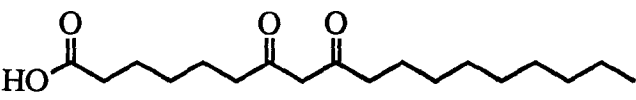
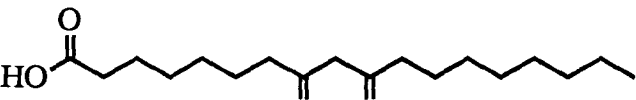
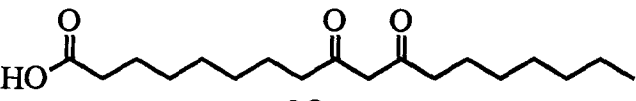
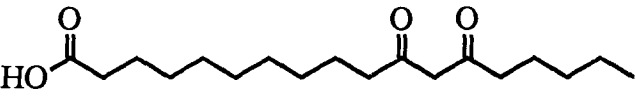
In all the ionomycin analogues studied so far, the number of carbons between the  $\beta$ -diketone and carboxyl groups was the same as that in ionomycin. This was based on the assumption that a seven-carbon chain separating these two functional groups would lead to favorable calcium transport. The requirement of the presence of the  $\beta$ -diketone and carboxyl



groups within the same molecule indicates that the distance between the two functional groups may be important. We proceeded to study the effect of the distance between these groups on calcium transport.

Compounds **33** and **34** which had the same lipid solubility ( $\log P$ ) as compound **28** but had the  $\beta$ -diketone moved two carbons closer to and two carbons further away from the carboxyl group respectively were synthesized. In addition, compound **35** which had the  $\beta$ -diketone in an 'unnatural' position, i.e., the  $\beta$ -diketone and carboxyl groups were in positions which would not be expected from normal polyketide biosynthesis,<sup>57</sup> was prepared. The number of methylene units ( $n$ ) between the two functional groups and the calcium transport rate ( $J$ ) of these compounds are given in Table VII. A graph of the calcium transport rate ( $J$ ) versus the number of methylene units ( $n$ ) is shown in Figure 13.

Table VII. Number of Methylene Units ( $n$ ) between the Two Functional Groups and Calcium Transport Rates ( $J$ ) of Compounds **33**, **35**, **28** and **34**.

Compound	$n$	$J$ ( $10^{-8}$ mole $\text{cm}^{-2}$ $\text{h}^{-1}$ )
 <b>33</b>	5	$3.5 \pm 0.4$
 <b>35</b>	6	$9.5 \pm 0.9$
 <b>28</b>	7	$15 \pm 2$
 <b>34</b>	9	$0.9 \pm 0.1$

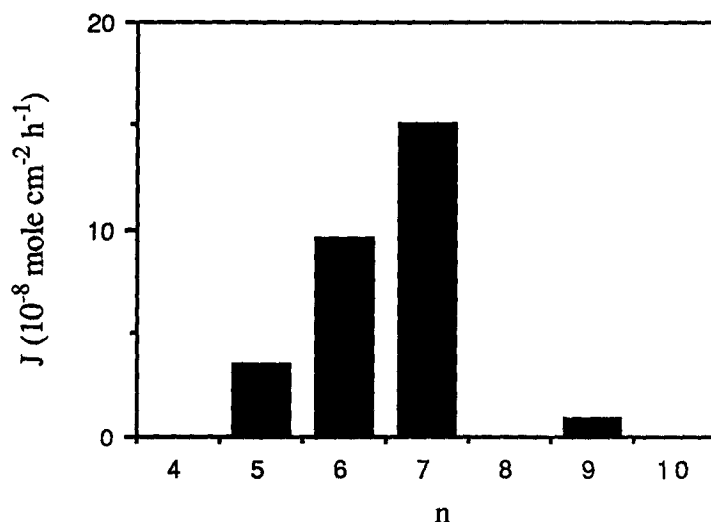
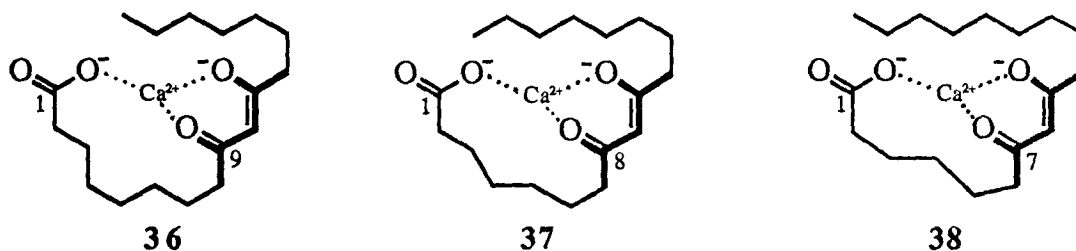


Figure 13. Graph of calcium transport rate ( $J$ ) versus number of methylene units ( $n$ ) separating the  $\beta$ -diketone and carboxyl groups.

Figure 13 shows that moving the  $\beta$ -diketone closer to or further away from the carboxyl group results in a significant decrease of calcium transport rate. The low calcium transport rate of compound **34** is likely due to the large unfavorable entropy change associated with the formation of its calcium complex. The first step in calcium transport is the binding of the ionophore with calcium to form the calcium complex (Section 1.4). As the  $\beta$ -diketone is moved further away from the carboxyl group, more entropy would need to be overcome to bring the two functional groups together for the binding and transport of calcium, resulting in a less effective calcium binding and transport. This trend can be expected to continue until the  $\beta$ -diketone is so far away from the carboxyl group that the two functional groups act essentially as in separate molecules, in which case no transport of calcium would be observed. Our findings on the transport behavior of compounds **31** and **32** are illustrative of the entropy effect on calcium binding and transport.

On the other hand, as the  $\beta$ -diketone is moved closer to the carboxyl group, the enthalpy of the calcium complex would increase due to the increasing steric strains (bond angle strain, torsional angle strain and transannular hydrogen interactions) in the chelate rings. This

unfavorable enthalpy may outweigh the more favorable entropy especially when the size of chelate ring is reduced from 12-membered to 11-membered or 10-membered as in the calcium complexes **36**, **37** and **38** of compounds **28**, **33** and **35**. The enolate of the  $\beta$ -diketone in the complexes could also increase the enthalpy in the order of  $36 < 37 < 38$ . The seven atoms of the enolate are planar (bonds between these atoms shown in bold), which, together with the fixed geometry of the carboxylate and enolate in the calcium complexes, restricts the number of bonds that can undergo rotations in the chelate rings to nine, eight and seven for complexes **36**, **37** and **38** respectively. This steric strain would increase in the order of  $36 < 37 < 38$  and may be responsible for the transport rate of compounds  $28 > 33 > 35$ .

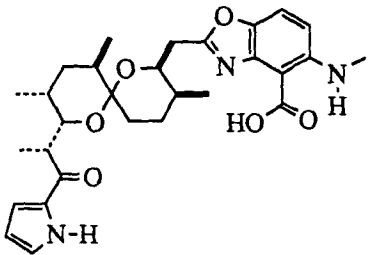
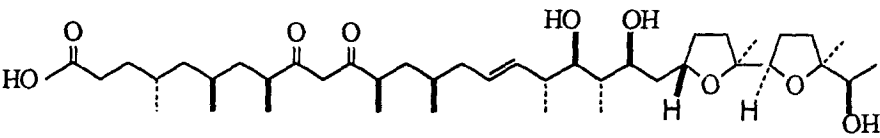
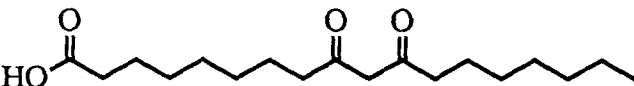
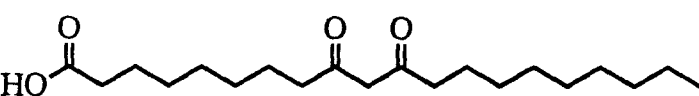
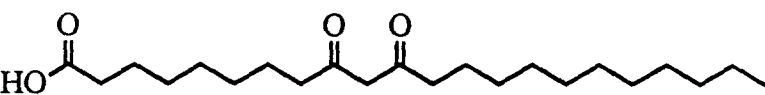


It appears that the competing role of enthalpy and entropy may be minimized when seven methylene units separate the two functional groups. It would also appear that ionomycin was biosynthesized with the optimal distance between the two functional groups.

## 2.5 Comparison of Ionomycin Analogues to Calcimycin and Ionomycin

To compare compounds **28-30** with known calcium ionophores, we carried out the transport experiments on ionomycin (**3**) and calcimycin (**2**). The results are given in Table VIII.

Table VIII. Calcium Transport Rates (J) for Calcimycin, Ionomycin and Compounds **28-30**.

Calcium ionophore	J ( $10^{-8}$ mole $\text{cm}^{-2}$ $\text{h}^{-1}$ )
 <p style="text-align: center;"><b>2</b></p>	$12 \pm 1$
 <p style="text-align: center;"><b>3</b></p>	$21 \pm 2$
 <p style="text-align: center;"><b>28</b></p>	$15 \pm 2$
 <p style="text-align: center;"><b>29</b></p>	$15 \pm 2$
 <p style="text-align: center;"><b>30</b></p>	$13 \pm 1$

Calcium transport by ionomycin is about twice as fast as calcimycin at the same molar concentration. This is in agreement with the transport results obtained for these two ionophores in other transport systems<sup>33</sup> and is due to the difference in the mole ratio of the ionophore-calcium complex. Ionomycin transports calcium as a 1:1 complex while calcimycin transports calcium as a 2:1 complex.

Calcium transport by analogues **28**, **29** and **30** is slower than ionomycin. The higher calcium transport rate of ionomycin compared to compounds **28-30** may be attributed to the smaller entropy change associated with the formation of ionomycin-calcium complex. Although the  $\beta$ -diketone and carboxyl groups in both ionomycin and compounds **28-30** are separated by a seven-carbon chain, there are three methyl substituents on this chain in ionomycin. These three methyl substituents, with their particular stereochemistry, may destabilize undesired rotomers of the acyclic bonds and reduce the number of conformations to those suitable for calcium complexation. This would reduce the entropy lost in the formation of calcium complex and thus increase the calcium transport rate for ionomycin.

Nevertheless, the comparative experiment demonstrates the high efficiency of compounds **28-30** as carriers for calcium transport across artificial membranes such as a chloroform liquid membrane.

## 2.6 Cation Selectivity in Transport

The comparable calcium transport efficiency of compounds **28-30** to calcimycin and ionomycin was very encouraging. However, a useful calcium ionophore should transport calcium both efficiently and selectively. In particular, it should have selectivity for calcium over sodium and potassium because of the ubiquitous presence of potassium and sodium ions in biological systems. Calcimycin and ionomycin both have selectivity for calcium over sodium and potassium.<sup>19,34</sup> Ionomycin is also selective for calcium over magnesium.<sup>34</sup>

To study the cation selectivity of our compounds, three transport experiments were carried out on analogue **28**. For each experiment, a solution of equimolar concentration of calcium chloride (250 mM) and chloride of the competing cation (magnesium chloride, sodium chloride and potassium chloride respectively) was placed in the source phase. Samples were withdrawn from the receiving phase and analyzed for calcium and the competing cation by atomic absorption spectroscopy. The results are given in Table IX.

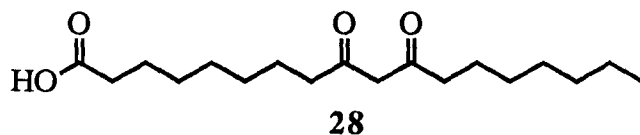


Table IX. Calcium, Magnesium, Sodium and Potassium Transport Rates for Analogue **28**.

Competing cations	Ca <sup>2+</sup>	Mg <sup>2+</sup>	Ca <sup>2+</sup>	Na <sup>+</sup> (or K <sup>+</sup> )
J (10 <sup>-8</sup> mole cm <sup>-2</sup> h <sup>-1</sup> )	2.2 ± 0.2	3.1 ± 0.3	5.5 ± 0.5	0

As seen from Table IX, the requirement of cation selectivity for calcium over sodium and potassium was met in analogue **28**. No detectable transport of sodium or potassium was observed. Unlike ionomycin, analogue **28** transported magnesium faster than calcium.

The cation selectivity of compound **28** in transport is likely due to the selectivity in binding which is expected to follow the order of ionic potentials of the cations  $\text{Mg}^{2+} > \text{Ca}^{2+} > \text{Na}^+ > \text{K}^+$ . Magnesium ion and calcium ion are both doubly charged and will bind to the enolate of  $\beta$ -diketone and the carboxylate more strongly than singly charged cations such as  $\text{Na}^+$  and  $\text{K}^+$ . On the other hand, the smaller magnesium cation (0.65 Å) will bind to the enolate of  $\beta$ -diketone and the carboxylate more strongly than calcium ion (0.99 Å).

The cation selectivity of ionomycin for calcium over magnesium in transport may be due to the size-match selectivity<sup>58</sup> and/or the coordination of the cations by additional oxygen atoms along the backbone of the ionophore. Ionomycin may have a limited number of low-energy conformations in which the size of the chelating portion of the molecule matches the size of a calcium ion but not the size of a magnesium ion. The coordination of cations by the additional oxygen atoms of ionomycin could also be the source of its selectivity for calcium over magnesium. The magnesium ion is small and its coordination with other oxygen atoms of the ionophore would increase steric crowding of the molecule more than the coordination of a larger calcium ion. The less favorable enthalpy in the magnesium complex may lead to the reversed cation selectivity in transport by ionomycin.

If one of the goals in the development of calcium ionophores based on ionomycin is to maintain the cation selectivity for calcium over magnesium in transport, two approaches should be considered. One is to design molecules that have the carboxyl and the  $\beta$ -diketone groups held in the geometry found in the crystal structure of the calcium salt of ionomycin.<sup>30</sup> The other approach would be to introduce additional oxygen atoms on appropriate positions into compounds such as **28**. The oxygen atoms should be on the hydrocarbon chain separating the carboxyl and  $\beta$ -diketone groups in an effort to ensure that the coordination of magnesium ions is less favorable.

## 2.7 Calcium Transport in Cultured Human Leukemic Cells

Analogues **6**, **27**, **28**, **29** and **33** were submitted to Merck Frosst Canada for *in vivo* testing of calcium transport in cultured human leukemic cells (THP-1 cells). Intracellular calcium,  $[Ca^{2+}]_i$ , was determined using a calcium-specific fluorescent probe.<sup>59</sup> The calcium ionophores calcimycin bromide and ionomycin were used as positive controls. Cumulative dose-responses were obtained and the cell fluorescence was monitored continuously for 3-5 minutes. Data from two separate experiments, one for positive control and the other for our analogues, are shown in Figure 14 - 18. Each curve represents the mean value of 2-3 determinations.

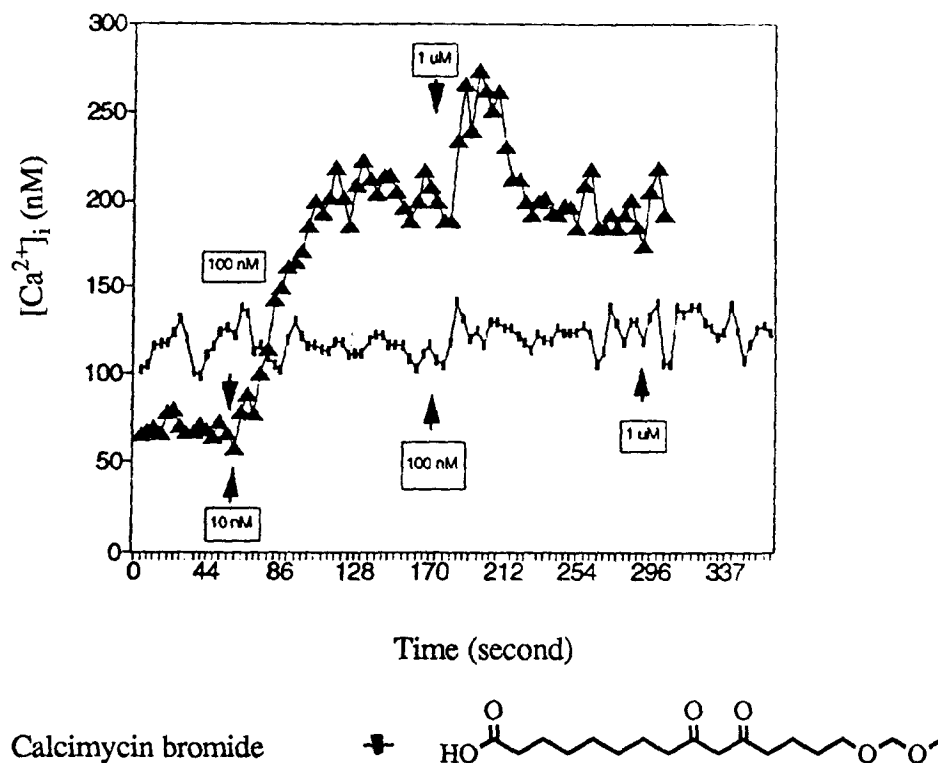
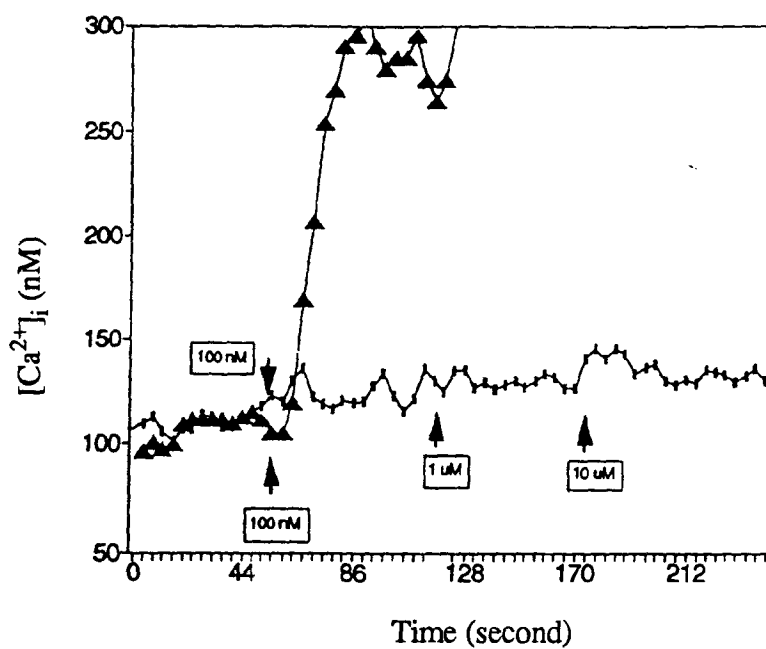


Figure 14.  $[Ca^{2+}]_i$  in THP-1 cell stimulated by calcimycin bromide and analogue 6.





▲ Ionomycin

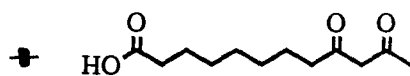
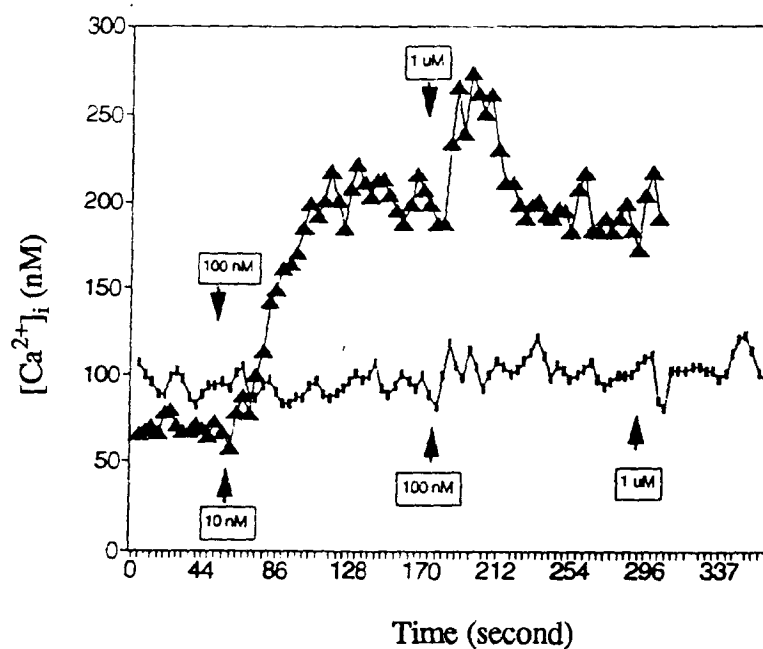


Figure 15.  $[Ca^{2+}]_i$  in THP-1 cell stimulated by ionomycin and analogue 27.



▲ Calcimycin bromide

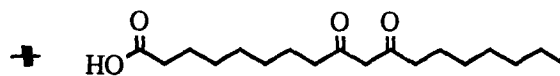


Figure 16.  $[Ca^{2+}]_i$  in THP-1 cell stimulated by calcimycin bromide and analogue 28.



As seen from Figure 14-18, the resting  $[Ca^{2+}]_i$  in THP-1 cells was in the range of 60-110 nM, in line with observations in other cell types.<sup>13</sup> The THP-1 cells responded to either calcimycin bromide or ionomycin stimulation with large (up to 10-fold) and sustained increases in  $[Ca^{2+}]_i$  in a dose-dependent manner. Only analogues **29** and **33** (Figure 17 & 18) induced a clear response at or greater than 1  $\mu$ M. These responses were transient and were significantly smaller than those of calcimycin bromide or ionomycin. Analogues **6** and **27** did not transport calcium across the membrane of THP-1 cell. This result is in agreement with those of the transport experiments using chloroform as the artificial membrane and is likely due to the low lipophilicity of the compounds in the cell membrane.

The transient and smaller responses induced by analogues **29** and **33** relative to the natural ionophores may be due to the lower chemical stability of the former compounds in the cell membranes. The analogues might undergo relatively rapid transformation such as transesterification in the cell membranes, which would result in the need for more compound and the transient calcium transport. It is also possible that the binding of the analogues with calcium is too low to allow the complexation and the transport of calcium at the given extracellular concentrations.

Surprisingly, no calcium transport in THP-1 cells was observed for analogue **28** which showed efficient calcium transport across a chloroform phase. The chemical stability of the analogues in biological membranes and its effect on calcium transport remained to be investigated.

One correlation can be made between the cylindrical glass cell experiments and the *in vivo* experiments. Compounds that show no calcium transport in the cylindrical glass cell would not transport calcium across biological membranes. The cylindrical glass cell experiments can be used to eliminate compounds from *in vivo* testing.

## 2.8 Effect of Substrate Concentration on Calcium Transport

To gain insight into the transport behavior of the analogues, we next investigated the effect of substrate concentration and pH on calcium transport. The first step in the transport of calcium across the chloroform phase is the binding of the ionophore to calcium at the interface of the chloroform and the aqueous source phase. This is followed by the diffusion of the calcium complex across the chloroform phase and the release of calcium into the aqueous receiving phase. If the binding of calcium is reversible, the ionophore-catalyzed calcium transport would show saturation kinetics which could be treated in the same fashion as enzyme kinetics.<sup>60</sup>

In the case of an enzyme-catalyzed reaction, the substrate (S) binds reversibly to the enzyme (E) to form an enzyme-substrate complex (ES) which then reacts to give the product (P) with the regeneration of the free enzyme. This kinetic behavior was first described by Michaelis and Menten under equilibrium conditions<sup>61</sup> and later extended by Briggs and Haldane with the steady-state approximation (Figure 19).<sup>62</sup>

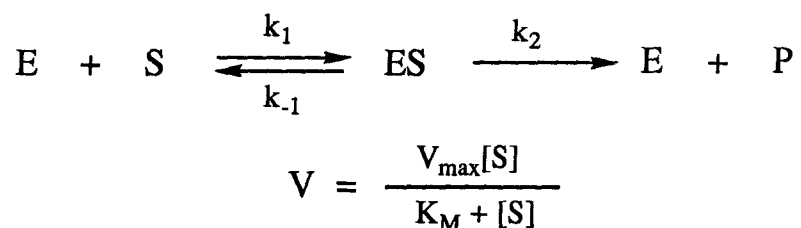


Figure 19. The Michaelis-Menten expression for enzyme catalysis.

This is formally the same as the ionophore (L) and calcium (Ca) forming an ionophore-calcium complex (CaL) which then diffuses across the membrane and releases calcium with the regeneration of the ionophore. The transport rate (J) can be related to the maximal rate (J<sub>max</sub>) through the Michealis-Menten equation (Equation 2) if the binding of calcium is reversible (Figure 20).

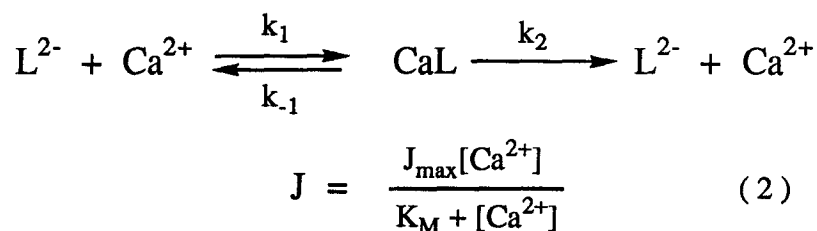


Figure 20. The Michaelis-Menten expression for ionophore-catalyzed calcium transport.

The thermodynamic parameter  $K_M$  represents  $(k_2 + k_{-1})/k_1$ . It is approximately equal to the equilibrium dissociation constant of the enzyme-substrate complex or the ionophore-calcium complex if  $k_2 \ll k_{-1}$  (the equilibrium assumption<sup>61</sup>).

The transport experiments were carried out on analogue **28** with various concentrations of calcium chloride in the source phase. The results are summarized in Table X.

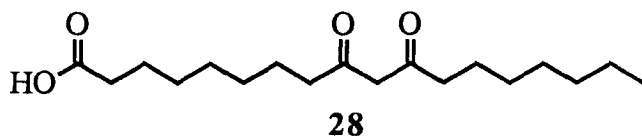


Table X. Calcium Transport Rates (J) at Various Calcium Concentrations in the Source Phase.

[Ca <sup>2+</sup> ] (mM)	10	50	100	250	500	1000
J (10 <sup>-8</sup> mole cm <sup>-2</sup> h <sup>-1</sup> )	0.6 ± 0.1	4.4 ± 0.4	5.9 ± 0.6	13 ± 1	15 ± 2	16 ± 2

When we fitted the transport rates (J) and substrate concentration ([Ca<sup>2+</sup>]) into the Michaelis-Menten equation (Equation 2) by non-linear regression, we obtained a hyperbolic curve (Figure 21) with a standard error of less than 10%, which could be taken as confirmation of the adherence to the Michaelis-Menten kinetics.<sup>63</sup>

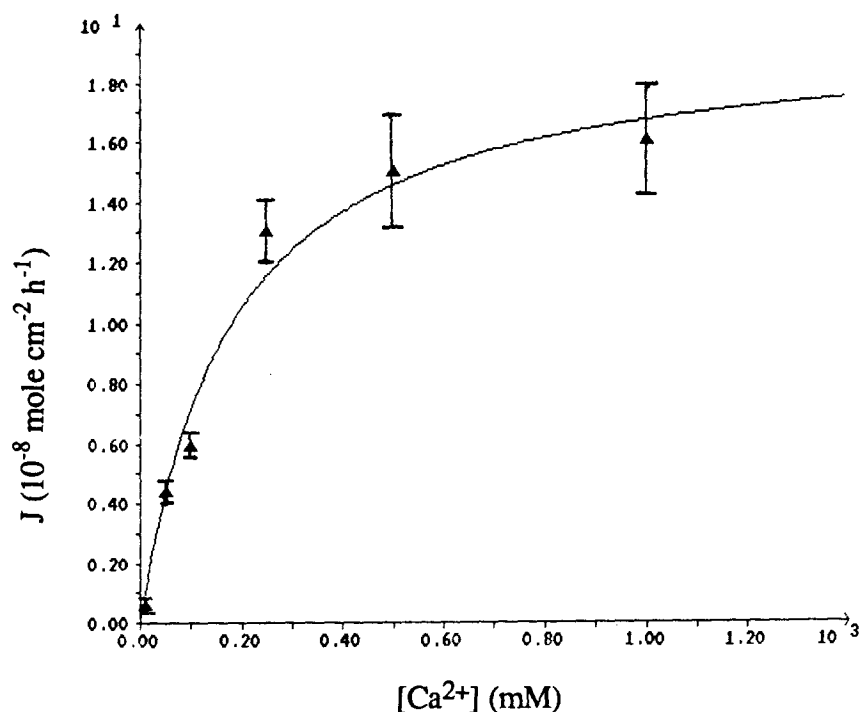


Figure 21. Curve of the dependence of transport rates on calcium concentration of the source phase. The points represent the experimental values, the solid line is fitted to the data by non-linear regression analysis according to Equation 2.

Therefore, calcium transport across the chloroform layer by analogue **28** is a saturable process which obeys the Michaelis-Menten kinetics. The values of the Michaelis-Menten constant  $K_M$  and the maximal transport rate  $J_{max}$  were found to be  $K_M = 170$  mM and  $J_{max} = 20 \times 10^{-8}$  mole  $\text{cm}^{-2} \text{h}^{-1}$  respectively by the above non-linear regression analysis.<sup>63</sup> The large  $K_M$  indicates the binding of calcium by analogue **28** is weak ( $k_{-1} \gg k_1$ ) and/or the diffusion of the analogue-calcium complex and the release of calcium is very fast compared to the binding of calcium ( $k_2 \gg k_1$ ).

The rate limiting step in the transport of calcium by analogue **28** is likely the diffusion of the calcium complex across the chloroform layer. This could be verified by the studies of the dependence of calcium transport on the stirring speed.<sup>27e</sup>

## 2.9 Effect of pH on Calcium Transport

The exchange of calcium ions from the ionophore-calcium complex (CaL) in the chloroform layer for protons from the aqueous receiving phase is the final step of the ionophore-catalyzed transport cycle. If this process is irreversible as suggested by the Michealis-Menten kinetics, a small change in the concentration of hydrogen ions in the receiving phase should not significantly affect the transport rate. The previous transport experiments were carried out with the aqueous receiving phase buffered at pH = 7.0.

The transport experiments were carried out on analogue **28** with various pH in the receiving phase. The pH of the aqueous source phase was buffered at pH = 9.5 as before and the results are given in Table XI.

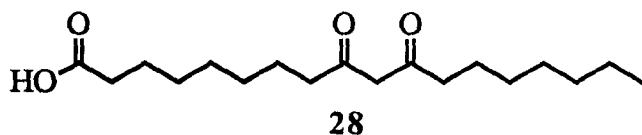
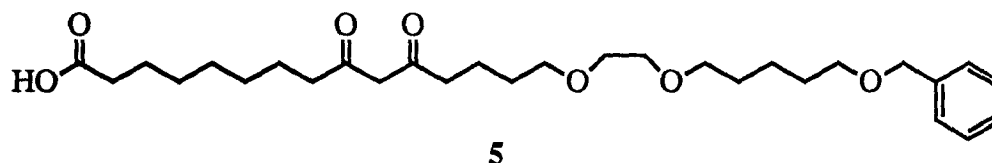


Table XI. Calcium Transport Rates (J) at Various pH in the Receiving Phase.

pH	8.0	7.0	6.0	5.0
J (10 <sup>-8</sup> mole cm <sup>-2</sup> h <sup>-1</sup> )	15 ± 2	16 ± 2	16 ± 2	15 ± 2

As seen from Table XI, the calcium transport rate is essentially independent of the pH of the receiving phase in the pH range of 5.0-8.0. Thus, the exchange of calcium ions for protons, i.e., the release of calcium ions from the ionophore-calcium complex (a Michaelis complex), can be treated as an irreversible process in this pH range, or at pH = 7.0 at least.

The transport experiments were carried out on analogue 5 with various pH's in the source phase. The concentration of the analogue in the chloroform layer was 300  $\mu\text{M}$  and the pH of the receiving phase was buffered at pH = 6.5. The results are summarized in Table XII (no detectable transport of calcium was found when the source phase was buffered at pH  $\leq$  7.0).



pH	7.5	8.0	8.5	9.0	9.5	10.0
$J (10^{-8} \text{ mole cm}^{-2} \text{ h}^{-1})$	$1.3 \pm 0.1$	$1.5 \pm 0.1$	$2.5 \pm 0.2$	$4.6 \pm 0.4$	$9.0 \pm 0.9$	$14 \pm 1$

The logarithm of calcium transport rate ( $\log J$ ) is linear with the pH in the source phase (Figure 22). Thus, transport of calcium by analogue **5** is directly dependent on the hydroxide concentration in the source phase. The dependence of calcium transport on the hydroxide concentration in the source phase suggests that the formation of the carboxylate and/or the enolate of the  $\beta$ -diketone of analogue **5** is required for the transport of calcium.



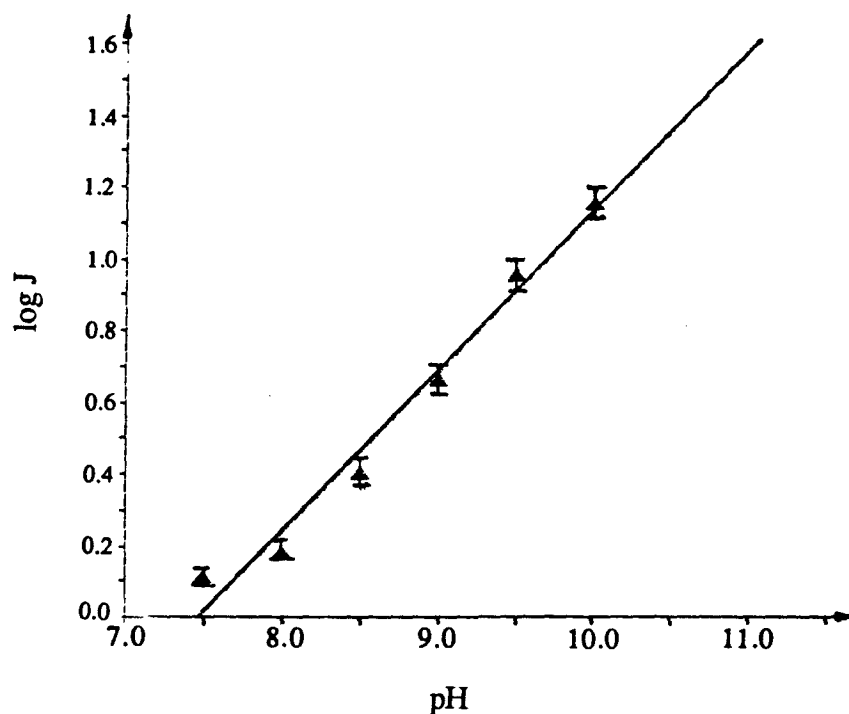


Figure 22. Plot of  $\log J$  as a function of pH in the source phase. The points represent the experimental values.

Non-linear regression analysis of the transport rate data versus pH using Equation 3 derived from the Henderson-Hasselbalch equation<sup>64</sup> gave a typical plot (Figure 23) for the ionization of a monoprotic acid with a  $pK_a$  of  $9.6 \pm 0.1$ .

$$J = \frac{J_{\min} + J_{\max} \times 10^{(pH - pK_a)}}{10^{(pH - pK_a)} + 1} \quad (3)$$

In their studies of competitive alkaline-earth cations extraction from aqueous solution into chloroform by polyether dicarboxylic acids, Kang et al. demonstrated that the carboxyl groups of the alkanic acids were deprotonated completely at the interface of the aqueous solution and chloroform at pH (pH in the aqueous phase) lower than 7.0 and that the resulting dicarboxylates extracted divalent cations as neutral complexes into the chloroform phase.<sup>65a</sup>

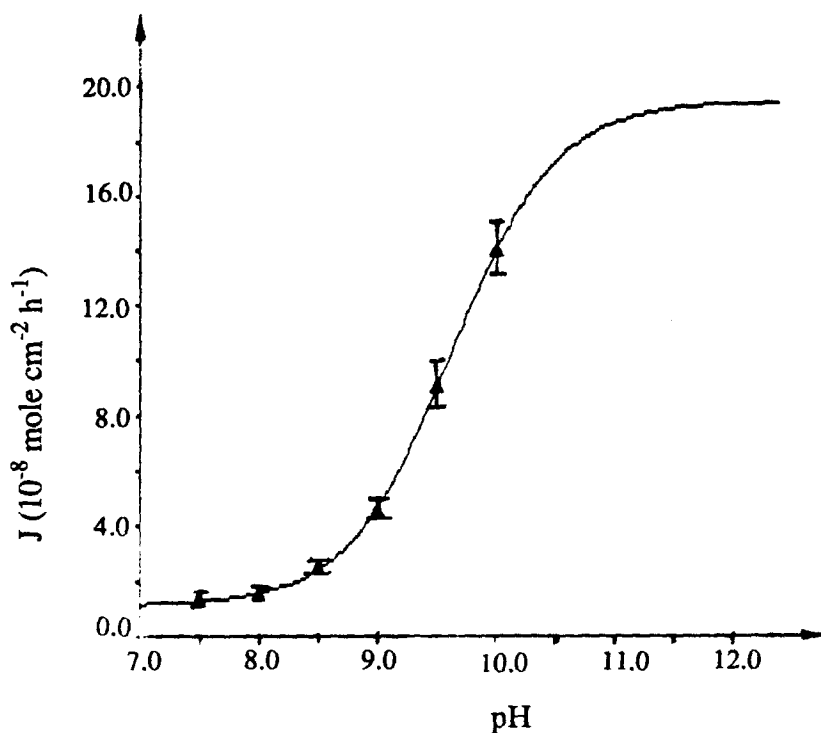


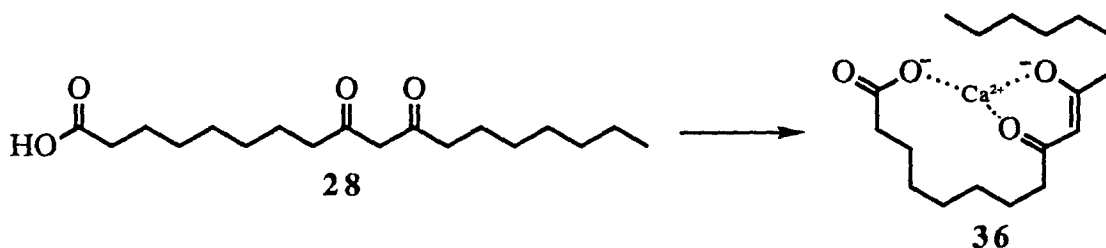
Figure 23. Plot of the dependence of transport rates on pH of the source phase. The points represent the experimental values and the solid line is determined by non-linear regression analysis according to Equation 3.

Based on the results reported by Kang et al., the  $pK_a$  of 9.6 was assigned to the  $pK_a$  of the  $\beta$ -diketone of analogue 5. Such a dependence of transport rate on pH of the source phase indicated that the ionization of the  $\beta$ -diketone at the interface of the aqueous source phase and chloroform was required for calcium transport. The transport rate (section 2.4) and the  $pK_a$  (see later) depend on the distance between the  $\beta$ -diketone group and the carboxyl group. We therefore associate this  $pK_a$  with the ionization of the  $\beta$ -diketone.

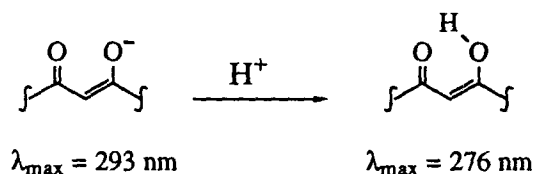
The formation of the carboxylate and the enolate of the  $\beta$ -diketone at the interface of the aqueous source phase and chloroform in the transport of calcium, the requirement of both the carboxyl and  $\beta$ -diketone groups within the same molecule for calcium transport (section 2.4) and the requirement of electrical neutrality of the calcium complex in chloroform<sup>65a</sup> indicates that the stoichiometry of the calcium complex involved in transport is 1:1.

## 2.10 Characterization of Calcium Complex of Analogue 28

Further evidence for the formation and involvement of the neutral 1:1 calcium complex in calcium transport could be obtained by determining the stoichiometry of the calcium complex in the solid state. To this end, the calcium salt of analogue 28 was isolated by reaction of the analogue with calcium hydroxide.



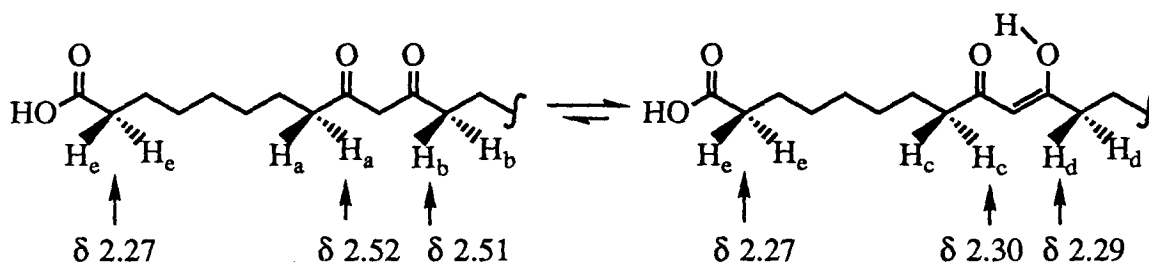
The UV spectrum of the calcium salt 36 in methanol showed an absorbance at 293 nm, indicating the presence of the enolate of the  $\beta$ -diketone. When hydrochloric acid was added to the solution of the calcium salt in methanol, the absorbance maximum was shifted from 293 nm to 276 nm, indicating the generation of the enol form of the  $\beta$ -diketone from the enolate. Ionization of the  $\beta$ -diketone group in the formation of calcium salt was thus confirmed.



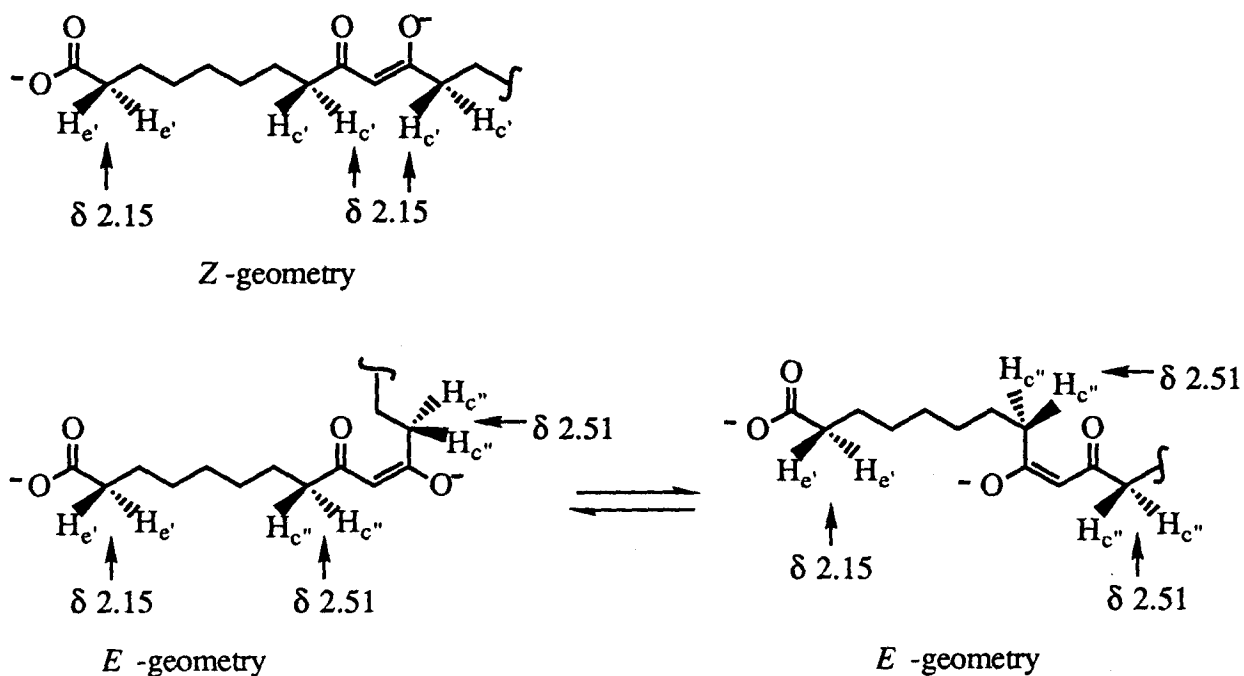
The solid state IR spectrum of analogue 28 showed absorptions at  $1719 \text{ cm}^{-1}$  due to the free acid, and at  $1688$  and  $1642 \text{ cm}^{-1}$  due to the ketone and the enol of the  $\beta$ -diketone respectively. In contrast, the solid state IR spectrum of the calcium salt 36 had absorptions at  $1577$  and  $1439 \text{ cm}^{-1}$  ascribable to the C=O asymmetric and symmetric stretches of the carboxylate respectively, which indicated that both the carboxylate oxygens were coordinated to the calcium ions.<sup>65b</sup> The absorption at  $1511 \text{ cm}^{-1}$  could be assigned to the enolate of the  $\beta$ -diketone. The calcium salt also

had weak absorptions at 3644 and 3527  $\text{cm}^{-1}$  assigned to the O-H stretching absorptions of water molecules perhaps bound to the calcium ions. Finally, it had a peak at 711  $\text{cm}^{-1}$  assigned to Ca-O stretching. Thus, the formation of the enolate of the  $\beta$ -diketone group and the coordination of calcium with both the carboxylate oxygens were established from the IR. The presence of water molecules in the complex was suggested from the IR.

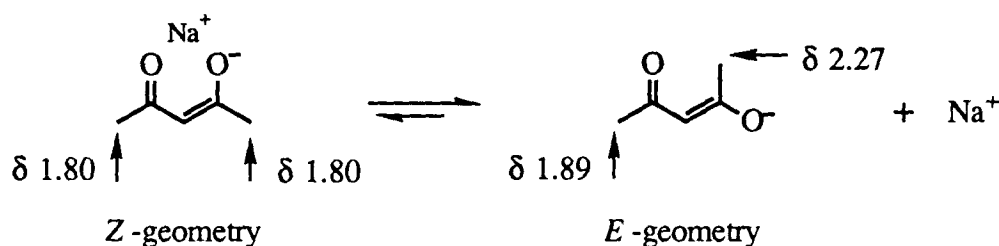
The  $^1\text{H}$  NMR spectrum of **28** in  $\text{MeOH-d}_4$  showed two sets of triplets at 2.52 and 2.51 p.p.m., which were assigned to two sets of methylene protons  $\text{H}_a$  and  $\text{H}_b$  of the keto form of the  $\beta$ -diketone. Three sets of partially overlapped triplets at 2.30, 2.29 and 2.27 p.p.m. were assigned to the methylene protons  $\text{H}_c$  and  $\text{H}_d$  of the enol form of the  $\beta$ -diketone and to the methylene protons  $\text{H}_e$  in both tautomers. The ratio of the enol tautomer to the keto tautomer was 7:3 as indicated by the relative intensity of  $\text{H}_c$  (or  $\text{H}_d$ ) to  $\text{H}_a$  (or  $\text{H}_b$ ).



The  $^1\text{H}$  NMR spectrum of the calcium salt **36** in  $\text{MeOH-d}_4$  showed a broad peak at 2.15 p.p.m. and a less intense broad peak at 2.51 p.p.m. The peak at 2.15 p.p.m. could be assigned to the methylene protons  $\text{H}_c'$  alpha to the enolate anion of the  $\beta$ -diketone in the *Z*-geometry (78% by integration) and the methylene protons  $\text{H}_e'$  alpha to the carboxylate of the complex. The upfield shifts of these methylene protons resulted from the formation of the enolate and carboxylate. The less intense peak at 2.51 p.p.m. was assigned to the methylene protons ( $\text{H}_c''$ ) alpha to the enolate anion of the "free" ligand in the *E*-geometry (22%). The protons ( $\text{H}_c''$ ) of the two methylene groups had an averaged chemical shift at 2.51 p.p.m. presumably due to the fast equilibrium between the two *E*-geometries as shown below.



The  $^1\text{H}$  NMR spectra of alkali metal acetylacetonates in  $\text{MeOH-d}_4$  at  $-57^\circ\text{C}$  were studied by Raban and coworkers.<sup>66a</sup> The methyl region of the  $^1\text{H}$  NMR spectrum of sodium acetylacetonate showed three singlets, two of which were of equal intensity. The singlet which appeared at higher field ( $\delta$  1.80) was assigned to the methyl protons of the complex in the Z-geometry (23%). The two equally intense singlets at lower field ( $\delta$  1.89, 2.27) were assigned to the methyl protons of the free ligand in the E-geometry (77%).<sup>66a</sup> Based on this analogy, we suggest that the species with the  $\delta$  2.51  $^1\text{H}$  NMR signal is the "free" ligand. However, calcium ions may be bound to the carboxylate (Figure 24) and/or the enolate of the  $\beta$ -diketone in the E-geometry.



Raban and coworkers demonstrated that this dissociation was strongly dependent on the nature of the cation and represented a measurement of the ability of the acetylacetonate anion to complex with a cation.<sup>66a</sup> For example, the binding constant of acetylacetonate anion with  $\text{Li}^+$  is  $6.0 \times 10^2 \text{ M}^{-1}$  and lithium acetylacetonate was found to exist only as lithium complex in solution.<sup>66a,b</sup> The binding constant of acetylacetonate with  $\text{Na}^+$  is  $4.0 \times 10 \text{ M}^{-1}$  and sodium acetylacetonate existed predominantly as the dissociated enolate anion (77%).<sup>66a,b</sup>

The presence of the "free" enolate anion in the solution NMR of the calcium complex **36** indicated the existence of a similar equilibrium in  $\text{MeOH-d}_4$  (Figure 24). Additional evidence for such an equilibrium was obtained from temperature-dependent  $^1\text{H}$  NMR studies. The percentage of the "free" enolate anion changed from 15% to 22% and 24% when the temperature was increased from  $-25^\circ\text{C}$  to  $25^\circ\text{C}$  and  $45^\circ\text{C}$  respectively. Because the percentage of the "free" enolate anion from the calcium complex **36** was lower than that of sodium acetylacetonate and higher than that of the lithium acetylacetonate, we predicted the binding constant of analogue **28** with calcium to be in the range of  $4.0 \times 10$  to  $6.0 \times 10^2 \text{ M}^{-1}$  in  $\text{MeOH}$ , which was significantly lower than the binding constant of ionomycin with calcium ( $1.9 \times 10^6 \text{ M}^{-1}$  in 80%  $\text{MeOH-H}_2\text{O}$ ).<sup>32</sup>

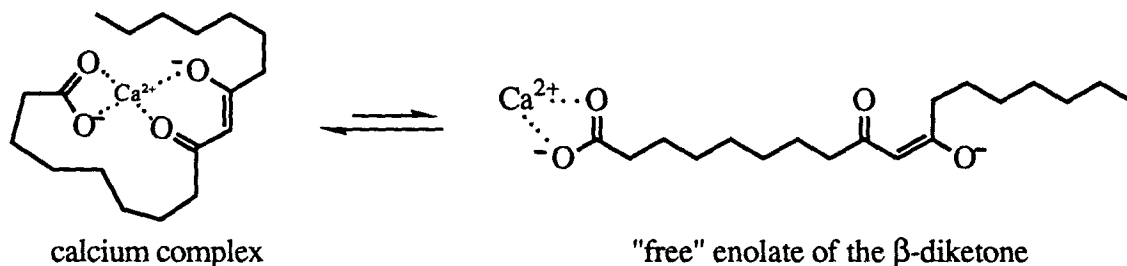
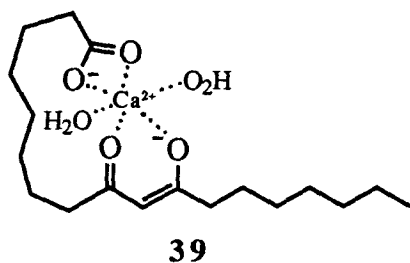


Figure 24. Equilibrium between the calcium complex and the free ions in  $\text{MeOH-d}_4$ .

The mass spectrum of the calcium salt was obtained using fast atom bombardment (FAB) ionization technique. The prominent ion peaks at  $m/z = 388$ , 351 and 313 were assigned to the ions  $[\text{CaL} \cdot 2\text{H}_2\text{O} + \text{H} + \text{H}]^+$ ,  $[\text{CaL} + \text{H}]^+$  and  $[\text{H}_2\text{L} + \text{H}]^+$  where  $\text{H}_2\text{L}$  represents analogue **28** and  $\text{CaL}$  represents the 1:1 calcium complex. The formation of 1:1 analogue-calcium complex was thus confirmed. The presence of two molecules of water in the complex was likely but not conclusive.

Assuming two molecules of water are indeed present in the 1:1 calcium complex and the calcium ion has its usual six coordinations, we suggest structure **39** for the calcium salt of analogue **28**. In this structure both oxygens of the carboxylate are involved in complexation.



Efforts to obtain a crystal of the calcium salt suitable for X-ray crystal structure analysis were unsuccessful. However, the preparation and characterization of the calcium salt of analogue **28** demonstrated that both the  $\beta$ -diketone and the carboxyl groups were ionized in the formation of the calcium salt and the stoichiometry of the complex was 1:1. It also showed that the binding constant of analogue **28** with calcium was 4-5 orders of magnitude lower than that of ionomycin with calcium.

### 2.11 Binding of Ionomycin Analogues with Calcium Ions

The second phase of this project was to investigate the binding of ionomycin analogues with calcium and other metal ions and determine if there was any correlation between calcium binding and transport. The determination of binding constants of the analogues with calcium, the stoichiometry and cation selectivity in binding might also provide insight into the structural features controlling the calcium specificity of ionomycin.

To systematically study the binding of the analogues with metal ions, we needed to develop a general experimental procedure. There are many methods to determine the binding constant between an ionophore and a metal cation.<sup>67</sup> The most widely used experimental approach is by spectrophotometric titration. In this method, a solution of the ionophore is titrated with the metal cation of interest while its absorbance is monitored as a function of the cation concentration. The essential requirement for the use of this method is that a significant spectral change occurs on the formation of the ionophore-cation complex.<sup>67</sup>

In many cases the stoichiometry of the ionophore complex and the binding constant may be determined by the mole ratio method.<sup>68</sup> In this method the total ionophore concentration ( $L_t$ ) is held constant and the cation concentration ( $M_t$ ) is varied. A plot of the maximal absorbance difference at a chosen wavelength versus the ratio of ionophore and cation is examined for discontinuities or abrupt changes of slope corresponding to the stoichiometric ratio. Suppose the binding constant  $\beta = \infty$  in such a system and for each  $m$  moles of the ionophore ( $L$ ) in the solution, addition of  $n$  moles of the cation ( $M$ ) resulted in the formation of exactly one mole of  $L_mM_n$ . The concentration of complex and thus the maximal absorbance difference will increase until  $L_t/M_t = m/n$ ; beyond this value no more complex can form because no more ionophore is available. Thus a break in the plot will be seen at this point (Figure 25, line A).<sup>68b</sup> As the binding constant decreases the extent of the complex dissociation increases, so the break becomes a gently rounded curve (Figure 25, lines B and C).<sup>68b</sup> The discontinuity is then located by



extrapolation of the linear segments over considerable ranges. Obviously, the lower the binding constant is, the less accurate the determination of the stoichiometry will be.

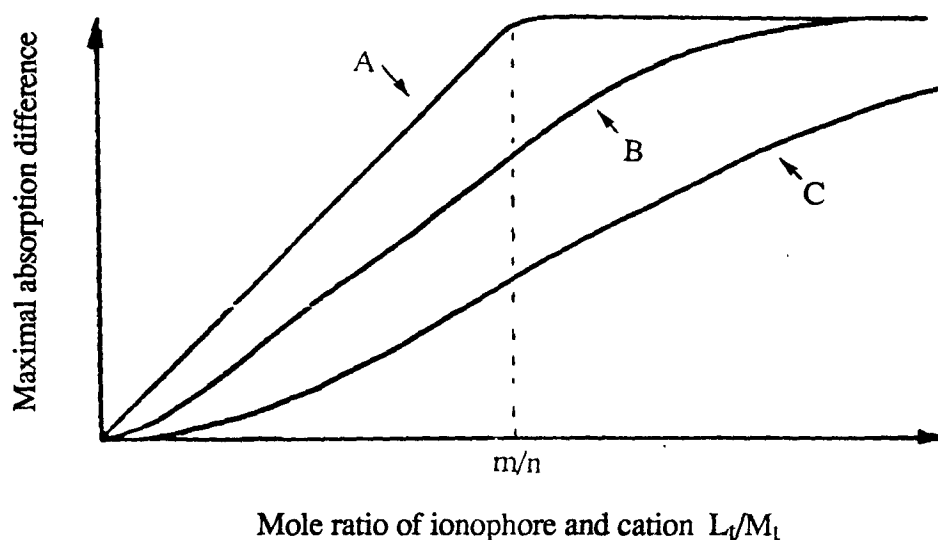


Figure 25. Representative mole ratio plots of complexes of various stabilities. Line A is typical of a relatively completely formed complex. Lines B and C are typical of successively weaker complexes.<sup>68</sup>

The other common method used in the determination of the stoichiometry in binding is the continuous variation method, often called Job's method.<sup>69</sup> In this method, a series of ionophore and cation solutions having identical total molar concentrations but different mole fractions of the two components are prepared. If a single, strong complex is formed, a plot of the maximal absorbance difference versus mole fraction of the solution gives a characteristic triangular plot (Figure 26, line A).<sup>67</sup> The mole fraction of the maximum of this plot, the apex of the triangle, indicates the stoichiometry of the complex. However, if a weak complex is formed, a curved plot results (Figure 26, line B and C).<sup>67</sup> The stoichiometry of the complex can be obtained from the point of intersection of the tangents to the curves. Again, the lower the binding constant, the less accurate the determination of the stoichiometry will be.

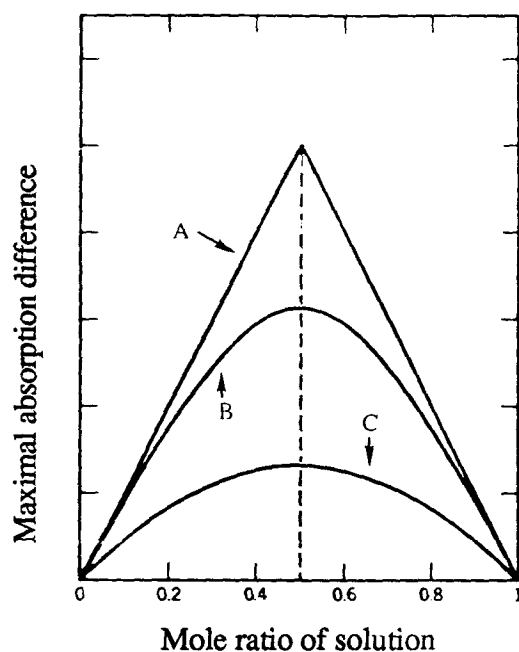


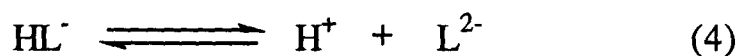
Figure 26. Continuous variation curves plotted for hypothetical systems with a stoichiometry of 1:1 and binding constant (from line A to line C)  $\beta = \infty, 10^3, 10^2$ .

Since the extent of curvature in both the mole ratio and the continuous variation methods depends on the binding constant, it is possible to extract an estimate of the binding constant from the same data used to obtain the stoichiometric ratio. Many authors have described ways to do this.<sup>67,69</sup> For example, the extinction coefficients of the ionophore and the complex can be determined (the former from the absorbance in the absence of the metal cation and the latter from the absorbance at complete complexation). These extinction coefficients are then used, in conjunction with the known absorbance of the mixture, to calculate the concentration of the complex at each titration point, from which the concentration of the free ligand and free cation is calculated. The stoichiometry determined from either the mole ratio or the continuous variation method is used to define the equation of the binding constant. The values of the concentrations of the complex, free ligand and cation are used in this equation to calculate the binding constant at each titration point. The consistency of the calculated binding constants would indicate the accuracy of the stoichiometry and the binding constant itself.<sup>70</sup>

A more accurate method to deduce the binding constant is to fit the titration data, after certain manipulation, into the Scatchard equation by non-linear regression computer software programs.<sup>63,71</sup> Both the binding constant and the stoichiometry can be obtained from such an analysis. Again, the accuracy of the calculation depends on the magnitude of the binding constant because the technique was developed to study complexes with high binding constants, such as those between enzymes and substrates.<sup>67</sup>

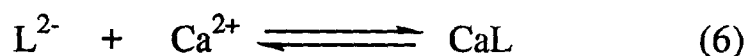
In principle, the UV spectrophotometric titration method is applicable to the binding of our analogues because the UV absorption of the enol form of the  $\beta$ -diketone group is shifted to longer wavelength upon complexation with cations. However, the mole ratio and the continuous variation methods may not be suitable for the determination of the binding constants of the analogues with calcium which, based on the transport results and the  $^1\text{H}$  NMR data of the calcium salt, may be small. If the transport selectivity is due to the selectivity in binding, we would expect the binding constant of the analogues with sodium and potassium to be even smaller than with calcium. Examination of cation selectivity using the mole ratio or the continuous variation methods would then be impossible.

Clearly, a method for the determination of small binding constants is needed in our studies. The measurement of the binding constant of the enolate of a  $\beta$ -diketone with a cation can be carried out by measuring the difference of  $\text{pK}_a$  of the  $\beta$ -diketone group in the absence and the presence of a large excess of metal ions. Let  $\text{HL}^-$  represent a  $\beta$ -diketo  $\omega$ -carboxylate, the dissociation of the enol form of a  $\beta$ -diketone group to the enolate of the  $\beta$ -diketone ( $\text{L}^{2-}$ ) and proton ( $\text{H}^+$ ) is given by Equation 4. The acid dissociation constant  $K_a$  is given by Equation 5.



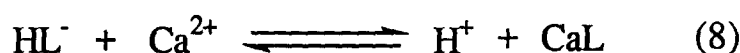
$$K_a = \frac{[\text{H}^+][\text{L}^{2-}]}{[\text{HL}^-]} \quad (5)$$

The binding of the enolate  $\text{L}^{2-}$  with a divalent cation such as calcium ion is given by Equation 6 and the binding constant  $\beta$  by Equation 7, assuming a 1:1 stoichiometry in binding.



$$\beta = \frac{[\text{CaL}]}{[\text{Ca}^{2+}][\text{L}^{2-}]} \quad (7)$$

In the presence of a large excess of calcium ions, the dissociation of the  $\beta$ -diketo  $\omega$ -carboxylate is given by Equation 8. The acid dissociation constant  $K_{a'}$  can thus be defined by Equation 9 which is also applicable to the determination of the binding constant of the enolate  $\text{L}^{2-}$  with monovalent cations such as potassium and sodium ions under the assumption that the stoichiometry of the potassium (or sodium) complex is 1:2.



$$K_{a'} = \frac{[\text{H}^+][\text{CaL}]}{[\text{HL}^-][\text{Ca}^{2+}]} = \frac{[\text{CaL}]}{[\text{Ca}^{2+}][\text{L}^{2-}]} \frac{[\text{H}^+][\text{L}^{2-}]}{[\text{HL}^-]} = \beta K_a$$

$$\log \beta = \text{p}K_a - \text{p}K_{a'} \quad (9)$$

## 2.12 Determination of $pK_a$ of $\beta$ -Diketones by Ultraviolet Spectrophotometric Titration

Measurement of the  $pK_a$  of the  $\beta$ -diketone group of the analogues by UV spectrophotometric titration is based on the different maximal absorptions of the enol form of the  $\beta$ -diketone and its conjugated base, the enolate of the  $\beta$ -diketone. Figure 27 shows changes in the UV absorption spectra of analogue 33 in 80% MeOH-H<sub>2</sub>O as the pH of the solution is raised from 5.80 to 13.0 by addition of tetramethylammonium hydroxide (Me<sub>4</sub>NOH). As the pH is increased the concentration of the enolate rises. The absorption peak shifts to longer wavelength and increases in magnitude. A clean isosbestic point is observed at 278 nm. The same general behavior was observed for all the analogues studied.

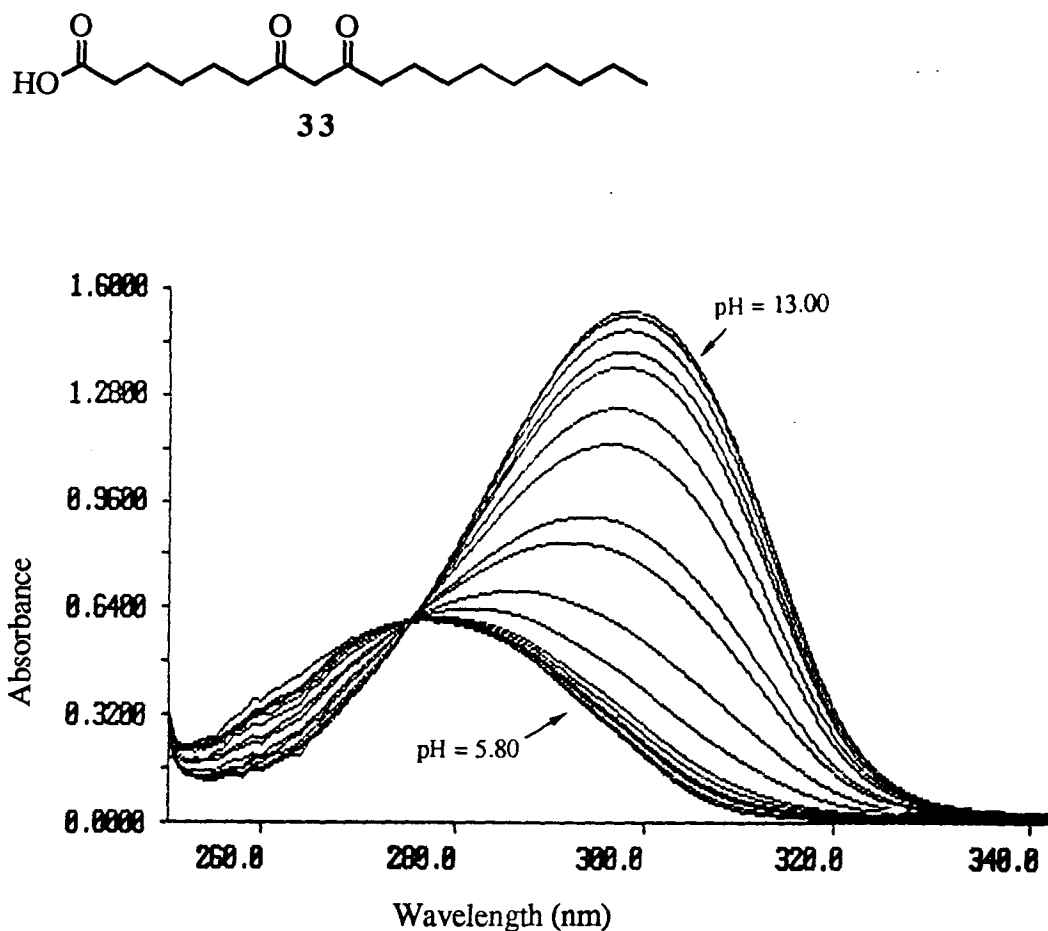


Figure 27. UV spectrophotometric absorption spectra of analogue 33 as the pH of the solution increased from 5.80 to 13.00.

The absorbance at 298 nm (ascribable to the enolate of the  $\beta$ -diketone) versus pH was fitted to a modified Henderson-Hasselbalch equation (3) by non-linear regression to calculate the  $pK_a$  value.<sup>63</sup> A  $pK_a$  of  $11.16 \pm 0.02$  was obtained. The curve calculated by such non-linear regression method is shown in Figure 28.

$$A = \frac{A_{\min} + A_{\max} \times 10^{(\text{pH} - pK_a)}}{10^{(\text{pH} - pK_a)} + 1} \quad (3)$$

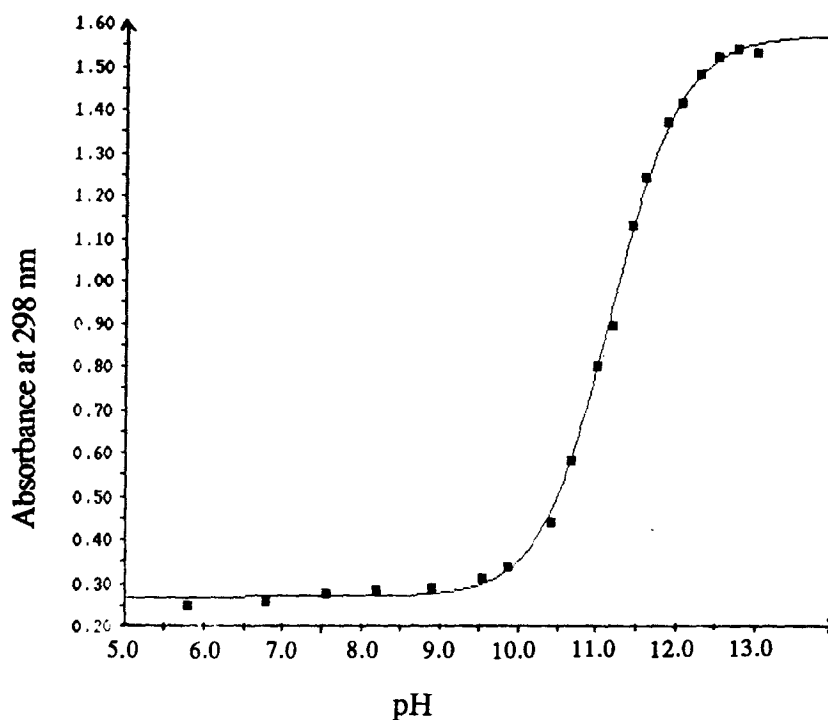
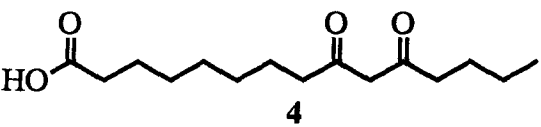
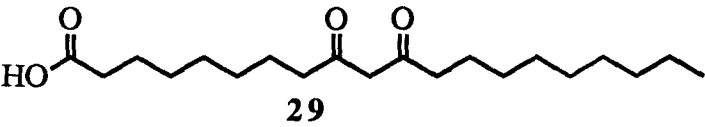
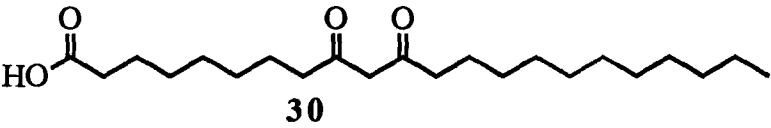
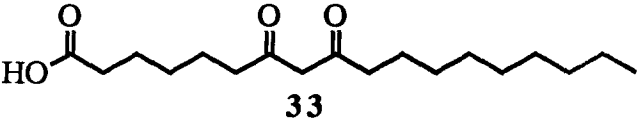
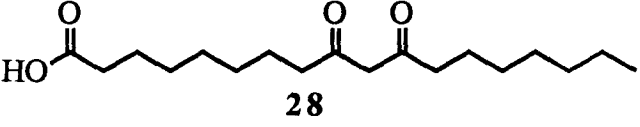
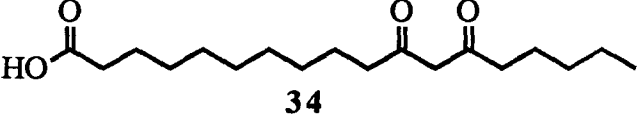
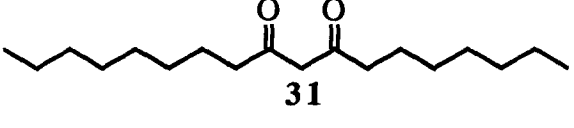
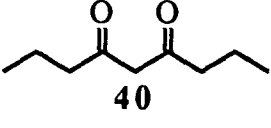


Figure 28. Plot of absorbance at 298 nm versus pH for analogue 33. The points represent the experimental values and the solid line is determined by non-linear regression using Equation 3.

Using this technique, we determined the  $pK_a$  of the  $\beta$ -diketone group of a number of analogues (Table XIII). The  $pK_a$  values of the  $\beta$ -diketone group of ionomycin and of 4,6-nonanedione (40) were taken from the literature.<sup>32</sup>

Table XIII.  $pK_a$  of the  $\beta$ -Diketone Group of Ionomycin and of Analogues.

Analogue	$pK_a (\pm 0.02)$
Ionomycin	11.94
 4	10.92
 29	11.04
 30	11.07
 33	11.16
 28	11.03
 34	10.90
 31	10.86
 40	10.78

As seen from Table XIII, analogues with higher lipid solubility have higher  $pK_a$  values. Since binding of metal ions generally follows the same order as the binding of protons, a higher  $pK_a$  would imply a stronger cation binding by the ligand. The solvent used in the  $pK_a$  determination (80% MeOH-H<sub>2</sub>O) has been shown to mimic the interface of water and phospholipid.<sup>32</sup> The increasing lipid solubility of the analogue by the addition of methylene units on the hydrocarbon side chain not only enhances the partition of cation complex into the chloroform phase but also result in stronger cation binding.

Moving the  $\beta$ -diketone group closer to the carboxylate results in an increase of its  $pK_a$  value. This is likely due to the formation of a less stable enolate anion with the increasing charge repulsion between the enolate anion and the carboxylate as the  $\beta$ -diketone group is moved closer to the carboxylate.

The  $pK_a$  value of the  $\beta$ -diketone group of ionomycin is significantly higher than that of the  $\beta$ -diketone group of the analogues. We suspect that the higher  $pK_a$  of ionomycin is due to the lower stability of its dianion in polar solvent such as 80% MeOH-H<sub>2</sub>O. Ionomycin has several alkyl groups which could destabilize its anion in a polar solvent. A similar hydrophobic effect can be seen by comparing analogues 4, 29 and 30. Based on these  $pK_a$  differences, the binding of calcium and other metal ions by synthetic analogues of ionomycin is expected to be weaker than that of ionomycin.

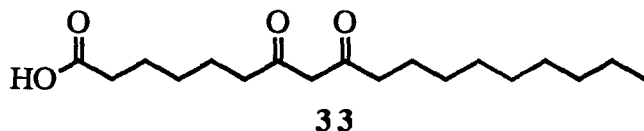


### 2.13 Binding of Calcium and Other Metal Ions by Ionomycin Analogues

The binding of calcium and other metal ions by ionomycin analogues was determined by measuring the  $pK_a'$  values of the  $\beta$ -diketone in the presence of a large excess of calcium or other metal ion and applying Equation 9.

$$\log \beta = pK_a - pK_a' \quad (9)$$

For example, the UV spectrophotometric titration of analogue **33** was carried out in the presence of a large excess of calcium chloride (molar ratio of calcium to analogue > 200). Determination of  $pK_a'$  of analogue **33** was performed in the same way as in the determination of  $pK_a$ . A  $pK_a'$  value of  $8.69 \pm 0.02$  was obtained from which the binding constant of analogue **33** with calcium was calculated to be  $\beta (Ca^{2+}) = (3.0 \pm 0.2) \times 10^2 M^{-1}$ .



In a same manner, the binding constants of analogue **33** with magnesium, potassium and sodium were determined as were the binding constants of other analogues with calcium, magnesium, potassium and sodium. The results are given in Table XIV and Table XV. The binding constants of ionomycin with calcium and magnesium ions were taken from the literature.<sup>32</sup>

Table XIV. Binding Constants of Ionomycin<sup>32</sup> and Analogues with Calcium and Magnesium.

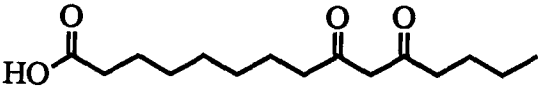
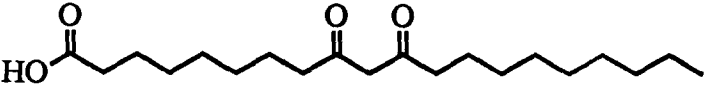
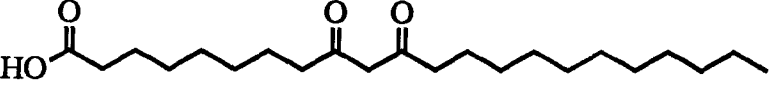
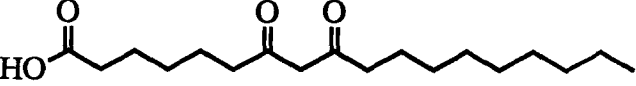
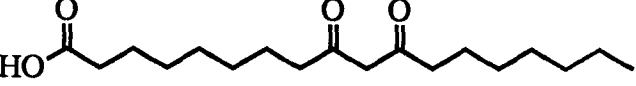
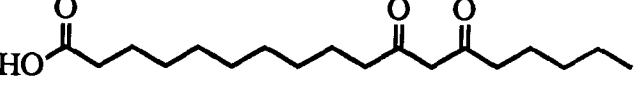
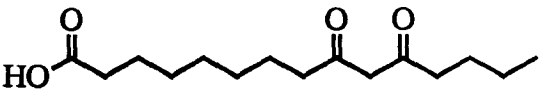
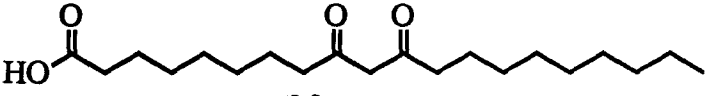
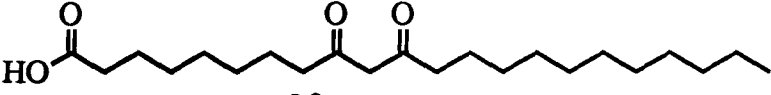
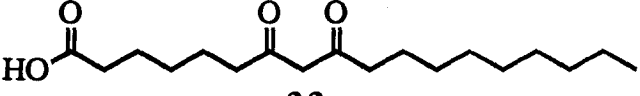
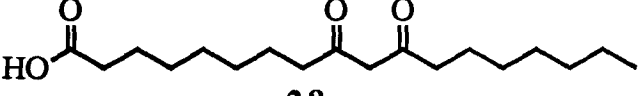
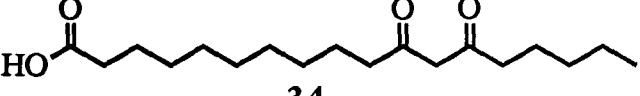
Analogue	$\beta$ (Ca <sup>2+</sup> ) x 10 <sup>2</sup> M <sup>-1</sup>	$\beta$ (Mg <sup>2+</sup> ) x 10 <sup>3</sup> M <sup>-1</sup>
Ionomycin	1.9 x 10 <sup>4</sup>	8.9 x 10 <sup>3</sup>
 <b>4</b>	1.7 ± 0.1	4.4 ± 0.2
 <b>29</b>	2.2 ± 0.2	5.6 ± 0.2
 <b>30</b>	2.0 ± 0.1	5.7 ± 0.3
 <b>33</b>	3.0 ± 0.2	7.6 ± 0.4
 <b>28</b>	1.8 ± 0.1	3.4 ± 0.2
 <b>34</b>	1.2 ± 0.1	1.9 ± 0.1

Table XV. Binding Constants of Analogues with Potassium and Sodium.

Analogue	$\beta$ (K <sup>+</sup> ) M <sup>-2</sup>	$\beta$ (Na <sup>+</sup> ) M <sup>-2</sup>
 <b>4</b>	$0.8 \pm 0.1$	$1.0 \pm 0.1$
 <b>29</b>	$0.8 \pm 0.1$	$1.2 \pm 0.1$
 <b>30</b>	$0.8 \pm 0.1$	$1.1 \pm 0.1$
 <b>33</b>	$1.3 \pm 0.1$	$1.8 \pm 0.1$
 <b>28</b>	$0.9 \pm 0.1$	$1.2 \pm 0.1$
 <b>34</b>	$0.9 \pm 0.1$	$0.8 \pm 0.1$

As seen from Tables XIV and XV, binding of the metal ions follows the same trend, which is  $\text{Mg}^{2+} > \text{Ca}^{2+} \gg \text{Na}^+ > \text{K}^+$ , for all the analogues studied. The ionomycin analogues were selective for divalent cations over monovalent cation in binding and were selective for magnesium over calcium. Thus the cation transport selectivity results from the cation binding selectivity.

The binding constants of analogues with different cations correlates with the  $\text{pK}_a$  values of the  $\beta$ -diketone group. This is especially evident for analogues with same lipid solubility but with

the  $\beta$ -diketone group at different positions. Moving the  $\beta$ -diketone group closer to the carboxyl group increases the  $pK_a$  of the  $\beta$ -diketone group and its binding with cations in the order, **33** > **28** > **34**.

The binding constant of analogue **28** with calcium  $\beta$  ( $Ca^{2+}$ ) =  $(1.8 \pm 0.1) \times 10^2 M^{-1}$  is consistent with the binding constant determined from the  $^1H$  NMR data of the calcium complex of analogue **28**  $\beta = 0.4 - 6.0 \times 10^2 M^{-1}$  (Section 2.10). Ionomycin binds to calcium and magnesium 3-4 orders of magnitude stronger than do the analogues. This is likely due to the fact that ionomycin has a limited number of conformations available compared to the analogues and consequently the loss of entropy in binding of ionomycin is significantly less than the loss of entropy in binding of the analogues.

In contrast to the mole ratio or the continuous variation method, the  $pK_a$  and  $pK_a'$  method permits the determination of small binding constants such as those of the analogues with potassium and sodium. However, this method assumes a certain stoichiometry in binding and can not be used to determine the stoichiometry of the complex. Because the binding constants of the analogues with magnesium ions are significantly higher, it may be possible to determine the stoichiometry of magnesium binding using the mole ratio method. The results from the mole ratio method would test the accuracy of the  $pK_a$  and  $pK_a'$  method. To this end, a solution of analogue **33** in 80% MeOH-H<sub>2</sub>O was buffered at pH = 9.10 and titrated with a solution of magnesium chloride. The pH of the solution was chosen so as not to induce significant ionization of the  $\beta$ -diketone group of the analogue but to force complete ionization of the  $\beta$ -diketone group when sufficient magnesium ions were added, which was clearly demonstrated in the measurements of  $pK_a$  and  $pK_a'(Mg^{2+})$  for the analogue.

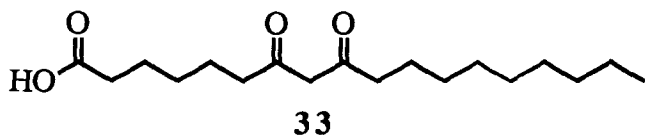


Figure 29 shows changes in the UV absorption spectra of analogue 33 as the concentration of magnesium chloride was increased from 0.00 to  $1.34 \times 10^{-3}$  M. As the concentration of magnesium chloride increased the concentration of the enolate rose. The absorption peak shifted to a longer wavelength and increased slightly in magnitude.

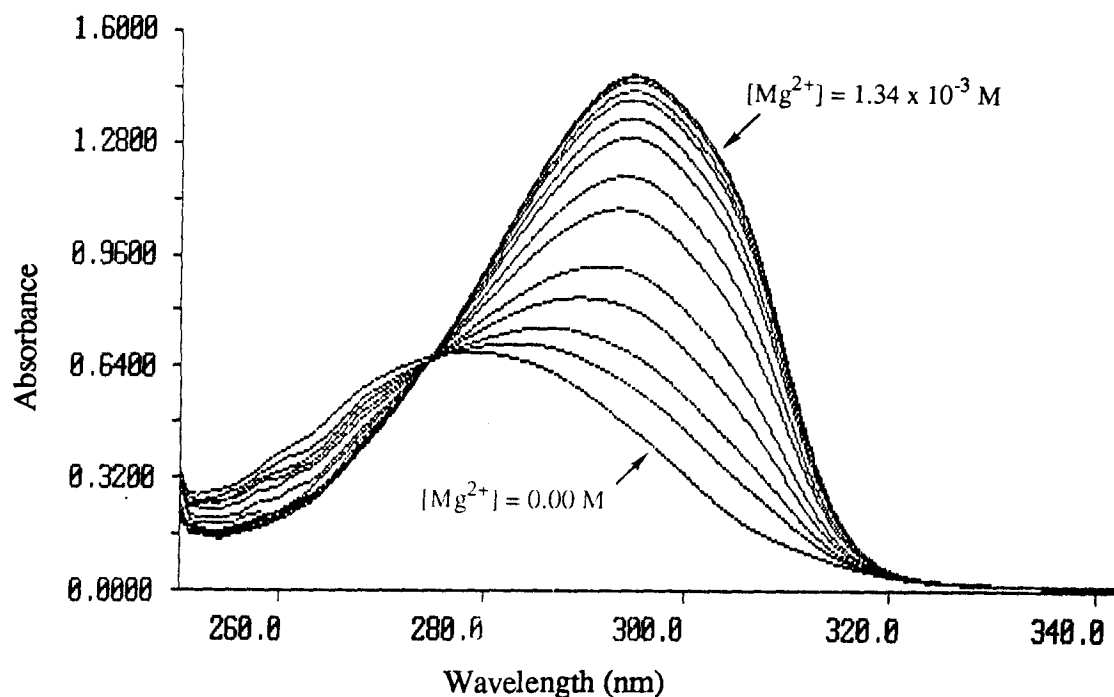


Figure 29. UV spectrophotometric absorption spectra of analogue 33 as the concentration of  $\text{MgCl}_2$  increased from 0.00 to  $1.34 \times 10^{-3}$  M at pH = 9.10.

From the absorbance at 298 nm in the absence of magnesium ion ( $A_0$ ), the absorbance at complete complexation ( $A_{\text{max}}$ ) and the absorbance at each titration point ( $A$ ), the concentration of the magnesium complex at equilibrium  $[\text{Mg}_x\text{L}_y]$  was calculated using Equation 10. From the total concentrations of the analogue  $[\text{L}]_t$  and magnesium  $[\text{Mg}]_t$  and the concentration of magnesium complex at each titration point, the concentrations of free analogue  $[\text{L}]$  and free magnesium  $[\text{Mg}]$  were calculated respectively based on mass balances. Assuming the stoichiometry in binding was  $n = x/y = 1/1$ , the binding constant  $\beta_{1:1} (\text{Mg}^{2+})$  could be calculated using Equation 11. Table XVI shows the results of these calculations.

$$[\text{Mg}_x\text{L}_y] = \frac{(A - A_0) [\text{L}]_t}{A_{\text{max}} - A_0} \quad (10)$$

$$\beta_{1:1}(\text{Mg}^{2+}) = \frac{[\text{MgL}]}{[\text{Mg}^{2+}] [\text{L}^{2-}]} \quad (11)$$

Table XVI. Total Concentrations of Analogue **33** and Magnesium, Absorbance, Concentrations of the Complex, Analogue and Magnesium at Each Titration Point and Binding Constants Based on 1:1 Stoichiometry.

$[\text{L}]_t$ $\times 10^{-4} \text{ M}$	$[\text{Mg}^{2+}]_t$ $\times 10^{-4} \text{ M}$	$A_{298}$	$[\text{Mg}_x\text{L}_y]$ $\times 10^{-4} \text{ M}$	$[\text{Mg}^{2+}]$ $\times 10^{-4} \text{ M}$	$[\text{L}]$ $\times 10^{-4} \text{ M}$	$\beta_{1:1}$ $\times 10^3$
0.80	0.00	0.384	-----	-----	0.08	-----
0.79	0.50	0.608	0.17	0.33	0.62	8.3
0.79	0.98	0.741	0.27	0.71	0.52	7.3
0.78	1.47	0.853	0.35	1.12	0.43	7.2
0.78	2.68	1.032	0.48	2.20	0.30	7.2
0.78	3.88	1.132	0.56	3.32	0.22	7.7
0.77	6.28	1.246	0.63	5.65	0.14	8.0
0.77	8.65	1.302	0.68	7.97	0.09	9.4

The calculated binding constants were consistent, which proved that the stoichiometry of the complex was 1:1. The average value of the binding constant of analogue **33** with magnesium

was  $\beta (\text{Mg}^{2+}) = (7.9 \pm 0.5) \times 10^3 \text{ M}^{-1}$  which was essentially the same as the value of  $\beta (\text{Mg}^{2+}) = (7.6 \pm 0.4) \times 10^3 \text{ M}^{-1}$  obtained using the  $\text{pK}_a$  and  $\text{pK}_a'$  method.

Alternatively, and more accurately, data of the number of moles of substrate (magnesium) bound per mole of ligand (analogue)  $v = [\text{Mg}_x\text{L}_y]/[\text{L}]_t$  versus the concentration of substrate (magnesium)  $[\text{S}] = [\text{Mg}^{2+}]$  were fitted to the Scatchard equation (11) by non-linear regression.<sup>63,71</sup> The curve so obtained is shown in Figure 30. The binding constant of the analogue with magnesium  $\beta (\text{Mg}^{2+}) = 1/K_d$  was calculated to be  $\beta = (7.1 \pm 0.1) \times 10^3 \text{ M}^{-1}$  and the stoichiometry of binding was  $n = x/y = 1.0$  by this non-linear regression method.<sup>63</sup>

$$v = n - K_d v/[\text{S}] \quad (11)$$

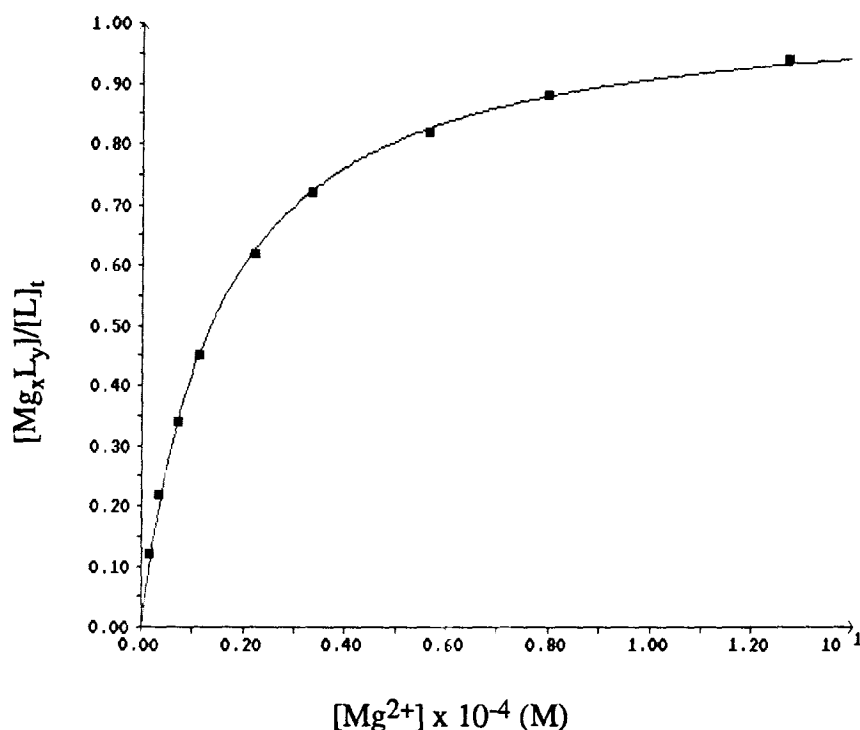
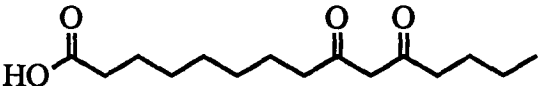
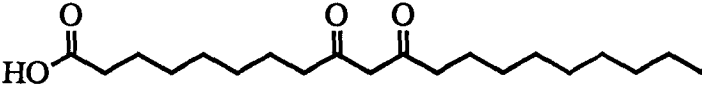
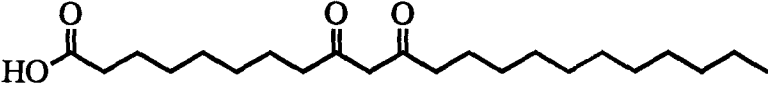
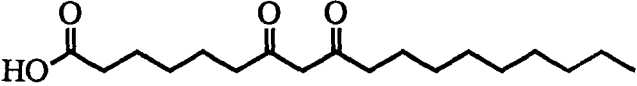
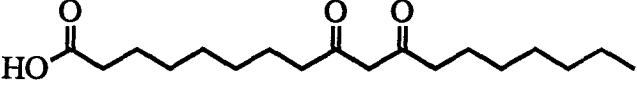
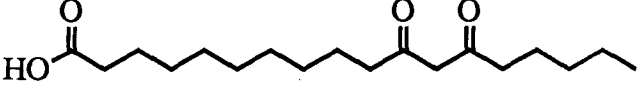


Figure 30. Plot of the number of moles of magnesium bound per mole of analogue **33** versus concentration of magnesium. The points represent the experimental values and the solid line is determined by non-linear regression using Equation 11.

Using the mole ratio method and the non-linear regression data treatments, we determined the binding constants of the other analogues with magnesium and the stoichiometry of binding. The stoichiometry in binding for all the analogues studied was 1:1. The binding constants obtained from the  $pK_a$  and  $pK_a'$  method and the mole ratio method are given in Table XVII.

Table XVII. Binding Constants of Analogues with Magnesium Using the  $pK_a$  and  $pK_a'$  Method (Method I) and the Mole Ratio Method (Method II).

Analogue	$\beta$ ( $Mg^{2+}$ ) $\times 10^3 M^{-1}$ (method I)	$\beta$ ( $Mg^{2+}$ ) $\times 10^3 M^{-1}$ (method II)
 4	$4.4 \pm 0.2$	$5.5 \pm 0.1$
 29	$5.6 \pm 0.2$	$6.2 \pm 0.1$
 30	$5.7 \pm 0.3$	$6.2 \pm 0.1$
 33	$7.6 \pm 0.4$	$7.1 \pm 0.1$
 28	$3.4 \pm 0.2$	$5.6 \pm 0.1$
 34	$1.9 \pm 0.1$	$4.5 \pm 0.1$



The binding constants of the analogues with magnesium determined by these two methods are consistent. Therefore, the assumption of the stoichiometry of the calcium (or magnesium) complex and the sodium (or potassium) complex in the  $pK_a$  and  $pK_a'$  method is correct. The binding constants of the analogues with calcium ions determined by the  $pK_a$  and  $pK_a'$  could be compared with the binding constants of ionomycin and other calcium ionophores with calcium determined by the mole ratio method.

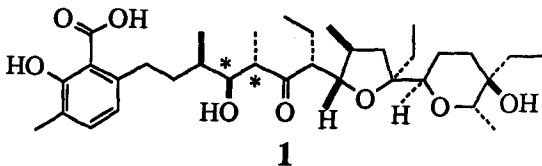
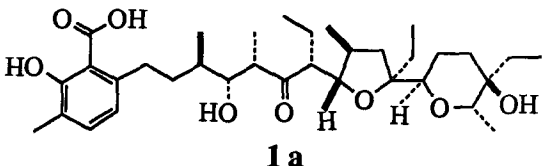
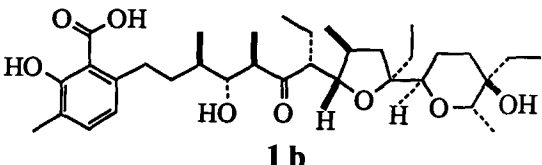
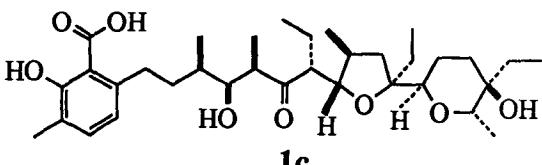
All the experimental results, i.e., the stoichiometry of magnesium binding, the 1:1 stoichiometry in the isolated calcium salt, the requirement of the presence of the carboxyl and  $\beta$ -diketone groups within the same molecule and the formation of both the carboxylate and enolate of the  $\beta$ -diketone in transport, suggested that the calcium complex had a 1:1 stoichiometry in binding and transport.

Because the binding of calcium by synthetic analogues of ionomycin is weaker than that by ionomycin, the synthetic analogues could possibly be further modified to achieve a stronger binding. This might be achieved by introducing some rigid structural elements into the molecules to reduce the entropy losses on binding.

## 2.14 Incorporation of Rigid Elements into Ionomycin Analogues

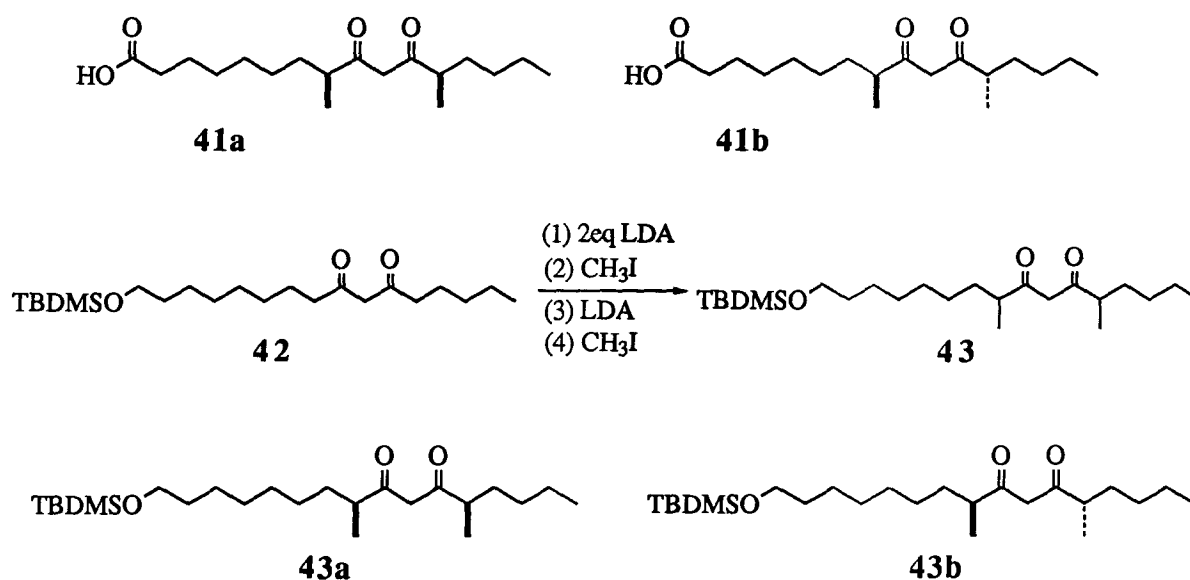
The polyether antibiotic calcium ionophores are unique in that they are stereochemically complex acyclic chains of ligands. It has been proposed by Still and co-workers that particular arrays of chiral centers in these molecules could destabilize undesired rotomers of these acyclic chains and reduce the available conformations to those suitable for polydentate ion binding.<sup>23</sup> In their elegant work towards the rational design of synthetic host molecules, Still and co-workers showed that two chiral centers (shown by an asterisk) in lasalocid A (**1**) were partially responsible for the high affinity of lasalocid A for barium ions.<sup>23a</sup> The natural stereoisomer **1** binds barium 2-3 orders of magnitude more tightly than the three epimers **1a**, **1b** and **1c** (Table XVIII).

Table XVIII. Binding Constants of Various Stereoisomers of Lasalocid A with Barium Ions.<sup>23a</sup>

Stereoisomer	$\beta$ (Ba <sup>2+</sup> )
 <p style="text-align: center;"><b>1</b></p>	$2.1 \times 10^6$
 <p style="text-align: center;"><b>1 a</b></p>	$3.9 \times 10^4$
 <p style="text-align: center;"><b>1 b</b></p>	$8.8 \times 10^3$
 <p style="text-align: center;"><b>1 c</b></p>	$7.8 \times 10^3$

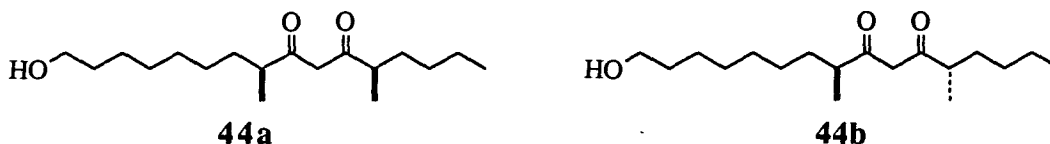
Although the substitutional and stereochemical arrays present in ionomycin might function in the same way as those in lasalocid A to reduce the available conformations to those suitable for calcium binding, there is no experimental data at this point as yet. The low binding constants of the analogues with calcium are suggestive, but not conclusive, that the stereochemical arrays in ionomycin are, at least, partially responsible for its high affinity for calcium.

To test the possibility of improving the ionophoric properties of the analogues by restricting the available conformations for calcium complexation through the introduction of chiral centers to the molecules, we set out to prepare analogues **41a** and **41b**. We envisaged the preparation of these two compounds through dimethylation of an appropriate  $\beta$ -diketo compound and separation of the diastereomeric mixture. To this end, compound **42** was treated with two equivalents of LDA and subsequently one equivalent of methyl iodide. Upon completion of the first methylation as shown by thin layer chromatography (TLC), one more equivalent of LDA and then an additional equivalent of methyl iodide was added to the reaction mixture. The dimethylated product **43**, which was thought to be a mixture of diastereomers **43a** and **43b** and their enantiomers, showed a single spot on TLC.



Interestingly, subjection of product **43** to gas liquid chromatography (GC) revealed the presence of two components in a ratio of 94:6. These two components had identical gas-liquid chromatography mass spectra (GCMS) in which there were two major peaks at  $m/z = 413$  and 355 corresponding to the molecular ion of  $[M + H]^+$  and the fragment of  $[M - CH_3]^+$ . These two components were found to be **43a** and **43b** by  $^1H$  NMR spectrometry. Thus, the dimethylation of compound **42** proceeded with high diastereoselectivity. The higher percentage of the enol form of the  $\beta$ -diketone and the downfield chemical shifts of the methine protons alpha to the enol and keto form of the  $\beta$ -diketone of the major isomer in the  $^1H$  NMR spectrum of the mixture suggested that the major isomer was **43b** with the two methyl groups "*trans*" to each other.

Unfortunately, efforts to separate **43a** and **43b** using column chromatography or high performance liquid chromatography (HPLC) were unsuccessful. Attempts to separate the alcohols **44a** and **44b**, or the acids **41a** and **41b** also failed.



The ratio of two diastereomeric alcohols and the acids prepared from the mixture of **43a** and **43b** were consistent with the ratio of 96:4 for **43a** and **43b**. The transport experiment on the mixture of **41a** and **41b** gave a transport rate comparable to its structural isomer, analogue **28**. Unfortunately no conclusion of the effect of substitution and stereochemistry of analogues **41a** and **41b** on calcium transport could be drawn at this stage because the configuration of the chiral centers of the major isomer **41b** are opposite to those found in ionomycin.

## 2.15 Conclusions and Future Consideration

The syntheses of simple analogues of ionomycin, namely a series of  $\beta$ -diketo  $\omega$ -carboxylic acids, were achieved by consecutive alkylation of the dianion of 2,4-pentanedione with appropriate bromides and subsequent oxidation of the  $\beta$ -diketo  $\omega$ -alcohols. This synthetic route permitted us to vary the number of methylene units between the  $\beta$ -diketone and the carboxyl groups and hence to probe the effect of the chain length between these two functional groups on calcium binding and transport. It also allowed us to incorporate various alkyl side chains to determine the effects of lipid solubility on calcium transport. Using this route gram quantities of each ionophore analogue was readily available.

Transport of calcium across an organic barrier by these synthetic analogues of ionomycin was determined in a cylindrical glass cell using chloroform as the artificial membrane. The basic structural requirements for efficient calcium transport are the presence of the  $\beta$ -diketone and the carboxyl groups within the same molecule, and a simple alkyl side chain with sufficient lipid solubility. The lipid solubility of a  $\beta$ -diketo  $\omega$ -carboxylic acid could be represented by the logarithm of its partition coefficient ( $\log P$ ) which was calculated by the hydrophobic fragmental constant method. The  $\log P$  value of a good calcium ionophore is in the range of 6-8.

The distance between the  $\beta$ -diketone and the carboxyl groups is important in controlling the efficiency of calcium transport. Optimum calcium transport is achieved when the  $\beta$ -diketone group is separated from the carboxyl group by seven methylene units identical to the backbone found in ionomycin. It appeared that additional oxygen binding sites on the side chain of the analogues did not significantly contribute to the chelation and transport of calcium.

Simple analogues with sufficient lipid solubility are comparable to calcimycin and ionomycin in terms of calcium transport and selectivity. Two of the analogues were found to cause calcium flux in human leukemic cells. The calcium response induced by the analogues was

transient and small, presumably due to the low chemical stability of these molecules in the cell membrane.

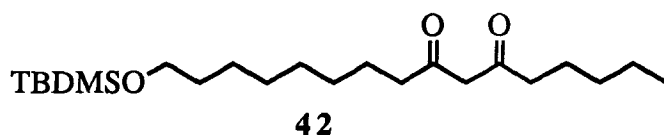
Transport of calcium by synthetic analogues of ionomycin is a saturable process which obeys Michaelis-Menten kinetics. Calcium transport is dependent of the pH in the aqueous source phase and independent of the pH in the receiving phase. Both the carboxyl and the  $\beta$ -diketone groups are ionized in the transport of calcium, indicating that the stoichiometry of calcium complex in transport is 1:1.

The characterization of calcium salt of analogue **28** showed that the stoichiometry of the calcium complex in the solid state was 1:1. It also revealed the weak binding of the analogue with calcium.

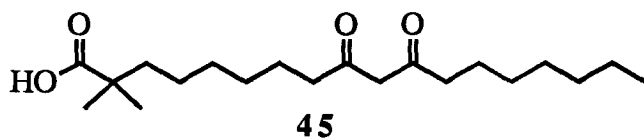
The  $pK_a$  of the  $\beta$ -diketone group of the analogues was measured by UV spectrophotometric titration and found to be much lower than that of the  $\beta$ -diketone group in ionomycin. They were directly related to the lipid solubility of the molecules and the hydrocarbon chain length between the  $\beta$ -diketone and the carboxyl groups.

The binding constants of the analogues with sodium, potassium, calcium and magnesium were determined by measuring the  $pK_a$  of the  $\beta$ -diketone group in the presence and absence of the cation. The selectivity in binding was the same as the selectivity in transport, which was  $Mg^{2+} > Ca^{2+} \gg Na^+, K^+$ . Calcium and magnesium binding by the analogues were 3-4 orders of magnitude lower than that of ionomycin. The mole ratio method was used to determine the binding constants of the analogues with magnesium. This established the 1:1 stoichiometry in the magnesium complex and verified the utility of the  $pK_a$  method used for the measurements of binding constants of the analogues with sodium, potassium and calcium.

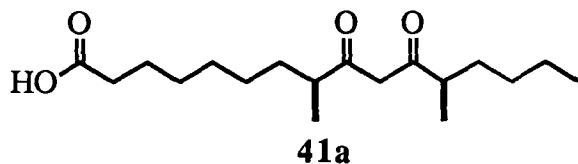
Dimethylation of the  $\beta$ -diketone **42** in a one pot reaction proceeded with high diastereoselectivity. The major diastereomers had the two methyl groups *trans* to each other.



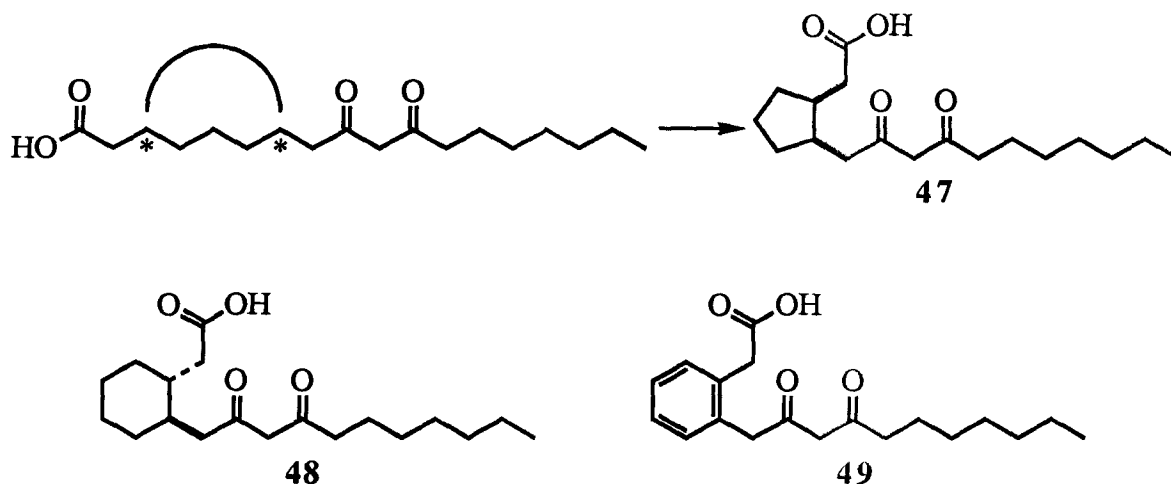
Future work on this project should address the two problems that have prevented the use of the analogues in biological systems: one is the proposed chemical instability of the analogues in cells. It is very likely that the structurally simple analogues undergo rapid transformation within the cell which results in the transient nature of the effect of calcium mobilization in THP-1 cells. These synthetic compounds may be transesterified and incorporated into the cell membrane. Introduction of bulky alkyl groups, such as a dimethyl group in **45**,  $\alpha$  to the carboxyl group, may prevent the compound from being incorporated into the cell membrane and achieve a greater and more sustained calcium transport into the cell.



The second problem is the relative low binding constants of the analogues with calcium compared to ionomycin. This problem is likely due to the presence of too many undesired rotomers associated with the acyclic chain of the synthetic analogues. This may be partially solved by introducing two methyl groups *cis* to each other and adjacent to the  $\beta$ -diketone group as in analogue **41a**.



Alternatively and likely more effectively, the entropy problem may be solved by connecting the  $\beta$ -carbons (shown by an asterisk) of the carboxyl and the  $\beta$ -diketone groups to form a molecule such as analogue **47**. Other derivatives such as analogues **48** and **49** are also worthy of testing. The *cis* and *trans* stereochemistry in analogues **47** and **48** respectively is to bring the  $\beta$ -diketone and the carboxyl groups closer to each other to reduce the entropy losses on binding.



In conclusion, the study of calcium binding and transport of synthetic analogues based on ionomycin has shed light on the structural features controlling calcium binding and transport by ionomycin and by its simple analogues. It has also paved the way to the rational design of new calcium ionophores both as potential biochemical tools and therapeutic agents.



## CHAPTER THREE

### EXPERIMENTAL

#### 3.1 General

**Solvents, reagents and equipment setup.** Solvents were dried as follows: diethyl ether (ether) and tetrahydrofuran (THF) were distilled from sodium benzophenone ketyl radical under a dry nitrogen atmosphere. Methylene chloride was distilled from calcium hydride and methanol from magnesium methoxide.

Unless otherwise specified, all reagents were supplied by the Aldrich Chemical Company and purified according to the procedure given in the literature.<sup>72</sup> n-Butyllithium (in hexanes) was standardized by titration against 2,2-diphenylacetic acid in THF at room temperature to the faintest appearance of a yellow color.

Nitrogen was supplied by Union Carbide and prior to use was passed through two columns of indicating Drierite ( $\text{CaSO}_4$  impregnated with  $\text{CoCl}_2$ ). Syringes and needles were oven-dried at 120 °C for a minimum of 3-4 hours and stored in a desiccator. Unless stated otherwise, all reactions were carried out under a dry nitrogen atmosphere in an anhydrous solvent. The glassware (including the Teflon-coated magnetic stirring bar) was assembled and connected to a vacuum pump and flame-dried under vacuum. After the glassware had cooled, dry nitrogen was introduced to the system. Cold temperatures were maintained using either an ice/water bath (0 °C) or an acetone/dry ice bath (-78 °C). The concentration or evaporation of solvents under reduced pressure refers to the use of a Buchi rotary evaporator. Petroleum ether refers to the fraction which boils between 30-60 °C.

**Reaction monitoring.** All reactions were monitored by thin layer chromatography (TLC). Analytical TLC was performed on aluminum backed, precoated silica ( $\text{SiO}_2$ ) gel plates (E. Merck, type 5554). The plates were visualized by ultraviolet fluorescence or by heating the plates after spraying them with a mixture of methanol, acetic acid, sulfuric acid and anisaldehyde (90:10:5:1 by volume). Analytical gas liquid chromatography (GC) was performed on a Hewlett Packard model 5880A gas chromatography using a 15 m x 0.2 mm capillary DB-210 column and with the following temperature program: 100 °C for 2 min, then a temperature increase to 220 °C at a rate of 20 °C per min, and a final time of 8 min at 220 °C.

**Product purification.** Unless otherwise stated, all reaction products were purified by flash chromatography using 230-400 mesh ASTM silica gel supplied by E. Merck Co. In those cases that a large amount of silica gel was used, the silica gel was recycled after column chromatography. This involved discarding the upper 2-4 cm of silica gel in the column and flushing the remaining silica gel with methanol until clean. A hose connected to a water aspirator was attached to the column spigot and the silica gel was sucked to dryness (powder dry). The silica gel was subsequently regenerated by oven heating for 6-8 hours at 120 °C.

**Product characterization.** Proton nuclear magnetic resonance ( $^1\text{H}$  NMR) spectra were recorded at 400 MHz on a Bruker WH-400 spectrometer or at 300 MHz on a Varian XL-300 spectrometer in deuteriochloroform ( $\text{CDCl}_3$ ) with signal positions given in parts per million (ppm) from the internal standard of tetramethylsilane (0.00 ppm) on the  $\delta$  scale. They are reported in the form: chemical shift (number of protons, signal multiplicities). The abbreviations used in reporting the data are: s = singlet, d = doublet, t = triplet, q = quartet, p = pentet, m = multiplet, dd = double doublet, dt = double triplet.

Infrared (IR) spectra were recorded on a Bomem Michelson 100 FT-IR spectrophotometer using internal calibration. Liquid samples were applied directly between two 3 mm NaCl plates. Solid samples were dissolved in chloroform and the spectra were taken and subsequently

subtracted from a spectrum of chloroform. Solid state IR spectra were determined using pressed discs of the samples in KBr. Absorption positions are given in  $\text{cm}^{-1}$ .

Low and high resolution mass spectra were determined on a Kratos-AEI model MS 50 spectrometer. The parent peak as well as major ion fragments are reported as percentages of the base peak. Gas chromatography mass spectra were determined on a Kratos-MSAD mass spectrometer. All instruments were operated at 70 eV. Melting points were determined on a Mel-Temp II melting point apparatus and were not corrected.

Microanalyses were carried out at the microanalytical laboratory of the University of British Columbia using a Carlo Erba Elemental Analyzer 1106.

**Determination of metal ion transport.** The transport of metal ions across a chloroform liquid membrane by synthetic analogues of ionomycin was determined in a cylindrical glass cell of internal diameter of 5.0 cm (Figure 11). The height of the cell is 6.3 cm and the glass divider is 0.4 cm wide and 5.3 cm from the top of the vessel.

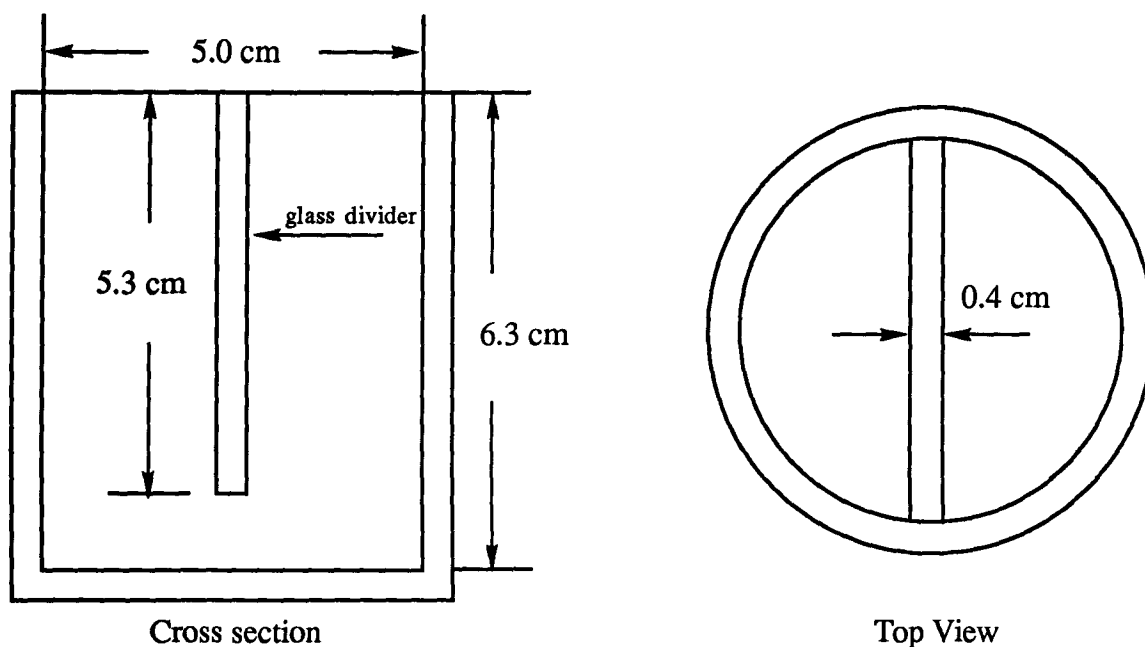


Figure 11. Cross section and top view of the cylindrical glass cell for the studies of calcium transport across a chloroform liquid membrane.

To determine the calcium transport efficiency of the various analogues, a solution of 200  $\mu\text{M}$  analogue in 40 mL of glass distilled chloroform (OmniSolv BDH Inc.) was placed at the bottom of the transport vessel. A solution of 500 mM of calcium chloride and 40 mM of CHES/ $\text{Me}_4\text{NOH}$  buffer in 10 mL of distilled deionized water at  $\text{pH} = 9.50$  was placed on one side of the transport vessel as the source phase. A solution of 40 mM MOPS/ $\text{Me}_4\text{NOH}$  buffer in 10 mL of distilled deionized water at  $\text{pH} = 7.00$  was placed on the other side of the transport vessel as the receiving phase. The chloroform solution was stirred continuously with a 10 x 3 mm microstirring bar at a constant speed of  $400 \pm 20$  r.p.m. as indicated by a chronometric speedcounter.

An aliquot of 200  $\mu\text{L}$  of the receiving phase was withdrawn with a microsyringe at the end of 12, 16, 20 and 24 h, diluted with 4.80 mL of distilled deionized water and analyzed for the calcium concentration by calcium atomic absorption spectrophotometry. The concentration of calcium in the receiving phase increased linearly with time when the amount of calcium transported was small. The transport rate ( $J$ ) is expressed as the moles of calcium transported per square centimeter of the organic phase per hour. Results from separate runs were reproducible within  $\pm 10\%$ . The reported  $J$  value is the average of two or three separate runs. For reason of simplicity, only one plot of the amount of calcium in the receiving phase versus time from a representative analogue is given.

Cation selectivity in transport was determined using a source phase of 10 mL of distilled deionized water containing equimolar concentration (250 mM) of calcium chloride and chloride of the competing cation (magnesium, sodium and potassium ions respectively), and 40 mM of CHES/ $\text{Me}_4\text{NOH}$  buffer at  $\text{pH} = 9.50$ . The samples taken from the receiving phase were analyzed for the concentrations of both cations by atomic absorption spectrometry.

Calcium, magnesium, potassium and sodium atomic absorption spectrometry was carried out on a Perkin-Elmer model 560 atomic absorption spectrometer. The setting of the instrument was: integration time = 3 seconds, lamp current = 6 mA, slit setting = 0.7 for calcium, magnesium and sodium, slit setting = 1.4 for potassium, wavelength = 422.7, 202.6, 589.0 and 766.5 nm for calcium, magnesium, sodium and potassium lamp respectively.

Calcium, magnesium or potassium solutions of 1.25, 2.50 and 5.00 ppm and sodium solutions of 0.25, 0.50 and 1.25 ppm prepared from 990 ppm atomic absorption standard solution (Aldrich) were used to standardized the instrument. The absorbances were linear against the concentrations of the metal ions up to 5.00 ppm for calcium, magnesium and potassium, and up to 1.25 ppm for sodium. The linear equations were used to calculate the cation concentration of the unknown samples whose absorbances were determined.

Buffers which had negligible affinity for magnesium, calcium, sodium and potassium ions were used to control the pH in the source phase and the receiving phase. They were prepared by mixing an aqueous solution of 10% tetramethylammonium hydroxide with an acid that has a  $pK_a$  close to the desired working pH and diluting the solution with distilled deionized water to a final concentration of 40 mM (Appendix 2).

The effect of five selective analogues on intracellular calcium mobilization was examined in cultured human leukemic cells known as THP-1 cells by Dr. C. Chan of Merck Frosst Centre For Therapeutic Research.<sup>73</sup> THP-1 cells were suspended in L15 medium (Sigma, pH 7.4, with 1 mM Hepes) at  $10^7$  cells/mL and were incubated with fura-2 acetocymethyl ester at 2  $\mu$ g/mL for 20 min at 37 °C. The cells were then washed three times with 20 mL of L15 to remove free dye and finally resuspended in L15 at  $2 \times 10^6$  cells/mL. Cell fluorescence (2 mL cell suspension) was monitored using a Perkin-Elmer spectrofluorometer with excitation settings at 340 nm and 380 nm. The ratio of fura-2 fluorescence with excitation at 340 nm to that at 380 nm was used as an index to calculate intracellular calcium concentration according to the method of Grynkiewicz.<sup>59</sup>

All compounds were dissolved in dimethylsulfoxide (DMSO) at 1000 times the final concentration (i.e. 2  $\mu$ L DMSO/compound in 2 mL cells). Calcimycin bromide and ionomycin were used as positive controls. Cumulative dose-responses were obtained and the cell fluorescence were monitored continuously for 3-4 minutes. The cells were constantly stirred and were kept at 37 °C during the course of the measurement.

**Determination of  $pK_a$  of  $\beta$ -diketones.** The  $pK_a$  of the  $\beta$ -diketone group of the synthetic analogues of ionomycin was determined in 80% MeOH-H<sub>2</sub>O by UV spectrophotometric titration at 25 °C on a Perkin-Elmer UV-Visible Lambda 2 Spectrometer with a thermostated sample cell. An aliquot of 1.0 mL 80% MeOH-H<sub>2</sub>O in a disposable cuvette (1.0 cm pathlength, InterScience) was placed in the sample cell and the baseline was recorded from 260 nm to 350 nm and stored. The solvent was then replaced by a solution of 80  $\mu$ M analogue and 50 mM Et<sub>4</sub>NClO<sub>4</sub> in 1.0 mL of 80% MeOH-H<sub>2</sub>O. Small aliquots (4 to 20  $\mu$ L) of 0.1%, 0.25%, 0.5% and 5.0% Me<sub>4</sub>NOH (the titrant) in 80% MeOH-H<sub>2</sub>O were added and the spectra were recorded. The addition of the titrant was terminated when the maximum absorption of the spectrum remained constant.

The values of pH at each titration point were determined with the same solutions on a 5-fold greater scale on a PHM82 STANDARD pH meter (Bach-Simpson Limited). The pH meter was standardized with pH = 7.0 and pH = 10.0 aqueous buffer solutions. No correction was made for differences in the pH readings between pure aqueous solutions and 80% MeOH-H<sub>2</sub>O solutions.

The absorbance at 298 nm versus pH was computer fitted to a modified Henderson-Hasselbalch equation by non-linear regression using Enzfitter developed by Leatherbarrow to calculate the  $pK_a$  values.<sup>63</sup>

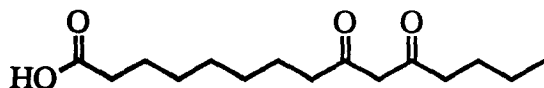
**Determination of metal ion binding constants.** The binding constant of the analogues with various metal ions was determined in 80% MeOH-H<sub>2</sub>O by UV spectrophotometric

titration at 25 °C. The UV spectrophotometric titration of the analogues was carried out in the presence of 50 mM NaCl, 50 mM KBr, 16.7 mM of CaCl<sub>2</sub> and 16.7 mM MgCl<sub>2</sub> respectively (in place of Et<sub>4</sub>NClO<sub>4</sub>). The absorbance at 298 nm versus pH was computer fitted to a modified Henderson-Hasselbalch equation by non-linear regression to calculate the conditional pK<sub>a</sub>' of a β-diketone in the presence of the metal ion. The difference between pK<sub>a</sub>' and pK<sub>a</sub> gave the logarithm of the dissociation constant of the analogue-cation complex.

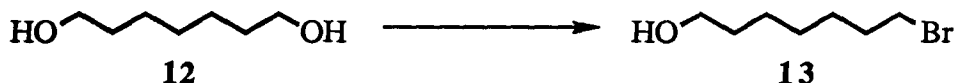
The binding constant of the analogues with magnesium was also determined using the mole ratio method. A solution of 80 μM analogue and 50 mM CHES/Me<sub>4</sub>NOH buffer in 80% MeOH-H<sub>2</sub>O was titrated with a solution of 5, 10, 25, 50, 100 and 250 mM MgCl<sub>2</sub> in 80% MeOH-H<sub>2</sub>O. Calculation of the number of moles of magnesium bound per mole of the analogue versus the concentration of free magnesium ions at each titration point were computer fitted to the Scatchard equation by non-linear regression to determine the binding constant.<sup>63</sup> This method also allowed the determination of the stoichiometry of the complex.

For reason of simplicity, only one set of the titration and the data fitting curves for the determination of pK<sub>a</sub>, pK<sub>a</sub>', the magnesium binding constant and stoichiometry of a representative analogue is presented. Results for other analogues are reported as absorbance at each pH or at each magnesium ion concentration and the calculated binding constant and stoichiometry.

### 3.2 Synthesis of 9,11-Dioxopentadecanoic Acid (4)



#### 3.2.1 7-Bromo-1-heptanol (13)



A suspension of 1,7-heptanediol (**12**) (5.8 g, 44 mmol) in 7.5 mL of 48% HBr (66 mmol) was prepared in a 1-L liquid-liquid continuous extractor. The suspension was heated to 90 °C and was extracted with 300 mL of heptane at this temperature for 72 h. The extract was cooled, washed twice with saturated NaHCO<sub>3</sub> and once with brine. The organic layer was dried over MgSO<sub>4</sub> and concentrated under reduced pressure. The crude oil was purified by column chromatography using petroleum ether : ethyl acetate (6:1) as eluent to give the monobrominated alcohol (6.2 g, 72%) as a colorless liquid, which was one spot by TLC.

**R<sub>f</sub>** (1:1 petroleum ether : ethyl acetate eluent) 0.54.

**<sup>1</sup>H NMR** (300 MHz, CDCl<sub>3</sub>) δ 3.66 (2H, t), 3.42 (2H, t), 1.87 (2H, p), 1.57 (2H, p), 1.52-1.25 (7H, m).

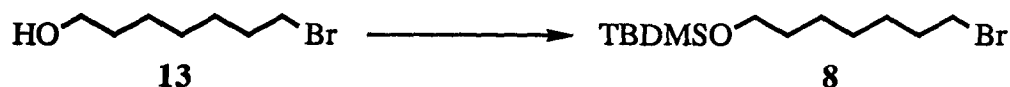
**IR** (neat, cm<sup>-1</sup>) 3347, 2930, 2858, 1452, 1254, 1054, 726.

**LRMS** (m/z) 195 (Br<sup>81</sup>: M<sup>+</sup> - H, 0.2), 193 (Br<sup>79</sup>: M<sup>+</sup> - H, 0.2), 150 (55), 148 (56), 137 (2), 136 (2), 135 (2), 134 (2), 109 (3), 107 (3), 98 (3), 97 (52), 96 (5), 95 (6), 83 (5), 81 (34), 70 (34), 69 (90), 68 (51), 67 (47), 57 (34), 56 (55), 55 (100), 44 (21), 43 (66), 42 (57), 41 (87), 40 (23), 39 (61), 31 (71).

**HRMS** calcd for C<sub>7</sub>H<sub>15</sub>Br<sup>81</sup>O - H: 195.0204, found: 195.0213; calcd for C<sub>7</sub>H<sub>15</sub>Br<sup>79</sup>O - H: 193.0224, found: 193.0228.



### 3.2.2 1-Bromo-7-(tert-butyldimethylsilyloxy)-heptane (8)



Freshly distilled triethylamine (1.68 mL, 12.0 mmol) was injected into a solution of the alcohol **13** (1.17 g, 6.0 mmol) in 100 mL of  $\text{CH}_2\text{Cl}_2$  at room temperature. A catalytic amount of 4-dimethylaminopyridine (DMAP) and 1.36 g (9.0 mmol) of tert-butyldimethylsilyl chloride (TBDMS-Cl) were added. The reaction was stirred at room temperature for 24 h. The mixture was then quenched with 1N HCl and extracted with ether three times. The combined organic layers were washed twice with saturated  $\text{NaHCO}_3$  and once with brine. The organic phase was dried over  $\text{MgSO}_4$  and concentrated under reduced pressure. Purification of the crude product by column chromatography using petroleum ether : ethyl acetate (15:1) as eluent gave the silyl ether **8** (1.50 g, 82%) as a colorless oil, which was one spot by TLC.

**R<sub>f</sub>** (6:1 petroleum ether : ethyl acetate eluent) 0.83.

**<sup>1</sup>H NMR** (400 MHz,  $\text{CDCl}_3$ )  $\delta$  3.64 (2H, t), 3.44 (2H, t), 1.86 (2H, p), 1.53-1.31 (8H, m), 0.89 (9H, s), 0.05 (6H, s).

**IR** (neat,  $\text{cm}^{-1}$ ) 2937, 2858, 1466, 1388, 1361, 1254, 1101, 1006, 938, 838, 776.

**LRMS** ( $m/z$ ) 253 ( $\text{Br}^{81}$ :  $\text{M}^+ - \text{C}_4\text{H}_9$ , 4.4), 251 ( $\text{Br}^{79}$ :  $\text{M}^+ - \text{C}_4\text{H}_9$ , 4.6), 173 (2), 171 (7), 170 (4), 169 (38), 167 (33), 140 (4), 139 (34), 138 (4), 137 (33), 101 (25), 99 (17), 98 (29), 97 (75), 96 (12), 93 (9), 89 (25), 76 (12), 75 (53), 74 (12), 73 (44), 70 (9), 69 (50), 68 (8), 67 (13), 61 (21), 60 (8), 59 (35), 58 (22), 57 (28), 56 (34), 55 (100), 47 (24), 45 (33), 43 (42), 41 (43), 39 (22).

**HRMS** calcd for  $\text{C}_{13}\text{H}_{29}\text{SiBr}^{81}\text{O} - \text{C}_4\text{H}_9$ : 253.0438, found: 253.0450; calcd for  $\text{C}_{13}\text{H}_{29}\text{SiBr}^{79}\text{O} - \text{C}_4\text{H}_9$ : 251.0458, found: 251.0460.

### 3.2.3 12-(Tert-butyldimethylsilyloxy)-2,4-dodecanedione (22)



Sodium hydride (610 mg, 50% in oil, 12.7 mmol) was added to a 100 mL, two-neck round bottom flask and washed twice with 20 mL of THF. Then 20 mL of THF was added and the resulting suspension was cooled to 0 °C. A solution of 2,4-pentanedione (7) (1.36 mL, 12.7 mmol) in 15 mL of THF was added through an addition funnel. The resulting white solution was stirred for 30 min and 7.84 mL of *n*-BuLi (1.62 M, 12.7 mmol) was added. The orange solution was stirred for 20 min. A solution of the bromide 8 (3.26 g, 10.6 mmol) in 10 mL of THF was slowly added through the addition funnel and the mixture was stirred at 0 °C for 1 h and at room temperature for 20 min. The mixture was quenched with saturated NH<sub>4</sub>Cl, acidified with 1N HCl and extracted with ether three times. The combined organic layers were washed twice with saturated NaHCO<sub>3</sub> and once with brine, dried over MgSO<sub>4</sub> and concentrated under reduced pressure. Purification of the crude product by column chromatography using a mixture of petroleum ether : ethyl acetate (15:1) as eluent gave the β-diketone 22 (2.20 g) and the bromide 8 (700 mg). The reaction yield, based on the recovered bromide, was 81%.

**R<sub>f</sub>** (6:1 petroleum ether : ethyl acetate eluent) 0.61.

**<sup>1</sup>H NMR** (400 MHz, CDCl<sub>3</sub>) δ 15.50 (0.8 H, s), 5.49 (0.8 H, s), 3.61 (2H, t), 3.58 (0.4 H, s), 2.51 (0.4 H, t), 2.27 (1.6 H, t), 2.24 (0.6 H, s), 2.06 (2.4 H, s), 1.65-1.26 (12H, m), 0.89 (9H, s), 0.04 (6H, s).

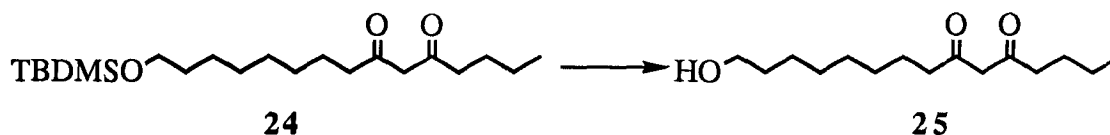
**IR** (neat, cm<sup>-1</sup>) 2934, 2857, 1709, 1614, 1465, 1253, 1100, 1006, 939, 838, 776.

**LRMS** (*m/z*) 313 (M<sup>+</sup> - CH<sub>3</sub>, 6), 274 (3), 273 (14), 272 (44), 271 (100), 253 (2), 229 (1), 171 (6), 169 (8), 157 (5), 145 (4), 143 (6), 131 (4), 117 (4), 115 (10), 101 (8), 100 (4), 99 (23), 85 (22), 75 (55), 73 (24), 69 (10), 67 (7), 61 (6), 59 (9), 58 (3), 57 (4), 55 (24), 43 (39), 41 (18).

**HRMS** calcd for C<sub>18</sub>H<sub>36</sub>SiO<sub>3</sub> - CH<sub>3</sub>: 313.2190, found: 313.2208.



### 3.2.5 15-Hydroxyl-5,7-pentadecanedione (25)



To a solution of the silyl ether **24** (444 mg, 1.20 mmol) in 40 mL of THF was injected a solution of tetrabutylammonium fluoride in THF (1.0 M, 2.40 mL, 2.4 mmol). The solution was stirred at room temperature for 12 h. The solvent was removed under reduced pressure and the residue was taken up in ether. The organic layer was washed twice with brine, dried over  $\text{MgSO}_4$  and concentrated under reduced pressure. Purification of the crude product by column chromatography using petroleum ether : ethyl acetate (6:1) as eluent gave the alcohol **25** (277 mg, 91%) as a colorless solid, which was one spot by TLC.

**R<sub>f</sub>** (1:1 petroleum ether : ethyl acetate eluent) 0.58.

**mp** 41.5 °C

**<sup>1</sup>H NMR** (400 MHz,  $\text{CDCl}_3$ )  $\delta$  15.50 (0.7H, s), 5.48 (0.7H, s), 3.65 (2H, t), 3.53 (0.6H, s), 2.52-2.51 (1.2H, dt), 2.29-2.27 (2.8H, dt), 1.66-1.25 (17H, m), 0.93 (3H, t).

**IR** ( $\text{CHCl}_3$ ,  $\text{cm}^{-1}$ ) 3621, 3462, 2934, 2859, 1723, 1700, 1605, 1460, 1355, 1307, 1149, 1098, 1005, 957, 916.

**LRMS** ( $m/z$ ) 256 ( $\text{M}^+$ , 1), 239 (0.2), 238 (1), 214 (1), 213 (1), 181 (1), 157 (2), 156 (2), 155 (6), 143 (2), 142 (22), 141 (4), 128 (3), 127 (30), 114 (3), 113 (12), 101 (3), 100 (38), 99 (4), 98 (3), 97 (14), 86 (6), 85 (100), 84 (9), 83 (8), 71 (14), 70 (5), 69 (33), 68 (4), 67 (13), 58 (19), 57 (79), 56 (12), 55 (87), 44 (20), 43 (65), 42 (8), 41 (65), 40 (34).

**HRMS** calcd for  $\text{C}_{15}\text{H}_{28}\text{O}_3$ : 256.2031, found: 256.2031.

### 3.2.6 9,11-Dioxopentadecanoic Acid (**4**)



To the alcohol **25** (384 mg, 1.34 mmol) in 15 mL of  $\text{CH}_2\text{Cl}_2$  and 15 mL of DMSO was added 1,3-dicyclohexylcarbodiimide (DCC) (1.67 g, 7.95 mmol) and dichloroacetic acid (53  $\mu\text{L}$ , 0.69 mmol). The mixture was stirred for 2 h, diluted with ethyl acetate and treated with oxalic acid (1.02 g, 7.95 mmol). The mixture was poured into brine, filtered to remove the urea precipitate and extracted with ethyl acetate. The organic layer was concentrated under reduced pressure. The resulting oil was dissolved in 24 mL 50% THF-  $\text{H}_2\text{O}$ . Silver nitrate (1.85 g, 10.8 mmol) and NaOH (0.86 g, 22 mmol) were added and the mixture was stirred for 4 h. The precipitate was filtered and washed with ethyl acetate and water. The aqueous layer was acidified with 1N HCl and was then extracted with ethyl acetate. The organic extract was washed with brine, dried over  $\text{MgSO}_4$  and concentrated under reduced pressure. The crude product was purified by recrystallization from hexanes to give the acid **4** (270 mg, 69%) as a colorless crystal.

**R<sub>f</sub>** (5% HOAc in 3:1 petroleum ether : ethyl acetate eluent) 0.54.

**mp** 43.0 °C.

**<sup>1</sup>H NMR** (300 MHz,  $\text{CDCl}_3$ )  $\delta$  15.50 (0.7H, s), 5.48 (0.7H, s), 3.53 (0.6H, s), 2.52-2.51 (1.2H, dt), 2.33 (2H, t), 2.28-2.26 (2.8H, dt), 1.70-1.27 (15H, m), 0.93 (3H, t).

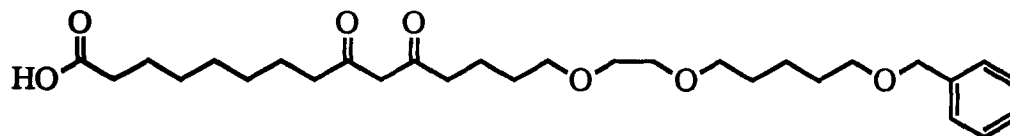
**IR** ( $\text{CHCl}_3$ ,  $\text{cm}^{-1}$ ) 3346-2480, 2937, 2861, 1713, 1601, 1459, 1286, 1116, 968, 903.

**LRMS** ( $m/z$ ) 270 ( $\text{M}^+$ , 4.0), 252 (1), 229 (1), 228 (8), 227 (3), 210 (2), 196 (2), 195 (15), 182 (3), 171 (25), 167 (5), 155 (10), 143 (4), 142 (33), 127 (51), 125 (16), 113 (18), 111 (8), 100 (37), 98 (6), 97 (17), 85 (100), 84 (9), 83 (17), 69 (22), 57 (32), 55 (32), 43 (25), 41 (24).

**HRMS** calcd for  $\text{C}_{15}\text{H}_{26}\text{O}_4$ : 270.1824, found: 270.1828.

**Elem. Anal.** calcd for  $\text{C}_{15}\text{H}_{26}\text{O}_4$ : C, 66.67; H, 9.63. found: C, 66.60; H, 9.65.

### 3.3 Synthesis of 15-[2-(5-Benzyloxy)-pentyloxy]-ethoxy-9,11-dioxopentadecanoic Acid (5)



#### 3.3.1 5-Benzyloxy-1-pentanol (16)



Sodium hydride (4.58 g, 80% in oil, 153 mmol) was added to a 500-mL two-neck round bottom flask and washed twice with 20 mL of THF. A solution of 1,5-pentanediol (**15**) (7.95 g, 76.4 mmol) in 20 mL of THF and 200 mL of THF was then added. The mixture was stirred at room temperature for 30 min. Benzyl bromide (9.1 mL, 77 mmol) was slowly added and the mixture was refluxed overnight. The reaction mixture was quenched with H<sub>2</sub>O. The organic layer was washed once with 1N HCl and twice with brine, dried over MgSO<sub>4</sub> and concentrated under reduced pressure. The crude product was chromatographed on a silica gel column using petroleum ether : ethyl acetate (3:1) as eluent to give the alcohol **16** (7.98 g, 54%) as a clear oil, which was one spot by TLC.

**R<sub>f</sub>** (1:1 petroleum ether : ethyl acetate eluent) 0.38.

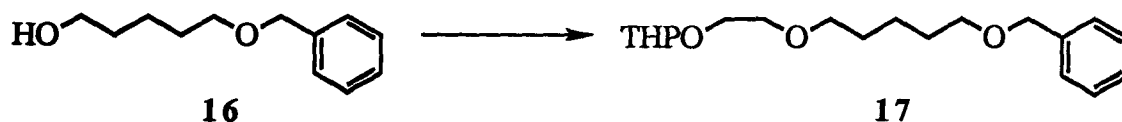
**<sup>1</sup>H NMR** (400 MHz, CDCl<sub>3</sub>) δ 7.40-7.24 (5H, m), 4.52 (2H, s), 3.65 (2H, t), 3.52 (2H, t), 1.70-1.40 (7H, m).

**IR** (neat, cm<sup>-1</sup>) 3372, 3090, 3063, 3030, 2897, 2850, 1496, 1454, 1363, 1206, 1077, 903.

**LRMS** (m/z) 194 (M<sup>+</sup>, 7), 176 (0.1), 131 (1), 118 (1), 117 (2), 109 (2), 108 (30), 107 (75), 106 (4), 105 (9), 92 (50), 91(100), 90 (5), 89 (6), 85 (24), 79 (23), 78 (6), 77 (13), 69 (15), 67 (7), 65 (30), 63 (5), 57 (15), 55 (12), 51 (11), 44 (4), 43 (16), 42 (6), 41 (32).

**HRMS** calcd for C<sub>12</sub>H<sub>18</sub>O<sub>2</sub>: 194.1302, found: 194.1304.

### 3.3.2 5-Benzyloxy-1-(2-tetrahydropyranyloxy)-ethoxy-pentane (17)



A 25-mL, three-neck round bottom flask was charged with 50% sodium hydroxide (4.0 mL, 50 mmol), 1-bromo-2-tetrahydropyranyloxy-ethane (4.18 g, 20.0 mmol) and the alcohol **16** (0.97 g, 5.0 mmol). Tetrabutylammonium hydrogen sulfate (0.15 g, 0.44 mmol) was added. The two-phase mixture was stirred vigorously and heated to 65 °C for 72 h. The reaction mixture was cooled to room temperature and taken up into 100 mL of ether. The organic layer was washed with H<sub>2</sub>O, brine, dried over MgSO<sub>4</sub> and concentrated under reduced pressure. Purification of the crude product by column chromatography using petroleum ether : ethyl acetate (6:1) as eluent gave the desired compound **17** (1.34 g, 83%) as a light yellow oil, which was one spot by TLC.

**R<sub>f</sub>** (6:1 petroleum ether : ethyl acetate eluent) 0.16.

**<sup>1</sup>H NMR** (300 MHz, CDCl<sub>3</sub>) δ 7.40-7.24 (5H, m), 4.64 (1H, t), 4.50 (2H, s), 3.94-3.46 (10H, m), 1.90-1.40 (12H, m).

**IR** (neat, cm<sup>-1</sup>) 3086, 3060, 3029, 2935, 2861, 1495, 1453, 1359, 1269, 1201, 1184, 1106, 1032, 988, 929, 906, 872, 814, 739.

**LRMS** (m/z) 322 (M<sup>+</sup>, 0.2), 321 (0.1), 238 (0.6), 237 (2), 177 (0.4), 176 (1), 132 (1), 131 (9), 119 (0.4), 118 (2), 117 (1), 108 (2), 107 (8), 106 (2), 105 (4), 92 (13), 91 (100), 86 (4), 85 (67), 84 (5), 79 (6), 78 (2), 77 (7), 67 (7), 66 (1), 65 (13), 57 (11), 56 (7), 55 (11), 45 (10), 43 (8), 41 (23).

**HRMS** calcd for C<sub>19</sub>H<sub>30</sub>O<sub>4</sub>: 322.2136, found: 322.2152.

### 3.3.3 2-(5-Benzoyloxy)-pentyloxy-1-ethanol (**18**)



Pyridinium p-toluenesulfonate (42 mg, 0.16 mmol) was added to a solution of the THP ether **17** (550 mg, 1.60 mmol) in 15 mL of MeOH. The mixture was stirred at room temperature for 12 h. The solvent was removed under reduced pressure and the residue was taken up in ether, washed with saturated NaHCO<sub>3</sub> and brine, dried over MgSO<sub>4</sub> and concentrated under reduced pressure. The crude oil was chromatographed on a silica gel column using petroleum ether : ethyl acetate (6:1) as eluent to give the alcohol **18** (368 mg, 91%) as a light yellow oil, which was one spot by TLC.

**R<sub>f</sub>** (1:1 petroleum ether : ethyl acetate eluent) 0.30.

**<sup>1</sup>H NMR** (300 MHz, CDCl<sub>3</sub>)  $\delta$  7.40-7.24 (5H, m), 4.52 (2H, s), 3.72 (2H, m), 3.53 (2H, t), 3.49 (4H, t), 2.04 (1H, s), 1.69-1.40 (6H, m).

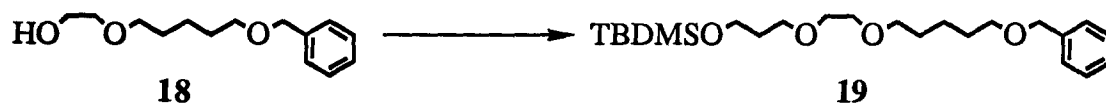
**IR** (neat, cm<sup>-1</sup>) 3414, 3082, 3063, 3030, 2932, 2862, 1495, 1454, 1362, 1207, 1086, 893, 740.

**LRMS** (m/z) 238 (M<sup>+</sup>, 0.6), 208 (0.2), 177 (0.1), 176 (1), 175 (1), 148 (0.2), 147 (1), 133 (1), 132 (3), 131 (3), 108 (2), 107 (10), 106 (3), 105 (5), 92 (14), 91(100), 85 (20), 79 (7), 78 (3), 77 (8), 65 (14), 63 (8), 57 (5), 56 (2), 55 (4), 45 (15), 44 (2), 43 (4), 42 (3), 41 (10).

**HRMS** calcd for C<sub>14</sub>H<sub>22</sub>O<sub>3</sub>: 238.1563, found: 238.1559.



### 3.3.4 5-Benzyloxy-1-[2-(3-tert-butyldimethylsilyloxy)propyloxy]-ethoxy-pentane (**19**)



Following the procedure outlined on section 3.3.2, the alcohol **18** (300 mg, 1.26 mmol) was reacted with 1-bromo-3-tert-butyldimethylsilyloxy-propane (1.28 g, 5.04 mmol) to give the corresponding ether. The crude product was purified by column chromatography using petroleum ether : ethyl acetate (6:1) as eluent to give the TBDMS ether **19** (1.34 g, 83%) as a light yellow oil, which was one spot by TLC.

**R<sub>f</sub>** (6:1 petroleum ether : ethyl acetate eluent) 0.20.

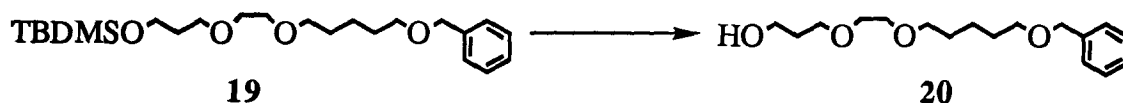
**<sup>1</sup>H NMR** (300 MHz, CDCl<sub>3</sub>) δ 7.36-7.24 (5H, m), 4.50 (2H, s), 3.70 (2H, s), 3.58-3.45 (10H, m), 1.79 (2H, p), 1.69-1.40 (6H, m), 0.89 (9H, s), 0.04 (6H, s).

**IR** (neat, cm<sup>-1</sup>) 3087, 3064, 3030, 2934, 2862, 1463, 1360, 1253, 1108, 1015, 841, 777, 737.

**LRMS** (m/z) 410 (M<sup>+</sup>, 0.3), 354 (0.2), 353 (1), 268 (0.2), 267 (1), 248 (0.3), 247 (1), 209 (1), 205 (2), 178 (2), 177 (22), 176 (2), 175 (3), 173 (4), 161 (5), 159 (3), 133 (13), 132 (3), 131 (12), 119 (8), 118 (3), 117 (24), 116 (2), 115 (11), 105 (12), 103 (6), 101 (9), 92 (42), 91 (100), 89 (13), 87 (10), 86 (5), 85 (32), 79 (10), 77 (8), 75 (26), 73 (20), 69 (12), 57 (12), 56 (10), 45 (14), 44 (5), 43 (9), 41 (27).

**HRMS** calcd for C<sub>23</sub>H<sub>42</sub>SiO<sub>4</sub>: 410.2841, found: 410.2861.

### 3.3.5 3-[2-(5-Benzyloxy)-pentyloxy]-ethoxy-1-propanol (**20**)



To a solution of the silyl ether **19** (430 mg, 1.05 mmol) in 15 mL of THF was injected a solution of tetrabutylammonium fluoride in THF (1.0 M, 2.10 mL, 2.1 mmol). The solution was stirred at room temperature for 12 h. The solvent was removed under reduced pressure and the residue was taken up in ether. The organic layer was washed with brine, dried over  $\text{MgSO}_4$  and concentrated under reduced pressure. Purification of the crude product by column chromatography using petroleum ether : ethyl acetate (3:1) as eluent gave the alcohol **20** (275 mg, 89%) as a colorless oil, which was one spot by TLC.

**R<sub>f</sub>** (1:1 petroleum ether : ethyl acetate eluent) 0.20.

**<sup>1</sup>H NMR** (400 MHz,  $\text{CDCl}_3$ )  $\delta$  7.38-7.26 (5H, m), 4.50 (2H, s), 3.78 (2H, s), 3.69 (2H, t), 3.62-3.54 (4H, m), 3.47 (2H, t), 3.45 (2H, t), 2.48 (1H, s), 1.83 (2H, p), 1.69-1.40 (6H, m).

**IR** (neat,  $\text{cm}^{-1}$ ) 3426, 3085, 3063, 3030, 2932, 2863, 1495, 1454, 1361, 1296, 1204, 1091, 740.

**LRMS** ( $m/z$ ) 236 ( $\text{M}^+ - \text{C}_3\text{H}_8\text{O}$ , 0.1), 223 (0.1), 222 (1), 192 (1), 191 (3), 190 (2), 187 (1), 176 (2), 175 (1), 149 (2), 148 (1), 147 (2), 131 (14), 124 (4), 123 (40), 122 (20), 121 (10), 108 (6), 107 (23), 106 (25), 105 (100), 104 (18), 103 (12), 101 (13), 100 (10), 99 (20), 92 (27), 91 (99), 90 (6), 89 (21), 87 (31), 86 (20), 85 (84), 79 (11), 78 (8), 77 (57), 75 (14), 73 (11), 71 (13), 70 (13), 69 (74), 68 (27), 67 (12), 65 (10), 59 (38), 58 (16), 57 (18), 56 (14), 55 (17).

**HRMS** calcd for  $\text{C}_{17}\text{H}_{28}\text{O}_4 - \text{C}_3\text{H}_8\text{O}$ : 236.1407, found: 236.1400.

### 3.3.6 5-Benzyloxy-1-[2-(3-bromo)-propyloxy]-ethoxy-heptane (**10**)



A 25-mL round bottom flask was charged with the alcohol **20** (296 mg, 1.00 mmol) in 12 mL of CH<sub>2</sub>Cl<sub>2</sub>. The solution was cooled to 0 °C. Freshly recrystallized triphenylphosphine (340 mg, 1.30 mmol) and carbon tetrabromide (415 mg, 1.25 mmol) were added. The mixture was stirred at 0 °C for 30 min, allowed to warm up to room temperature and diluted with ether. The organic layer was washed with H<sub>2</sub>O, brine, dried over MgSO<sub>4</sub> and concentrated under reduced pressure. The crude product was purified by column chromatography using petroleum ether : ethyl acetate (9:1) as eluent to give the bromide **10** (315 mg, 88%) as a colorless oil, which was one spot by TLC.

**R<sub>f</sub>** (9:1 petroleum ether : ethyl acetate eluent) 0.14.

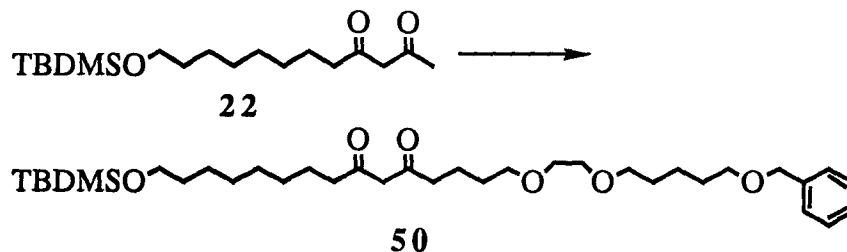
**<sup>1</sup>H NMR** (400 MHz, CDCl<sub>3</sub>) δ 7.38-7.25 (5H, m), 4.50 (2H, s), 3.66-3.44 (12H, m), 2.12 (2H, p), 1.69-1.40 (6H, m).

**IR** (neat, cm<sup>-1</sup>) 3080, 3063, 3030, 2930, 2862, 1495, 1454, 1360, 1256, 1209, 1110.

**LRMS** (m/z) 360 (Br<sup>81</sup>: M<sup>+</sup>, 3.5), 358 (Br<sup>79</sup>: M<sup>+</sup>, 3.9), 269 (2), 267 (2), 197 (2), 195 (2), 185 (30), 183 (34), 177 (5), 176 (26), 168 (18), 167 (20), 166 (21), 165 (18), 153 (22), 151 (24), 140 (15), 138 (21), 131 (25), 123 (53), 121 (42), 108 (16), 107 (42), 106 (25), 105 (52), 92 (50), 91 (100), 90 (10), 89 (10), 87 (33), 86 (39), 85 (81), 84 (22), 79 (20), 77 (31), 71 (23), 70 (31), 69 (57), 68 (28), 67 (23), 65 (32), 59 (18), 57 (36), 56 (18), 55 (31).

**HRMS** calcd for C<sub>17</sub>H<sub>27</sub>Br<sup>81</sup>O<sub>3</sub>: 360.1116, found: 360.1109; calc. for C<sub>17</sub>H<sub>27</sub>Br<sup>79</sup>O<sub>3</sub>: 358.1136, found: 358.1139.

**3.3.7 1-[2-(5-Benzoyloxy)pentyl]oxy-15-(tert-butyldimethylsilyloxy)-5,7-pentadecanedione (**50**)**



Following the procedure outlined in section 3.2.4, the  $\beta$ -diketone **22** (426 mg, 1.30 mmol) was alkylated with the bromide **10** (359 mg, 1.00 mmol) to give the  $\beta$ -diketone **50**. The crude product was purified by column chromatography using silica gel and petroleum ether : ethyl acetate (9:1) to give the  $\beta$ -diketone **50** (270 mg) as a clear oil and the bromide **10** (104 mg). The reaction yield, based on the recovered bromide, was 85%.

**R<sub>f</sub>** (9:1 petroleum ether : ethyl acetate eluent) 0.12.

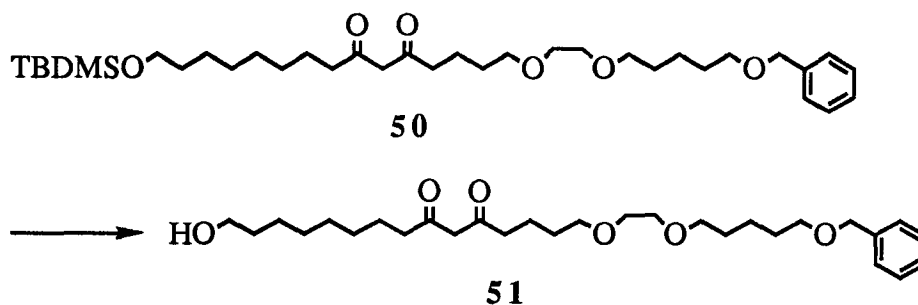
**<sup>1</sup>H NMR** (400 MHz, CDCl<sub>3</sub>)  $\delta$  15.48 (0.8H, s), 7.38-7.26 (5H, m), 5.47 (0.8H, s), 4.51 (2H, s), 3.65-3.44 (12.4H, m), 2.59-2.49 (0.8H, dt), 2.35-2.24 (3.2H, dt), 1.72-1.25 (22H, m), 0.90 (9H, s), 0.50 (6H, s).

**IR** (neat, cm<sup>-1</sup>) 3080, 3060, 3026, 1710, 1703, 1609, 1460, 1360, 1252, 1110, 840.

**LRMS** (m/z) 606 (M<sup>+</sup>, 0.7), 591 (0.5), 551 (3), 550 (9), 549 (24), 458 (0.6), 457 (2), 444 (0.6), 443 (2), 312 (3), 311 (12), 298 (0.3), 297 (2), 284 (1), 283 (4), 272 (2), 271 (10), 170 (2), 169 (9), 132 (2), 131 (9), 107 (7), 106 (3), 105 (9), 101 (9), 99 (10), 97 (9), 95 (12), 92 (12), 91 (100), 85 (26), 77 (14), 75 (45), 73 (15), 71 (8), 70 (4), 69 (24), 57 (13), 56 (96), 55 (21), 43 (17), 41 (23).

**HRMS** calcd for C<sub>35</sub>H<sub>62</sub>SiO<sub>6</sub>: 606.4299, found: 606.4313.

### 3.3.8 1-[2-(5-Benzyloxy)pentyloxy]-ethoxy-15-hydroxyl-5,7-pentadecanedione (**51**)



Following the procedure outlined in section 3.2.5, the silyl ether **50** (1.40 g, 2.58 mmol) was converted to the corresponding alcohol **51**. The crude product was purified by column chromatography using petroleum ether : ethyl acetate (6:1) as eluent to give the alcohol **51** (993 mg, 87%) as a colorless oil, which was one spot by TLC.

**R<sub>f</sub>** (1:1 petroleum ether : ethyl acetate eluent) 0.30.

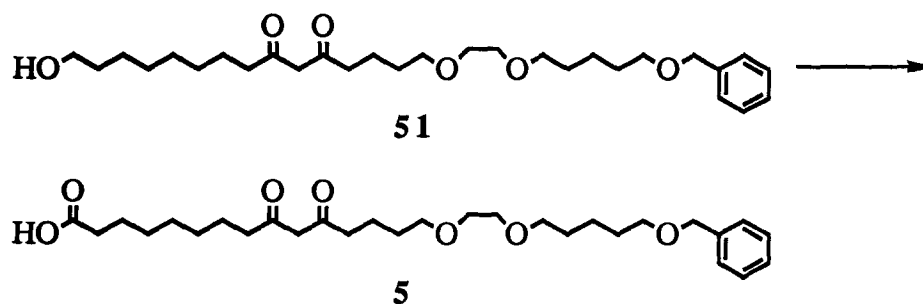
**<sup>1</sup>H NMR** (400 MHz, CDCl<sub>3</sub>) δ 15.50 (0.8H, s), 7.38-7.24 (5H, m), 5.48 (0.8H, s), 4.50 (2H, s), 3.64 (2H, t), 3.57 (4H, m), 3.53 (0.4H, s), 3.50-3.43 (6H, m), 2.58-2.47 (0.8H, dt), 2.35-2.24 (3.2H, dt), 1.72-1.25 (23H, m).

**IR** (neat, cm<sup>-1</sup>) 3437, 3080, 3060, 3030, 2930, 2863, 1710, 1702, 1606, 1453, 1361, 1096, 739.

**LRMS** (m/z) 492 (M<sup>+</sup>, 1.3), 474 (0.4), 386 (1), 317 (1), 257 (2), 256 (6), 255 (37), 254 (10), 253 (13), 198 (1), 197 (7), 178 (1), 177 (4), 176 (11), 154 (3), 153 (13), 141 (9), 140 (22), 139 (12), 131 (13), 125 (20), 108 (4), 107 (12), 101 (12), 100 (4), 99 (19), 98 (10), 97 (17), 95 (7), 92 (13), 91 (100), 85 (31).

**HRMS** calcd for C<sub>29</sub>H<sub>48</sub>O<sub>6</sub>: 492.3438, found: 492.3445.

### 3.3.9 15-[2-(5-Benzyloxy)-pentyloxy]-ethoxy-9,11-dioxopentadecanoic Acid (**5**)



Following the procedure outlined in section 3.2.6, the alcohol **51** (2.11 g, 4.29 mmol) was converted to the corresponding acid **5**. The crude product was purified by column chromatography using petroleum ether : ethyl acetate (6:1) which also contained 5% acetic acid as eluent to give the acid **5** (1.58 g, 74%) as a clear oil, which was one spot by TLC.

**R<sub>f</sub>** (5% HOAc in 3:1 petroleum ether : ethyl acetate eluent) 0.30.

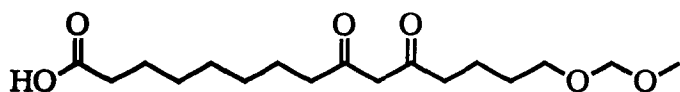
**<sup>1</sup>H NMR** (400 MHz, CDCl<sub>3</sub>)  $\delta$  15.50 (0.8H, s), 7.38-7.24 (5H, m), 5.47 (0.8H, s), 4.50 (2H, s), 3.60-3.55 (4H, m), 3.53 (0.4H, s), 3.50-3.42 (6H, m), 2.58-2.46 (0.8H, m), 2.36-2.22 (5.2H, m), 1.72-1.25 (21H, m).

**IR** (neat, cm<sup>-1</sup>) 3120, 3080, 3060, 3028, 2933, 2859, 1726, 1604, 1455, 1360, 1246, 1105, 928, 738.

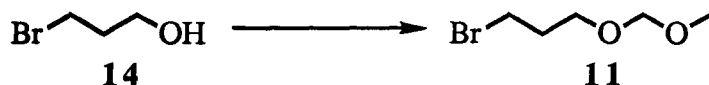
**LRMS** (m/z) 506 (M<sup>+</sup>, 2), 488 (0.3), 463 (0.3), 462 (0.8), 416 (0.7), 415 (1), 401 (0.3), 400 (1), 332 (0.4), 331 (2), 314 (1), 313 (3), 270 (7), 269 (38), 268 (29), 267 (7), 252 (94), 251 (19), 250 (12), 249 (7), 172 (5), 171 (42), 153 (27), 141 (15), 140 (37), 125 (49), 124 (8), 123 (29), 113 (8), 112 (15), 111 (12), 107 (11), 106 (9), 105 (81), 101 (26), 100 (10), 99 (22), 98 (22), 97 (38), 92 (8), 91 (80), 87 (18), 86 (10), 85 (63), 84 (15), 83 (33), 77 (14), 71 (12), 70 (9), 69 (100), 68 (19), 67 (12), 57 (13), 56 (10), 55 (48).

**HRMS** calcd for C<sub>29</sub>H<sub>46</sub>O<sub>7</sub>: 506.3231, found: 506.3237.

### 3.4 Synthesis of 15-Methoxymethoxy-9,11-dioxopentadecanoic Acid (6)



#### 3.4.1 1-Bromo-3-methoxymethoxypropane (11)



To a solution of 3-bromo-1-propanol (**14**) (3.08 g, 22.1 mmol) in 35 mL of  $\text{CH}_2\text{Cl}_2$  was added dimethoxymethane (30.3 g, 399 mmol). The solution was cooled to 0 °C and phosphorus pentoxide (approximately 1.0 g at a time) was added every 10 min until the reaction was completed as shown by TLC. The mixture was poured into 200 ml of an ice-cooled saturated  $\text{NaHCO}_3$  and the gummy residue remaining in the reaction flask carefully quenched with saturated  $\text{NaHCO}_3$ . The aqueous layer from the combined work-up solutions was extracted with ether. The combined organic layers were washed with brine, dried over  $\text{MgSO}_4$  and concentrated under reduced pressure. Distillation of the crude product under reduced pressure (85 °C/32 torr) gave the bromide **11** (3.67 g, 91%) as a colorless oil.

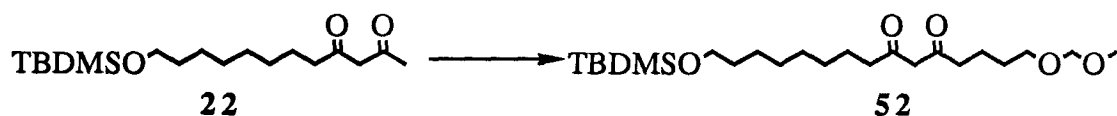
$^1\text{H}$  NMR (400 MHz,  $\text{CDCl}_3$ )  $\delta$  4.63 (2H, s), 3.67 (2H, t), 3.54 (2H, t), 3.38 (3H, s), 2.14 (2H, p).

IR (neat,  $\text{cm}^{-1}$ ) 2931, 2886, 1476, 1449, 1383, 1284, 1258, 1216, 1144, 1045, 919, 880, 766.

LRMS ( $m/z$ ) 183 ( $\text{Br}^{81}$ :  $\text{M}^+ - \text{H}$ , 16), 181 ( $\text{Br}^{79}$ :  $\text{M}^+ - \text{H}$ , 16), 154 (10), 153 (7), 152 (12), 151 (6), 123 (14), 122 (5), 121 (13), 95 (2), 93 (2), 75 (52), 61 (6), 45 (100), 41 (31).

HRMS calcd for  $\text{C}_5\text{H}_{11}\text{Br}^{81}\text{O}_2 - \text{H}$ : 182.9841, found: 182.9847.

### 3.4.2 1-Methoxymethoxy-15-(tert-butyldimethylsilyloxy)-5,7-pentadecanedione (**52**)



Following the procedure outlined in section 3.2.4, the  $\beta$ -diketone **22** (2.16 g, 6.59 mmol) was alkylated with the bromide **11** (1.08 g, 5.93 mmol) to give **52**. The crude product was purified by column chromatography using petroleum ether : ethyl acetate (15:1) as eluent to give the purified product **52** (1.56 g, 73% based on recovered starting material) as a clear oil, which was one spot by TLC.

**R<sub>f</sub>** (6:1 petroleum ether : ethyl acetate eluent) 0.24.

**<sup>1</sup>H NMR** (400 MHz, CDCl<sub>3</sub>)  $\delta$  15.50 (0.8H, s), 5.48 (0.8H, s), 4.62 (1.6H, s), 4.61 (0.4H, s), 3.61 (2H, t), 3.57 (0.4H, s), 3.56 (2H, t), 3.38 (3H, s), 2.59-2.49 (0.8H, dt), 2.35-2.24 (3.2H, dt), 1.88-1.25 (16H, m), 0.90 (9H, s), 0.50 (6H, s).

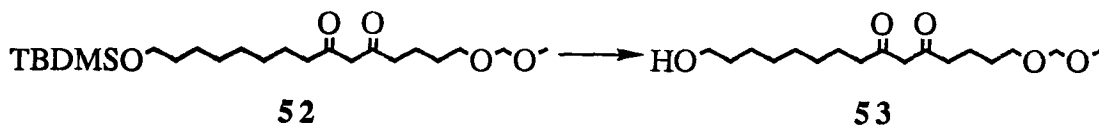
**IR** (neat, cm<sup>-1</sup>) 2936, 2858, 1708, 1701, 1611, 1463, 1387, 1253, 1148, 1103, 1044, 924.

**LRMS** (m/z) 415 (M<sup>+</sup> - CH<sub>3</sub>, 1.7), 400 (0.1), 375 (5), 374 (17), 373 (63), 343 (4), 342 (5), 341 (18), 313 (4), 312 (6), 311 (21), 284 (1), 283 (6), 242 (3), 241 (17), 214 (3), 213 (18), 125 (11), 171 (5), 169 (5), 115 (25), 111 (21), 109 (7), 107 (7), 105 (6), 101 (12), 97 (12), 95 (16), 89 (15), 85 (12), 83 (12), 81 (15), 79 (7), 77 (10), 75 (67), 73 (30), 71 (9), 69 (30), 67 (14), 59 (10), 57 (11), 56 (10), 55 (43), 45 (100), 44 (5), 43 (21), 42 (7), 41 (25).

**HRMS** calcd for C<sub>23</sub>H<sub>46</sub>SiO<sub>5</sub> - CH<sub>3</sub>: 415.2868, found: 415.2875.



### 3.4.3 1-Methoxymethoxy-15-hydroxyl-5,7-pentadecanedione (**53**)



Following the procedure outlined in section 3.2.5, the silyl ether **52** (215 mg, 0.50 mmol) was converted to the alcohol **53**. The crude product was purified by column chromatography using petroleum ether : ethyl acetate (6:1) as eluent to give the alcohol **53** (136 mg, 86%) as a colorless solid, which was one spot by TLC.

**R<sub>f</sub>** (1:1 petroleum ether : ethyl acetate eluent) 0.36.

**mp** 42.0 °C.

**<sup>1</sup>H NMR** (400 MHz, CDCl<sub>3</sub>)  $\delta$  15.50 (0.8H, s), 5.48 (0.8H, s), 4.62 (1.6H, s), 4.61 (0.4H, s), 3.65 (2H, t), 3.56 (0.4H, s), 3.55 (2H, t), 3.37 (3H, s), 2.59-2.49 (0.8H, dt), 2.35-2.25 (3.2H, dt), 1.77-1.25 (17H, m).

**IR** (CHCl<sub>3</sub>, cm<sup>-1</sup>) 3635, 3458, 2932, 2860, 1704, 1610, 1452, 1217, 1148, 1112, 1039, 923.

**LRMS** (m/z) 316 (M<sup>+</sup>, 2.5), 298 (0.3), 284 (10), 267 (10), 266 (15), 256 (8), 255 (33), 254 (31), 253 (27), 239 (5), 238 (9), 237 (4), 236 (9), 202 (18), 182 (4), 181 (19), 171 (10), 170 (43), 157 (20), 155 (37), 153, (41), 152 (24), 142 (26), 141 (21), 140 (62), 139 (47), 127 (33), 126 (26), 125 (76), 124 (31), 121 (30), 115 (30), 113 (39), 112 (34), 111 (50), 110 (24), 109 (37), 101 (54), 100 (40), 99 (47), 98 (60), 97 (75), 96 (22), 95 (41), 85 (63), 84 (51), 83 (54), 82 (31), 81 (41), 79 (22), 71 (51), 70 (37), 69 (90), 68 (22), 67 (41), 57 (48), 56 (34), 55 (84), 45 (100), 43 (76), 42 (43), 41 (60).

**HRMS** calcd for C<sub>17</sub>H<sub>32</sub>O<sub>5</sub>: 316.2241, found: 316.2247.

#### 3.4.4 15-Methoxymethoxy-9,11-dioxopentadecanoic Acid (**6**)



Following the procedure outlined in section 3.2.6, the alcohol **53** (128 mg, 0.40 mmol) was converted to the corresponding acid **6**. The crude product was purified by recrystallization from hexanes to give the acid **6** (94 mg, 73%) as a clear solid, which was one spot by TLC.

**R<sub>f</sub>** (5% HOAc in 3:1 petroleum ether : ethyl acetate eluent) 0.34.

**mp** 43.0 °C.

**<sup>1</sup>H NMR** (300 MHz, CDCl<sub>3</sub>) δ 15.50 (0.8H, s), 5.49 (0.8H, s), 4.63 (1.6H, s), 4.62 (0.4H, s), 3.57-3.52 (2.4H, m), 3.38 (3H, s), 2.59-2.48 (0.8H, dt), 2.36 (2H, t), 2.34-2.25 (3.2H, dt), 1.77-1.25 (15H, m).

**IR** (CHCl<sub>3</sub>, cm<sup>-1</sup>) 3116, 2932, 2860, 1717, 1611, 1461, 1416, 1221, 1148, 1111, 1039, 923.

**LRMS** (m/z) 330 (M<sup>+</sup>, 0.5), 312 (0.2), 298 (6), 281 (6), 280 (4), 269 (14), 268 (24), 267 (21), 251 (7), 250 (8), 249 (15), 239 (7), 196 (5), 195 (29), 172 (9), 171 (55), 170 (36), 155 (24), 153 (38), 140 (55), 127 (18), 126 (19), 125 (79), 113 (25), 112 (19), 111 (34), 101 (44), 100 (22), 99 (29), 98 (50), 97 (64), 85 (58), 84 (39), 83 (53), 81 (26), 71 (35), 70 (18), 69 (77), 68 (13), 67 (22), 57 (25), 56 (19), 55 (81), 45 (100), 44 (10), 43 (72), 42 (25), 41 (53).

**HRMS** calcd for C<sub>17</sub>H<sub>30</sub>O<sub>6</sub>: 330.2034, found: 330.2036.

**Elem. Anal.** calcd for C<sub>17</sub>H<sub>30</sub>O<sub>6</sub>: C, 61.78; H, 9.09. found: C, 61.72; H, 9.08.



### 3.5.2 9,11-Dioxododecanoic Acid (**27**)



Following the procedure outlined in section 3.2.6, the alcohol **54** (750 mg, 3.50 mmol) was converted to the corresponding acid **27**. The crude product was purified by recrystallization from hexanes to give the acid **27** (480 mg, 60%) as a colorless solid, which was one spot by TLC.

**R<sub>f</sub>** (5% HOAc in 3:1 petroleum ether : ethyl acetate eluent) 0.48.

**mp** 41.5 °C.

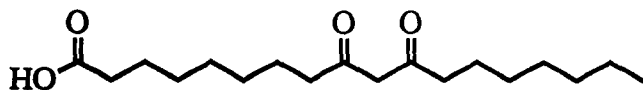
**<sup>1</sup>H NMR** (400 MHz, CDCl<sub>3</sub>) δ 15.48 (0.8H, s), 5.48 (0.8H, s), 3.57 (0.4H, s), 2.48 (0.4H, t), 2.39 (2H, t), 2.23 (1.6H, t), 2.21 (0.6H, s), 2.03 (2.4H, s), 1.66-1.28 (11H, m).

**IR** (CHCl<sub>3</sub>, cm<sup>-1</sup>) 3340-2500, 2935, 2860, 1712, 1607, 1460, 1410, 1364, 1290, 1135, 1097, 954, 915.

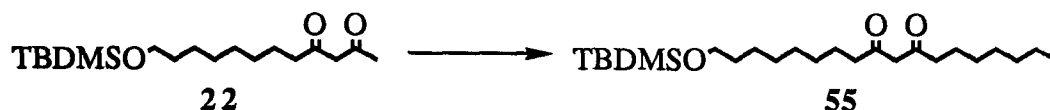
**LRMS** (m/z) 228 (M<sup>+</sup>, 0.4), 210 (0.4), 195 (0.3), 193 (0.4), 191 (0.3), 186 (0.6), 184 (0.6), 182 (0.5), 171 (3), 169 (3), 168 (9), 141 (1), 140 (5), 113 (3), 112 (3), 111 (35), 101 (3), 100 (9), 99 (3), 98 (18), 97 (15), 85 (20), 84 (14), 83 (39), 82 (13), 81 (11), 73 (17), 72 (4), 71 (29), 70 (7), 69 (28), 68 (10), 67 (15), 60 (23), 59 (17), 58 (97), 57 (11), 56 (9), 55 (60), 45 (17), 44 (14), 43 (100), 42 (12), 41 (27).

**HRMS** calcd for C<sub>12</sub>H<sub>20</sub>O<sub>4</sub>: 228.1356, found: 228.1362.

### 3.6 Synthesis of 9,11-Dioxooctadecanoic Acid (28)



#### 3.6.1 18-(Tert-butyldimethylsilyloxy)-8,10-octadecanedione (55)



Following the procedure outlined in section 3.2.4, the  $\beta$ -diketone **22** (4.00 g, 12.2 mmol) was alkylated with freshly distilled 1-bromohexane (1.81 g, 11.0 mmol) to give the corresponding  $\beta$ -diketone **55**. The crude product was purified by column chromatography using petroleum ether : ethyl acetate (20:1) as eluent to give the  $\beta$ -diketone **55** (3.50 g, 85 % based on the recovered  $\beta$ -diketone **22**) as a clear oil, which was one spot by TLC.

**R<sub>f</sub>** (6:1 petroleum ether : ethyl acetate eluent) 0.76.

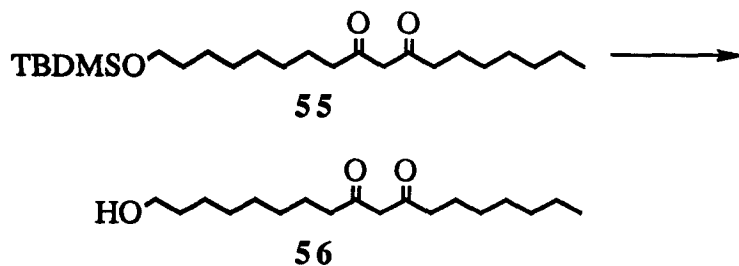
**<sup>1</sup>H NMR** (400 MHz, CDCl<sub>3</sub>)  $\delta$  15.50 (0.8H, s) 5.48 (0.8H, s), 3.61 (2H, t), 3.53 (0.4H, s), 2.50 (0.8H, t), 2.27 (3.2H, t), 1.66-1.25 (22H, m), 0.90 (9H, s), 0.88 (3H, t), 0.06 (6H, s).

**IR** (neat, cm<sup>-1</sup>) 2931, 2857, 1711, 1612, 1463, 1392, 1365, 1252, 1101, 837, 776.

**LRMS** (m/z) 397 (M<sup>+</sup> - CH<sub>3</sub>, 2.4), 357 (7), 356 (26), 355 (100), 314 (0.4), 313 (2), 272 (0.2), 271 (1), 269 (0.4), 171 (2), 170 (1), 169 (4), 128 (2), 127 (7), 109 (2), 107 (3), 100 (1), 99 (1), 97 (2), 95 (3), 93 (2), 89 (2), 85 (4), 83 (2), 82 (1), 81 (4), 77 (2), 76 (1), 75 (18), 73 (8), 71 (2), 69 (6), 67 (3), 61 (1), 59 (2), 58 (1), 57 (16), 55 (10), 43 (7), 42 (1) 41 (6).

**HRMS** calcd for C<sub>24</sub>H<sub>48</sub>SiO<sub>3</sub> - CH<sub>3</sub>: 397.3126, found: 397.3137.

### 3.6.2 18-Hydroxyl-8,10-octadecanedione (**56**)



Following the procedure outlined in section 3.2.5, the silyl ether **55** (2.66 g, 6.46 mmol) was converted to the corresponding alcohol **56**. The crude product was purified by recrystallization from hexanes to give the alcohol **56** (1.68 g, 87%) as a colorless solid, which was one spot by TLC.

**R<sub>f</sub>** (1:1 petroleum ether : ethyl acetate eluent) 0.62.

**mp** 56.0 °C.

**<sup>1</sup>H NMR** (400 MHz, CDCl<sub>3</sub>) δ 15.50 (0.8H, s), 5.48 (0.8H, s), 3.66 (2H, t), 3.53 (0.4H, s), 2.51 (0.8H, t), 2.27 (3.2H, t), 1.66-1.20 (23H, m), 0.88 (3H, t).

**IR** (CHCl<sub>3</sub>, cm<sup>-1</sup>) 3623, 3460, 2932, 2857, 1724, 1708, 1604, 1460, 1372, 1294, 1146, 1112, 917.

**LRMS** (m/z) 298 (M<sup>+</sup>, 3.1), 281 (1), 280 (4), 262 (1), 238 (0.6), 237 (1), 215 (1), 214 (6), 198 (2), 197 (14), 185 (4), 184 (24), 170 (7), 169 (58), 167 (4), 140 (4), 139 (27), 138 (12), 137 (5), 128 (14), 127 (100), 126 (9), 125 (6), 124 (7), 123 (7), 114 (7), 113 (32), 112 (6), 111 (14), 110 (5), 109 (14), 101 (9), 100 (88), 99 (5), 98 (9), 97 (31), 96 (5), 95 (10), 85 (32), 84 (11), 83 (12), 71 (7), 70 (3), 69 (22), 68 (2), 67 (5), 58 (3), 57 (16), 56 (2), 55 (11).

**HRMS** calcd for C<sub>18</sub>H<sub>34</sub>O<sub>3</sub>: 298.2499, found: 298.2499.

### 3.6.3 9,11-Dioxooctadecanoic Acid (**28**)



Following the procedure outlined in section 3.2.6, the alcohol **56** (850 mg, 2.85 mmol) was converted to the corresponding acid **28**. The crude product was purified by recrystallization from hexanes to give the acid **28** (500 mg, 56%) as a clear solid, which was one spot by TLC.

**R<sub>f</sub>** (5% HOAc in 3:1 petroleum ether : ethyl acetate eluent) 0.55.

**mp** 57.0 °C.

**<sup>1</sup>H NMR** (300 MHz, CDCl<sub>3</sub>) δ 15.50 (0.8H, s), 5.48 (0.8H, s), 3.53 (0.4H, s), 2.50 (0.8H, t), 2.36 (2H, t), 2.28 (3.2H, t), 1.70-1.24 (21H, m), 0.90 (3H, t).

**IR** (CHCl<sub>3</sub>, cm<sup>-1</sup>) 3310-2480, 2932, 2859, 1707, 1609, 1466, 1407, 1290, 1132, 951, 916.

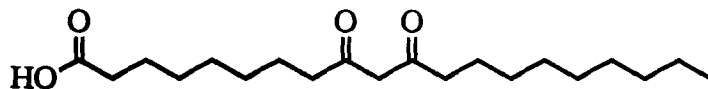
**IR** (KBr, cm<sup>-1</sup>) 3543, 3483, 2931, 2849, 1719, 1688, 1642, 1461, 1440, 1421, 1310, 1237, 1188, 1138, 903.

**LRMS** (m/z) 312 (M<sup>+</sup>, 5.9), 295 (1), 294 (3), 277 (0.5), 276 (2), 267 (0.6), 266 (2), 249 (0.2), 248 (1), 229 (3), 228 (21), 211 (2), 210 (9), 198 (2), 197 (13), 196 (4), 195 (26), 185 (4), 184 (22), 183 (3), 182 (13), 172 (7), 171 (77), 170 (9), 169 (71), 168 (4), 154 (2), 153 (11), 152 (11), 151 (8), 128 (10), 127 (76), 126 (12), 125 (33), 124 (11), 114 (6), 113 (30), 112 (6), 111 (16), 101 (10), 100 (100), 99 (7), 98 (17), 97 (40), 96 (4), 95 (7), 86 (4), 85 (62), 84 (20), 83 (32), 82 (6), 81 (14), 71 (15), 70 (5), 69 (37), 68 (5), 67 (12), 57 (54), 55 (49), 43 (40), 41 (21).

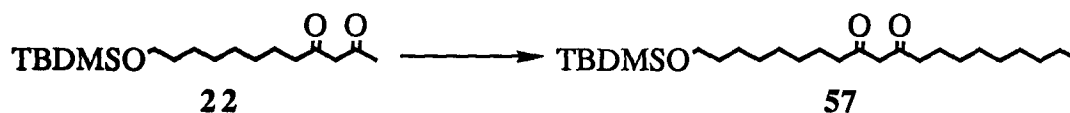
**HRMS** calcd for C<sub>18</sub>H<sub>32</sub>O<sub>4</sub>: 312.2292, found: 312.2293.

**Elem. Anal.** calcd for C<sub>18</sub>H<sub>32</sub>O<sub>4</sub>: C, 69.23; H, 10.33. found: C, 69.22; H, 10.33.

### 3.7 Synthesis of 9,11-Dioxoeicosanoic Acid (29)



#### 3.9.1 1-(Tert-butyldimethylsilyloxy)-9,11-eicosanedione (57)



Following the procedure outlined in section 3.2.4, the  $\beta$ -diketone **22** (1.97 g, 6.0 mmol) was alkylated with freshly distilled 1-bromooctane (1.04 g, 5.4 mmol) to give the  $\beta$ -diketone **57**. The crude product was purified by column chromatography using petroleum ether : ethyl acetate (20:1) as eluent to give the  $\beta$ -diketone **57** (1.52 g, 73 % based on the recovered  $\beta$ -diketone **22**) as a clear oil, which was one spot by TLC.

**R<sub>f</sub>** (6:1 petroleum ether : ethyl acetate eluent) 0.78.

**<sup>1</sup>H NMR** (400 MHz, CDCl<sub>3</sub>)  $\delta$  15.50 (0.8H, s), 5.48 (0.8H, s), 3.61 (2H, t), 3.54 (0.4H, s), 2.50 (0.8H, t), 2.27 (3.2H, m), 1.66-1.25 (26H, m), 0.90 (9H, s), 0.88 (3H, t), 0.07 (6H, s).

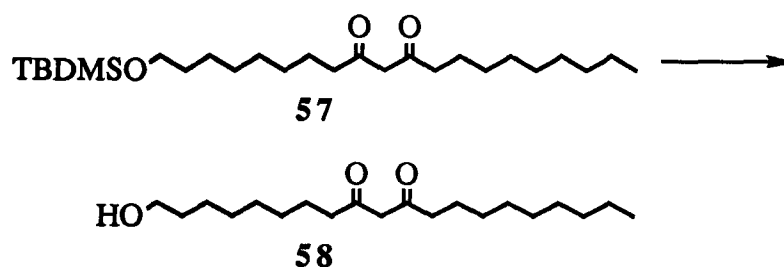
**IR** (neat, cm<sup>-1</sup>) 2930, 2856, 1707, 1611, 1463, 1366, 1253, 1100, 1044, 943, 837, 776.

**LRMS** (m/z) 440 (M<sup>+</sup>, 0.5), 386 (7), 385 (39), 384 (90), 383 (100), 366 (0.7), 365 (3), 326 (0.5), 297 (2), 284 (1), 283 (7), 272 (2), 271 (11), 230 (3), 229 (15), 172 (3), 171 (16), 170 (4), 169 (16), 157 (9), 156 (9), 155 (52), 132 (2), 131 (10), 129 (11), 128 (6), 116 (5), 115 (27), 110 (2), 109 (12), 108 (4), 107 (32), 102 (3), 101 (22), 100 (12), 99 (14), 98 (6), 97 (27), 95 (34), 90 (2), 89 (23), 88 (3), 87 (7), 86 (5), 85 (62), 84 (10), 83 (20), 82 (6), 81 (32), 76 (11), 75 (86), 74 (7), 73 (64), 72 (4), 71 (49), 70 (6), 69 (51).

**HRMS** calcd for C<sub>26</sub>H<sub>52</sub>SiO<sub>3</sub>: 440.3672, found: 440.3654.



### 3.7.2 1-Hydroxyl-9,11-eicosanedione (**58**)



Following the procedure outlined in section 3.2.5, the silyl ether **57** (1.40 g, 3.2 mmol) was converted to the corresponding alcohol **58**. The crude product was purified by recrystallization from hexanes to give the alcohol **58** (940 g, 91%) as a colorless solid, which was one spot by TLC.

**R<sub>f</sub>** (1:1 petroleum ether : ethyl acetate eluent) 0.65.

**mp** 64.5 °C.

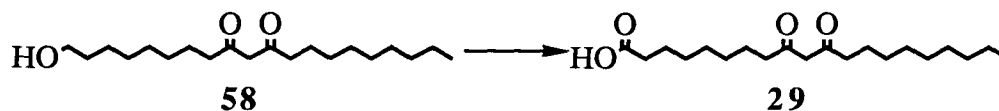
**<sup>1</sup>H NMR** (400 MHz, CDCl<sub>3</sub>) δ 15.50 (0.8H, s), 5.48 (0.8H, s), 3.66 (2H, t), 3.54 (0.4H, s), 2.50 (0.8H, t), 2.27 (3.2H, t), 1.64-1.22 (27H, m), 0.88 (3H, t).

**IR** (CHCl<sub>3</sub>, cm<sup>-1</sup>) 3622, 2930, 2857, 1724, 1700, 1608, 1460, 1364, 1308, 1047, 905.

**LRMS** (m/z) 326 (M<sup>+</sup>, 3.5), 309 (2), 308 (9), 291 (0.6), 290 (3), 279 (0.7), 278 (2), 266 (0.6), 265 (2), 254 (0.5), 253 (0.6), 252 (2), 227 (2), 226 (2), 225 (8), 215 (1), 214 (7), 213 (2), 212 (8), 199 (6), 198 (5), 197 (37), 196 (12), 195 (3), 194 (16), 158 (1), 157 (7), 156 (10), 155 (42), 142 (6), 141 (2), 140 (4), 139 (33), 138 (30), 137 (10), 136 (20), 135 (10), 125 (6), 124 (10), 123 (5), 122 (3), 121 (22), 120 (8), 119 (2), 114 (8), 113 (23), 112 (97), 111 (17), 109 (11), 108 (5), 107 (4), 101 (9), 100 (100), 99 (6), 98 (11), 97 (38), 96 (8), 95 (27), 94 (11), 93 (9), 86 (4), 85 (38), 84 (16), 83 (18), 82 (6), 81 (29), 71 (48), 70 (7), 69 (75), 67 (19), 57 (40), 55 (67).

**HRMS** calcd for C<sub>20</sub>H<sub>38</sub>O<sub>3</sub>: 326.2811, found: 326.2814.

### 3.7.3 9,11-Dioxoeicosanoic Acid (**29**)



Following the procedure outlined in section 3.2.6, the alcohol **58** (630 mg, 2.11 mmol) was converted to the corresponding acid **29**. The crude product was purified by recrystallization from hexanes to give the acid **29** (520 mg, 79%) as a clear solid, which was one spot by TLC.

**R<sub>f</sub>** (5% HOAc in 3:1 petroleum ether : ethyl acetate eluent) 0.56.

**mp** 64.0 °C.

**<sup>1</sup>H NMR** (300 MHz, CDCl<sub>3</sub>) δ 15.50 (0.8H, s), 5.48 (0.8H, s), 3.53 (0.4H, s), 2.49 (0.8H, t), 2.36 (2H, t), 2.28 (3.2H, t), 1.70-1.22 (25H, m), 0.90 (3H, t).

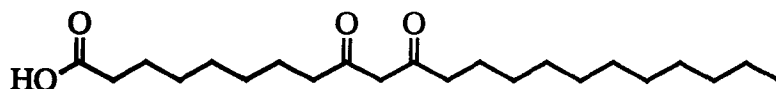
**IR** (CHCl<sub>3</sub>, cm<sup>-1</sup>) 3355-2490, 2931, 2858, 1708, 1606, 1459, 1413, 1292, 1134, 1104, 953.

**LRMS** (m/z) 340 (M<sup>+</sup>, 2.8), 323 (1), 322 (3), 305 (0.7), 304 (1), 295 (0.5), 294 (2), 282 (0.7), 281 (1), 229 (3), 228 (17), 226 (2), 225 (12), 198 (9), 197 (61), 196 (5), 195 (31), 183 (2), 182 (14), 172 (10), 171 (100), 170 (3), 169 (8), 168 (4), 167 (11), 156 (10), 155 (70), 154 (7), 153 (13), 144 (2), 143 (17), 141 (4), 140 (5), 127 (7), 126 (8), 125 (45), 124 (11), 115 (3), 114 (6), 113 (26), 102 (1), 101 (11), 100 (94), 99 (6), 98 (20), 97 (53), 96 (5), 95 (14), 93 (5), 86 (4), 85 (45), 84 (23), 83 (41), 82 (8), 81 (19), 80 (4), 71 (46), 70 (8), 69 (29), 68 (7), 67 (12), 58 (10), 57 (34), 56 (8), 55 (65).

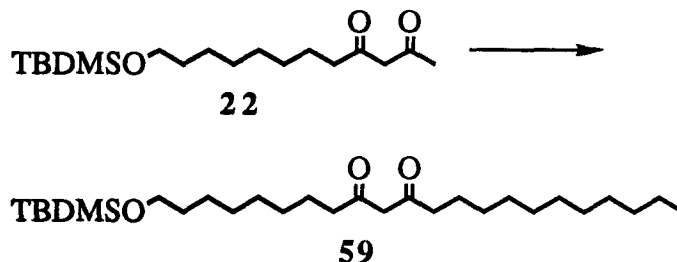
**HRMS** calcd for C<sub>20</sub>H<sub>36</sub>O<sub>4</sub>: 340.2604, found: 340.2620.

**Elem. Anal.** calcd for C<sub>20</sub>H<sub>36</sub>O<sub>4</sub>: C, 70.59; H, 10.58. found: C, 70.32; H, 10.66.

### 3.8 Synthesis of 9,11-Dioxodoeicosanoic Acid (30)



#### 3.8.1 1-(Tert-butyltrimethylsilyloxy)-9,11-doeicosanedione (59)



Following the procedure outlined in section 3.2.4, the  $\beta$ -diketone **22** (1.67 g, 5.1 mmol) was alkylated with freshly distilled 1-bromodecane (1.12 g, 5.1 mmol) to give the  $\beta$ -diketone **59**. The crude product was purified by column chromatography using petroleum ether : ethyl acetate (20:1) as eluent to give the  $\beta$ -diketone **59** (0.95 g, 70% based on the recovered  $\beta$ -diketone **22**) as a clear oil, which was one spot by TLC.

**R<sub>f</sub>** (6:1 petroleum ether : ethyl acetate eluent) 0.80.

**<sup>1</sup>H NMR** (400 MHz, CDCl<sub>3</sub>)  $\delta$  15.50 (0.8H, s), 5.48 (0.8H, s), 3.60 (2H, t), 3.54 (0.4H, s), 2.50 (0.8H, t), 2.27 (3.2H, m), 1.66-1.22 (30H, m), 0.90 (9H, s), 0.89 (3H, t), 0.07 (6H, s).

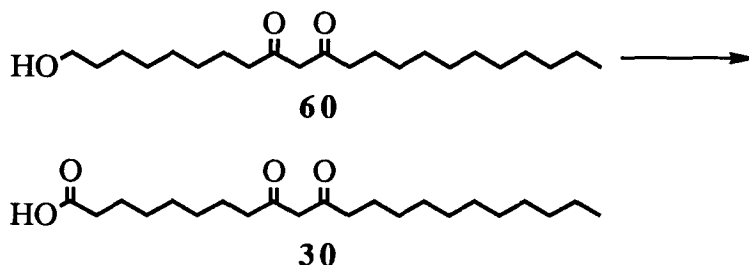
**IR** (neat, cm<sup>-1</sup>) 2928, 2856, 1711, 1611, 1463, 1390, 1365, 1252, 1101, 1011, 944, 837.

**LRMS** (m/z) 467 (M<sup>+</sup>, 0.7), 453 (2), 439 (0.4), 412 (33), 413 (7), 412 (33), 411 (100), 384 (8), 383 (36), 313 (2), 283 (2), 272 (0.5), 271 (4), 263 (0.4), 262 (2), 230 (0.6), 229 (2), 187 (1), 185 (1), 183 (6), 181 (2), 171 (3), 170 (1), 169 (3), 157 (2), 156 (1), 155 (5), 110 (1), 109 (5), 108 (2), 107 (10), 100 (3), 99 (5), 98 (2), 97 (8), 96 (1), 95 (10), 85 (14), 84 (2), 83 (10), 76 (4), 75 (50), 74 (3), 73 (19), 59 (5), 58 (5), 57 (18), 56 (7), 55 (27).

**HRMS** calcd for C<sub>28</sub>H<sub>56</sub>SiO<sub>3</sub>: 467.3906, found: 467.3960.



### 3.8.3 9,11-Dioxodoeicosanoic Acid (**30**)



Following the procedure outlined in section 3.2.6, the alcohol **60** (450 mg, 1.27 mmol) was converted to the acid **30**. The crude product was purified by recrystallization from hexanes to give the acid **30** (140 mg, 34%) as a colorless solid, which was one spot by TLC.

**R<sub>f</sub>** (5% HOAc in 3:1 petroleum ether : ethyl acetate eluent) 0.57.

**mp** 69.5 °C.

**<sup>1</sup>H NMR** (300 MHz, CDCl<sub>3</sub>) δ 15.50 (0.8H, s), 5.48 (0.8H, s), 3.54 (0.4H, s), 2.50 (0.8H, t), 2.36 (2H, t), 2.26 (3.2H, t), 1.72-1.22 (29H, m), 0.89 (3H, t).

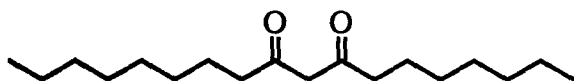
**IR** (CHCl<sub>3</sub>, cm<sup>-1</sup>) 3370-2510, 2929, 2857, 1718, 1607, 1460, 1408, 1292, 1135, 1090, 952.

**LRMS** (m/z) 368 (M<sup>+</sup>, 9.8), 351 (3), 350 (10), 333 (1), 332 (3), 323 (0.7), 322 (3), 305 (0.4), 304 (2), 280 (0.6), 279 (1), 254 (2), 253 (11), 241 (4), 240 (10), 229 (5), 228 (36), 226 (8), 225 (51), 211 (4), 210 (17), 196 (4), 195 (32), 184 (5), 183 (32), 182 (18), 172 (9), 171 (83), 151 (5), 150 (24), 149 (5), 126 (10), 125 (35), 124 (12), 114 (5), 113 (22), 112 (97), 111 (18), 110 (6), 109 (12), 108 (6), 107 (11), 101 (10), 100 (100), 99 (8), 98 (18), 97 (48), 96 (5), 95 (17), 85 (33), 84 (21), 83 (40), 71 (34), 70 (7), 69 (27), 58 (10), 57 (54), 56 (10), 55 (86).

**HRMS** calcd for C<sub>22</sub>H<sub>40</sub>O<sub>4</sub>: 368.2916, found: 368.2935.

**Elem. Anal.** calcd for C<sub>22</sub>H<sub>40</sub>O<sub>4</sub>: C, 71.74; H, 10.87. found: C, 71.20; H, 10.94.

### 3.9 Synthesis of 8,10-Octadecanedione (31)



#### 3.9.1 2,4-Undecanedione (61)



Following the procedure outlined in section 3.2.3, 2,4-pentanedione (**7**) (4.10 mL, 40.0 mmol) was alkylated with 1-bromohexane (4.50 mL, 32.0 mmol) to give the  $\beta$ -diketone **61**. Distillation of the crude product under reduced pressure (155 °C/50 torr) gave the purified  $\beta$ -diketone **61** (3.70 g, 63 %) as a colorless oil, which was one spot by TLC.

**R<sub>f</sub>** (6:1 petroleum ether : ethyl acetate eluent) 0.60.

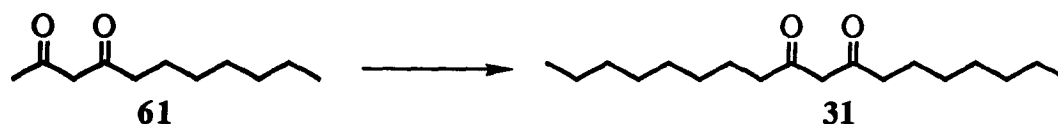
**<sup>1</sup>H NMR** (400 MHz, CDCl<sub>3</sub>)  $\delta$  15.50 (0.8H, s), 5.49 (0.8H, s), 3.58 (0.4H, s), 2.51 (0.4H, t), 2.27 (1.6H, t), 2.26 (0.6H, s), 2.06 (2.4H, s), 1.65-1.20 (10H, m), 0.89 (3H, t).

**IR** (neat, cm<sup>-1</sup>) 2930, 2858, 1711, 1613, 1446, 1364, 1254, 947.

**LRMS** (m/z) 184 (M<sup>+</sup>, 20), 170 (1), 169 (10), 167 (1), 166 (10), 143 (1), 142 (15), 128 (8), 127 (24), 126 (8), 114 (9), 113 (70), 101 (28), 100 (33), 99 (5), 98 (11), 97 (8), 86 (15), 85 (37), 84 (17), 83 (10), 82 (10), 81 (7), 73 (2), 72 (44), 71 (2), 70 (4), 69 (17), 68 (3), 67 (13), 59 (8), 58 (54), 57 (100), 56 (9), 55 (25), 44 (8), 43 (50), 42 (16), 41 (53).

**HRMS** calcd for C<sub>11</sub>H<sub>20</sub>O<sub>2</sub>: 184.1458, found: 184.1459.

### 3.9.2 8.10-Octadecanedione (**31**)



Following the procedure outlined in section 3.2.4, the  $\beta$ -diketone **61** (756 mg, 4.11 mmol) was alkylated with 1-bromoheptane (660 mg, 3.69 mmol) to give the  $\beta$ -diketone **30**. Purification of the crude product by column chromatography using petroleum ether : ethyl acetate (20:1) gave the desired  $\beta$ -diketone **31** (803 mg, 77%) as a colorless oil, which was one spot by TLC.

**R<sub>f</sub>** (6:1 petroleum ether : ethyl acetate eluent) 0.78.

**<sup>1</sup>H NMR** (400 MHz, CDCl<sub>3</sub>)  $\delta$  15.50 (0.8H, s), 5.48 (0.8H, s), 3.53 (0.4H, s), 2.50 (0.8H, t), 2.26 (3.2H, t), 1.64 - 1.22 (22H, m), 0.89 (6H, t).

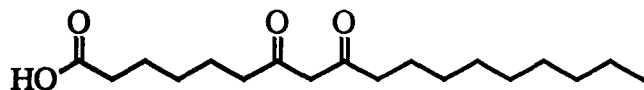
**IR** (neat, cm<sup>-1</sup>) 2934, 2857, 1704, 1613, 1455, 1276, 1142, 1102, 942.

**LRMS** (m/z) 282 (M<sup>+</sup>, 4.6), 265 (0.7), 264 (3), 241 (0.3), 240 (2), 227 (0.2), 226 (2), 212 (2), 211 (10), 199 (3), 198 (14), 197 (110), 185 (4), 184 (24), 183 (36), 170 (6), 169 (42), 142 (20), 141 (80), 139 (3), 138 (6), 128 (13), 127 (100), 126 (9), 114 (6), 113 (38), 112 (4), 111 (6), 101 (7), 100 (97), 99 (7), 98 (12), 97 (16), 86 (3), 85 (52), 84 (14), 71 (30), 70 (4), 69 (14), 58 (5), 57 (36), 56 (4), 55 (14).

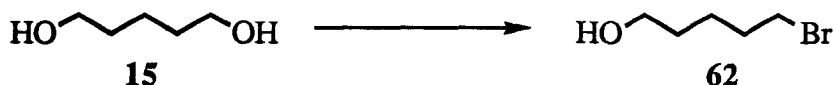
**HRMS** calcd for C<sub>18</sub>H<sub>34</sub>O<sub>2</sub>: 282.2550, found: 282.2565.

**Elem. Anal.** calcd for C<sub>18</sub>H<sub>34</sub>O<sub>2</sub>: C, 76.52; H, 12.14. found: C, 76.80; H, 12.16.

### 3.10 Synthesis of 7,9-Dioxooctadecanoic Acid (33)



#### 3.10.1 5-Bromo-1-pentanol (62)



Following the procedure outlined in section 3.2.1, 1,5-pentanediol (**15**) (15.0 g, 140 mmol) was converted to the corresponding bromide **62**. The crude product was purified by column chromatography using petroleum ether : ethyl acetate (6:1) as eluent to give the monobrominated alcohol **62** (12.4 g, 52%) as a colorless liquid, which was one spot by TLC.

**R<sub>f</sub>** (1:1 petroleum ether : ethyl acetate) 0.46.

**<sup>1</sup>H NMR** (400 MHz, CDCl<sub>3</sub>) δ 3.70 (2H, t), 3.42 (2H, t), 2.72 (1H, s), 1.92 (2H, p), 1.64 - 1.48 (4H, m).

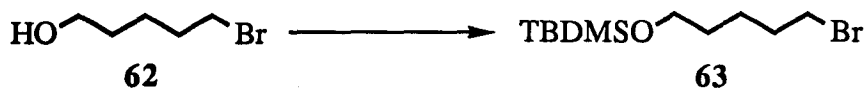
**IR** (neat, cm<sup>-1</sup>) 3346, 2936, 2865, 1456, 1434, 1274, 1238, 1137, 1061, 1014, 984, 950, 734.

**LRMS** (m/z) 167 (Br<sup>81</sup>: M<sup>+</sup> - H, 0.1), 165 (Br<sup>79</sup>: M<sup>+</sup> - H, 0.1), 137 (3), 135 (3), 123 (0.3), 121 (0.3), 109 (2), 107 (2), 97 (5), 87 (1), 86 (2), 85 (4), 84 (1), 79 (4), 71 (2), 70 (8), 69 (100), 68 (18), 67 (10), 57 (15), 56 (16), 55 (40), 45 (8), 44 (7), 43 (17), 42 (17), 41 (73).

**HRMS** calcd for C<sub>5</sub>H<sub>11</sub>Br<sup>81</sup>O - H: 166.9892, found: 166.9902; calcd for C<sub>5</sub>H<sub>11</sub>Br<sup>79</sup>O - H: 164.9912, found: 164.9911.



### 3.10.2 1-Bromo-5-(tert-butyldimethylsilyloxy)-pentane (**63**)



Following the procedure outlined in section 3.2.2, the alcohol **62** (2.90 g, 17.4 mmol) was converted to the corresponding ether **63**. The crude product was purified by column chromatography using petroleum ether : ethyl acetate (15:1) as eluent to give the silyl ether **63** (3.81 g, 81%) as a colorless oil, which was one spot by TLC.

**R<sub>f</sub>** (6:1 petroleum ether : ethyl acetate) 0.80.

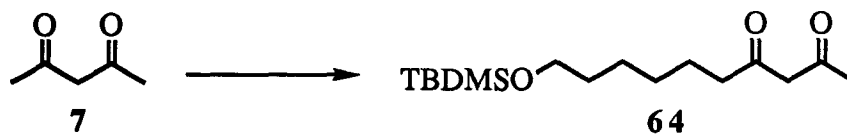
**<sup>1</sup>H NMR** (400 MHz, CDCl<sub>3</sub>) δ 3.61 (2H, t), 3.41 (2H, t), 1.88 (2H, p), 1.58-1.45 (4H, m), 0.90 (9H, s), 0.07 (6H, s).

**IR** (neat, cm<sup>-1</sup>) 2940, 2858, 1467, 1388, 1361, 1254, 1102, 1006, 835, 775.

**LRMS** (m/z) 281 (Br<sup>81</sup>: M<sup>+</sup> - H, 0.2), 227 (0.4), 225 (0.4), 201 (0.1), 181 (0.1), 171 (0.2), 169 (2), 167 (2), 139 (3), 137 (3), 89 (2), 87 (1), 85 (2), 81 (2), 77 (1), 76 (1), 75 (16), 73 (11), 71 (2), 70 (6), 69 (100), 68 (2), 67 (3), 59 (5), 58 (2), 57 (5), 56 (3), 55 (5), 53 (1), 43 (5), 42 (3), 41 (25).

**HRMS** calcd for C<sub>11</sub>H<sub>25</sub>SiBr<sup>81</sup>O - H: 281.0753, found: 281.0527; calcd for C<sub>11</sub>H<sub>25</sub>SiBr<sup>79</sup>O - H: 279.0771, found: 279.0772.

### 3.10.3 10-(Tert-butyldimethylsilyloxy)-2,4-decanedione (**64**)



Following the procedure outlined in section 3.2.3, 2,4-pentanedione (**7**) (1.72 g, 17.2 mmol) was converted to the  $\beta$ -diketone **64**. The crude product was purified by column chromatography using petroleum ether : ethyl acetate (15:1) as eluent to give the  $\beta$ -diketone **64** (2.12 g, 60% based on the recovered bromide), which was one spot by TLC.

**R<sub>f</sub>** (6:1 petroleum ether : ethyl acetate) 0.56.

**<sup>1</sup>H NMR** (400 MHz, CDCl<sub>3</sub>)  $\delta$  15.50 (0.8 H, s), 5.49 (0.8 H, s), 3.60 (2H, t), 3.59 (0.4 H, s), 2.52 (0.4 H, t), 2.26 (1.6 H, t), 2.24 (0.6 H, s), 2.07 (2.4 H, s), 1.68-1.25 (8H, m), 0.90 (9H, s), 0.06 (6H, s).

**IR** (neat, cm<sup>-1</sup>) 2936, 2858, 1716, 1614, 1465, 1361, 1252, 1100, 1005, 936, 837, 775.

**LRMS** (m/z) 285 (M<sup>+</sup> - CH<sub>3</sub>, 7.5), 246 (1), 245 (10), 244 (40), 243 (100), 227 (2), 225 (2), 186 (3), 185 (20), 171 (4), 170 (2), 169 (13), 167 (3), 159 (2), 158 (2), 157 (7), 156 (3), 155 (7), 145 (5), 144 (2), 143 (11), 142 (1), 141 (3), 118 (1), 117 (11), 116 (3), 115 (29), 102 (2), 101 (14), 100 (5), 99 (9), 97 (4), 95 (6), 87 (11), 85 (53), 83 (14), 82 (2), 81 (14), 79 (10), 78 (2), 77 (30), 76 (19), 75 (97), 74 (10), 73 (81), 69 (31), 61 (22), 60 (5), 59 (36), 58 (13), 57 (17), 56 (9), 55 (58), 45 (22), 44 (6), 43 (90), 42 (7), 41 (59).

**HRMS** calcd for C<sub>16</sub>H<sub>32</sub>SiO<sub>3</sub> - CH<sub>3</sub>: 285.1879, found: 285.1884.

### 3.10.4 1-(Tert-butyldimethylsilyloxy)-7,9-octadecanedione (**65**)



Following the procedure outlined in section 3.2.4, the  $\beta$ -diketone **64** (1.2 g, 4.2 mmol) was alkylated with freshly distilled 1-bromooctane (0.77 g, 4.0 mmol) to give the  $\beta$ -diketone **65**. The crude product was purified by column chromatography using petroleum ether : ethyl acetate (20:1) as eluent to give the  $\beta$ -diketone **65** (0.77 g, 75 % based on the recovered  $\beta$ -diketone **64**) as a clear oil, which was one spot by TLC.

**R<sub>f</sub>** (6:1 petroleum ether : ethyl acetate) 0.74.

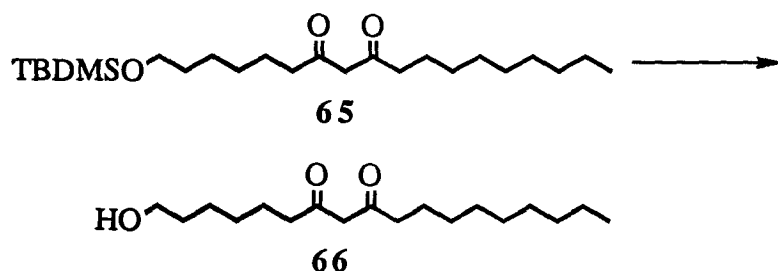
**<sup>1</sup>H NMR** (400 MHz, CDCl<sub>3</sub>)  $\delta$  15.50 (0.8H, s), 5.48 (0.8H, s), 3.61 (2H, t), 3.53 (0.4H, s), 2.50 (0.8H, dt), 2.27 (3.2H, dt), 1.66-1.22 (22H, m), 0.90 (9H, s), 0.89 (3H, t), 0.06 (6H, s).

**IR** (neat, cm<sup>-1</sup>) 2930, 2856, 1722, 1707, 1611, 1463, 1387, 1360, 1252, 1101, 1006, 937, 836, 812, 775.

**LRMS** (m/z) 412 (M<sup>+</sup>, 0.1), 398 (0.7), 397 (2), 357 (7), 356 (26), 355 (100), 297 (1), 283 (2), 282 (1), 281 (4), 271 (1), 270 (3), 269 (14), 257 (2), 256 (1), 255 (7), 187 (1), 186 (2), 185 (8), 171 (4), 170 (9), 169 (11), 167 (3), 157 (4), 156 (3), 155 (12), 114 (5), 113 (6), 111 (7), 110 (5), 109 (10), 86 (3), 85 (25), 84 (4), 83 (15), 77 (14), 76 (6), 75 (73), 74 (3), 73 (20), 72 (5), 71 (31), 70 (6), 69 (48), 57 (34), 56 (7), 55 (33), 43 (33), 42 (6), 41 (41).

**HRMS** calcd for C<sub>24</sub>H<sub>48</sub>SiO<sub>3</sub>: 412.3360, found: 412.3367.

### 3.10.5 1-Hydroxyl-7,9-octadecanedione (**66**)



Following the procedure outlined in section 3.2.5, the silyl ether **65** (640 mg, 1.55 mmol) was converted to the alcohol **66**. The crude product was purified by recrystallization from hexanes to give the alcohol **66** (410 mg, 89%) as a colorless solid, which was one spot by TLC.

**R<sub>f</sub>** (1:1 petroleum ether : ethyl acetate) 0.56.

**mp** 57.5 °C.

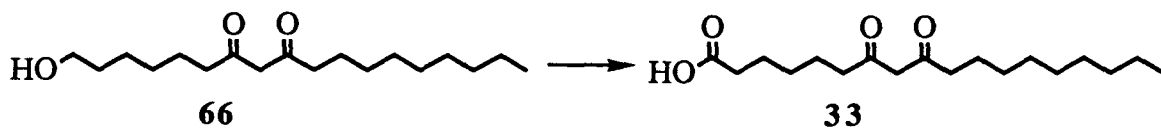
**<sup>1</sup>H NMR** (400 MHz, CDCl<sub>3</sub>) δ 15.50 (0.8H, s) 5.48 (0.8H, s), 3.64 (2H, t), 3.55 (0.4H, s), 2.51 (0.8H, dt), 2.27 (3.2H, dt), 1.70-1.18 (23H, m), 0.89 (3H, t).

**IR** (CHCl<sub>3</sub>, cm<sup>-1</sup>) 3623, 2930, 2858, 1607, 1459, 1329, 1141, 1052, 965, 904.

**LRMS** (m/z) 298 (M<sup>+</sup>, 1.0), 281 (1), 280 (3), 226 (2), 225 (10), 213 (2), 212 (8), 198 (7), 197 (56), 187 (1), 186 (12), 170 (3), 169 (5), 168 (11), 157 (2), 156 (15), 155 (86), 154 (7), 153 (21), 130 (4), 129 (39), 128 (6), 127 (34), 114 (6), 113 (33), 112 (10), 111 (56), 101 (8), 100 (100), 99 (10), 98 (15), 97 (27), 96 (5), 95 (18), 86 (5), 85 (54), 84 (22), 83 (57), 82 (10), 81 (46), 72 (5), 71 (58), 70 (10), 69 (75), 58 (15), 57 (42), 56 (8), 55 (77), 43 (47), 42 (7), 41 (26).

**HRMS** calcd for C<sub>18</sub>H<sub>34</sub>O<sub>3</sub>: 298.2499, found: 298.2505.

### 3.10.6 7,9-Dioxooctadecanoic Acid (**33**)



Following the procedure outlined in section 3.2.6, the alcohol **66** (298 mg, 1.00 mmol) was converted to the corresponding acid **33**. The crude product was purified by recrystallization from hexanes to give the acid **33** (210 mg, 67%) as a clear solid, which was one spot by TLC.

**R<sub>f</sub>** (5% HOAc in 3:1 petroleum ether : ethyl acetate) 0.52.

**mp** 58.0 °C.

**<sup>1</sup>H NMR** (300 MHz, CDCl<sub>3</sub>) δ 15.50 (0.8H, s), 5.49 (0.8H, s), 3.53 (0.4H, s), 2.51 (0.8H, dt), 2.36 (2H, t), 2.28 (3.2H, dt), 1.76-1.22 (21H, m), 0.90 (3H, t).

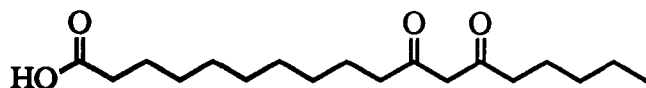
**IR** (CHCl<sub>3</sub>, cm<sup>-1</sup>) 3340-2490, 2930, 2858, 1709, 1607, 1460, 1409, 1291, 1131, 950, 907.

**LRMS** (m/z) 312 (M<sup>+</sup>, 4.1), 295 (1), 294 (4), 277 (2), 276 (4), 252 (1), 251 (2), 226 (1), 225 (8), 201 (4), 200 (30), 198 (9), 197 (53), 196 (2), 195 (9), 183 (4), 182 (27), 169 (4), 168 (6), 167 (32), 156 (8), 155 (49), 154 (9), 153 (6), 145 (2), 144 (8), 143 (100), 141 (9), 140 (28), 126 (9), 125 (88), 115 (9), 114 (13), 113 (20), 101 (10), 100 (51), 99 (14), 98 (32), 97 (61), 96 (12), 95 (24), 86 (7), 85 (42), 84 (23), 83 (26), 82 (8), 81 (24), 73 (26), 72 (4), 71 (53), 70 (20), 69 (85), 58 (14), 57 (38), 56 (11), 55 (78), 45 (7), 44 (33), 43 (46), 42 (12), 41 (27).

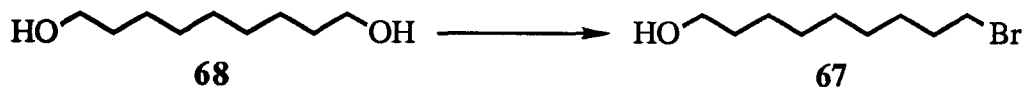
**HRMS** calcd for C<sub>18</sub>H<sub>32</sub>O<sub>4</sub>: 312.2292, found: 312.2291.

**Elem. Anal.** calcd for C<sub>18</sub>H<sub>32</sub>O<sub>4</sub>: C, 69.23; H, 10.33. found: C, 69.24; H, 10.33.

### 3.11 Synthesis of 11,13-Dioxooctadecanoic Acid (34)



#### 3.11.1 9-Bromo-1-nonanol (67)



Following the procedure outlined in section 3.2.1, 1,9-nonanediol (**68**) (10.0 g, 62.5 mmol) was converted to the corresponding bromide **67**. The crude product was purified by column chromatography using petroleum ether : ethyl acetate (6:1) as eluent to give the monobrominated alcohol **67** (9.78 g, 70%) as a colorless solid, which was one spot by TLC.

**R<sub>f</sub>** (1:1 petroleum ether : ethyl acetate) 0.58.

**mp** 34.0 °C.

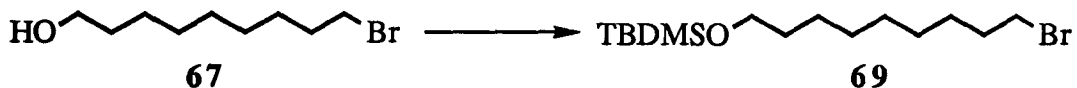
**<sup>1</sup>H NMR** (400 MHz, CDCl<sub>3</sub>) δ 3.64 (2H, t), 3.42 (2H, t), 1.83 (2H, p), 1.58 (2H, p), 1.48 - 1.30 (11H, m).

**IR** (CHCl<sub>3</sub>, cm<sup>-1</sup>): 3622, 3460, 2929, 2857, 1459, 1386, 1352, 1274, 1111, 1044, 889.

**LRMS** (m/z) 206 (Br<sup>81</sup>: M<sup>+</sup> - H<sub>2</sub>O, 0.1), 204 (Br<sup>79</sup>: M<sup>+</sup> - H<sub>2</sub>O, 0.1), 178 (12), 176 (12), 164 (21), 162 (22), 150 (35), 148 (36), 137 (50), 135 (50), 109 (10), 107 (10), 98 (11), 97 (68), 96 (11), 95 (18), 84 (10), 83 (63), 82 (42), 81 (40), 71 (7), 70 (40), 69 (88), 68 (50), 67 (39), 57 (43), 56 (48), 55 (100), 54 (38), 53 (23), 45 (9), 44 (13), 43 (62), 42 (51), 41 (86).

**HRMS** calcd for C<sub>9</sub>H<sub>19</sub>Br<sup>81</sup>O - H<sub>2</sub>O: 206.0489, found: 206.0494; calcd for C<sub>9</sub>H<sub>19</sub>Br<sup>79</sup>O - H<sub>2</sub>O: 204.0514, found: 204.0509.

### 3.11.2 1-Bromo-9-(tert-butyldimethylsilyloxy)-nonane (**69**)



Following the procedure outlined in section 3.2.2, the alcohol **67** (2.66 g, 11.9 mmol) was converted to the corresponding ether **69**. The crude product was purified by column chromatography using petroleum ether : ethyl acetate (15:1) as eluent to give the silyl ether **69** (3.60 g, 90%) as a colorless oil, which was one spot by TLC.

**R<sub>f</sub>** (6:1 petroleum ether : ethyl acetate) 0.84.

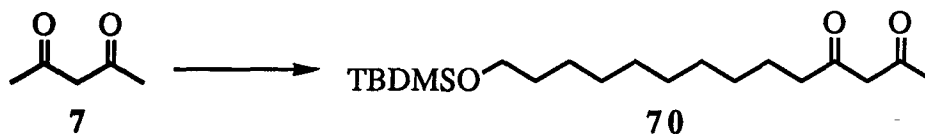
**<sup>1</sup>H NMR** (400 MHz, CDCl<sub>3</sub>)  $\delta$  3.60 (2H, t), 3.41 (2H, t), 1.86 (2H, p), 1.54 - 1.26 (12H, m), 0.89 (9H, s), 0.05 (6H, s).

**IR** (neat, cm<sup>-1</sup>) 2933, 2856, 1466, 1387, 1360, 1252, 1101, 1006, 839, 775, 717.

**LRMS** (m/z) 281 (Br<sup>81</sup>: M<sup>+</sup> - C<sub>4</sub>H<sub>9</sub>, 0.5), 279 (Br<sup>79</sup>: M<sup>+</sup> - C<sub>4</sub>H<sub>9</sub>, 0.5), 241 (0.3), 215 (0.1), 200 (2), 199 (13), 169 (14), 167 (14), 139 (15), 137 (14), 125 (11), 115 (9), 101 (14), 99 (7), 97 (1), 84 (10), 83 (97), 82 (3), 81 (14), 76 (9), 75 (92), 74 (4), 73 (36), 70 (13), 69 (100), 67 (11), 59 (10), 57 (25), 55 (55).

**HRMS** calcd for C<sub>15</sub>H<sub>33</sub>SiBr<sup>81</sup>O - C<sub>4</sub>H<sub>9</sub>: 281.0173, found: 281.0748; calcd for C<sub>15</sub>H<sub>33</sub>SiBr<sup>79</sup>O - C<sub>4</sub>H<sub>9</sub>: 279.0193, found: 279.0786.

### 3.11.3 14-(Tert-butyl(dimethyl)silyloxy)-2,4-tetradecanedione (70)



Following the procedure outlined in section 3.2.3, 2,4-pentanedione (**7**) (0.98 g, 9.4 mmol) was converted to the  $\beta$ -diketone **70**. The crude product was purified by column chromatography using petroleum ether : ethyl acetate (15:1) as eluent to give the  $\beta$ -diketone **70** (2.12 g, 79% based on the recovered bromide), which was one spot by TLC.

**R<sub>f</sub>** (6:1 petroleum ether : ethyl acetate) 0.66.

**<sup>1</sup>H NMR** (400 MHz, CDCl<sub>3</sub>)  $\delta$  15.50 (0.8H, s), 5.49 (0.8H, s), 3.59 (2H, t), 3.57 (0.4H, s), 2.49 (0.4H, t), 2.27 (1.6H, t), 2.24 (0.6H, s), 2.06 (2.4H, s), 1.65-1.24 (16H, m), 0.89 (9H, s), 0.06 (6H, s).

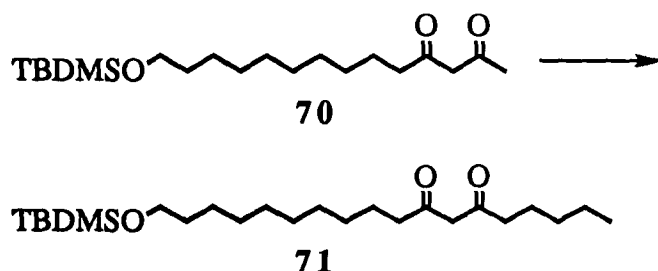
**IR** (neat, cm<sup>-1</sup>) 2932, 2856, 1709, 1616, 1465, 1387, 1361, 1251, 1100, 1006, 940, 838, 813, 776.

**LRMS** (m/z) 355 (M<sup>+</sup> - H, 0.1), 301 (6), 300 (25), 299 (100), 298 (0.1), 281 (0.1), 169 (4), 157 (2), 145 (1), 143 (3), 117 (0.7), 115 (4), 101 (3), 99 (2), 97 (1), 95 (4), 93 (2), 89 (3), 85 (14), 83 (1), 81 (6), 77 (5), 76 (2), 75 (46), 73 (13), 69 (8), 67 (6), 59 (6), 55 (14), 43 (29), 41 (15).

**HRMS** calcd for C<sub>20</sub>H<sub>40</sub>SiO<sub>3</sub> - H: 355.2658, found: 355.2676.



### 3.11.4 18-(Tert-butyldimethylsilyloxy)-6, 8-octadecanedione (**71**)



Following the procedure outlined in section 3.2.4, the  $\beta$ -diketone **70** (1.2 g, 3.2 mmol) was alkylated with freshly distilled 1-bromobutane (0.60 g, 3.2 mmol) to give the  $\beta$ -diketone **71**. The crude product was purified by column chromatography using petroleum ether : ethyl acetate (20:1) as eluent to give the  $\beta$ -diketone **71** (0.65 g, 77% based on the recovered  $\beta$ -diketone **70**) as a clear oil, which was one spot by TLC.

**R<sub>f</sub>** (6:1 petroleum ether : ethyl acetate) 0.77.

**<sup>1</sup>H NMR** (400 MHz, CDCl<sub>3</sub>)  $\delta$  15.52 (0.8H, s), 5.49 (0.8H, s), 3.61 (2H, t), 3.54 (0.4H, s), 2.49 (0.8H, t), 2.27 (3.2H, m), 1.66-1.22 (22H, m), 0.90 (12H, s), 0.06 (6H, s).

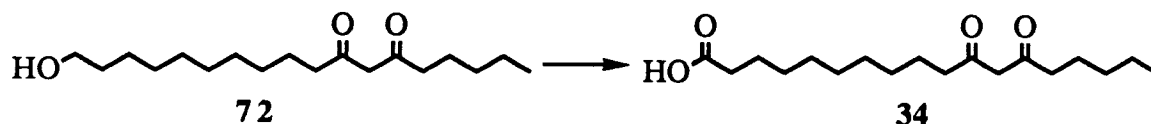
**IR** (neat, cm<sup>-1</sup>) 2934, 2856, 1730, 1707, 1612, 1463, 1386, 1361, 1252, 1100, 1006, 940, 838.

**LRMS** (m/z) 411 (M<sup>+</sup> - H, 0.2), 399 (0.2), 398 (1), 397 (3), 357 (8), 356 (30), 355 (100), 341 (2), 339 (2), 337 (2), 300 (0.4), 299 (2), 279 (0.6), 278 (1), 262 (2), 242 (0.5), 241 (3), 226 (2), 225 (7), 170 (2), 169 (11), 168 (1), 167 (3), 159 (2), 157 (3), 156 (3), 155 (3), 149 (8), 147 (8), 130 (2), 129 (28), 112 (8), 111 (12), 100 (7), 99 (25), 98 (2), 97 (12), 86 (2), 85 (16), 84 (7), 83 (19), 76 (6), 75 (64), 74 (2), 73 (19), 72 (4), 71 (42), 58 (4), 57 (33), 56 (10), 55 (36), 45 (10), 44 (3), 43 (36), 42 (7), 41 (33).

**HRMS** calcd for C<sub>24</sub>H<sub>48</sub>SiO<sub>3</sub> - H: 411.3282, found: 411.3287.



### 3.11.6 11, 13-Dioxooctadecanoic Acid (**34**)



Following the procedure outlined in section 3.2.6, the alcohol **72** (200 mg, 0.67 mmol) was converted to the acid **34**. The crude product was purified by recrystallization from hexanes to give the acid **34** (130 mg, 64%) as a colorless solid, which was one spot by TLC.

**R<sub>f</sub>** (5% HOAc in 3:1 petroleum ether : ethyl acetate) 0.56.

**mp** 56.5 °C.

**<sup>1</sup>H NMR** (300 MHz, CDCl<sub>3</sub>) δ 15.50 (0.8H, s), 5.48 (0.8H, s), 3.55 (0.4H, s), 2.50 (0.8H, t), 2.35 (2H, t), 2.27 (3.2H, t), 1.70-1.22 (21H, m), 0.90 (3H, t).

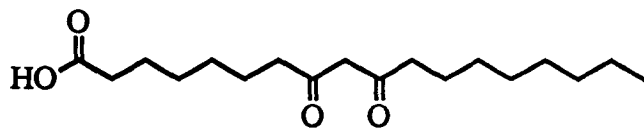
**IR** (CHCl<sub>3</sub>, cm<sup>-1</sup>) 3350-2500, 2933, 2859, 1710, 1605, 1458, 1395, 1281, 1138, 1047, 951, 879.

**LRMS** (m/z) 312 (M<sup>+</sup>, 6.1), 296 (0.8), 295 (5), 278 (0.4), 277 (2), 256 (8), 239 (6), 224 (4), 223 (26), 200 (5), 199 (33), 157 (7), 156 (39), 142 (11), 141 (65), 139 (11), 138 (18), 137 (4), 136 (4), 135 (21), 114 (13), 113 (27), 112 (13), 111 (23), 101 (10), 100 (68), 99 (72), 98 (38), 97 (47), 96 (7), 95 (22), 93 (12), 85 (43), 84 (42), 83 (38), 82 (7), 81 (28), 73 (25), 72 (9), 71 (75), 69 (85), 68 (12), 67 (36), 60 (37), 59 (12), 58 (24), 57 (51), 56 (23), 55 (88), 45 (36), 44 (17), 43 (100), 42 (52), 41 (81).

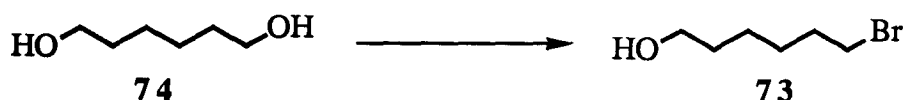
**HRMS** calcd for C<sub>18</sub>H<sub>32</sub>O<sub>4</sub>: 312.2292, found: 312.2294.

**Elem. Anal.** calcd for C<sub>18</sub>H<sub>32</sub>O<sub>4</sub>: C, 69.23; H, 10.33. found: C, 68.94; H, 10.25.

### 3.12 Synthesis of 8,10-Dioxooctadecanoic Acid (35)



#### 3.12.1 6-Bromo-1-hexanol (73)



Following the procedure outlined in section 3.2.1, 1,6-hexanediol (**74**) (5.9 g, 50 mmol) was converted to the corresponding bromide **73**. The crude product was purified by column chromatography using petroleum ether : ethyl acetate (6:1) as eluent to give the monobrominated alcohol **73** (4.2 g, 46%) as a colorless liquid, which was one spot by TLC.

**R<sub>f</sub>** (1:1 petroleum ether : ethyl acetate) 0.48.

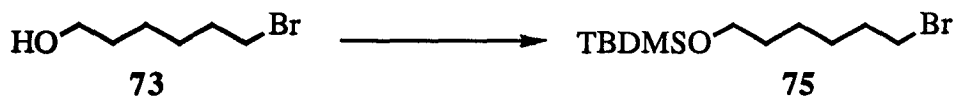
**<sup>1</sup>H NMR** (400 MHz, CDCl<sub>3</sub>)  $\delta$  3.68 (2H, t), 3.43 (2H, t), 1.88 (2H, p), 1.62 (2H, p), 1.52 - 1.34 (5H, m).

**IR** (neat, cm<sup>-1</sup>): 3335, 2932, 2860, 1447, 1260, 1055.

**LRMS** (*m/z*) 181 (Br<sup>81</sup>: M<sup>+</sup> - H, 1.0), 179 (Br<sup>79</sup>: M<sup>+</sup> - H, 1.2), 164 (3), 162 (3), 137 (3), 136 (19), 135 (3), 134 (19), 117 (11), 109 (5), 107 (6), 101 (12), 100 (6), 99 (18), 85 (21), 84 (10), 83 (100), 82 (38), 81 (19), 70 (6), 69 (28), 68 (6), 64 (27), 57 (17), 56 (11), 55 (86), 54 (10), 53 (5), 43 (6), 42 (6), 41 (12).

**HRMS** calcd for C<sub>6</sub>H<sub>13</sub>Br<sup>81</sup>O - H: 181.0048, found: 181.0043; calcd for C<sub>6</sub>H<sub>13</sub>Br<sup>79</sup>O - H: 179.0068, found: 179.0063.

### 3.12.2 1-Bromo-6-(tert-butyldimethylsilyloxy)-hexane (**75**)



Following the procedure outlined in section 3.2.2, the alcohol **73** (2.86 g, 15.8 mmol) was converted to the ether **75**. The crude product was purified by column chromatography using petroleum ether : ethyl acetate (15:1) as eluent to give the silyl ether **75** (4.12 g, 88%) as a colorless oil, which was one spot by TLC.

**R<sub>f</sub>** (6:1 petroleum ether : ethyl acetate) 0.82.

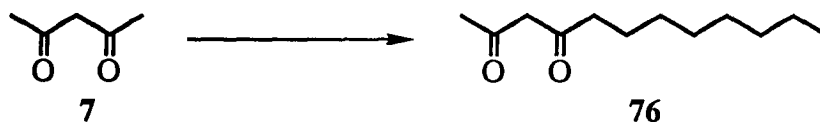
**<sup>1</sup>H NMR** (400 MHz, CDCl<sub>3</sub>) δ 3.61 (2H, t), 3.41 (2H, t), 1.87 (2H, p), 1.60-1.43 (6H, m), 0.90 (9H, s), 0.06 (6H, s).

**IR** (neat, cm<sup>-1</sup>) 2936, 2858, 1466, 1253, 1101, 837, 775.

**LRMS** (m/z) 295 (Br<sup>81</sup>: M<sup>+</sup> - H, 0.1), 293 (Br<sup>79</sup>: M<sup>+</sup> - H, 0.1), 239 (2), 237 (2), 200 (0.2), 199 (2), 170 (3), 169 (29), 168 (3), 167 (29), 159 (5), 158 (7), 157 (56), 139 (31), 138 (3), 137 (28), 129 (7), 127 (15), 115 (13), 101 (27), 99 (18), 90 (30), 89 (27), 88 (4), 87 (5), 85 (8), 84 (14), 83 (100), 82 (4), 77 (7), 76 (10), 75 (94), 74 (5), 73 (38), 61 (6), 59 (15), 58 (6), 57 (6), 56 (7), 55 (68).

**HRMS** calcd for C<sub>12</sub>H<sub>27</sub>SiBr<sup>81</sup>O - H: 295.2000, found: 295.0917; calcd for C<sub>12</sub>H<sub>27</sub>SiBr<sup>79</sup>O - H: 293.2020, found: 293.0928.

### 3.12.3 2,4-Dodecanedione (76)



Following the procedure outlined in section 3.2.3, 2,4-pentanedione (7) (3.00 g, 30.0 mmol) was alkylated with freshly distilled 1-bromoheptane (5.37 g, 30.0 mmol) to give the corresponding  $\beta$ -diketone 76. The crude product was purified by column chromatography using petroleum ether : ethyl acetate (15:1) as eluent to give the  $\beta$ -diketone 76 (2.70 g, 63% based on the recovered bromide) as a clear oil, which was one spot by TLC.

**R<sub>f</sub>** (6:1 petroleum ether : ethyl acetate) 0.64.

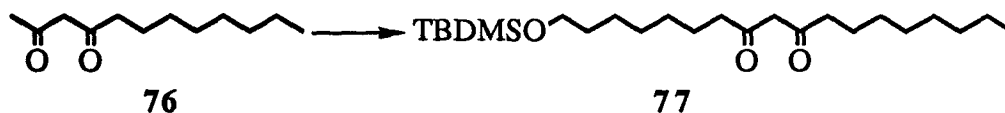
**<sup>1</sup>H NMR** (400 MHz, CDCl<sub>3</sub>)  $\delta$  15.50 (0.8H, s), 5.49 (0.8H, s), 3.58 (0.4H, s), 2.50 (0.4H, t), 2.27 (1.6H, t), 2.24 (0.6H, s), 2.07 (2.4H, s), 1.68-1.20 (12H, m), 0.89 (3H, t).

**IR** (neat, cm<sup>-1</sup>) 2931, 2856, 1713, 1614, 1449, 1363, 1241, 946, 777.

**LRMS** (m/z) 198 (M<sup>+</sup>, 3.3), 184 (0.4), 183 (4), 181 (0.4), 180 (2), 157 (0.2), 156 (2), 155 (1), 142 (4), 141 (10), 140 (3), 114 (4), 113 (33), 101 (14), 100 (98), 96 (4), 95 (9), 86 (7), 85 (100), 84 (9), 73 (2), 72 (21), 71 (24), 69 (12), 68 (6), 58 (14), 57 (20), 56 (4), 55 (18), 44 (4), 43 (45).

**HRMS** calcd for C<sub>12</sub>H<sub>22</sub>O<sub>2</sub>: 198.1614, found: 198.1626.

### 3.12.4 1-(Tert-butyldimethylsilyloxy)-8,10-octadecanedione (77)



Following the procedure outlined in section 3.2.4, the  $\beta$ -diketone **76** (2.50 g, 12.6 mmol) was alkylated with the bromide **75** (3.10 g, 10.5 mmol) to give the corresponding  $\beta$ -diketone **77**. The crude product was purified by column chromatography using petroleum ether : ethyl acetate (20:1) as eluent to give the  $\beta$ -diketone **77** (2.30 g, 75 % based on the recovered  $\beta$ -diketone **76**) as a clear oil, which was one spot by TLC.

**R<sub>f</sub>** (6:1 petroleum ether : ethyl acetate) 0.76.

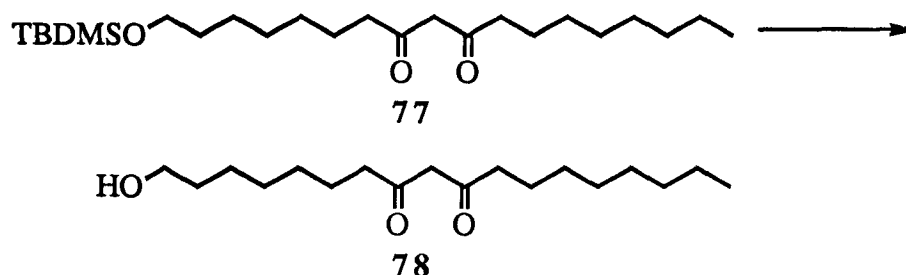
**<sup>1</sup>H NMR** (400 MHz, CDCl<sub>3</sub>)  $\delta$  15.50 (0.8H, s), 5.48 (0.8H, s), 3.61 (2H, t), 3.53 (0.4H, s), 2.50 (0.8H, t), 2.27 (3.2H, t), 1.66-1.22 (22H, m), 0.90 (9H, s), 0.89 (3H, t), 0.06 (6H, s).

**IR** (neat, cm<sup>-1</sup>) 2909, 2856, 1704, 1615, 1459, 1360, 1251, 1100, 945, 838, 775.

**LRMS** (m/z) 412 (M<sup>+</sup>, 0.1), 398 (0.9), 397 (3), 357 (7), 356 (26), 355 (100), 338 (0.5), 337 (2), 270 (0.4), 269 (2), 257 (2), 241 (1), 215 (3), 213 (2), 199 (3), 171 (2), 170 (1), 169 (4), 157 (3), 155 (1), 145 (2), 143 (4), 142 (2), 141 (12), 129 (3), 127 (2), 117 (2), 116 (1), 115 (5), 86 (1), 85 (6), 84 (2), 83 (5), 82 (1), 81 (7), 77 (5), 76 (4), 75 (43), 73 (14), 71 (12), 57 (13), 55 (13), 44 (7), 43 (6), 41(5).

**HRMS** calcd for C<sub>24</sub>H<sub>48</sub>SiO<sub>3</sub>: 412.3360, found: 412.3377.

### 3.12.5 1-Hydroxyl-8,10-octadecanedione (78)



Following the procedure outlined in section 3.2.5, the silyl ether **77** (2.00 g, 4.85 mmol) was converted to the alcohol **78**. The crude product was purified by recrystallization from hexanes to give the alcohol (1.26 g, 87%) as a colorless solid, which was one spot by TLC.

**R<sub>f</sub>** (1:1 petroleum ether : ethyl acetate) 0.64.

**mp** 57.0 °C.

**<sup>1</sup>H NMR** (400 MHz, CDCl<sub>3</sub>)  $\delta$  15.50 (0.8H, s), 5.48 (0.8H, s), 3.64 (2H, dt), 3.54 (0.4H, s), 2.51 (0.8H, dt), 2.26 (3.2H, dt), 1.70-1.20 (23H, m), 0.89 (3H, t).

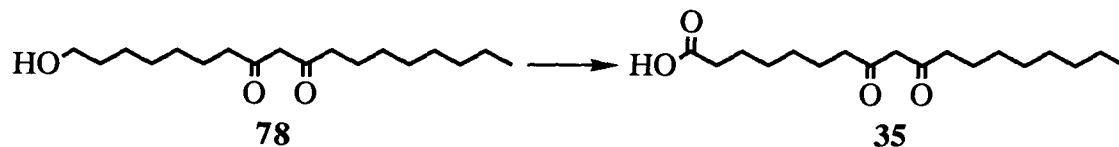
**IR** (CHCl<sub>3</sub>, cm<sup>-1</sup>) 3622, 3460, 2931, 2857, 1703, 1607, 1458, 1335, 1051, 902.

**LRMS** (m/z) 298 (M<sup>+</sup>, 1.0), 281 (0.8), 280 (2), 263 (0.6), 262 (2), 252 (0.4), 251 (1), 239 (1), 237 (2), 235 (1), 212 (3), 211 (14), 199 (2), 198 (10), 184 (8), 183 (58), 168 (2), 167 (13), 143 (13), 142 (14), 141 (100), 126 (5), 125 (42), 124 (20), 123 (15), 122 (18), 121 (10), 114 (8), 113 (32), 112 (10), 111 (16), 101 (9), 100 (83), 98 (19), 97 (63), 96 (16), 95 (41), 94 (8), 86 (4), 85 (38), 84 (24), 83 (31), 82 (14), 81 (37), 80 (12), 79 (15), 77 (11), 73 (10), 72 (6), 71 (75), 69 (73), 68 (11), 67 (24), 58 (15), 57 (68), 56 (12), 55 (99), 44 (7), 43 (34), 42 (6), 41 (21).

**HRMS** calcd for C<sub>18</sub>H<sub>34</sub>O<sub>3</sub>: 298.2499, found: 298.2514.



### 3.12.6 8,10-Dioxooctadecanoic Acid (**35**)



Following the procedure outlined in section 3.2.6, the alcohol **78** (596 mg, 2.00 mmol) was converted to the corresponding acid **35**. The crude product was purified by recrystallization from hexanes to give the acid **35** (306 mg, 50%) as a clear solid, which was one spot by TLC.

**R<sub>f</sub>** (5% HOAc in 3:1 petroleum ether : ethyl acetate) 0.53.

**mp** 58.5 °C.

**<sup>1</sup>H NMR** (400 MHz, CDCl<sub>3</sub>) δ 15.50 (0.8H, s), 5.49 (0.8H, s), 3.54 (0.4H, s), 2.51 (0.8H, dt), 2.34 (2H, dt), 2.27 (3.2H, dt), 1.72-1.20 (21H, m), 0.90 (3H, t).

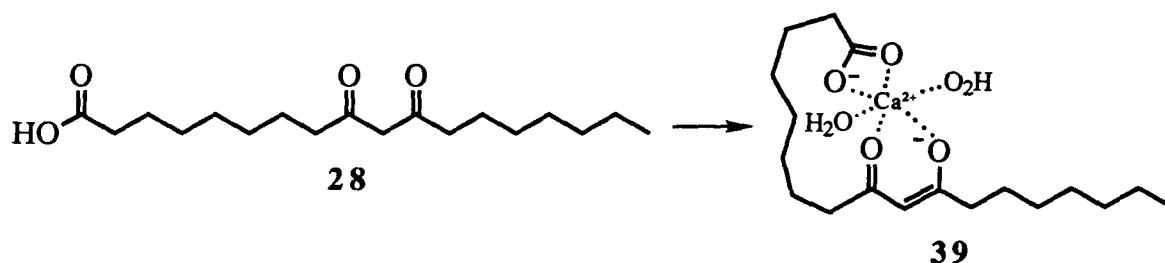
**IR** (CHCl<sub>3</sub>, cm<sup>-1</sup>) 3340-2480, 2931, 2858, 1708, 1608, 1459, 1300, 1127.

**LRMS** (m/z) 312 (M<sup>+</sup>, 6.4), 295 (0.9), 294 (3), 277 (0.2), 276 (0.8), 266 (1), 253 (1), 227 (1), 215 (4), 214 (32), 199 (7), 198 (10), 197 (3), 196 (17), 184 (7), 183 (63), 182 (3), 181 (27), 158 (9), 157 (100), 142 (9), 141 (58), 140 (7), 139 (27), 138 (12), 137 (6), 136 (14), 135 (4), 114 (4), 113 (24), 112 (10), 111 (38), 101 (5), 100 (79), 99 (5), 98 (9), 97 (26), 87 (5), 85 (23), 84 (17), 83 (41), 71 (52), 70 (4), 69 (46), 58 (8), 57 (63), 56 (7), 55 (48), 43 (52), 42 (8), 41 (57).

**HRMS** calcd for C<sub>18</sub>H<sub>32</sub>O<sub>4</sub>: 312.2292, found: 312.2307.

**Elem. Anal.** calcd for C<sub>18</sub>H<sub>32</sub>O<sub>4</sub>: C, 69.23; H, 10.33. found: C, 68.94; H, 10.38.

### 3.13 Synthesis of Calcium Salt of 9,11-Dioxooctadecanoic Acid (36)



To a solution of 9,11-dioxooctadecanoic acid (**28**) (60 mg, 0.19 mmol) in 8 mL of acetone was added calcium hydroxide (28 mg, 0.38 mmol) in 15 mL of distilled deionized water. The mixture was stirred at room temperature for 2 h. The solid precipitate was filtered, washed with distilled deionized water and acetone, and dried under reduced pressure to give 67 mg solid compound. The yield of the reaction, based on a 1:1 stoichiometry of the calcium complex **39** and on the assumption that two molecules of H<sub>2</sub>O were bound to each calcium ion, was 86%.

**mp** 200-220 °C.

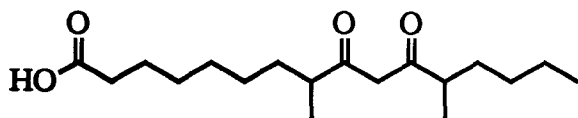
**<sup>1</sup>H NMR** (400 MHz, CD<sub>3</sub>OD)  $\delta$  2.51 (0.9H, m), 2.15 (5.1H, m), 1.64-1.52 (6H, m), 1.38-1.26 (14H, m), 0.95 - 0.87 (3H, m).

**IR** (KBr, cm<sup>-1</sup>) 3644, 3527, 2928, 2852, 1577, 1511, 1439, 711.

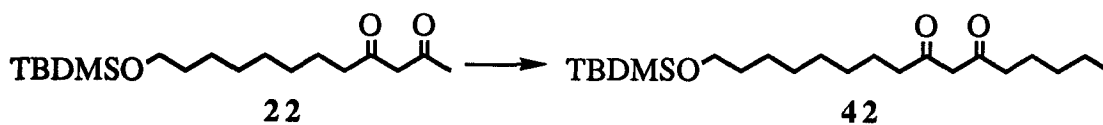
**FAB-MS** (m/z) 388 [CaC<sub>18</sub>H<sub>30</sub>O<sub>4</sub>(H<sub>2</sub>O)<sub>2</sub> + H + H]<sup>+</sup>, 351 [CaC<sub>18</sub>H<sub>30</sub>O<sub>4</sub> + H]<sup>+</sup>, 313 [C<sub>18</sub>H<sub>32</sub>O<sub>4</sub> + H]<sup>+</sup>, 235, 186, 169.

**Elem. Anal.** calcd for CaC<sub>18</sub>H<sub>30</sub>O<sub>4</sub>·(H<sub>2</sub>O)<sub>2</sub>: C, 55.91; H, 8.87. found: C, 54.79; H, 8.06.

### 3.14 Synthesis of 8,12-Dimethyl-9,11-dioxohexadecanoic Acid (41)



#### 3.14.1 16-(Tert-butyldimethylsilyloxy)-6,8-hexadecanedione (42)



Following the procedure outlined in section 3.2.4, the  $\beta$ -diketone **22** (4.26 g, 13.0 mmol) was alkylated with freshly distilled 1-bromobutane (1.64 g, 12.0 mmol) to give the  $\beta$ -diketone **42**. The crude product was purified by column chromatography using petroleum ether : ethyl acetate (20:1) as eluent to give the  $\beta$ -diketone **42** (2.33 g, 68% based on the recovered  $\beta$ -diketone **22**) as a clear oil, which was one spot by TLC.

**R<sub>f</sub>** (6:1 petroleum ether : ethyl acetate) 0.60.

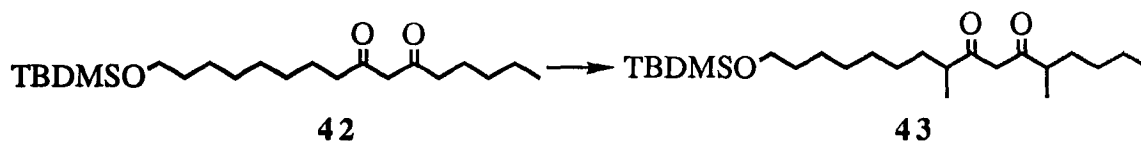
**<sup>1</sup>H NMR** (400 MHz, CDCl<sub>3</sub>)  $\delta$  15.50 (0.8H, s), 5.48 (0.8H, s), 3.60 (2H, t), 3.53 (0.4H, s), 2.49 (0.8H, t), 2.27 (3.2H, t), 1.66-1.22 (18H, m), 0.90 (9H, s), 0.89 (3H, t), 0.06 (6H, s).

**IR** (neat, cm<sup>-1</sup>) 2954, 2931, 2857, 1706, 1613, 1463, 1386, 1253, 1200, 1100, 1006, 949, 838, 776.

**LRMS** (m/z) 383 (M<sup>+</sup> - H, 0.7), 371 (0.3), 370 (1), 369 (3), 329 (7), 328 (26), 327 (100), 314 (0.5), 313 (2), 272 (0.3), 271 (1), 230 (0.3), 229 (2), 199 (2), 173 (2), 171 (3), 169 (3), 141 (3), 115 (4), 101 (3), 100 (3), 99 (22), 97 (3), 89 (4), 77 (4), 76 (2), 75 (29), 73 (11), 71 (19), 69 (8), 67 (5), 57 (4), 55 (13), 43 (15), 41 (8).

**HRMS** calcd for C<sub>22</sub>H<sub>44</sub>SiO<sub>3</sub> - H: 383.2970, found: 383.2975.

### 3.14.2 16-(Tert-butyldimethylsilyloxy)-5,9-dimethyl-6,8-hexadecanedione (**43**)



Lithium diisopropylamide (LDA, 8.4 mmol) was prepared at  $-78\text{ }^{\circ}\text{C}$  by addition of *n*-BuLi (6.2 mL, 1.35 M, 8.4 mmol) to a solution of diisopropylamine (1.3 mL, 8.8 mmol) in 20 mL of THF and stirring of the mixture for 30 min. It was then added to a solution of the  $\beta$ -diketone **42** (0.16 g, 4.2 mmol) in 80 mL of THF at  $-78\text{ }^{\circ}\text{C}$  through an addition funnel. The mixture was stirred at  $-78\text{ }^{\circ}\text{C}$  for 12 h. Iodomethane (0.59 g, 4.2 mmol) was injected and the mixture was stirred at  $0\text{ }^{\circ}\text{C}$  for 4 h. The mixture was cooled to  $-78\text{ }^{\circ}\text{C}$  and LDA (4.2 mmol) was added. The mixture was stirred overnight. Iodomethane (0.59 g, 4.2 mmol) was injected and the mixture was stirred at  $0\text{ }^{\circ}\text{C}$  for 2 h. The mixture was quenched with saturated  $\text{NH}_4\text{Cl}$ , acidified with 1N HCl and extracted with ether three times. The organic layers were washed with saturated  $\text{NaHCO}_3$ , brine, dried over  $\text{MgSO}_4$  and concentrated under reduced pressure. Purification of the crude product by column chromatography using petroleum ether : ethyl acetate (20:1) gave the dimethylated  $\beta$ -diketone **43** (1.25 g, 72%) as a colorless oil, which was one spot by TLC.

$R_f$  (6:1 petroleum ether : ethyl acetate) 0.86.

GC 94%,  $R_T = 9.68\text{ min}$ , 6%,  $R_T = 9.27\text{ min}$ .

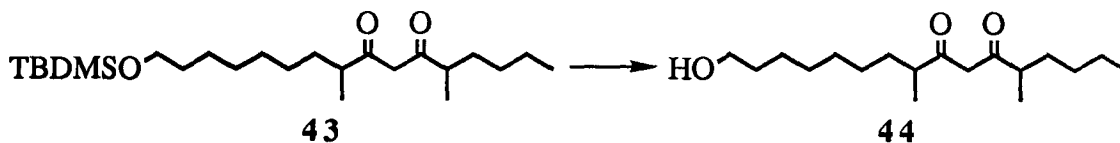
$^1\text{H NMR}$  (400 MHz,  $\text{CDCl}_3$ )  $\delta$  15.70 (0.8H, s), 5.47 (0.8H, s), 3.62 (0.4H, s), 3.59 (2H, t), 2.63 - 2.56 (0.38H, m), 2.50 - 2.42 (0.02H, m), 2.33 - 2.22 (1.52H, m), 2.14 - 2.08 (0.08H, m), 1.68-1.20 (18H, m), 1.16 - 1.06 (6H, dd), 0.92 - 0.86 (12H, m), 0.06 (6H, s).

IR (neat,  $\text{cm}^{-1}$ ) 2937, 2857, 1608, 1463, 1381, 1360, 1253, 1101, 1006, 940, 838, 776.

LRMS ( $m/z$ ) 412 ( $\text{M}^+$ , 0.1), 411 (0.3), 399 (0.4), 398 (2), 397 (5), 357 (7), 356 (26), 355 (100), 195 (1), 184 (1), 155 (3), 135 (2), 115 (2), 113 (4), 101 (1), 99 (2), 97 (1), 95 (2), 89 (2), 85 (12), 83 (2), 81 (2), 77 (1), 75 (11), 57 (3), 55 (6), 43 (8), 41 (4).

HRMS calcd for  $\text{C}_{24}\text{H}_{48}\text{SiO}_3$ : 412.3360, found: 412.3326.

### 3.14.3 16-Hydroxyl-5,9-dimethyl-6,8-hexadecanedione (**44**)



Following the procedure outlined in section 3.2.5, the silyl ether **43** (1.0 g, 2.4 mmol) was converted to the corresponding alcohol **44**. The crude product was purified by column chromatography using hexanes : ethyl acetate (3:1) as eluent to give the alcohol **44** (0.68 g, 94%) as a colorless oil, which was one spot by TLC.

**R<sub>f</sub>** (1:1 petroleum ether : ethyl acetate) 0.74.

**GC** 94%, **R<sub>T</sub>** = 7.85 min, 6%, **R<sub>T</sub>** = 7.68 min.

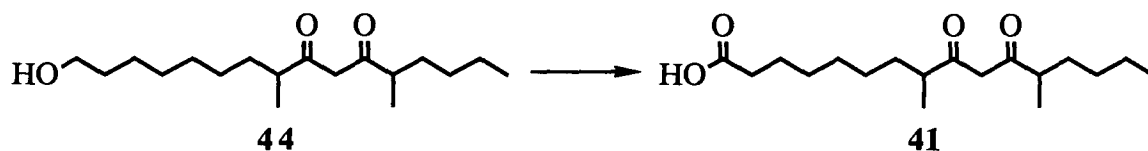
**<sup>1</sup>H NMR** (400 MHz, CDCl<sub>3</sub>)  $\delta$  15.70 (0.8H, s), 5.48 (0.8H, s), 3.64 (2H, t), 3.62 (0.4H, s), 2.66 - 2.44 (0.4H, m), 2.36 - 2.10 (1.6H, m), 1.70 - 1.20 (19H, m), 1.18 - 1.06 (6H, dd), 0.90 (3H, t).

**IR** (neat, cm<sup>-1</sup>) 3385, 2929, 2857, 1603, 1459, 1352, 1055, 793.

**LRMS** (m/z) 298 (M<sup>+</sup>, 2.5), 281 (0.1), 280 (0.6), 255 (0.4), 253 (0.7), 214 (0.5), 213 (4), 212 (2), 211 (2), 198 (1), 197 (5), 196 (1), 195 (7), 185 (5), 184 (39), 156 (11), 155 (100), 143 (7), 142 (3), 141 (18), 129 (3), 128 (19), 127 (5), 126 (5), 125 (12), 124 (4), 123 (20), 114 (7), 113 (69), 112 (15), 111 (19), 110 (4), 109 (11), 99(28), 98 (14), 97 (25), 95 (14), 86 (8), 85 (84), 84 (6), 83 (39), 82 (5), 81 (20), 72 (9), 71 (21), 70 (8), 69 (77), 57 (24), 56 (5), 55 (33).

**HRMS** calcd for C<sub>18</sub>H<sub>34</sub>O<sub>3</sub>: 298.2499, found: 298.2509.

### 3.14.4 8,12-Dimethyl-9,11-dioxohexadecanoic Acid (**41**)



Following the procedure outlined in section 3.2.6, the alcohol **44** (596 mg, 2.0 mmol) was converted to the acid **41**. The crude product was purified by column chromatography using hexane : ethyl acetate : acetic acid (6:1:0.7) to give the acid **41** (384 mg, 62%) as a clear oil, which was one spot by TLC.

**R<sub>f</sub>** (5% HOAc in 3:1 petroleum ether : ethyl acetate) 0.60.

**GC** 95%,  $R_T$  = 8.35 min, 5%,  $R_T$  = 8.15 min.

**<sup>1</sup>H NMR** (400 MHz, CDCl<sub>3</sub>)  $\delta$  15.70 (0.8H, s), 5.48 (0.8H, s), 3.62 (0.4H, s), 2.66-2.40 (0.4H, m), 2.36 (2H, t), 2.34-2.08 (1.6H, m), 1.70-1.20 (17H, m), 1.14-1.06 (6H, dd), 0.88 (3H, t).

**IR** (neat, cm<sup>-1</sup>) 3320-2480, 2939, 2860, 1720, 1600, 1449, 1377, 1287, 1224, 1099, 931.

**LRMS** (m/z) 312 (M<sup>+</sup>, 4), 295 (0.3), 294 (0.8), 257 (1), 256 (11), 239 (0.8), 238 (3), 210 (4), 209 (17), 185 (18), 184 (39), 182 (7), 181 (38), 157 (24), 156 (14), 155 (100), 141 (13), 140 (6), 139 (32), 137 (6), 128 (14), 114 (5), 113 (58), 112 (12), 111 (18), 99 (25), 98 (16), 97 (28), 95 (12), 86 (7), 85 (69), 71 (18), 70 (5), 69 (46), 57 (15), 56 (5), 55 (26).

**HRMS** calcd for C<sub>18</sub>H<sub>32</sub>O<sub>4</sub>: 312.2292, found: 312.2299.

**Elem. Anal.** calcd for C<sub>18</sub>H<sub>32</sub>O<sub>4</sub>: C, 69.23; H, 10.33. found: C, 69.08; H, 10.43.

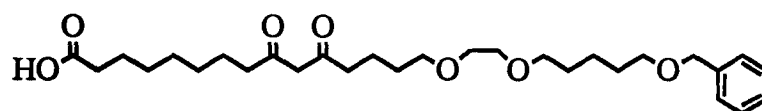
### 3.15 Transport of Calcium and Other Metal Ions by Synthetic Analogues of Ionomycin

#### 3.15.1 Transport of Calcium by Synthetic Analogues of Ionomycin

Source Phase: 500 mM  $\text{CaCl}_2$ , 40 mM CHES/ $\text{Me}_4\text{NOH}$  buffer, pH = 9.5

Receiving Phase: 40 mM MOPS/ $\text{Me}_4\text{NOH}$  buffer, pH = 7.0

Analogue: 15-[2-(5-Benzyloxy)-pentyloxy]-ethoxy-9,11-dioxopentadecanoic Acid (**5**)



Time (h)	12	16	20	24
$\text{Ca}^{2+}$ Transported ( $\mu\text{mol}$ )	$5.8 \pm 0.6$	$7.8 \pm 0.7$	$10 \pm 1$	$12 \pm 1$
Transport Rate ( $10^{-8} \text{ mole cm}^{-2} \text{ h}^{-1}$ )	$J = 7.3 \pm 0.7$			

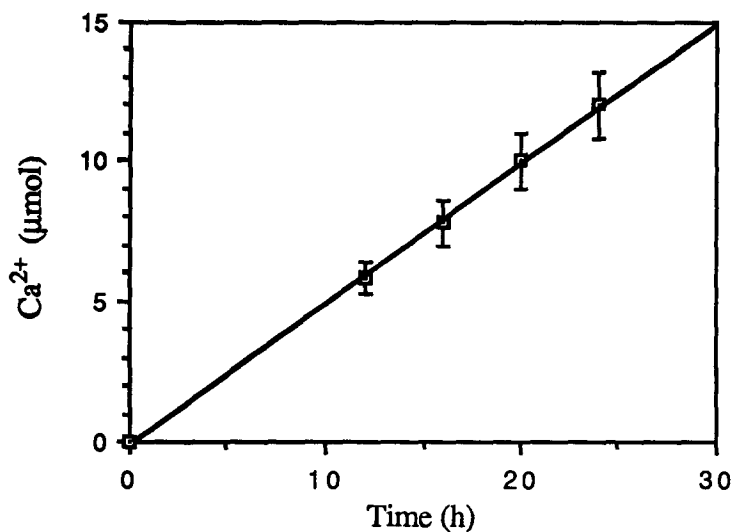
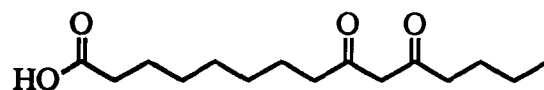


Figure 12. Plot of the amount of calcium in the receiving phase versus time.

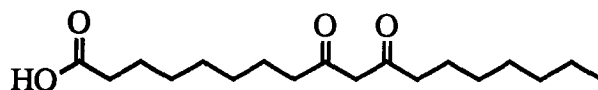
Analogue: 9,11-Dioxopentadecanoic Acid (4)



Time (h)	12	16	20	24
Ca <sup>2+</sup> Transported (μmol)	0.2 ± 0.1	0.3 ± 0.1	0.3 ± 0.1	0.4 ± 0.1
Transport Rate (10 <sup>-8</sup> mole cm <sup>-2</sup> h <sup>-1</sup> )	J = 0.3 ± 0.1			

-----

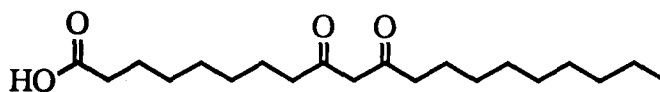
Analogue: 9,11-Dioxooctadecanoic Acid (28)



Time (h)	16	20	24
Ca <sup>2+</sup> Transported (μmol)	16 ± 1	20 ± 2	23 ± 2
Transport Rate (10 <sup>-8</sup> mole cm <sup>-2</sup> h <sup>-1</sup> )	J = 15 ± 2		

-----

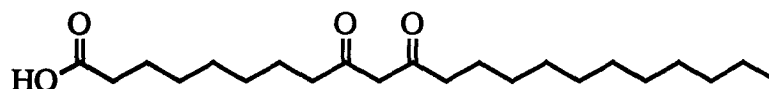
Analogue: 9,11-Dioxoeicosanoic Acid (29)



Time (h)	12	16	20	24
Ca <sup>2+</sup> Transported (μmol)	13 ± 1	17 ± 1	20 ± 1	24 ± 2
Transport Rate (10 <sup>-8</sup> mole cm <sup>-2</sup> h <sup>-1</sup> )	J = 15 ± 2			



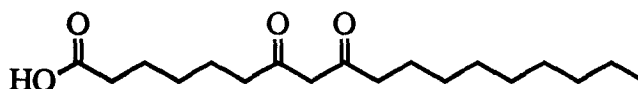
Analogue: 9,11-Dioxodoeicosanoic Acid (30)



Time (h)	12	16	20	24
Ca <sup>2+</sup> Transported (μmol)	11 ± 1	15 ± 1	18 ± 1	21 ± 2
Transport Rate (10 <sup>-8</sup> mole cm <sup>-2</sup> h <sup>-1</sup> )	J = 13 ± 1			

-----

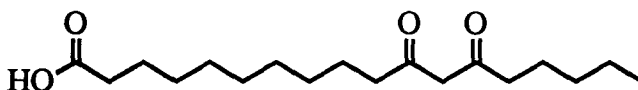
Analogue: 7,9-Dioxooctadecanoic Acid (33)



Time (h)	16	20	24
Ca <sup>2+</sup> Transported (μmol)	3.9 ± 0.4	4.9 ± 0.4	5.8 ± 0.6
Transport Rate (10 <sup>-8</sup> mole cm <sup>-2</sup> h <sup>-1</sup> )	J = 3.5 ± 0.4		

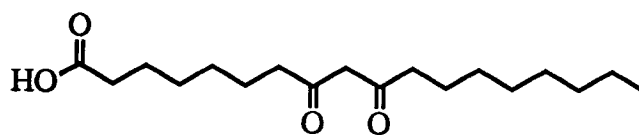
-----

Analogue: 11,13-Dioxooctadecanoic Acid (34)



Time (h)	12	16	20	24
Ca <sup>2+</sup> Transported (μmol)	0.9 ± 0.1	1.1 ± 0.1	1.2 ± 0.1	1.3 ± 0.1
Transport Rate (10 <sup>-8</sup> mole cm <sup>-2</sup> h <sup>-1</sup> )	J = 0.9 ± 0.1			

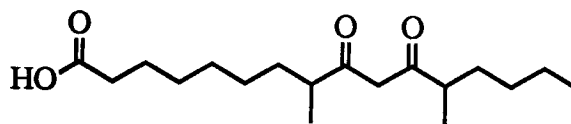
Analogue: 8,10-Dioxooctadecanoic Acid (35)



Time (h)	16	20	24
Ca <sup>2+</sup> Transported (μmol)	9.3 ± 0.9	13 ± 1	16 ± 1
Transport Rate (10 <sup>-8</sup> mole cm <sup>-2</sup> h <sup>-1</sup> )	J = 9.5 ± 0.9		

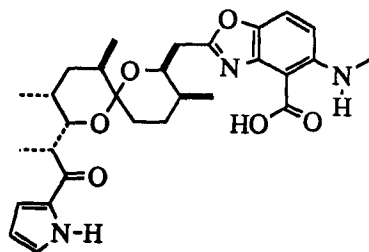
-----

Analogue: 8,12-Dimethyl-9,11-dioxohexadecanoic Acid (41)



Time (h)	16	20	24
Ca <sup>2+</sup> Transported (μmol)	10 ± 1	14 ± 1	16 ± 1
Transport Rate (10 <sup>-8</sup> mole cm <sup>-2</sup> h <sup>-1</sup> )	J = 10 ± 1		

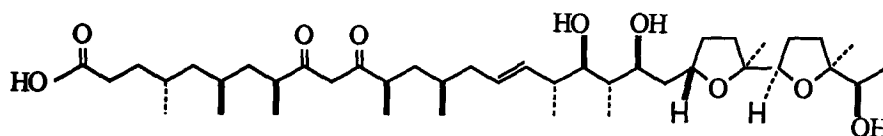
## Calcimycin (2)



Time (h)	12	16	20	24
Ca <sup>2+</sup> Transported (μmol)	14 ± 1	16 ± 1	18 ± 1	19 ± 2
Transport Rate (10 <sup>-8</sup> mole cm <sup>-2</sup> h <sup>-1</sup> )	J = 12 ± 1			

-----

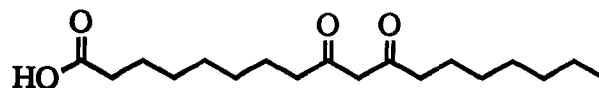
## Ionomycin (3)



Time (h)	16	20	24	40
Ca <sup>2+</sup> Transported (μmol)	20 ± 2	30 ± 2	36 ± 2	56 ± 2
Transport Rate (10 <sup>-8</sup> mole cm <sup>-2</sup> h <sup>-1</sup> )	J = 21 ± 2			

### 3.15.2 Cation Selectivity in Transport

Analogue: 9,11-dioxooctadecanoic Acid (28)



Receiving Phase: 40 mM MOPS/Me<sub>4</sub>NOH buffer, pH = 7.5

Source Phase: 40 mM CHES/Me<sub>4</sub>NOH buffer, pH = 9.5

250 mM CaCl<sub>2</sub>, 250 mM in MgCl<sub>2</sub>

Time (h)	16	20	24
Ca <sup>2+</sup> Transported (μmol)	3.0 ± 0.2	3.2 ± 0.2	3.5 ± 0.3
Mg <sup>2+</sup> Transported (μmol)	4.0 ± 0.3	4.4 ± 0.4	5.0 ± 0.4
Ca <sup>2+</sup> Transport Rate (10 <sup>-8</sup> mole cm <sup>-2</sup> h <sup>-1</sup> )	J = 2.2 ± 0.2		
Mg <sup>2+</sup> Transport Rate (10 <sup>-8</sup> mole cm <sup>-2</sup> h <sup>-1</sup> )	J = 3.1 ± 0.3		

Source Phase: 40 mM CHES/Me<sub>4</sub>NOH buffer, pH = 9.5

250 mM CaCl<sub>2</sub>, 250 mM in NaCl

Time (h)	16	24	40
Ca <sup>2+</sup> Transported (μmol)	6.7 ± 0.5	10 ± 1	15 ± 1
Na <sup>+</sup> Transported (μmol)	0.0	0.0	0.0
Ca <sup>2+</sup> Transport Rate (10 <sup>-8</sup> mole cm <sup>-2</sup> h <sup>-1</sup> )			J = 5.5 ± 0.5
Na <sup>+</sup> Transport Rate (10 <sup>-8</sup> mole cm <sup>-2</sup> h <sup>-1</sup> )			J = 0.0

-----

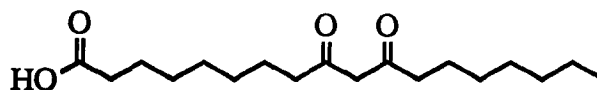
Source Phase: 40 mM CHES/Me<sub>4</sub>NOH buffer, pH = 9.5

250 mM CaCl<sub>2</sub>, 250 mM in KCl

Time (h)	16	24	40
Ca <sup>2+</sup> Transported (μmol)	6.7 ± 0.5	10 ± 1	15 ± 1
K <sup>+</sup> Transported (μmol)	0.0	0.0	0.0
Ca <sup>2+</sup> Transport Rate (10 <sup>-8</sup> mole cm <sup>-2</sup> h <sup>-1</sup> )			J = 5.5 ± 0.5
K <sup>+</sup> Transport Rate (10 <sup>-8</sup> mole cm <sup>-2</sup> h <sup>-1</sup> )			J = 0.0

### 3.15.3 Effect of Substrate Concentration on Calcium Transport

Analogue: 9,11-Dioxooctadecanoic Acid (28)



Receiving Phase: 40 mM MOPS/Me<sub>4</sub>NOH buffer, pH = 7.5

Source Phase: 40 mM CHES/Me<sub>4</sub>NOH buffer, pH = 9.5, 10 mM CaCl<sub>2</sub>

Time (h)	16	20	24
Ca <sup>2+</sup> Transported (μmol)	0.6 ± 0.1	0.8 ± 0.1	0.9 ± 0.1
Transport Rate (10 <sup>-8</sup> mole cm <sup>-2</sup> h <sup>-1</sup> )	J = 0.6 ± 0.1		

-----

Source Phase: 40 mM CHES/Me<sub>4</sub>NOH buffer, pH = 9.5, 50 mM CaCl<sub>2</sub>

Time (h)	16	20	24
Ca <sup>2+</sup> Transported (μmol)	4.6 ± 0.4	6.0 ± 0.4	7.1 ± 0.7
Transport Rate (10 <sup>-8</sup> mole cm <sup>-2</sup> h <sup>-1</sup> )	J = 4.4 ± 0.4		

Source Phase: 40 mM CHES/Me<sub>4</sub>NOH buffer, pH = 9.5, 100 mM CaCl<sub>2</sub>

Time (h)	16	20	24
Ca <sup>2+</sup> Transported (μmol)	7.4 ± 0.6	8.4 ± 0.7	9.4 ± 0.9
Transport Rate (10 <sup>-8</sup> mole cm <sup>-2</sup> h <sup>-1</sup> )	J = 5.9 ± 0.6		

Source Phase: 40 mM CHES/Me<sub>4</sub>NOH buffer, pH = 9.5, 250 mM CaCl<sub>2</sub>

Time (h)	16	20	24
Ca <sup>2+</sup> Transported (μmol)	14 ± 1	18 ± 1	21 ± 2
Transport Rate (10 <sup>-8</sup> mole cm <sup>-2</sup> h <sup>-1</sup> )	J = 13 ± 1		

Source Phase: 40 mM CHES/Me<sub>4</sub>NOH buffer, pH = 9.5, 500 mM CaCl<sub>2</sub>

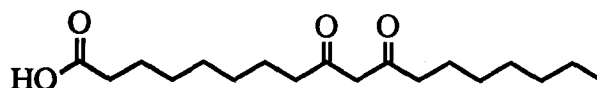
Time (h)	16	20	24
Ca <sup>2+</sup> Transported (μmol)	16 ± 2	20 ± 2	23 ± 2
Transport Rate (10 <sup>-8</sup> mole cm <sup>-2</sup> h <sup>-1</sup> )	J = 15 ± 2		

Source Phase: 40 mM CHES/Me<sub>4</sub>NOH buffer, pH = 9.5, 1000 mM CaCl<sub>2</sub>

Time (h)	16	20	24
Ca <sup>2+</sup> Transported (μmol)	16 ± 1	21 ± 2	28 ± 2
Transport Rate (10 <sup>-8</sup> mole cm <sup>-2</sup> h <sup>-1</sup> )	J = 16 ± 2		

### 3.15.4 Effect of pH in Receiving Phase on Calcium Transport

Analogue: 9,11-Dioxooctadecanoic Acid (28)



Source Phase: 500 mM CaCl<sub>2</sub>, 40 mM CHES/Me<sub>4</sub>NOH buffer, pH = 9.5

Receiving Phase: 40 mM Succinic Acid/Me<sub>4</sub>NOH buffer, pH = 5.0

Time (h)	16	20	24
Ca <sup>2+</sup> Transported (μmol)	13 ± 1	16 ± 1	21 ± 2
Transport Rate (10 <sup>-8</sup> mole cm <sup>-2</sup> h <sup>-1</sup> )	J = 15 ± 2		

-----

Receiving Phase: 40 mM MES/Me<sub>4</sub>NOH buffer, pH = 6.0

Time (h)	16	20	24
Ca <sup>2+</sup> Transported (μmol)	13 ± 1	17 ± 1	20 ± 2
Transport Rate (10 <sup>-8</sup> mole cm <sup>-2</sup> h <sup>-1</sup> )	J = 16 ± 2		



Receiving Phase: 40 mM MOPS/Me<sub>4</sub>NOH buffer, pH = 7.0

Time (h)	16	20	24
Ca <sup>2+</sup> Transported (μmol)	14 ± 1	17 ± 2	18 ± 2
Transport Rate (10 <sup>-8</sup> mole cm <sup>-2</sup> h <sup>-1</sup> )	J = 16 ± 2		

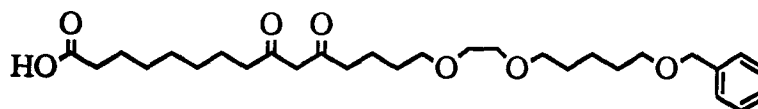
-----

Receiving Phase: 40 mM HEPPS/Me<sub>4</sub>NOH buffer, pH = 8.0

Time (h)	16	20	24
Ca <sup>2+</sup> Transported (μmol)	13 ± 1	16 ± 2	18 ± 2
Transport Rate (10 <sup>-8</sup> mole cm <sup>-2</sup> h <sup>-1</sup> )	J = 15 ± 2		

### 3.15.5 Effect of pH in Source Phase on Calcium Transport

Analogue: 15-[2-(5-Benzyloxy)-pentyloxy]]-ethoxy-9,11-dioxopentadecanoic Acid (5)



Concentration: 300  $\mu$ M

Receiving Phase: 40 mM MES/Me<sub>4</sub>NOH buffer, pH = 6.5

Source Phase: 500 mM CaCl<sub>2</sub>, 40 mM MOPS/Me<sub>4</sub>NOH buffer, pH = 7.5

Time (h)	16	20	24
Ca <sup>2+</sup> Transported ( $\mu$ mol)	1.2 $\pm$ 0.1	1.3 $\pm$ 0.1	1.6 $\pm$ 0.1
Transport Rate (10 <sup>-8</sup> mole cm <sup>-2</sup> h <sup>-1</sup> )	J = 1.3 $\pm$ 0.1		

-----

Source Phase: 500 mM CaCl<sub>2</sub>, 40 mM HEPPS/Me<sub>4</sub>NOH buffer, pH = 8.0

Time (h)	16	20	24
Ca <sup>2+</sup> Transported ( $\mu$ mol)	1.1 $\pm$ 0.1	1.2 $\pm$ 0.1	1.6 $\pm$ 0.1
Transport Rate (10 <sup>-8</sup> mole cm <sup>-2</sup> h <sup>-1</sup> )	J = 1.5 $\pm$ 0.1		

Source Phase: 500 mM CaCl<sub>2</sub>, 40 mM HEPPS/Me<sub>4</sub>NOH buffer, pH = 8.5

Time (h)	16	20	24
Ca <sup>2+</sup> Transported (μmol)	2.2 ± 0.2	2.8 ± 0.2	3.8 ± 0.4
Transport Rate (10 <sup>-8</sup> mole cm <sup>-2</sup> h <sup>-1</sup> )	J = 2.5 ± 0.2		

-----

Source Phase: 500 mM CaCl<sub>2</sub>, 40 mM MOPS/Me<sub>4</sub>NOH buffer, pH = 9.0

Time (h)	16	20	24
Ca <sup>2+</sup> Transported (μmol)	6.2 ± 0.4	6.6 ± 0.5	7.8 ± 0.7
Transport Rate (10 <sup>-8</sup> mole cm <sup>-2</sup> h <sup>-1</sup> )	J = 4.6 ± 0.4		

-----

Source Phase: 500 mM CaCl<sub>2</sub>, 40 mM CHES/Me<sub>4</sub>NOH buffer, pH = 9.5

Time (h)	16	20	24
Ca <sup>2+</sup> Transported (μmol)	11 ± 1	13 ± 1	14 ± 1
Transport Rate (10 <sup>-8</sup> mole cm <sup>-2</sup> h <sup>-1</sup> )	J = 9.0 ± 0.9		

-----

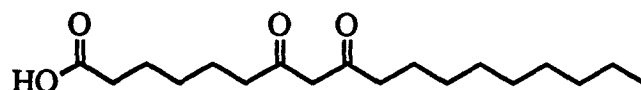
Source Phase: 500 mM CaCl<sub>2</sub>, 40 mM CHES/Me<sub>4</sub>NOH buffer, pH = 10.0

Time (h)	16	20	24
Ca <sup>2+</sup> Transported (μmol)	18 ± 1	20 ± 2	21 ± 2
Transport Rate (10 <sup>-8</sup> mole cm <sup>-2</sup> h <sup>-1</sup> )	J = 14 ± 1		

### 3.16 $pK_a$ of the $\beta$ -Diketone Group of Synthetic Analogues of Ionomycin

Solvent: 80% MeOH-H<sub>2</sub>OIonic Medium: 50 mM Et<sub>4</sub>NClO<sub>4</sub>Concentration: 80  $\mu$ MTitrant: Me<sub>4</sub>NOH

Analogue: 7,9-Dioxooctadecanoic Acid (33)



pH	5.80	6.80	7.56	8.20	8.90	9.54	9.86	10.42	10.66
A (298 nm)	0.248	0.257	0.276	0.283	0.288	0.310	0.336	0.439	0.581
pH	11.00	11.19	11.44	11.60	11.88	12.06	12.28	12.52	12.76
A (298 nm)	0.800	0.892	1.130	1.240	1.368	1.415	1.479	1.520	1.537

$$pK_a = 11.16 \pm 0.02$$

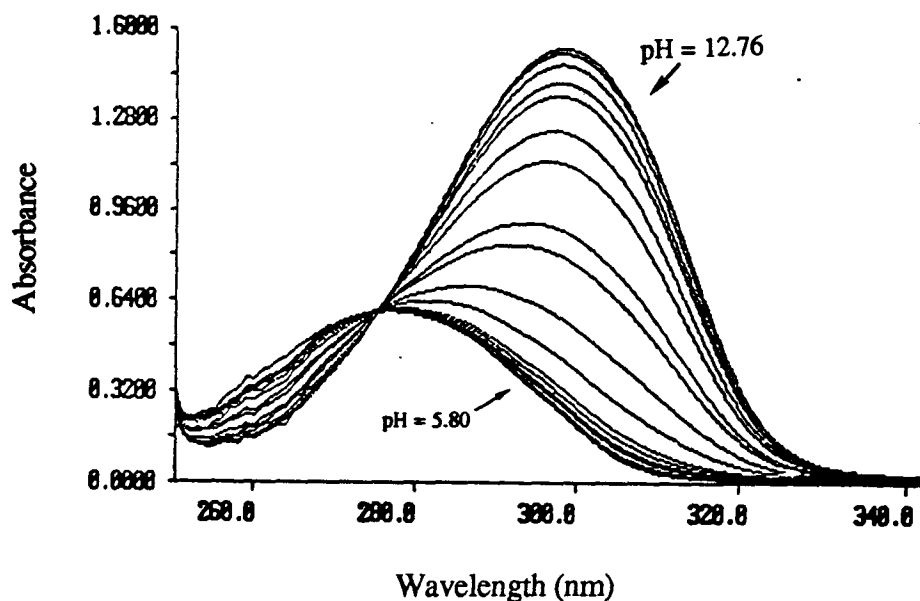


Figure 27. UV spectrophotometric absorption spectra of analogue 33 as the pH of the solution increased from 5.80 to 12.76.

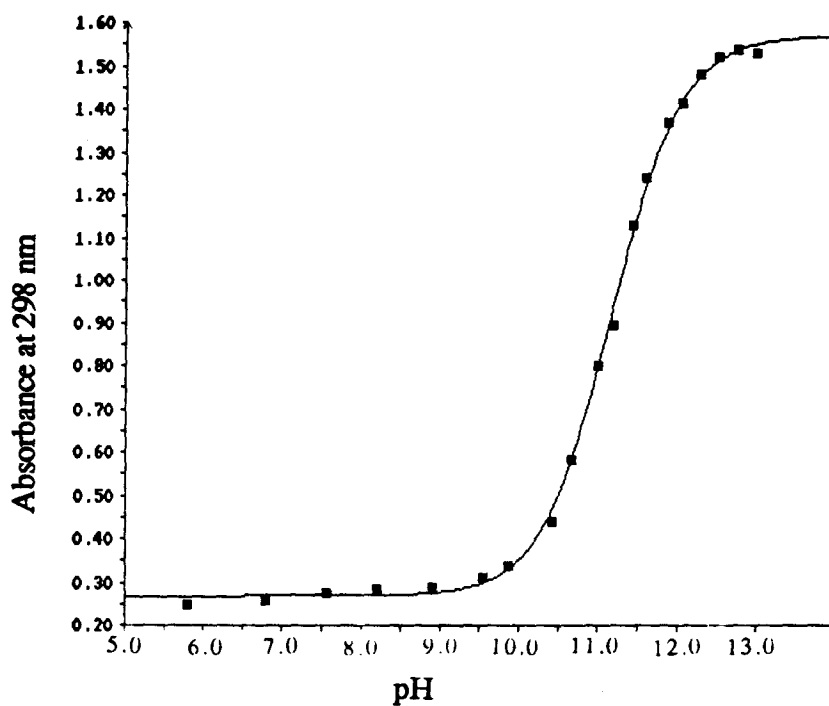
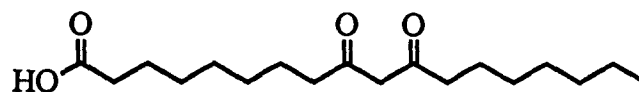


Figure 28. Plot of the UV absorbance at 298 nm versus pH for analogue 33.

-----

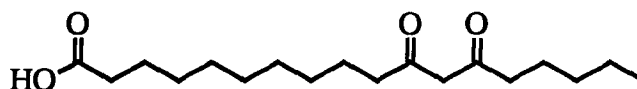
Analogue: 9,11-Dioxooctadecanoic Acid (28)



pH	5.80	6.80	7.56	8.20	8.90	9.54	9.86	10.42	10.66
A (298 nm)	0.275	0.294	0.320	0.324	0.335	0.361	0.370	0.544	0.698
pH	11.00	11.19	11.44	11.60	11.88	12.06	12.28	12.52	12.76
A (298 nm)	0.900	1.033	1.224	1.322	1.410	1.437	1.500	1.531	1.539

$$pK_a = 11.03 \pm 0.02$$

Analogue: 11,13-Dioxooctadecanoic Acid (34)



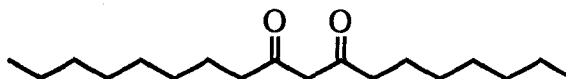
pH	5.80	6.80	7.56	8.20	8.90	9.54	9.86	10.42	10.66
A (298 nm)	0.315	0.324	0.348	0.366	0.375	0.403	0.451	0.724	0.902

pH	11.00	11.19	11.44	11.60	11.88	12.06	12.28	12.52	12.76
A (298 nm)	1.138	1.278	1.480	1.572	1.659	1.680	1.728	1.780	1.829

$pK_a = 10.90 \pm 0.02$

-----

Analogue: 8,10-Octadecanedione (31)

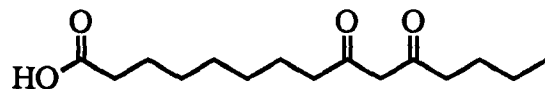


pH	5.80	6.80	7.56	8.20	8.90	9.54	9.86	10.42	10.66
A (298 nm)	0.208	0.211	0.211	0.221	0.235	0.256	0.286	0.484	0.595

pH	11.00	11.19	11.44	11.60	11.88	12.06	12.28	12.52	12.76
A (298 nm)	0.719	0.817	0.920	0.985	1.032	1.050	1.084	1.109	1.120

$pK_a = 10.86 \pm 0.02$

Analogue: 9,11-Dioxopentadecanoic Acid (4)



pH 5.80 6.80 7.56 8.20 8.90 9.54 9.86 10.42 10.66

A (298 nm) 0.279 0.293 0.310 0.323 0.350 0.381 0.421 0.664 0.834

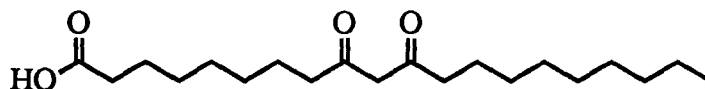
pH 11.00 11.19 11.44 11.60 11.88 12.06 12.28 12.52 12.76

A (298 nm) 1.033 1.137 1.348 1.448 1.520 1.553 1.613 1.634 1.665

$pK_a = 10.92 \pm 0.02$

-----

Analogue: 9,11-Dioxoeicosanoic Acid (29)



pH 5.80 6.80 7.56 8.20 8.90 9.54 9.86 10.42 10.66

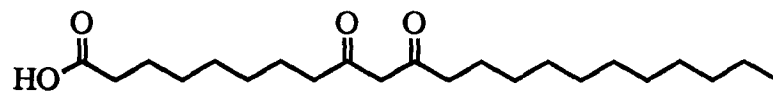
A (298 nm) 0.278 0.287 0.299 0.310 0.315 0.320 0.341 0.515 0.691

pH 11.00 11.19 11.44 11.60 11.88 12.06 12.28 12.52 12.76

A (298 nm) 0.936 1.009 1.255 1.373 1.481 1.508 1.551 1.593 1.611

$pK_a = 11.04 \pm 0.02$

Analogue: 9,11-Dioxodoeicosanoic Acid (**30**)



pH	5.80	6.80	7.56	8.20	8.90	9.54	9.86	10.42	10.66
----	------	------	------	------	------	------	------	-------	-------

A (298 nm)	0.282	0.288	0.306	0.315	0.318	0.318	0.329	0.561	0.657
------------	-------	-------	-------	-------	-------	-------	-------	-------	-------

pH	11.00	11.19	11.44	11.60	11.88	12.06	12.28	12.52	12.76
----	-------	-------	-------	-------	-------	-------	-------	-------	-------

A (298 nm)	0.932	1.009	1.188	1.332	1.440	1.474	1.523	1.570	1.593
------------	-------	-------	-------	-------	-------	-------	-------	-------	-------

$\text{pK}_a = 11.07 \pm 0.02$



### 3.17 Binding of Calcium and Other Metal Ions by Synthetic Analogues of Ionomycin

#### 3.17.1 Binding of Calcium

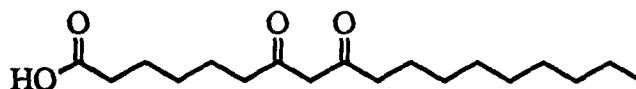
Solvent: 80% MeOH-H<sub>2</sub>O

Ionic Medium: 16,7 mM CaCl<sub>2</sub>

Concentration: 80  $\mu$ M

Titant: Me<sub>4</sub>NOH

Analogue: 7,9-Dioxooctadecanoic Acid (33)



pH	5.40	6.36	7.11	7.60	8.02	8.32	8.48	9.19	9.88
A (298 nm)	0.272	0.283	0.334	0.427	0.543	0.662	0.758	1.181	1.445

pH	10.62	10.94	11.27	11.46
A (298 nm)	1.503	1.504	1.510	1.515

$pK_a' = 8.69 \pm 0.02$

$\beta = (3.0 \pm 0.2) \times 10^2 \text{ M}^{-1}$

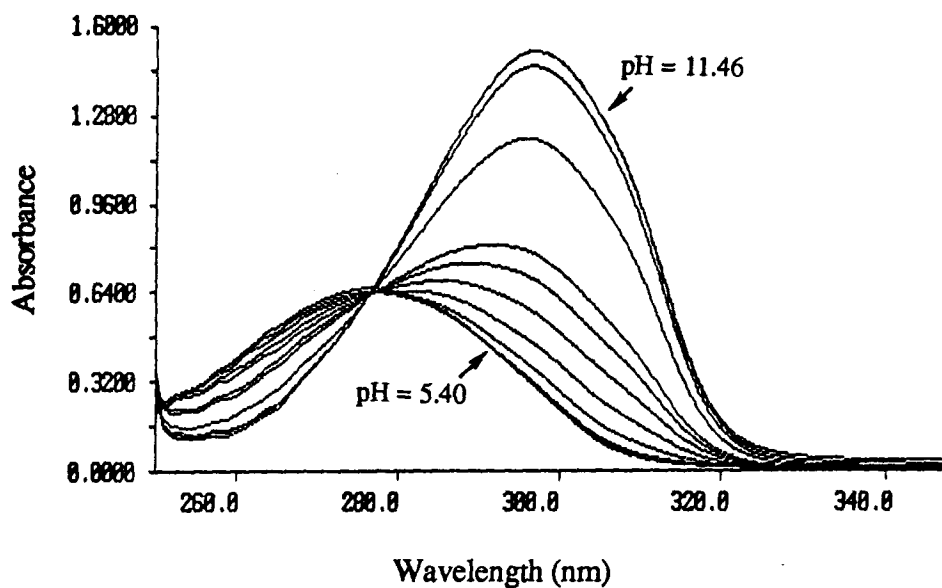


Figure 31. UV spectrophotometric absorption spectra of analogue 33 as the pH of the solution increased from 5.40 to 11.46 in the presence of CaCl<sub>2</sub>.

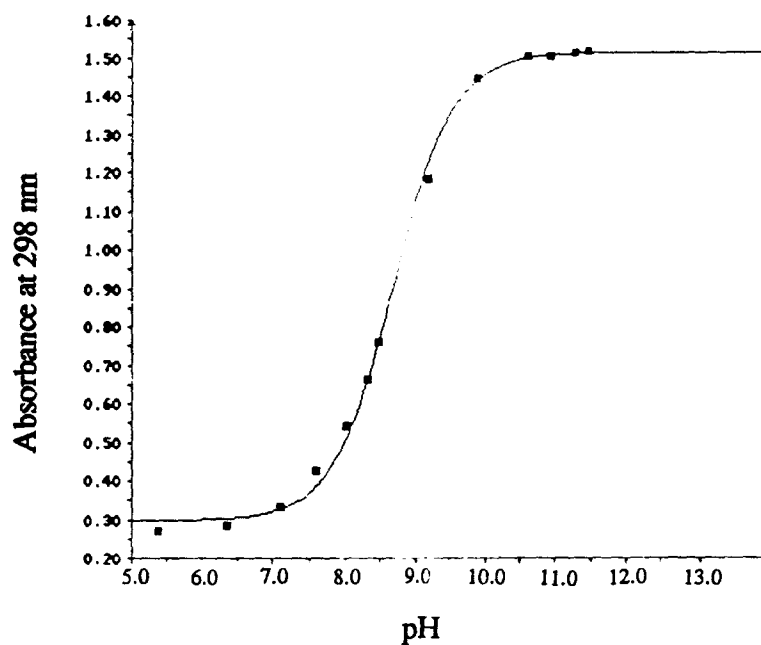
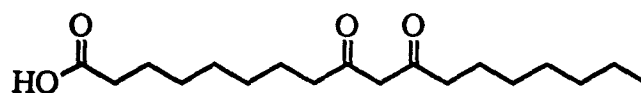


Figure 32. Plot of the UV absorbance at 298 nm versus pH for analogue 33 in the presence of  $\text{CaCl}_2$ .

Analogue: 9,11-Dioxooctadecanoic Acid (28)



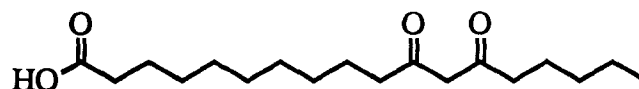
pH	5.40	6.36	7.11	7.60	8.02	8.32	8.48	9.19	9.88
A (298 nm)	0.323	0.334	0.382	0.472	0.584	0.724	0.840	1.470	1.743

pH	10.62	10.94	11.27	11.46
A (298 nm)	1.842	1.854	1.867	1.882

$\text{pK}_a' = 8.77 \pm 0.02$

$\beta = (1.8 \pm 0.1) \times 10^2 \text{ M}^{-1}$

Analogue: 11,13-Dioxooctadecanoic Acid (34)



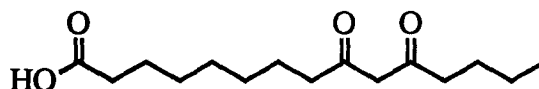
pH	5.40	6.36	7.11	7.60	8.02	8.32	8.48	9.19	9.88
A (298 nm)	0.310	0.324	0.369	0.436	0.531	0.626	0.755	1.267	1.560

pH	10.62	10.94	11.27	11.46
A (298 nm)	1.668	1.677	1.686	1.692

$pK_a' = 8.84 \pm 0.02$                        $\beta = (1.2 \pm 0.2) \times 10^2 \text{ M}^{-1}$

-----

Analogue: 9,11-Dioxopentadecanoic Acid (4)

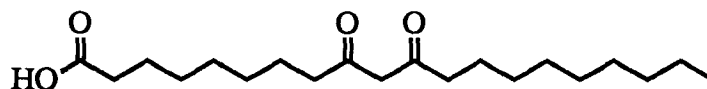


pH	5.40	6.36	7.11	7.60	8.02	8.32	8.48	9.19	9.88
A (298 nm)	0.282	0.296	0.389	0.481	0.632	0.727	0.805	1.286	1.576

pH	10.62	10.94	11.27	11.46
A (298 nm)	1.627	1.632	1.636	1.637

$pK_a' = 8.69 \pm 0.02$                        $\beta = (1.7 \pm 0.1) \times 10^2 \text{ M}^{-1}$

Analogue: 9,11-Dioxoeicosanoic Acid (29)



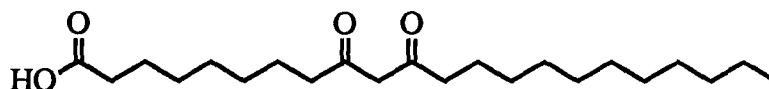
pH	5.40	6.42	7.14	7.61	8.03	8.27	8.38	8.98	9.60
A (298 nm)	0.257	0.274	0.334	0.435	0.561	0.624	0.723	1.039	1.367

pH	10.46	10.81	11.21	11.41
A (298 nm)	1.498	1.508	1.516	1.519

$pK_a' = 8.68 \pm 0.02$                        $\beta = (2.2 \pm 0.2) \times 10^2 \text{ M}^{-1}$

-----

Analogue: 9,11-Dioxodoeicosanoic Acid (30)



pH	5.46	6.42	7.14	7.61	8.03	8.27	8.38	8.98	9.60
A (298 nm)	0.251	0.276	0.322	0.405	0.488	0.543	0.590	1.012	1.262

pH	10.46	10.81	11.21
A (298 nm)	1.416	1.422	1.419

$pK_a' = 8.77 \pm 0.02$                        $\beta = (2.0 \pm 0.1) \times 10^2 \text{ M}^{-1}$

### 3.7.3 Binding of Magnesium

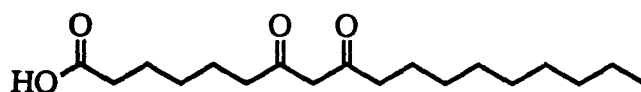
Solvent: 80% MeOH-H<sub>2</sub>O

Ionic Medium: 16,7 mM MgCl<sub>2</sub>

Concentration: 80  $\mu$ M

Titant: Me<sub>4</sub>NOH

Analogue: 7,9-Dioxooctadecanoic Acid (33)



pH	5.61	6.58	7.20	7.64	7.95	8.23	8.48	9.21	9.51
A (298 nm)	0.303	0.533	0.856	1.095	1.251	1.335	1.397	1.473	1.478

$pK_a' = 7.28 \pm 0.02$

$\beta = (7.6 \pm 0.4) \times 10^3 \text{ M}^{-1}$

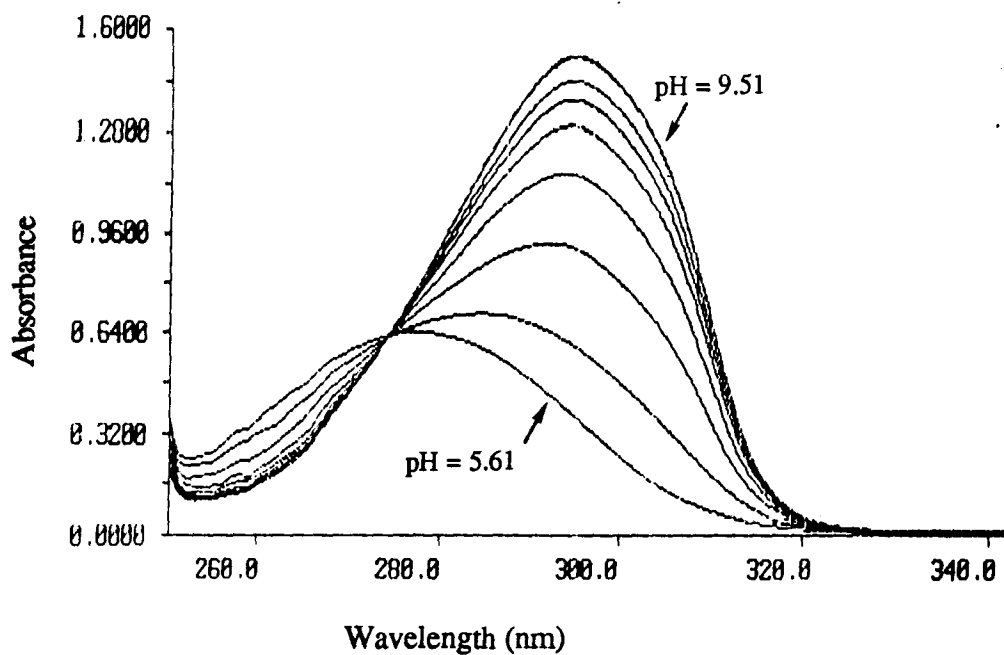


Figure 33. UV spectrophotometric absorption spectra of analogue 33 as the pH of the solution increased from 5.61 to 9.51 in the presence of MgCl<sub>2</sub>.

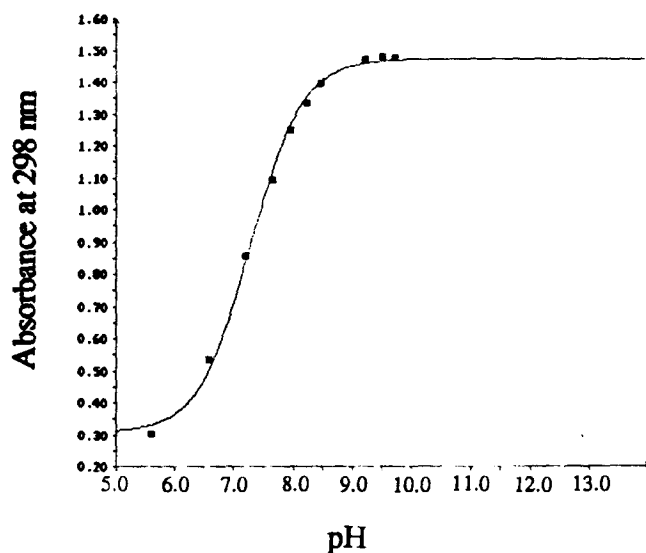
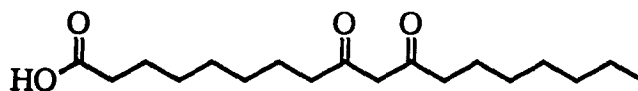


Figure 34. Plot of the UV absorbance at 298 nm versus pH for analogue 33 in the presence of  $\text{MgCl}_2$ .

-----  
Analogue: 9,11-Dioxooctadecanoic Acid (28)



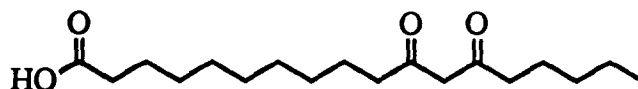
pH	5.50	6.49	7.10	7.56	7.95	8.22	8.53	9.28	9.54
A (298 nm)	0.351	0.556	0.828	1.134	1.376	1.534	1.626	1.764	1.775

$$\text{pK}_a' = 7.50 \pm 0.02$$

$$\beta = (3.4 \pm 0.2) \times 10^3 \text{ M}^{-1}$$

-----

Analogue: 11,13-Dioxooctadecanoic Acid (34)

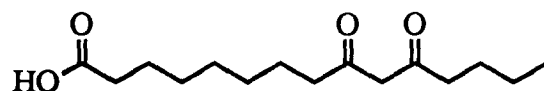


pH	5.61	6.58	7.20	7.64	7.95	8.23	8.48	9.21	9.51
A (298 nm)	0.341	0.493	0.769	1.045	1.280	1.436	1.549	1.678	1.699

$$\text{pK}_a' = 7.61 \pm 0.02$$

$$\beta = (1.9 \pm 0.1) \times 10^3 \text{ M}^{-1}$$

Analogue: 9,11-Dioxopentadecanoic Acid (4)



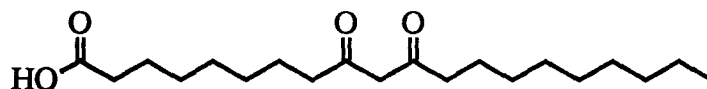
pH	5.50	6.49	7.10	7.56	7.95	8.22	8.53	9.28	9.54
A (298 nm)	0.307	0.586	0.764	1.198	1.356	1.479	1.535	1.596	1.599

$pK_a' = 7.28 \pm 0.02$

$\beta = (4.4 \pm 0.2) \times 10^3 \text{ M}^{-1}$

-----

Analogue: 9,11-Dioxoeicosanoic Acid (29)



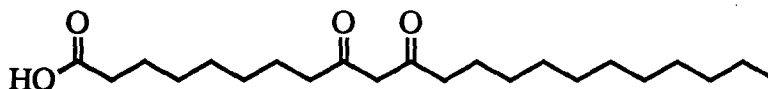
pH	5.50	6.49	7.10	7.56	7.95	8.22	8.53	9.28	9.54
A (298 nm)	0.278	0.448	0.749	1.047	1.263	1.337	1.398	1.473	1.473

$pK_a' = 7.29 \pm 0.02$

$\beta = (5.6 \pm 0.2) \times 10^3 \text{ M}^{-1}$

-----

Analogue: 9,11-Dioxodoeicosanoic Acid (30)



pH	5.61	6.58	7.20	7.64	7.95	8.23	8.48	9.21	9.51
A (298 nm)	0.288	0.392	0.798	1.059	1.203	1.288	1.338	1.436	1.440

$pK_a' = 7.31 \pm 0.02$

$\beta = (5.7 \pm 0.3) \times 10^3 \text{ M}^{-1}$

### 3.7.4 Binding of Sodium

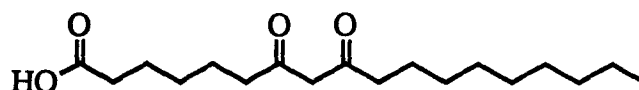
Solvent: 80% MeOH-H<sub>2</sub>O

Ionic Medium: 50 mM NaCl

Concentration: 80  $\mu$ M

Titant: Me<sub>4</sub>NOH

Analogue: 7,9-Dioxooctadecanoic Acid (33)



pH	5.84	6.82	7.52	8.12	8.74	9.34	9.70	10.34	10.60
A (298 nm)	0.270	0.276	0.289	0.307	0.325	0.345	0.375	0.663	0.768
pH	11.00	11.20	11.46	11.62	11.88	12.06	12.26	12.50	12.70
A (298 nm)	0.976	1.070	1.214	1.304	1.378	1.402	1.462	1.513	1.537

$$pK_a' = 11.16 \pm 0.02$$

$$\beta = 1.8 \pm 0.1 \text{ M}^{-2}$$

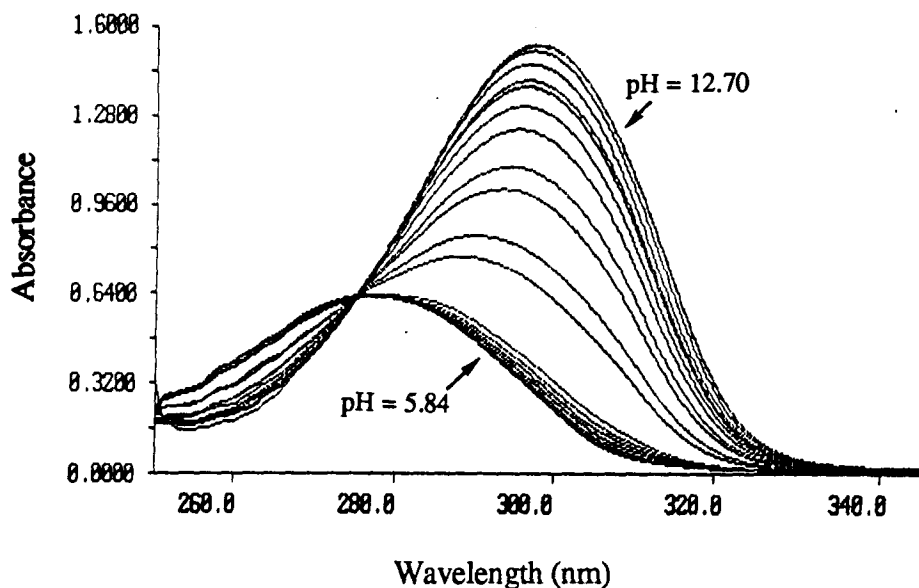
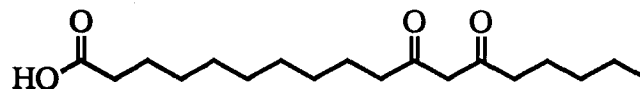


Figure 35. UV spectrophotometric absorption spectra of analogue 33 as the pH of the solution increased from 5.84 to 12.70 in the presence of NaCl.





Analogue: 11,13-Dioxooctadecanoic Acid (34)



pH 5.84 6.82 7.52 8.12 8.74 9.34 9.70 10.34 10.60

A (298 nm) 0.322 0.322 0.331 0.346 0.356 0.363 0.373 0.581 0.793

pH 11.00 11.20 11.46 11.62 11.88 12.06 12.26 12.50 12.70

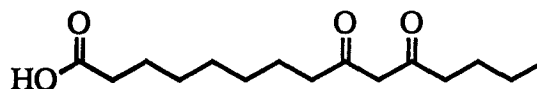
A (298 nm) 1.107 1.245 1.489 1.613 1.725 1.755 1.815 1.843 1.850

$\text{pK}_{\text{a}}' = 11.00 \pm 0.02$

$\beta = 0.8 \pm 0.1 \text{ M}^{-2}$

-----

Analogue: 9,11-Dioxopentadecanoic Acid (4)



pH 5.84 6.82 7.52 8.12 8.74 9.34 9.70 10.34 10.60

A (298 nm) 0.280 0.281 0.290 0.299 0.318 0.332 0.342 0.608 0.805

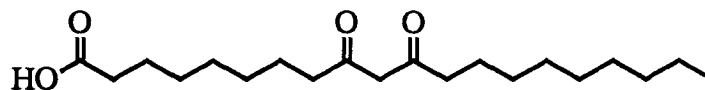
pH 11.00 11.20 11.46 11.62 11.88 12.06 12.26 12.50 12.76

A (298 nm) 1.058 1.184 1.311 1.422 1.524 1.557 1.612 1.636 1.664

$\text{pK}_{\text{a}}' = 10.90 \pm 0.02$

$\beta = 1.0 \pm 0.1 \text{ M}^{-2}$

Analogue: 9,11-Dioxoeicosanoic Acid (29)



pH 5.84 6.82 7.52 8.12 8.74 9.34 9.70 10.34 10.60

A (298 nm) 0.274 0.275 0.289 0.306 0.314 0.318 0.326 0.590 0.696

pH 11.00 11.20 11.46 11.62 11.88 12.06 12.26 12.50 12.76

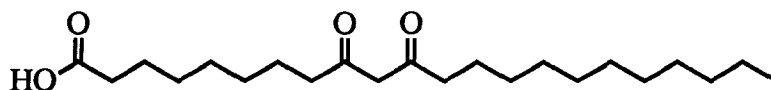
A (298 nm) 0.957 1.102 1.296 1.394 1.470 1.495 1.544 1.570 1.587

$\text{pK}_{\text{a}}' = 10.96 \pm 0.02$

$\beta = 1.2 \pm 0.1 \text{ M}^{-2}$

-----

Analogue: 9,11-Dioxodoeicosanoic Acid (30)



pH 5.84 6.82 7.52 8.12 8.74 9.34 9.70 10.34 10.60

A (298 nm) 0.252 0.255 0.262 0.275 0.282 0.287 0.292 0.411 0.655

pH 11.00 11.20 11.46 11.62 11.88 12.06 12.26 12.50 12.76

A (298 nm) 0.866 0.981 1.163 1.273 1.330 1.395 1.447 1.476 1.483

$\text{pK}_{\text{a}}' = 11.03 \pm 0.02$

$\beta = 1.1 \pm 0.1 \text{ M}^{-2}$

### 3.7.5 Binding of Potassium

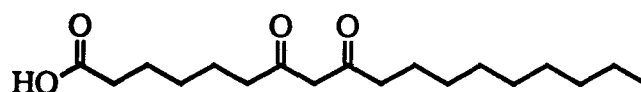
Solvent: 80% MeOH-H<sub>2</sub>O

Ionic Medium: 50 mM KCl

Concentration: 80  $\mu$ M

Titant: Me<sub>4</sub>NOH

Analogue: 7,9-Dioxooctadecanoic Acid (33)



pH	5.84	6.82	7.52	8.12	8.74	9.34	9.70	10.34	10.60
A (298 nm)	0.252	0.261	0.279	0.291	0.300	0.324	0.359	0.524	0.652

pH	11.00	11.20	11.46	11.62	11.88	12.06	12.26	12.50	12.70
A (298 nm)	0.854	0.978	1.164	1.248	1.349	1.380	1.436	1.468	1.482

$pK_a' = 11.03 \pm 0.02$

$\beta = 1.3 \pm 0.1 \text{ M}^{-2}$

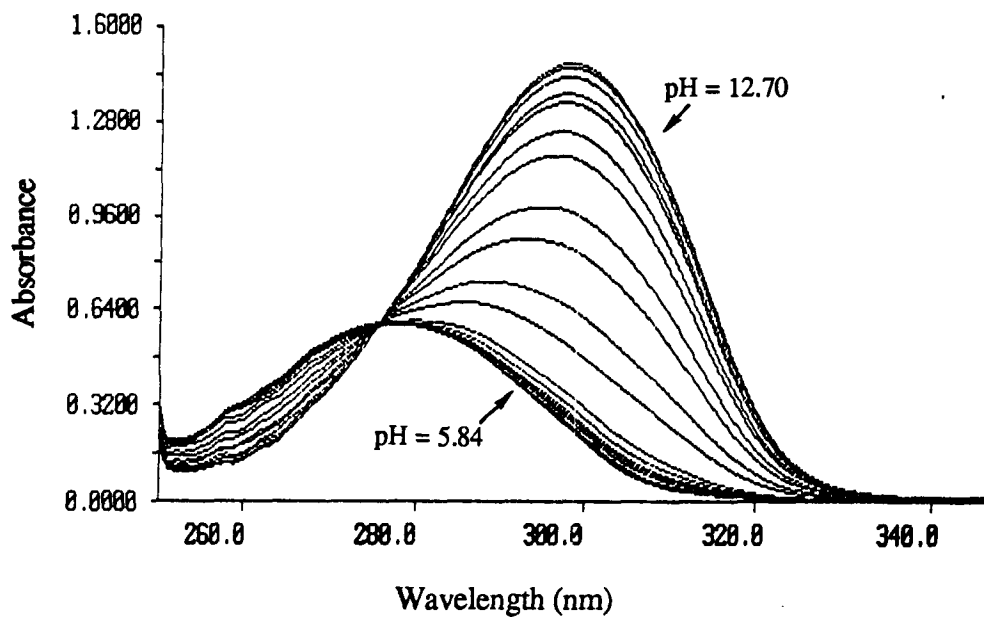


Figure 37. UV spectrophotometric absorption spectra of analogue 33 as the pH of the solution increased from 5.84 to 12.70 in the presence of KCl.

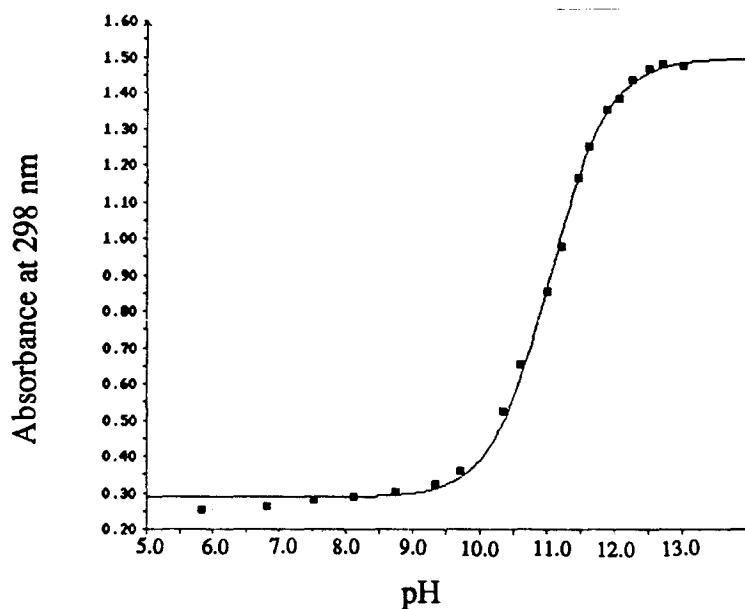
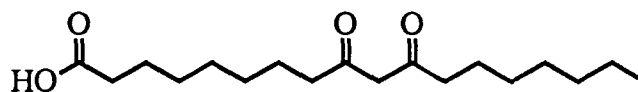


Figure 38. Plot of the UV absorbance at 298 nm versus pH for analogue **33** in the presence of KCl.

Analogue: 9,11-Dioxooctadecanoic Acid (**28**)



pH	5.84	6.82	7.52	8.12	8.74	9.34	9.70	10.34	10.60
----	------	------	------	------	------	------	------	-------	-------

A (298 nm)	0.260	0.278	0.299	0.312	0.330	0.332	0.352	0.500	0.618
------------	-------	-------	-------	-------	-------	-------	-------	-------	-------

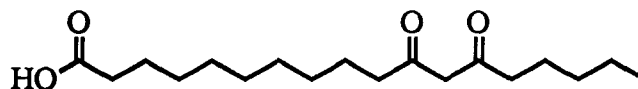
pH	11.00	11.20	11.46	11.62	11.88	12.06	12.26	12.50	12.70
----	-------	-------	-------	-------	-------	-------	-------	-------	-------

A (298 nm)	0.848	0.990	1.171	1.279	1.384	1.418	1.480	1.506	1.519
------------	-------	-------	-------	-------	-------	-------	-------	-------	-------

$pK_a' = 11.09 \pm 0.02$

$\beta = 0.9 \pm 0.1 \text{ M}^{-2}$

Analogue: 11,13-Dioxooctadecanoic Acid (34)



pH 5.84 6.82 7.52 8.12 8.74 9.34 9.70 10.34 10.60

A (298 nm) 0.293 0.304 0.327 0.350 0.356 0.377 0.427 0.671 0.814

pH 11.00 11.20 11.46 11.62 11.88 12.06 12.26 12.50 12.70

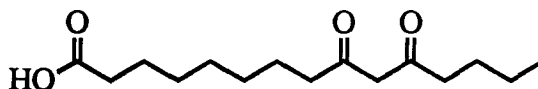
A (298 nm) 1.073 1.220 1.406 1.507 1.610 1.633 1.682 1.726 1.751

$\text{pK}_{\text{a}}' = 10.94 \pm 0.02$

$\beta = 0.9 \pm 0.1 \text{ M}^{-2}$

-----

Analogue: 9,11-Dioxopentadecanoic Acid (4)



pH 5.84 6.82 7.52 8.12 8.74 9.34 9.70 10.34 10.60

A (298 nm) 0.286 0.287 0.300 0.308 0.316 0.335 0.340 0.543 0.725

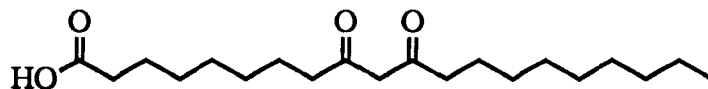
pH 11.00 11.20 11.46 11.62 11.88 12.06 12.26 12.50 12.76

A (298 nm) 0.991 1.060 1.308 1.441 1.543 1.576 1.618 1.662 1.680

$\text{pK}_{\text{a}}' = 11.00 \pm 0.02$

$\beta = 0.8 \pm 0.1 \text{ M}^{-2}$

Analogue: 9,11-Dioxoeicosanoic Acid (29)



pH 5.84 6.82 7.52 8.12 8.74 9.34 9.70 10.34 10.60

A (298 nm) 0.271 0.271 0.283 0.295 0.301 0.306 0.307 0.430 0.598

pH 11.00 11.20 11.46 11.62 11.88 12.06 12.26 12.50 12.76

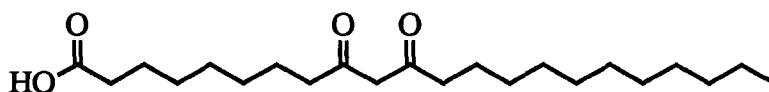
A (298 nm) 0.822 0.962 1.221 1.314 1.449 1.488 1.548 1.576 1.596

$pK_a' = 11.14 \pm 0.02$

$\beta = 0.8 \pm 0.1 \text{ M}^{-2}$

-----

Analogue: 9,11-Dioxodoeicosanoic Acid (30)



pH 5.84 6.82 7.52 8.12 8.74 9.34 9.70 10.34 10.60

A (298 nm) 0.251 0.255 0.270 0.278 0.277 0.278 0.280 0.409 0.557

pH 11.00 11.20 11.46 11.62 11.88 12.06 12.26 12.50 12.76

A (298 nm) 0.762 0.863 1.141 1.231 1.330 1.378 1.424 1.470 1.480

$pK_a' = 11.14 \pm 0.02$

$\beta = 0.8 \pm 0.1 \text{ M}^{-2}$

### 3.17.6 Binding of Magnesium

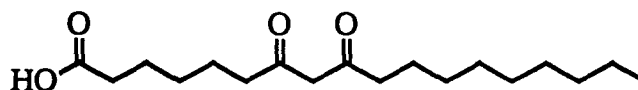
Solvent: 80% MeOH-H<sub>2</sub>O    Ionic Medium: 50 mM CHES/Me<sub>4</sub>NOH buffer

pH = 9.10

Concentration: 80  $\mu$ M

Titant: MgCl<sub>2</sub> (10<sup>-4</sup> M)

Analogue: 7,9-Dioxooctadecanoic Acid (33)



[MgCl <sub>2</sub> ]	0.25	0.50	0.98	1.47	2.68	3.88	6.28	8.65	13.40
A (298 nm)	0.511	0.608	0.741	0.853	1.032	1.132	1.246	1.302	1.359

$n = 1.0 \pm 0.1$

$\beta = (7.1 \pm 0.1) \times 10^3 \text{ M}^{-1}$

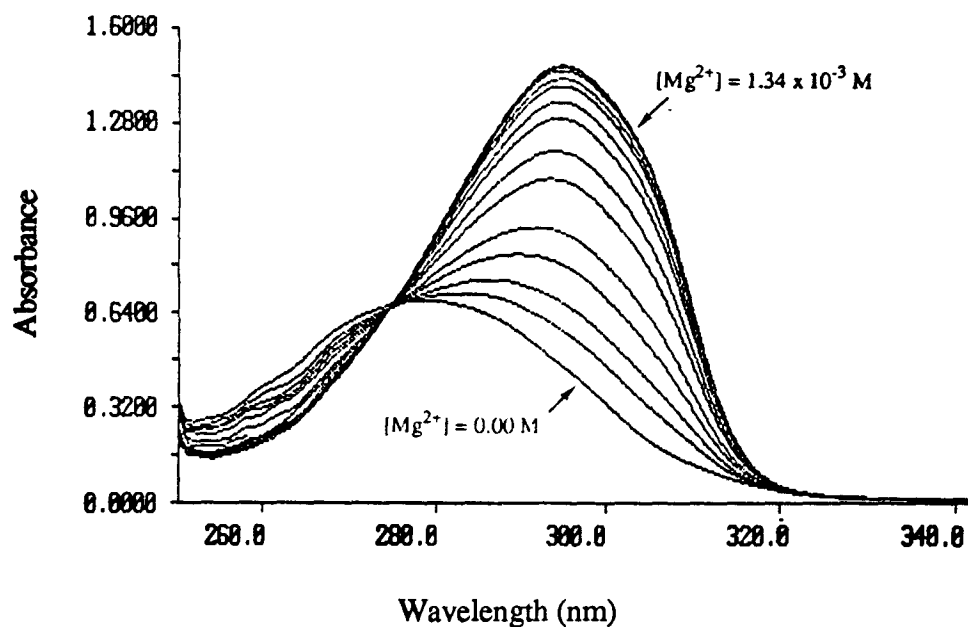


Figure 29. UV spectrophotometric absorption spectra of analogue 33 as the concentration of MgCl<sub>2</sub> increased from 0.25 to 1.34  $\times 10^{-3}$  M at pH = 9.10.



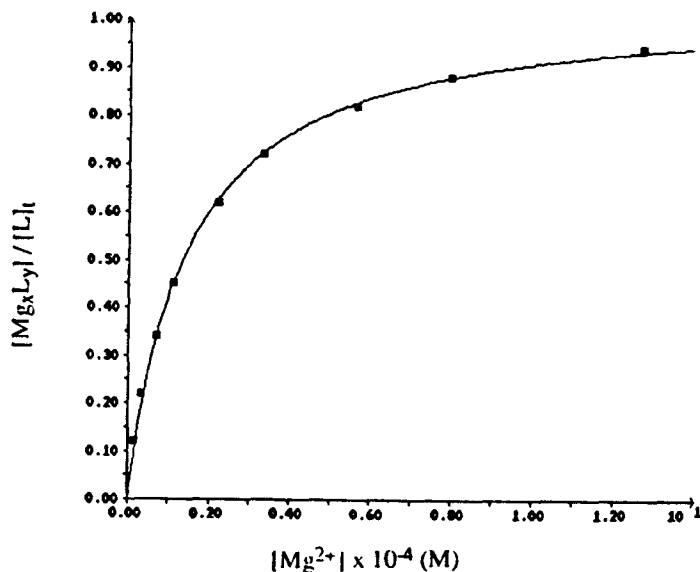
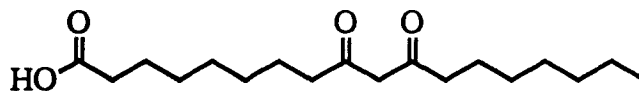


Figure 30. Plot of the number of moles of magnesium bound per mole of analogue 33 versus concentration of magnesium.

-----

Analogue: 9,11-Dioxooctadecanoic Acid (28)



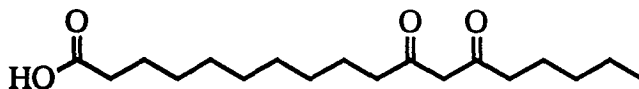
[MgCl <sub>2</sub> ]	0.25	0.50	0.98	1.47	2.68	3.88	6.28	8.65	13.40
A (298 nm)	0.526	0.630	0.804	0.913	1.128	1.259	1.409	1.496	1.581

$$n = 1.0 \pm 0.1$$

$$\beta = (5.6 \pm 0.1) \times 10^3 \text{ M}^{-1}$$

-----

Analogue: 11,13-Dioxooctadecanoic Acid (34)

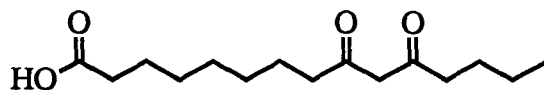


[MgCl <sub>2</sub> ]	0.25	0.50	0.98	1.47	2.68	3.88	6.28	8.65	13.40
A (298 nm)	0.536	0.618	0.785	0.890	1.091	1.239	1.380	1.468	1.554

$$n = 1.0 \pm 0.1$$

$$\beta = (4.5 \pm 0.1) \times 10^3 \text{ M}^{-1}$$

Analogue: 9,11-Dioxopentadecanoic Acid (4)



[MgCl <sub>2</sub> ]	0.25	0.50	0.98	1.47	2.68	3.88	6.28	8.65	13.40
----------------------	------	------	------	------	------	------	------	------	-------

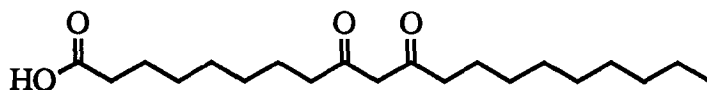
A (298 nm)	0.444	0.542	0.695	0.804	0.982	1.126	1.251	1.324	1.390
------------	-------	-------	-------	-------	-------	-------	-------	-------	-------

$n = 1.0 \pm 0.1$

$\beta = (5.5 \pm 0.1) \times 10^3 \text{ M}^{-1}$

-----

Analogue: 9,11-Dioxoeicosanoic Acid (29)



[MgCl <sub>2</sub> ]	0.25	0.50	0.98	1.47	2.68	3.88	6.28	8.65	13.40
----------------------	------	------	------	------	------	------	------	------	-------

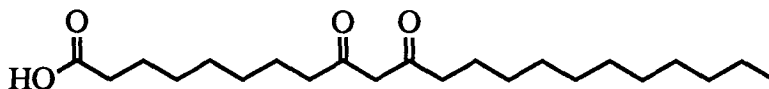
A (298 nm)	0.450	0.545	0.701	0.819	1.007	1.114	1.243	1.302	1.369
------------	-------	-------	-------	-------	-------	-------	-------	-------	-------

$n = 1.0 \pm 0.1$

$\beta = (6.2 \pm 0.1) \times 10^3 \text{ M}^{-1}$

-----

Analogue: 9,11-Dioxodoeicosanoic Acid (30)



[MgCl <sub>2</sub> ]	0.25	0.50	0.98	1.47	2.68	3.88	6.28	8.65	13.40
----------------------	------	------	------	------	------	------	------	------	-------

A (298 nm)	0.442	0.536	0.672	0.786	0.964	1.071	1.199	1.258	1.325
------------	-------	-------	-------	-------	-------	-------	-------	-------	-------

$n = 1.0 \pm 0.1$

$\beta = (6.2 \pm 0.1) \times 10^3 \text{ M}^{-1}$

## REFERENCES

- (1) (a) Berridge, M.J. *Sci. Am.* **1985**, 253 (4), 142; (b) Carafoli, E. and Penniston, J.T. *Sci. Am.* **1985**, 253 (5), 70; (c) Ochial, E. *J. Chem. Educ.* **1991**, 68, 10.
- (2) Davy, H. *Philos. Soc. Trans. R. Soc. London*, **1808**, 98, 333.
- (3) Ringer, S. *J. Physiol.* **1883**, 4, 29.
- (4) (a) Ringer, S. *J. Physiol.* **1886**, 7, 291; (b) Ringer, S. *J. Physiol.* **1890**, 11, 79.
- (5) Locke, F.S. *J. Physiol.* **1894**, 8, 166.
- (6) (a) Loeb, J. *The Dynamics of Living Matter*; Columbia University: New York, **1906**;  
(b) Mines, G.R. *J. Physiol.* **1910**, 40, 327; **1913**, 46, 188; (c) Loewi, O. *Pharmacol.* **1917**, 82, 131.
- (7) (a) Heilbrunn, L.V. and Wilbur, K.M. *Biol. Bull.* **1937**, 73, 557; (b) Heilbrunn, L.V. and Wiercinski, F.J. *J. Cell Comp. physiol.* **1947**, 29, 15.
- (8) Campbell, A.K. *Intracellular Calcium, Its Universal Role as Regulator*; John Wiley & Sons: Toronto, **1983**.
- (9) Nordin, B.E.C. *Calcium in Human Biology*; Springer-Verlag: Germany, **1988**.
- (10) (a) Berridge, M.J. and Irvine, R.F. *Nature*, **1989**, 341, 197; (b) Altman, J. *Nature*, **1988**, 331, 119.
- (11) Potter, J.D. and Johnson, J.D. *Calcium and Cell Function*; Academic: New York, **1982**, 2, 145.
- (12) (a) Lehninger, A.L. *Biochem. J.* **1970**, 119, 129; (b) Somlyo, A.P. Bond, M. and Somlyo, A.V. *Nature*, **1985**, 314, 622.

- (13) (a) Ashley, C.C. Campbell, A.K. *Detection and Measurement of Free Calcium in Cells*; Amsterdam, Elsevier/North-Holland, **1979**; (b) Blinks, J.R. Wier, W.G. Hess, P. and Prendergast, F.G. *Prog. Biophys. Mol. Biol.* **1982**, 1.
- (14) Kretsinger, R.H. *Calcium Binding Proteins and Calcium Function*; Amsterdam, Elsevier/North-Holland, **1977**, 63.
- (15) (a) Hagiwara, S. and Byerly, L. *Annu. Rev. Neurosci.* **1981**, 4, 69;  
(b) Blaustein, M.P. *Calcium in Biological System*; Plenum: New York, **1985**.
- (16) DeMeis, L. and Inesi, G. *Membrane Transport of Calcium*; Academic: New York, **1982**, 141.
- (17) Pressman, B.C. Harris, E.J. Jagger, W.S. and Johnson, J.H. *Proc. Natl. Acad.Sci.* **1967**, 58, 1949.
- (18) Berger, J. Rachlin, A.I. Scott, W.E. Sternbach, L.H. and Goldberg, M.W. *J. Am. Chem. Soc.* **1951**, 73, 5295.
- (19) (a) Reed, P.W. *Fedn Proc.* **1972**, 31, 432; (b) Reed, P.W. and Lardy, H.A. *J. Biol. Chem.* **1972**, 247, 6970.
- (20) (a) Westley, J.W. Evens, R.H. Jr. Williams, T. and Stempel, A. *J. Chem. Soc. Chem. Commun.* **1970**, 71; (b) Chaney, M.O. Demarco, P.V. Johes, N.D. and Occolowitz, J.L. *J. Am. Chem. Soc.* **1974**, 96, 1932.
- (21) Gale, E.F. Cundliffe, E. Reynolds, P.E. Richmond, M.H. and Waring, M.J. *The Molecular Basis of Antibiotic Action*; John Wiley and Sons: Toronto, **1972**, 154.
- (22) Johnson, S.M. Jerrin, J. Liu, S.J. and Paul, I.C. *J. Am. Chem. Soc.* **1970**, 92, 4428.
- (23) (a) Smith, G.D. and Duax, W.L. *J. Am. Chem. Soc.* **1976**, 98, 1578; (b) Deber, C.M. and Pfeiffer, D.R. *Biochemistry* **1976**, 15, 132.
- (24) (a) Still, W.C. Cai, D. Lee, D. Hauck, P. Bernardi, A. and Romero, A. *Lectures in Heterocyclic Chemistry*, **1987**, 9, 33, (b) Still, W.C. and Smith, W. *J. Am. Chem. Soc.* **1988**, 110, 7917, (c) Still, W.C. and Iimori T. *J. Am. Chem. Soc.* **1989**, 111, 3439, (d) Still, W.C. and Erickson, S.D. *Tetrahedron Lett.* **1990**, 31, 4253.

- (25) Riddell, F.G. *Chemistry in Britain*, **1992**, 533.
- (26) Westley, J.W. *Polyether Antibiotics - Naturally Occurring Acid Ionophores*; Marcel Dekker: New York, **1982**, 1.
- (27) (a) Umen, M.J. and Scarpa, A. *J. Med. Chem.* **1978**, 21, 505; (b) Hiratani, K. Sughara, H. Taguchi, K and Iio, K. *Chem. Lett.* **1983**, 1657; **1984**, 1457; (c) Ashton, R. and Steinrauf, L.K. *J. Mol. Biol.* **1970**, 49, 547; (d) Lehn, J.M. and Behr, J.P. *J. Am. Chem. Soc.* **1973**, 95, 6108; (e) Lehn, J.M. and Kirch, M. *Angew. Chem. Int. Ed. Engl.* **1975**, 14, 555; (f) Rebek, J. Jr. Askew, B. Nemeth, D. and Parris, K. *J. Am. Chem. Soc.* **1987**, 109, 2432; (g) Fyles, T.M. *Inclusion Aspects of Membrane Chemistry*; Kluwer Academic: Netherlands, **1991**, 59.
- (28) (a) Fenton, D.E. *Chem. Soc. Rev.* **1977**, 6, 325; (b) Stein, W.D. *Channels, Carriers, and Pumps*, Academic: New York, **1990**.
- (29) (a) Meyers, E. Slusarchyk, D.S. and Liu, W.C. *U.S. Patent 3 873 693*, **1975**; *Chem. Abstr.* **1975**, 83, 41512a; (b) Meyers, E. Slusarchyk, D.S. Liu, W.C. Astle, G. Trejo, W.H. and Brown, W.E. *J. Antibiot.* **1978**, 31, 815.
- (30) Toeplitz, B.K. Cohen, A.I. Funke, R.T. Parker, W.L. and Gougoutas, J.Z. *J. Am. Chem. Soc.* **1979**, 101, 3344.
- (31) Seco, M. *J. Chem. Ed.* **1989**, 66, 779.
- (32) Stiles, M.K. Craig, M.E. Gunnell, S.L.N. Pfeiffer, D.R. and Taylor, R.W. *J. Biol. Chem.* **1991**, 266, 8336.
- (33) Liu, C.M. and Hermann, T.E. *J. Biol. Chem.* **1978**, 253, 5892.
- (34) Kauffman, R.F. Taylor, R.W. and Pfeiffer, D.R. *J. Biol. Chem.* **1978**, 253, 5892.
- (35) Kauffman, R.F. Taylor, R.W. and Pfeiffer, D.R. *J. Biol. Chem.* **1980**, 255, 2735.
- (36) Bennett, J.P. Cockcroft, S. and Gomperts, B.D. *Nature*, **1979**, 282, 851.

- (37) Rittenhouse, S.E. and Horne, W.C. *Biochem. Biophys. Res. Commun.* **1984**, *123*, 393.
- (38) Rubin, R.P. Kelly, K.L. Halenda, S.P. and Laychock, S.G. *Prostaglandin*, **1982**, *24*, 179.
- (39) (a) Hanessian, S. Cooke, N.G. Dehoff, B. and Sakito, Y. *J. Am. Chem. Soc.* **1990**, *112*, 5276; (b) Evans, D.A. Low, R.L. Shih, T.L. Takacs, J.M. and Zahler, R. *J. Am. Chem. Soc.* **1990**, *112*, 5290; (c) Weiler, L. and Shelly, K. *Can. J. Chem.* **1988**, *66*, 1359; (d) Weiler, L. and Nicoll-Griffith, D.A. *Tetrahedron*, **1991**, *47*, 2733.
- (40) (a) Dijkstra, B.W. Kalk, K.H. Hol, W.G.J. and Drenth, J. *J. Mol. Biol.* **1981**, *147*, 97; (b) Kretsinger, R.H. *Ann. Rev. Biochem.* **1976**, *45*, 239; (c) Kretsinger, R.H. *Crit. Rev. Biochem.* **1980**, 114.
- (41) Carey, F.A. and Sundberg, R.J. *Advanced Organic Chemistry*; Plenum: New York, **1984**, *2*, 481.
- (42) (a) Gallagher, A.F. and Hibbert, H. *J. Am. Chem. Soc.* **1936**, *58*, 813; (b) Krespan, C.G. *J. Org. Chem.* **1974**, *39*, 2351; (c) Newcomb, M. Moore, S.S. and Cram, D.J. *J. Am. Chem. Soc.* **1977**, *99*, 6405.
- (43) (a) Huckin, S.N. and Weiler, L. *J. Am. Chem. Soc.* **1974**, *96*, 1082; (b) Sum, F.N. and Weiler, L. *J. Am. Chem. Soc.* **1979**, *101*, 4401.
- (44) Hendrich, C.A. *Tetrahedron*, **1977**, *33*, 1845.
- (45) Chandhary, S.K. and Hernandez, O. *Tetrahedron Lett.* **1979**, 99.
- (46) Fuji, K. Nakano, S. and Fujita, E. *Synthesis*, **1975**, 276.
- (47) Gibson, T. *J. Org. Chem.* **1980**, *45*, 1095.
- (48) Freedman, H.H. and Dubois, R.A. *Tetrahedron Lett.* **1975**, *38*, 3251.

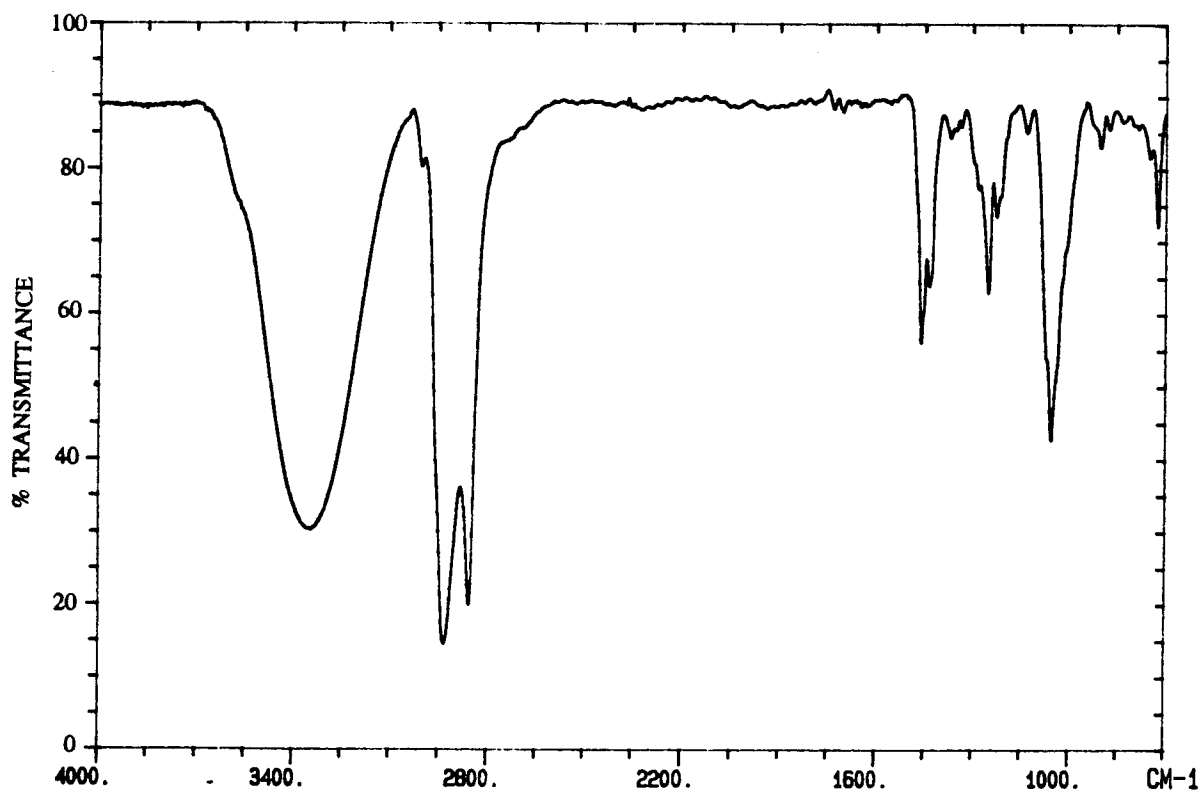
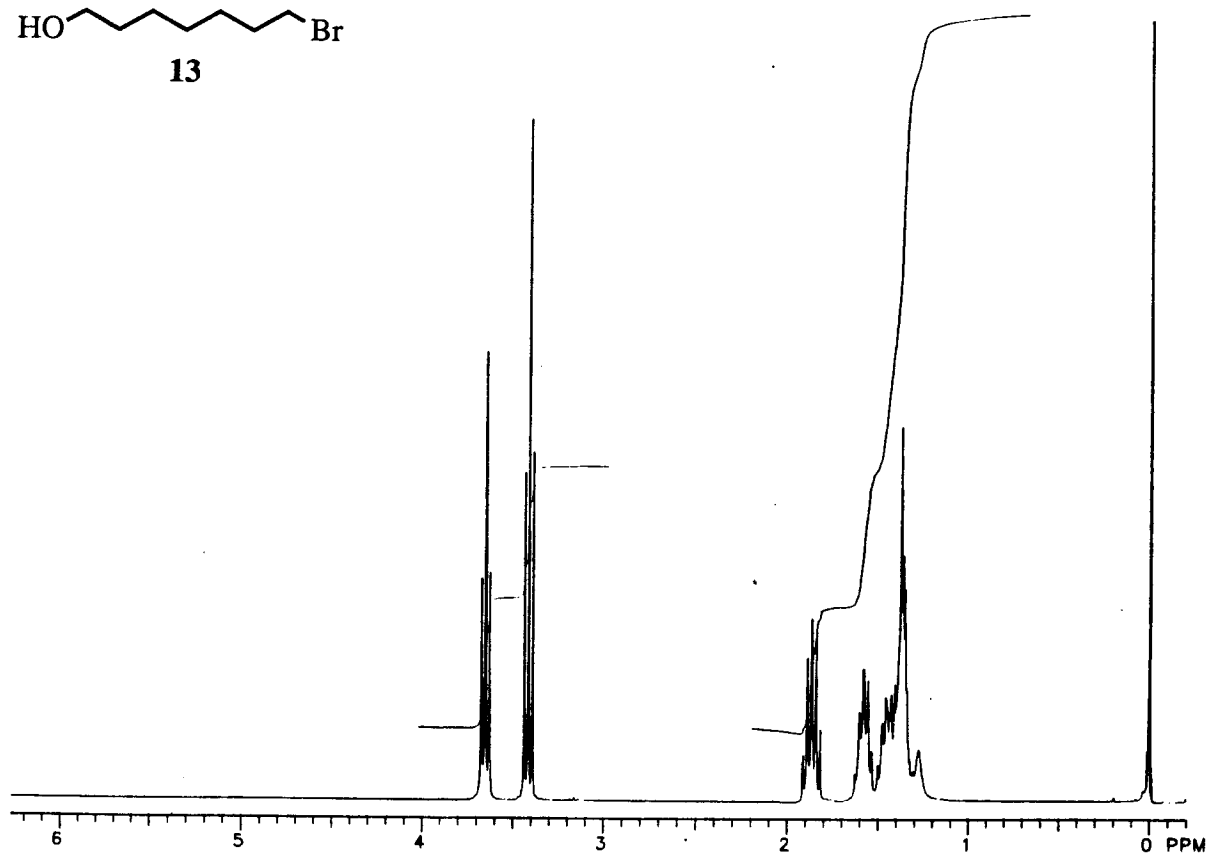
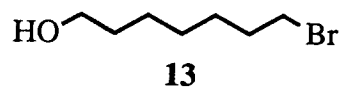
- (49) Corey, E.J. Niwa, H. and Knolle, J. *J. Am. Chem. Soc.* **1978**, *100*, 1942.
- (50) Corey, E.J. and Snider, B.B. *J. Am. Chem. Soc.* **1972**, *94*, 2549.
- (51) Appel, R. *Angew. Chem. Int. Ed. Engl.* **1975**, *14*, 801.
- (52) Moffatt, J.G. *J. Org. Chem.* **1971**, *36*, 1909.
- (53) Corey, E.J. and Das, J. *J. Am. Chem. Soc.* **1982**, *104*, 5551.
- (54) Bowden, K. Heilbon, I.M. Jones, E.R.H. and Weedon, B.C.L. *J. Chem. Soc.* **1946**, 39.
- (55) Smith, J. *Introduction to the Principle of Drug Design*; Hywel Williams Wright PSG, **1983**.
- (56) Rekker, R.F. *The Hydrophobic Fragmental Constant*; Elsevier Scientific: Germany, **1977**.
- (57) Westley, J.W. *Polyether antibiotics: naturally occurring acid ionophores*; Marcel Dekker: New York, **1982**.
- (58) Hancock, R.D. and Martell, A.E. *Chem. Rev.* **1989**, *89*, 1875.
- (59) Grynkiewicz, G. Peonie, M. and Tsien, R.Y. *J. Biol. Chem.* **1985**, *6*, 145.
- (60) (a) Christensen, H.N. *Biological Transport*, W.A.Benjamin Inc. **1975**;  
(b) Neame, K.D. and Richards, T.G. *Elementary Kinetics of Membrane Carrier Transport*; Blackwell Scientific: Oxford, England, **1972**.
- (61) Michaelis, L. and Menten, M.L. *Biochem. J.* **1913**, *49*, 333.
- (62) Briggs, G.E. and Haldane, J.B.S. *Biochem. J.* **1925**, *19*, 338.
- (63) Leatherbarrow, R.J. *Enzfitter*; Elsevier: Amsterdam, The Netherlands, **1987**.

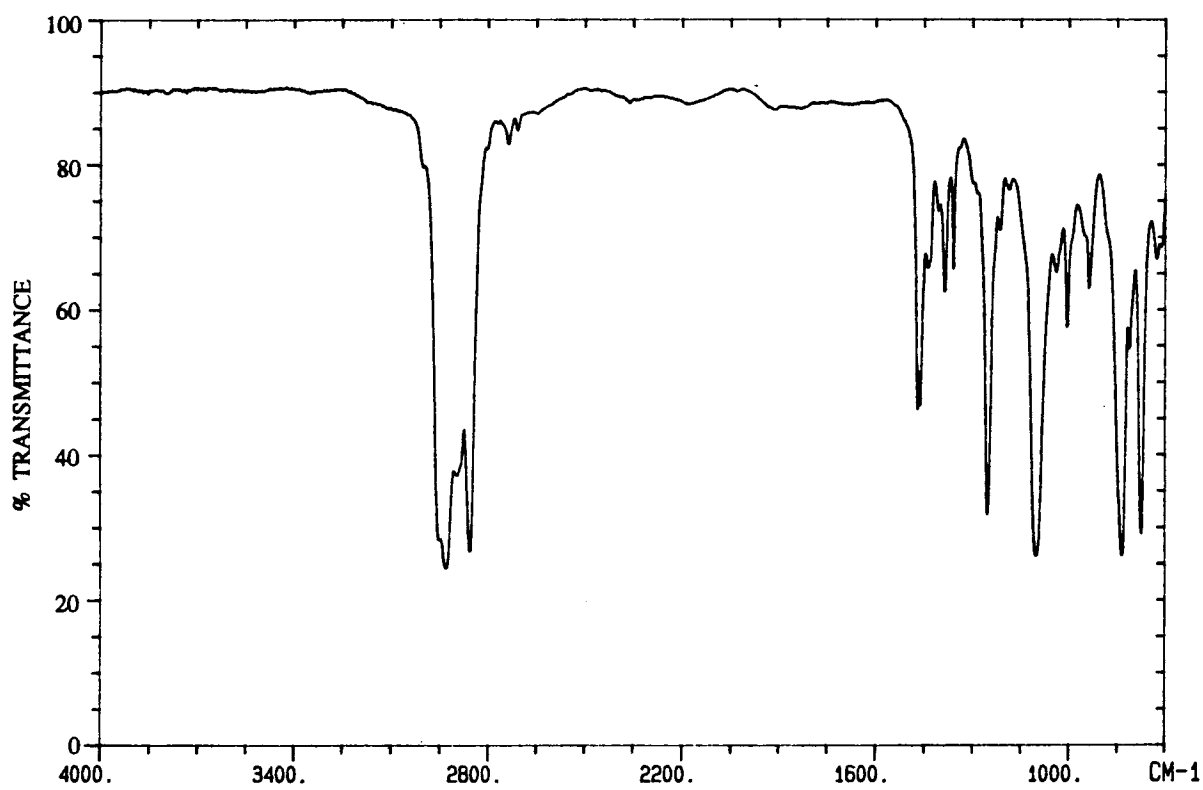
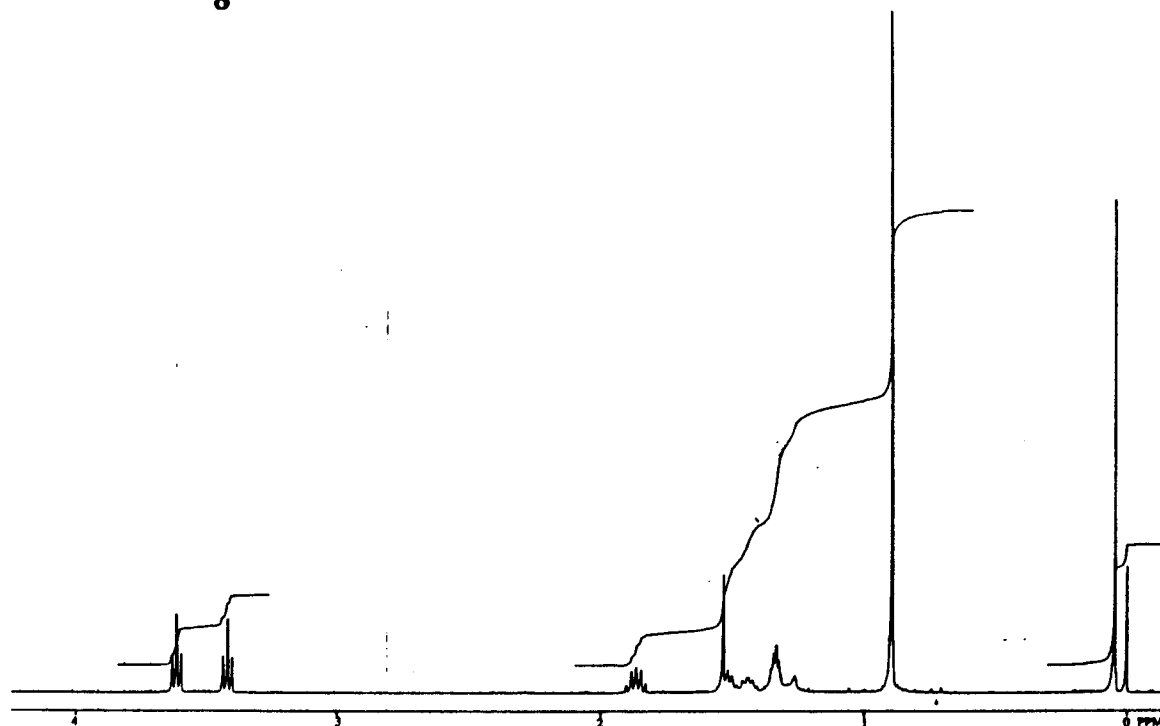
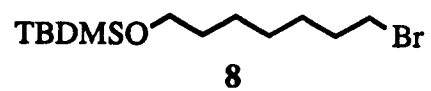
- (64) Brady, J.E. and Humiston, G.E. *General Chemistry*, John Wiley & Sons: Toronto, **1982**.
- (65) (a) Kang, S.I. Czech, A. Czeck, B.P. Stewart, L.E. and Bartsch, R.A. *Anal. Chem.* **1985**, 57, 1713; (b) Sawyer, D.T. and Paulsen, P.J. *J. Am. Chem. Soc.* **1959**, 81, 819.
- (66) (a) Raban, M. Noe, E.A. and Yamamoto, G. *J. Am. Chem. Soc.* **1977**, 99, 6527; (b) Luehrs, D.C. Iwamoto, R.T. and Kleinberg, J. *Inorg. Chem.* **1965**, 4, 1739.
- (67) Connors, K.A. *Binding Constants*; John Wiley & Sons: Toronto, **1987**.
- (68) (a) Yoe, J.H. and Harvey, A.E. *J. Am. Chem. Soc.* **1948**, 70, 648; (b) Chriswell, C.D. and Schilt, A.A. *Anal. Chem.* **1975**, 47, 1623.
- (69) (a) Job, P. *Ann. Chim.* **1928**, 9, 113; (b) Likussar, W. and Boltz, D.F. *Anal. Chem.* **1971**, 43, 1265.
- (70) Poh, B.L. Seah, L.H. and Lia, C.S. *Tetrahedron*, **1990**, 46, 4379.
- (71) Scatchard, G. *Ann. N.Y. Acad. Sci.* **1949**, 51, 660.
- (72) Perrin, D.D. and Armarego, W.L.F. *Purification of Laboratory Chemicals*; Permagon: Toronto, **1988**.
- (73) Chan, C. personal communication, **1992**.

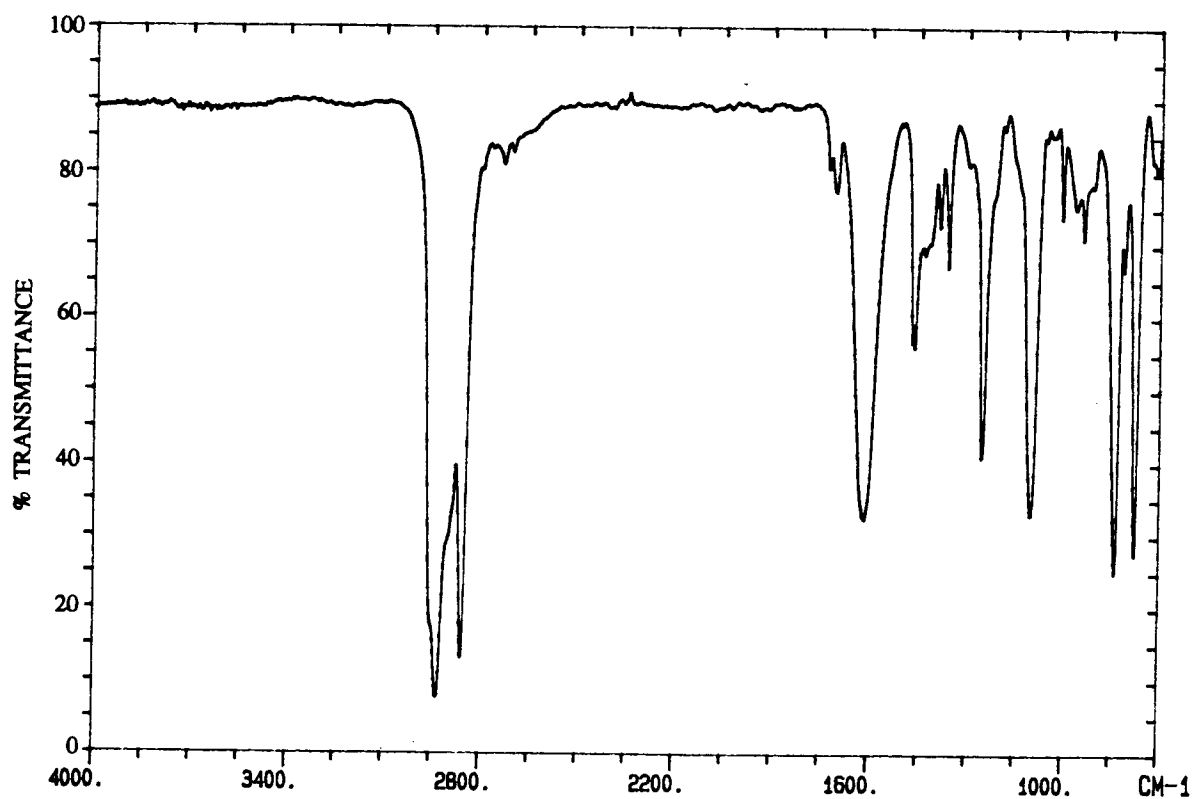
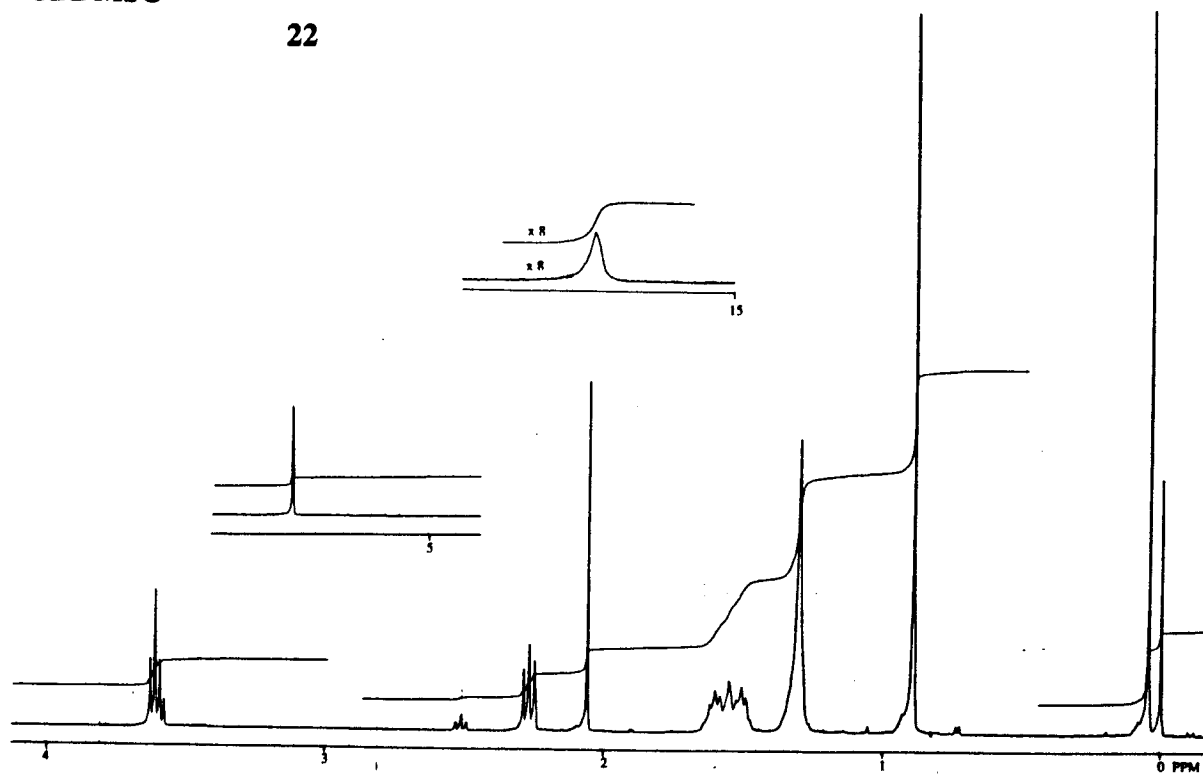
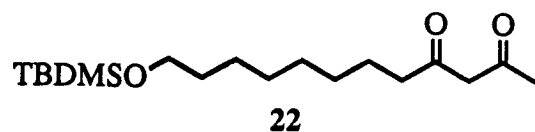


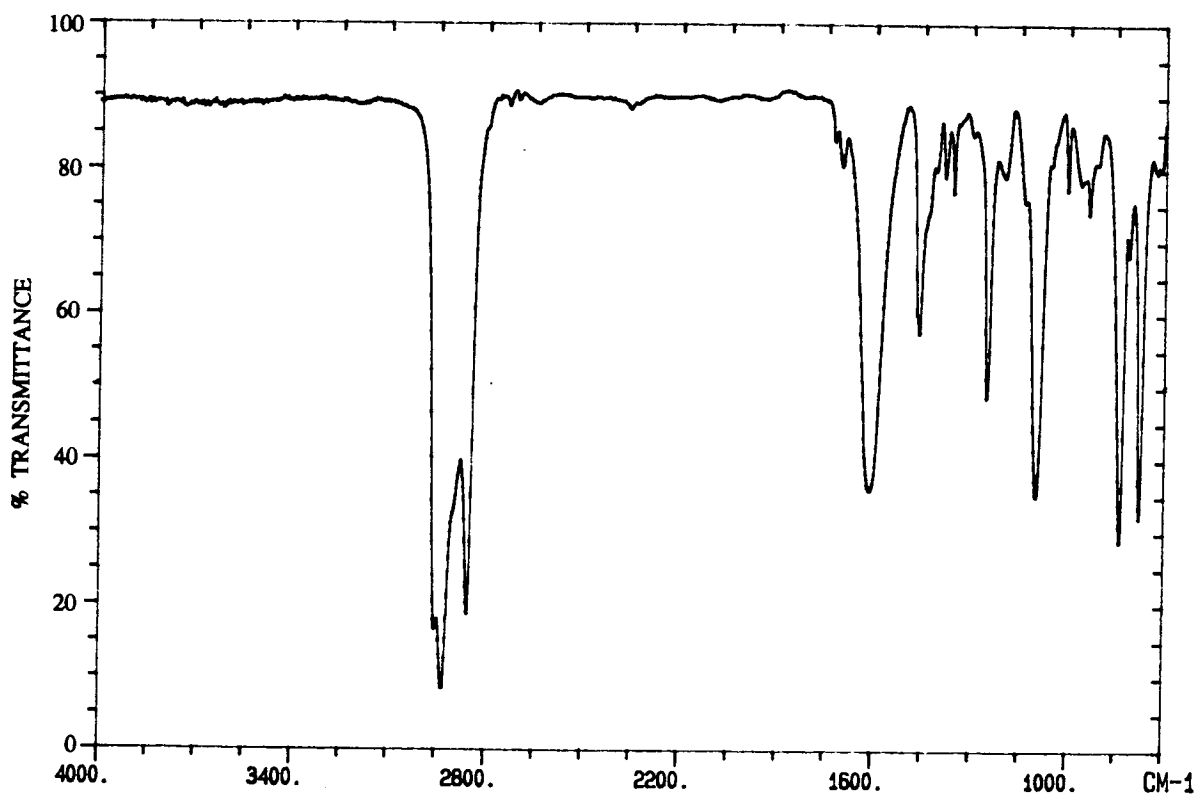
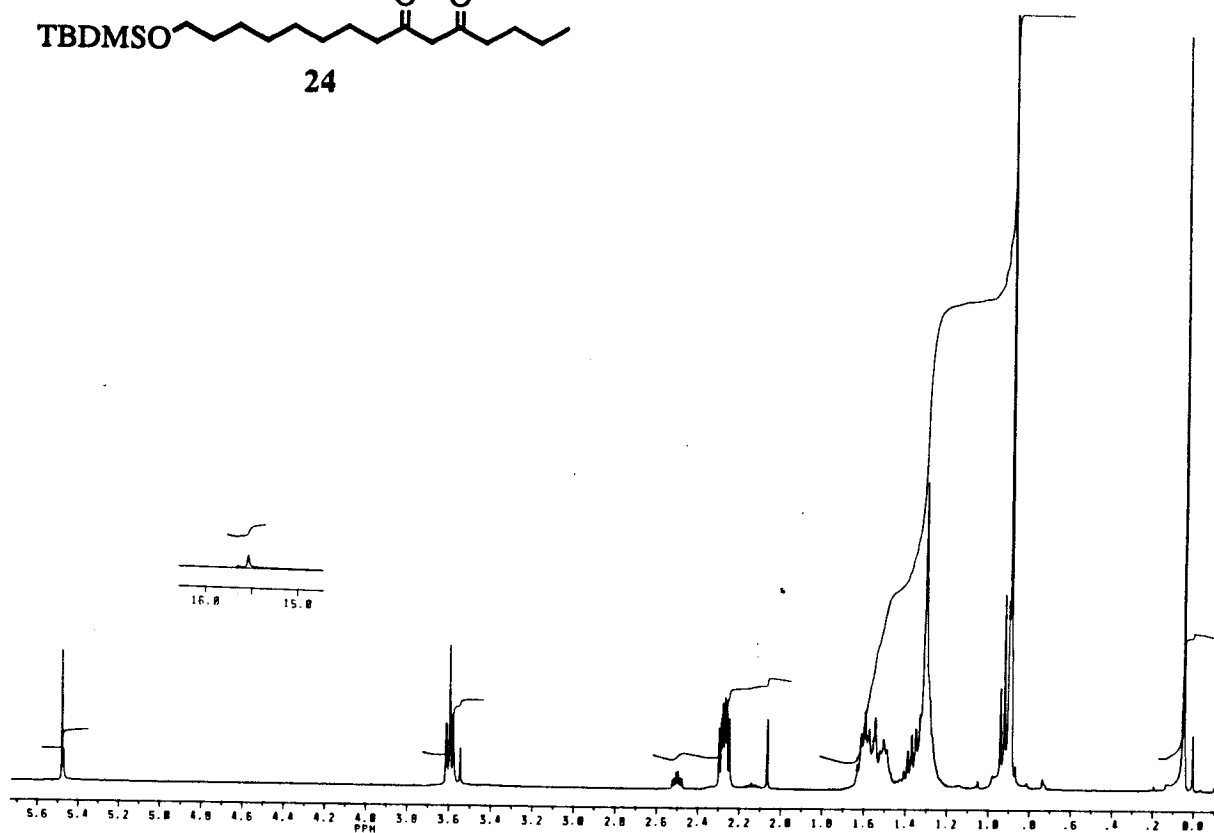
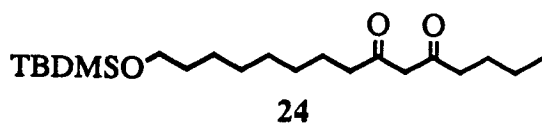
## APPENDIX 1

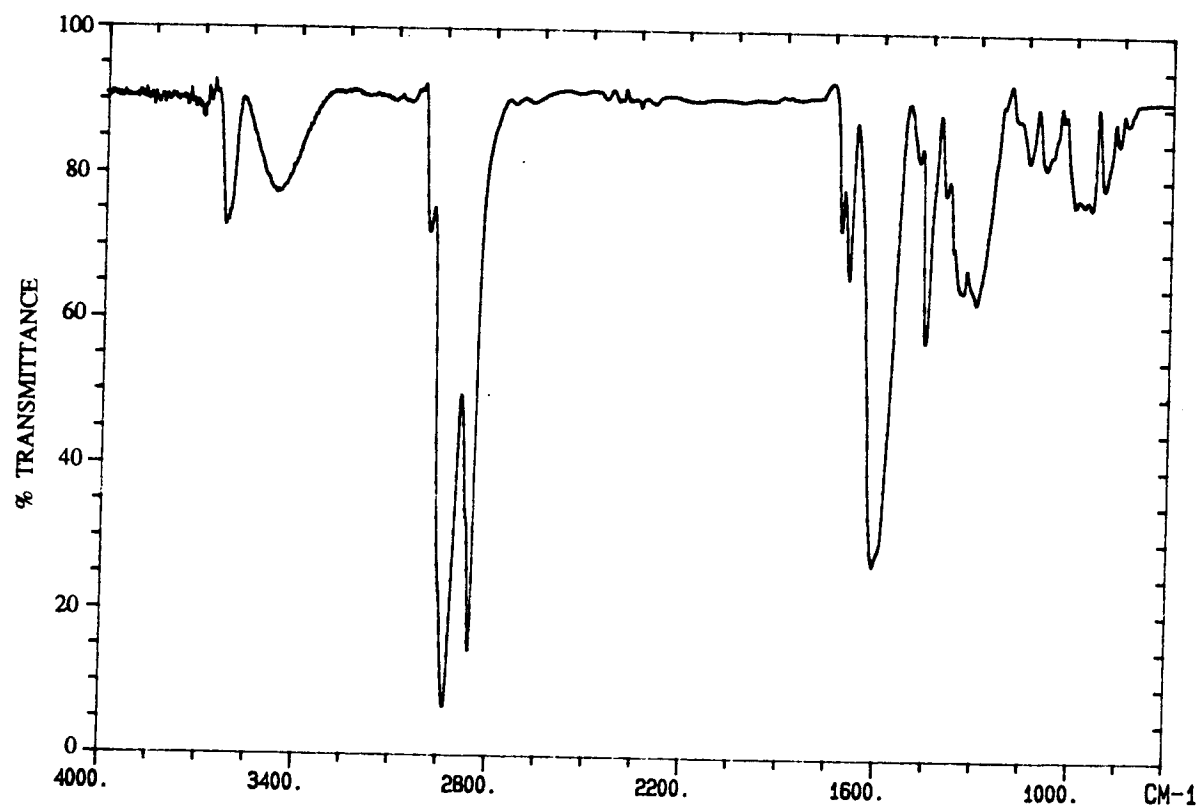
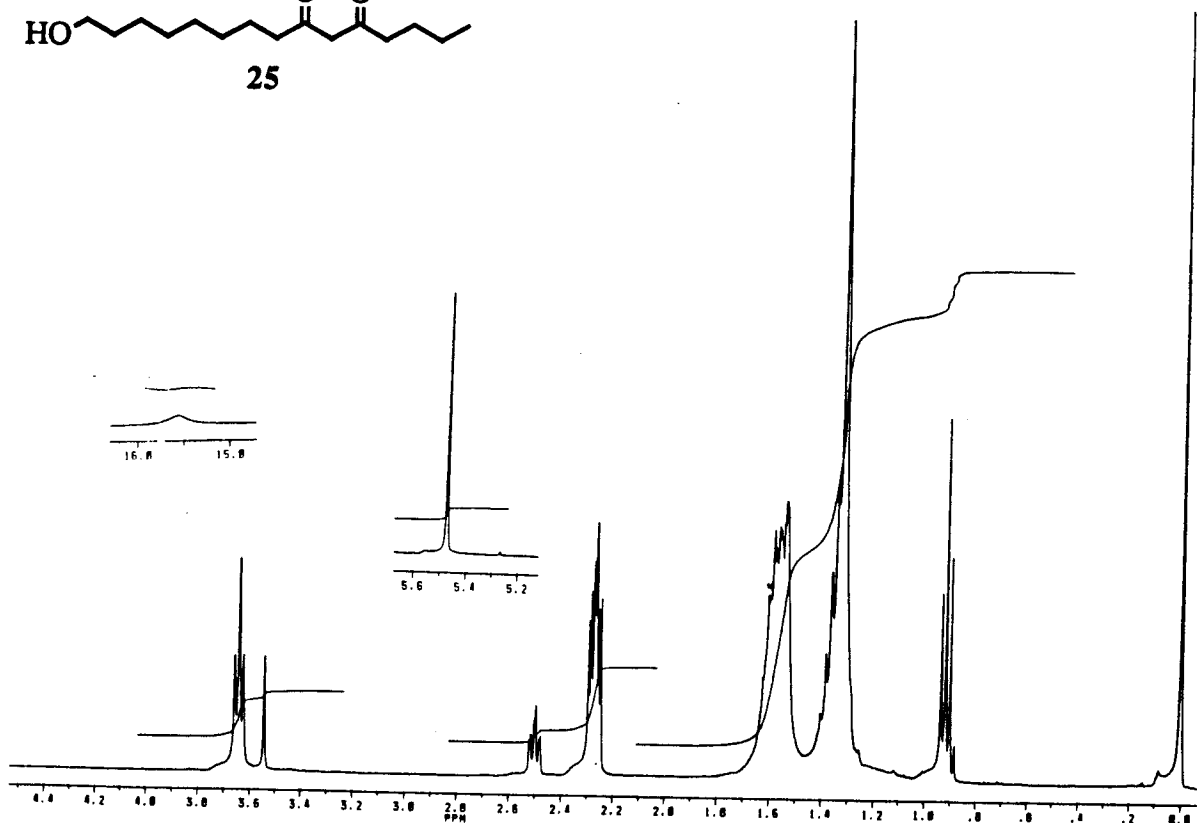
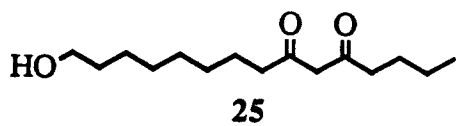
## NMR AND IR SPECTRAL

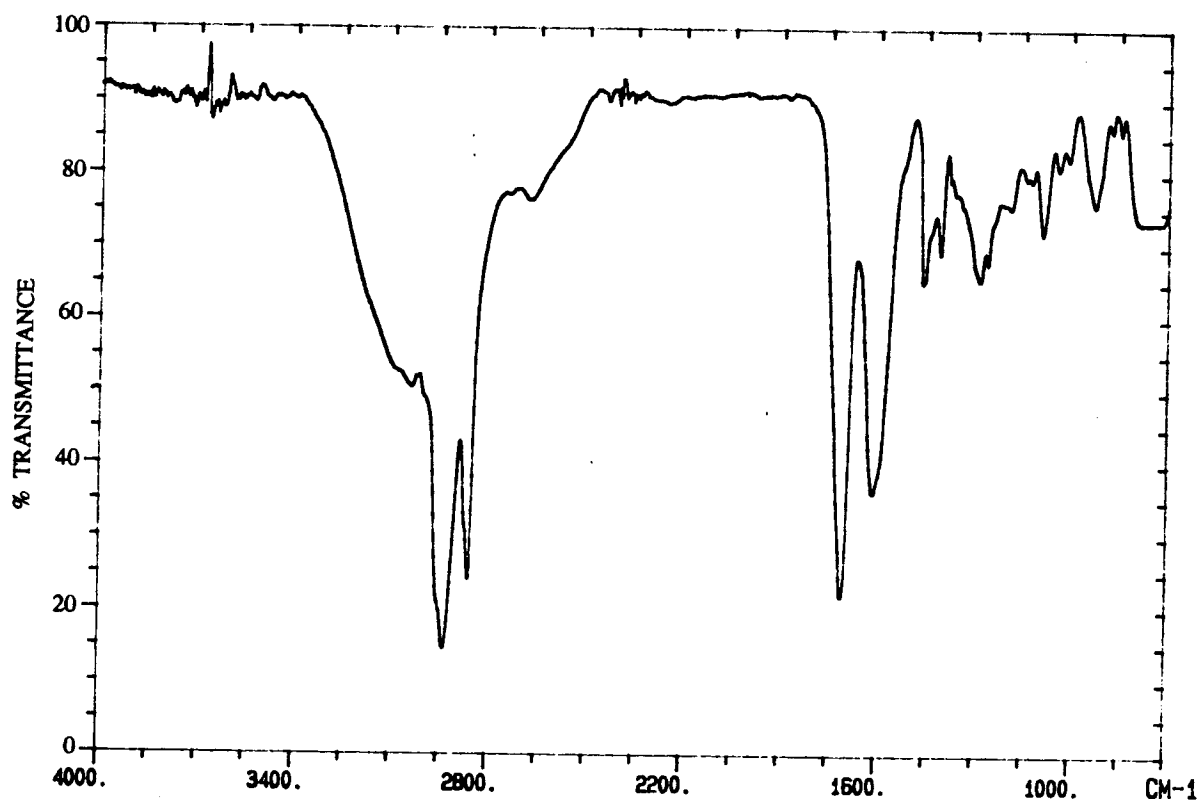
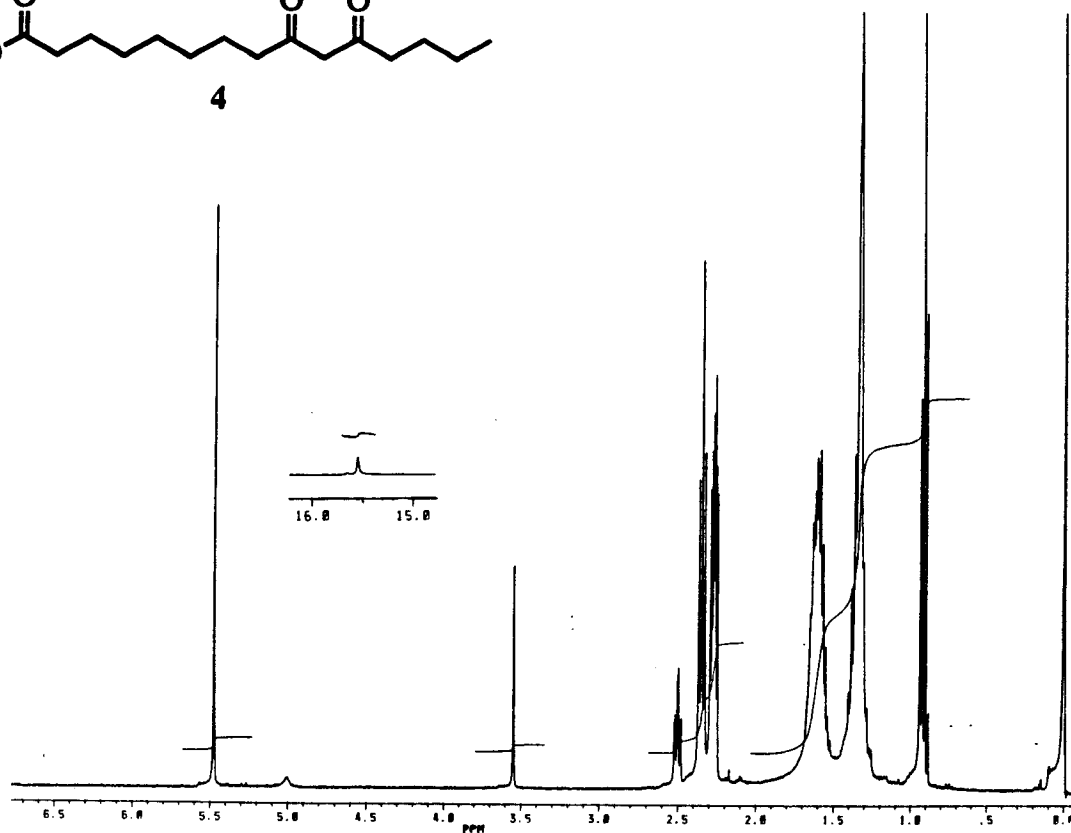
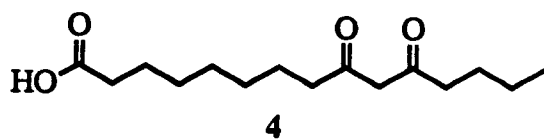


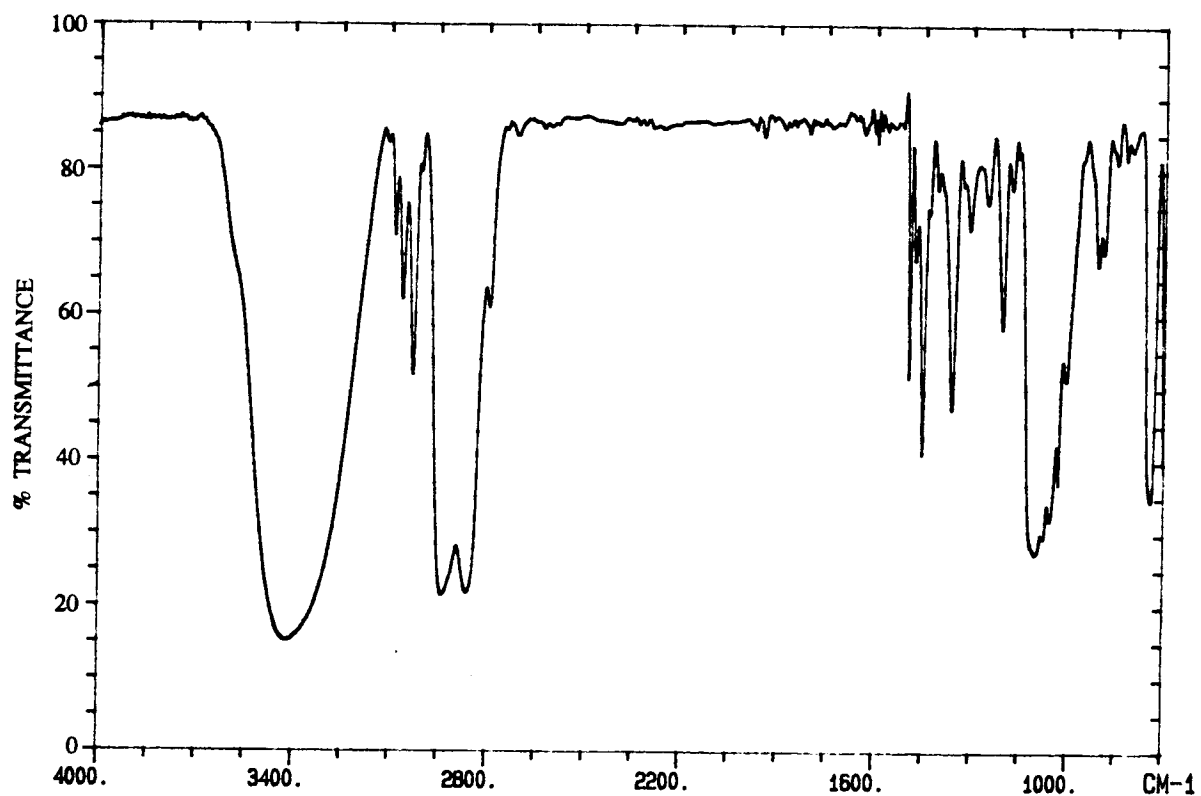
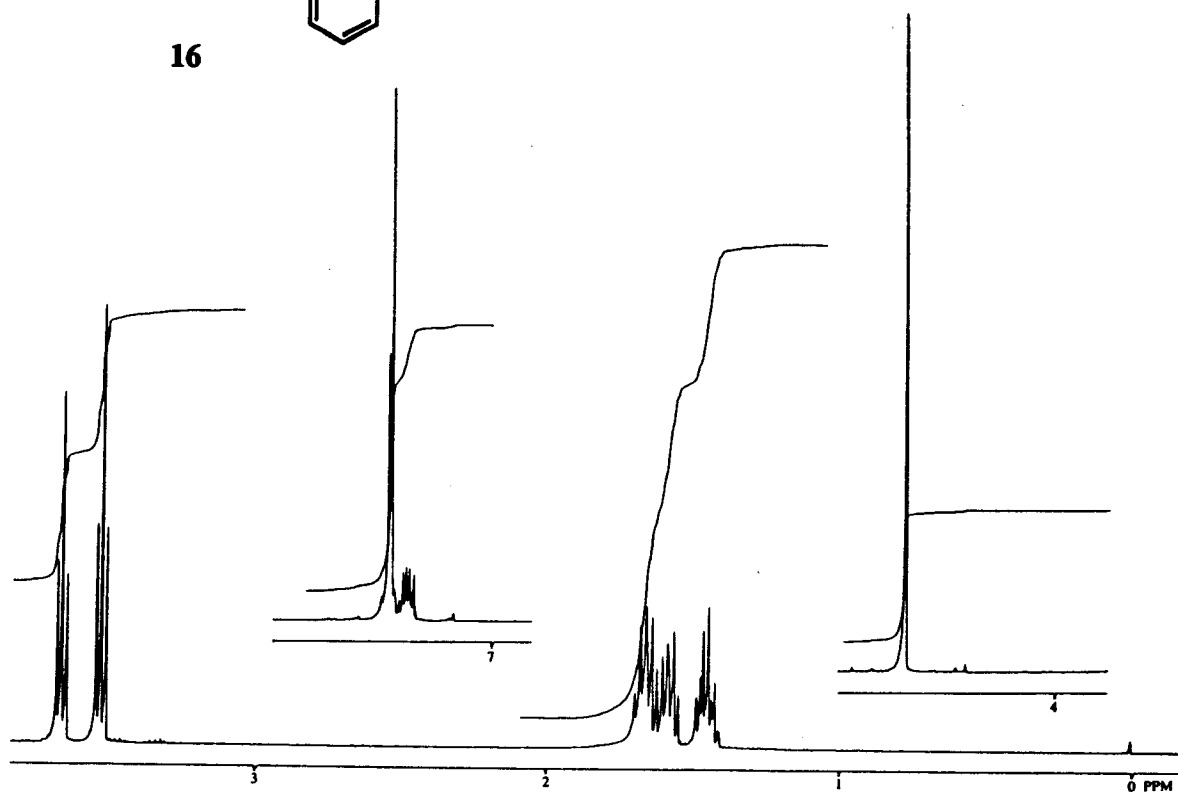
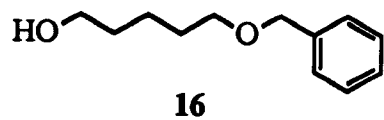




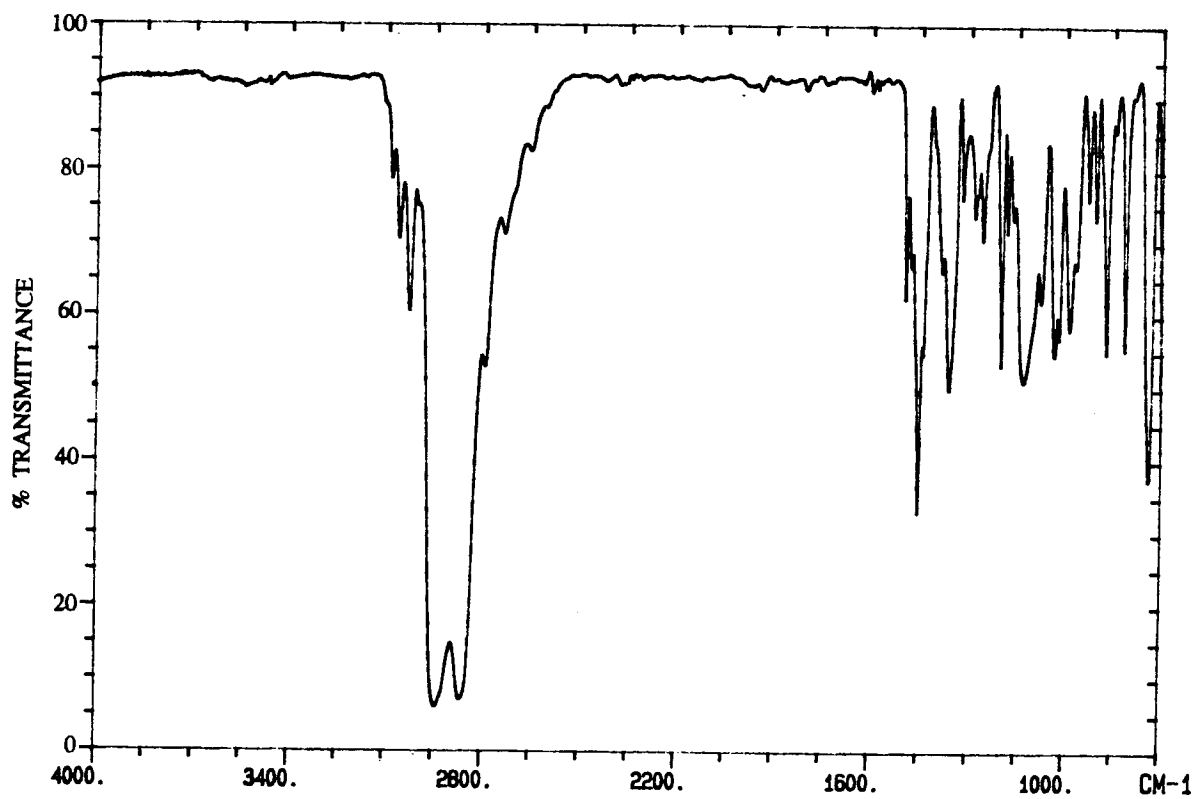
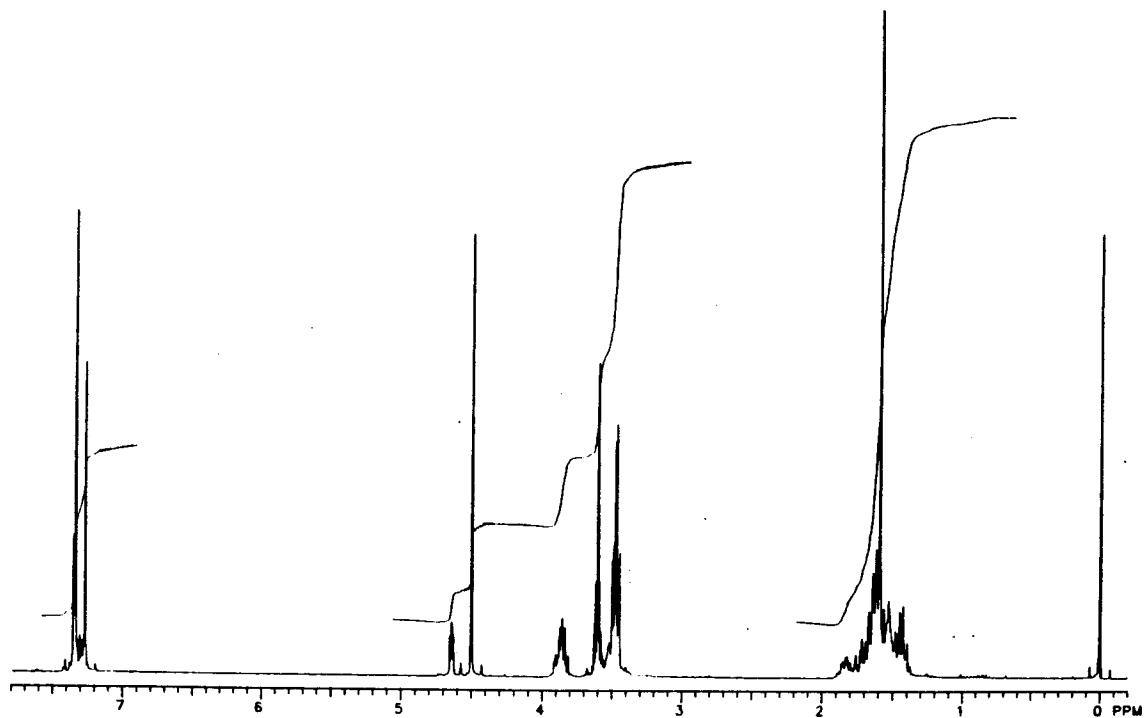
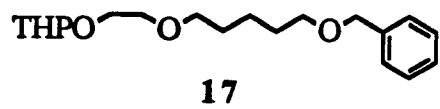


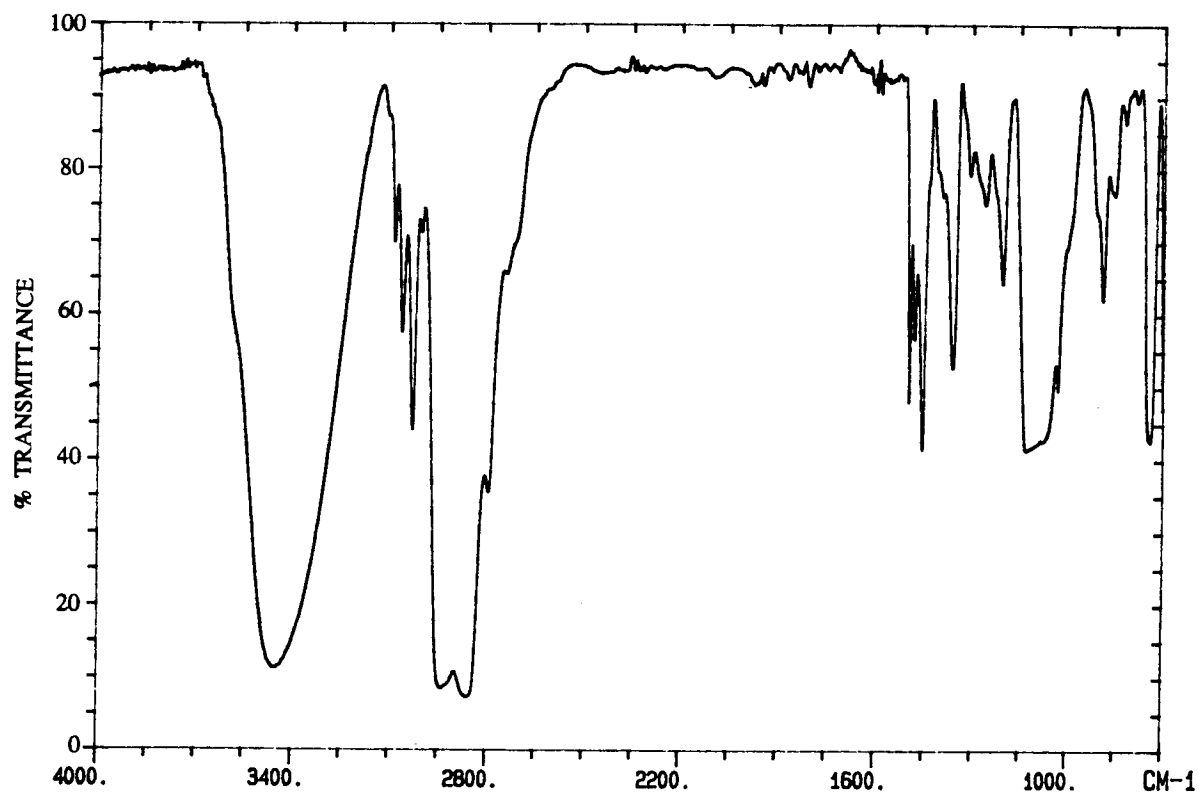
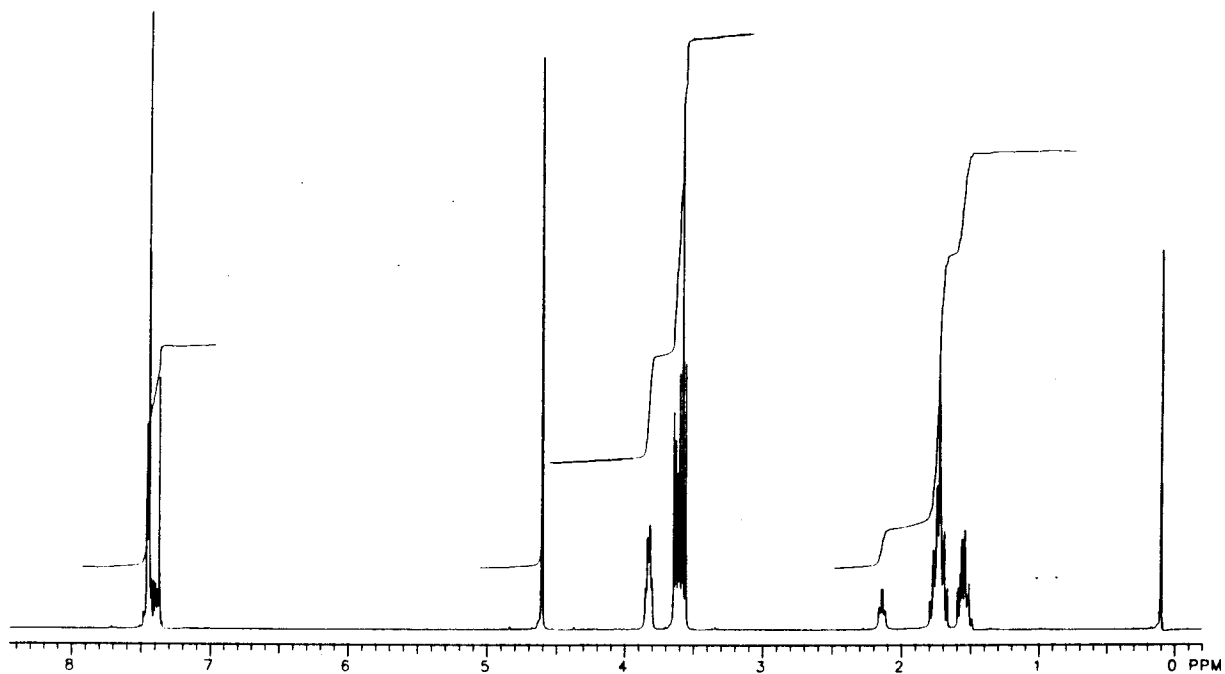
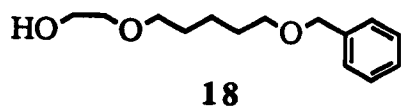


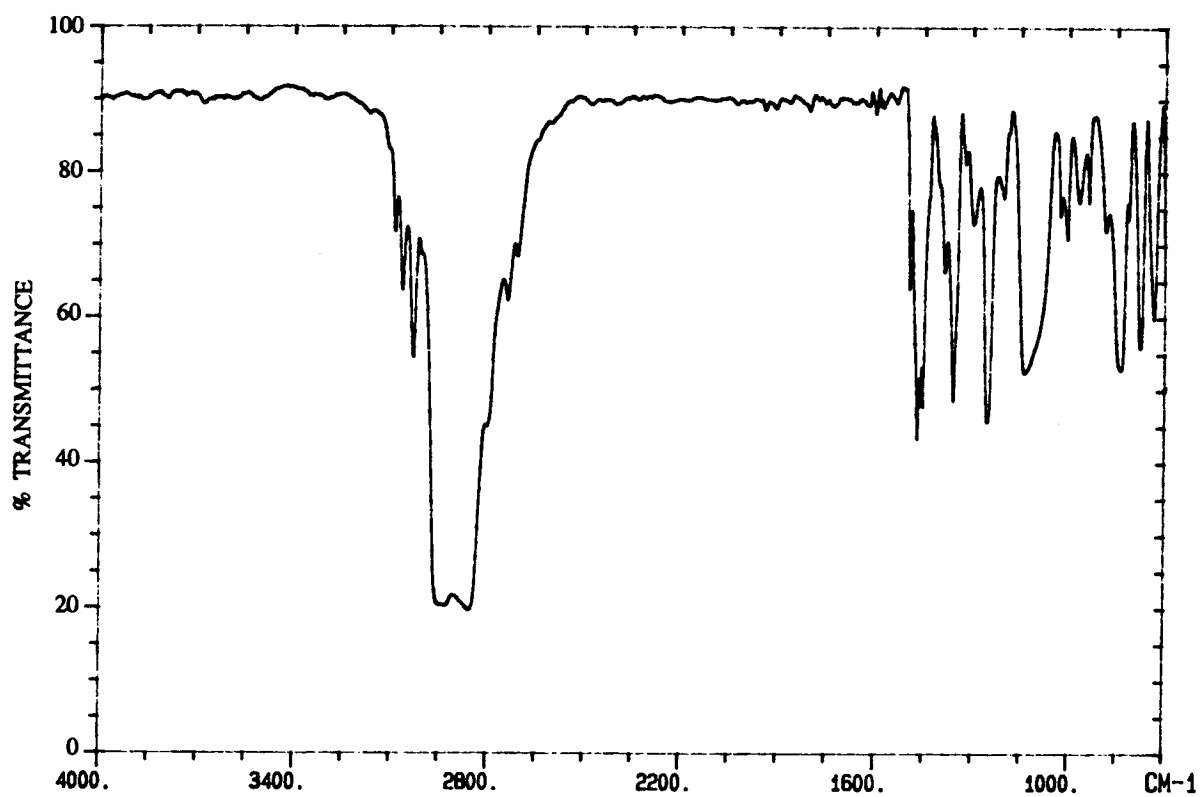
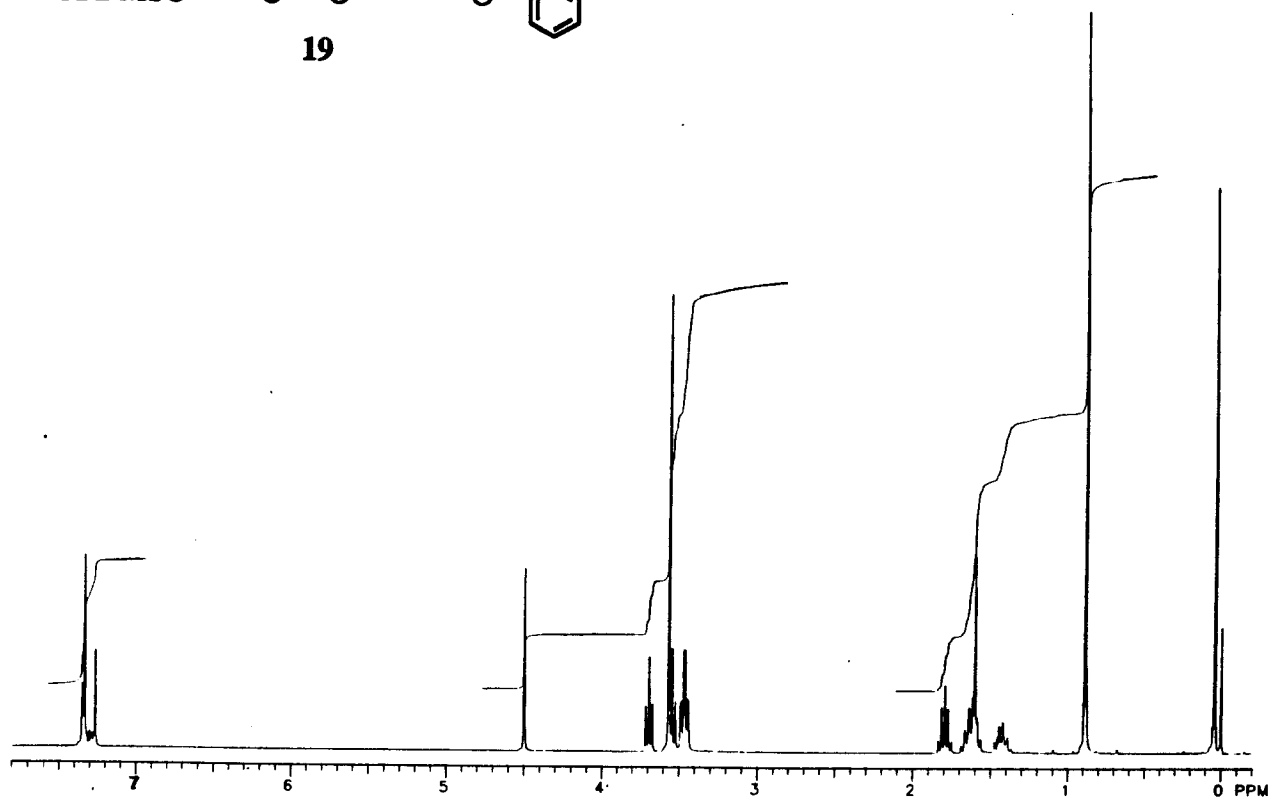
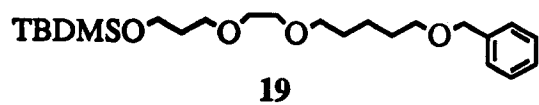


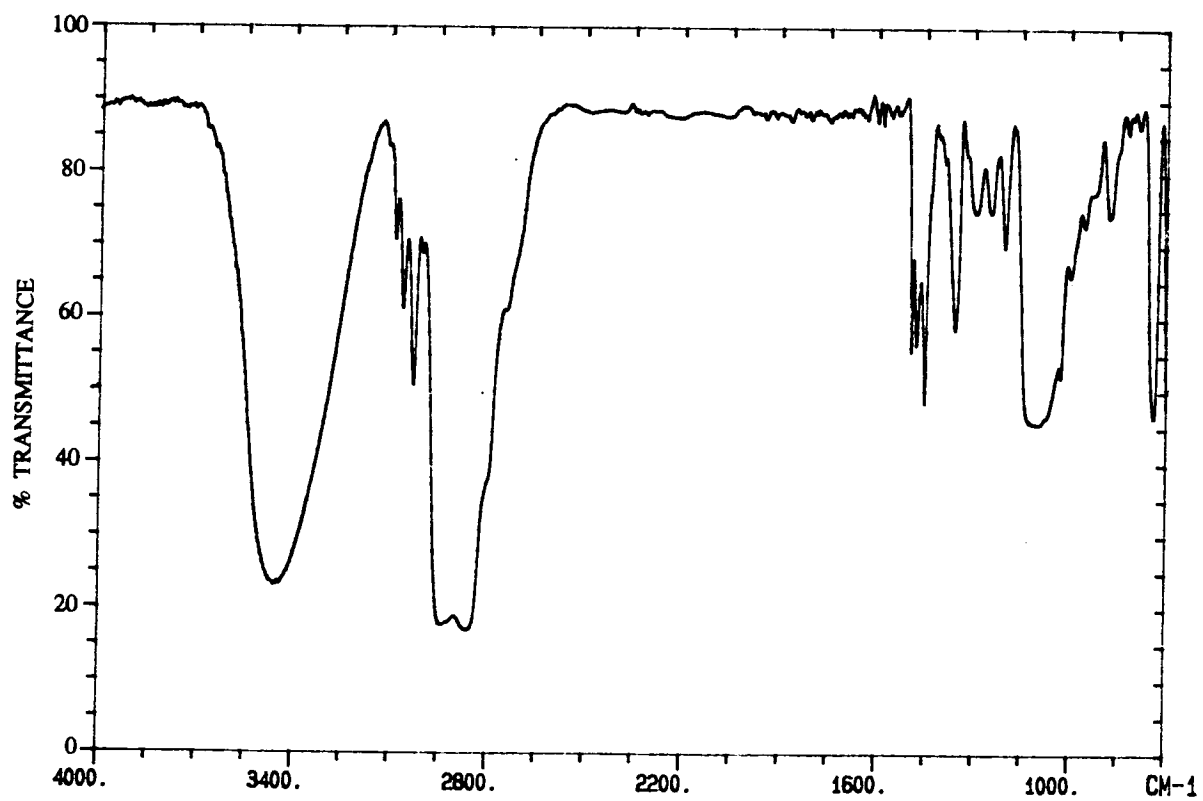
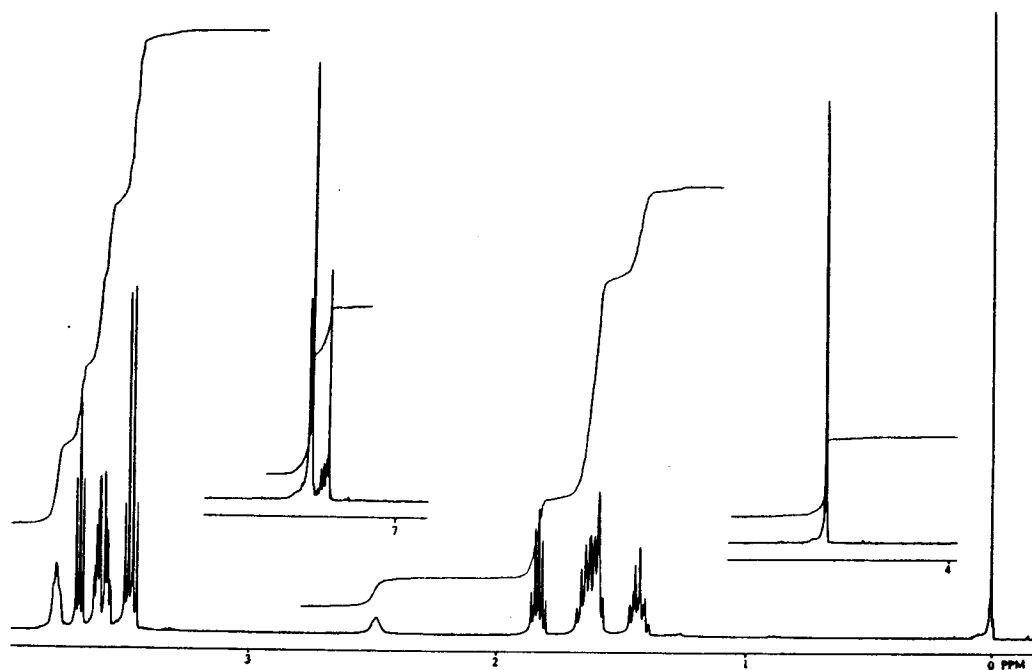
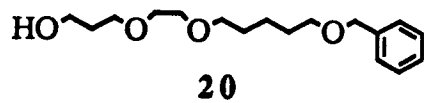


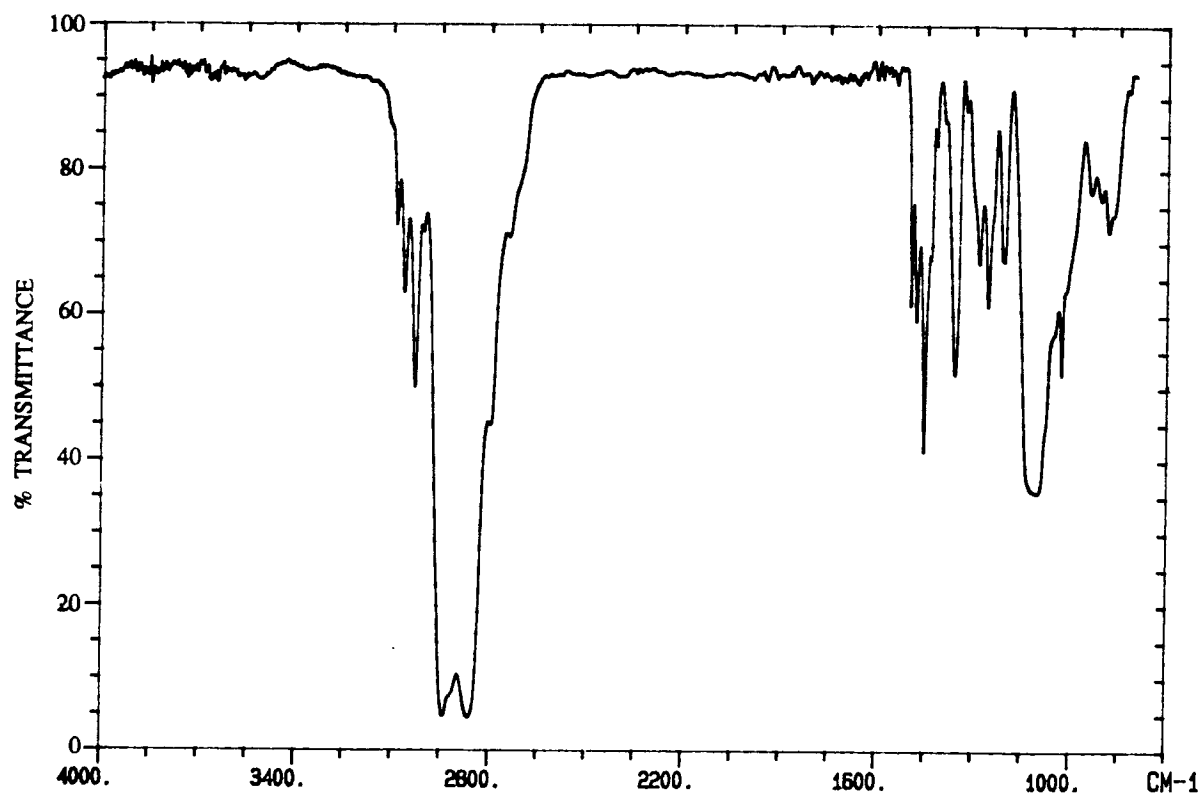
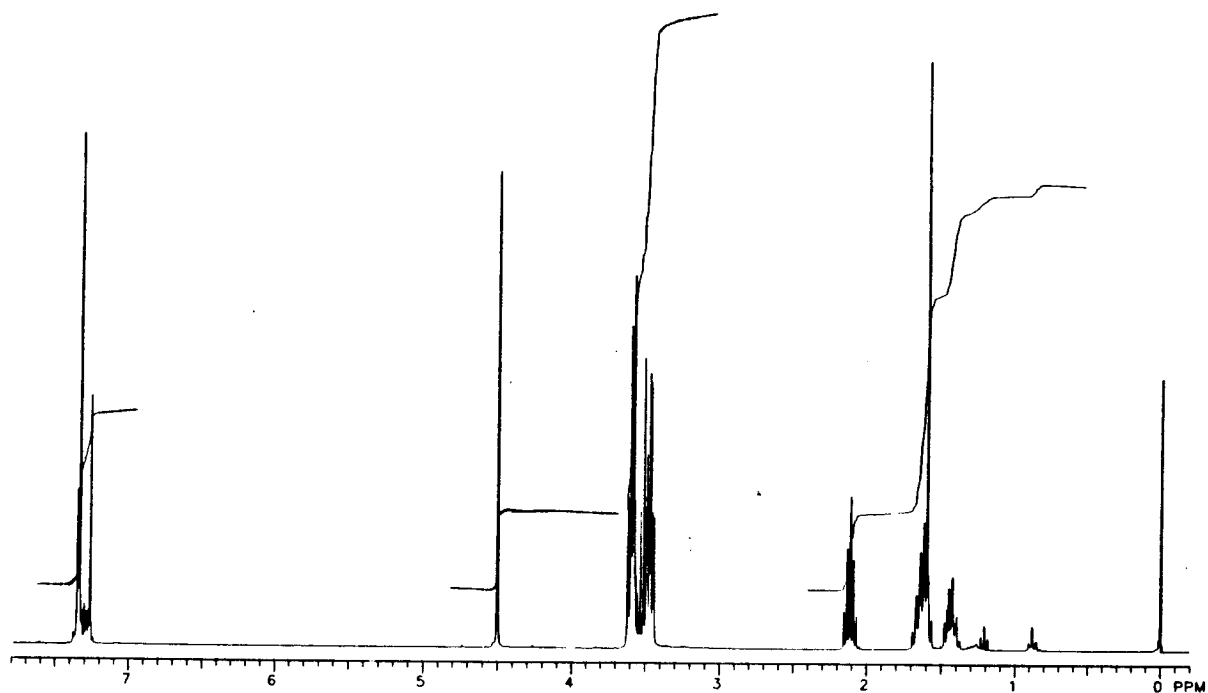
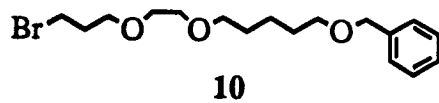


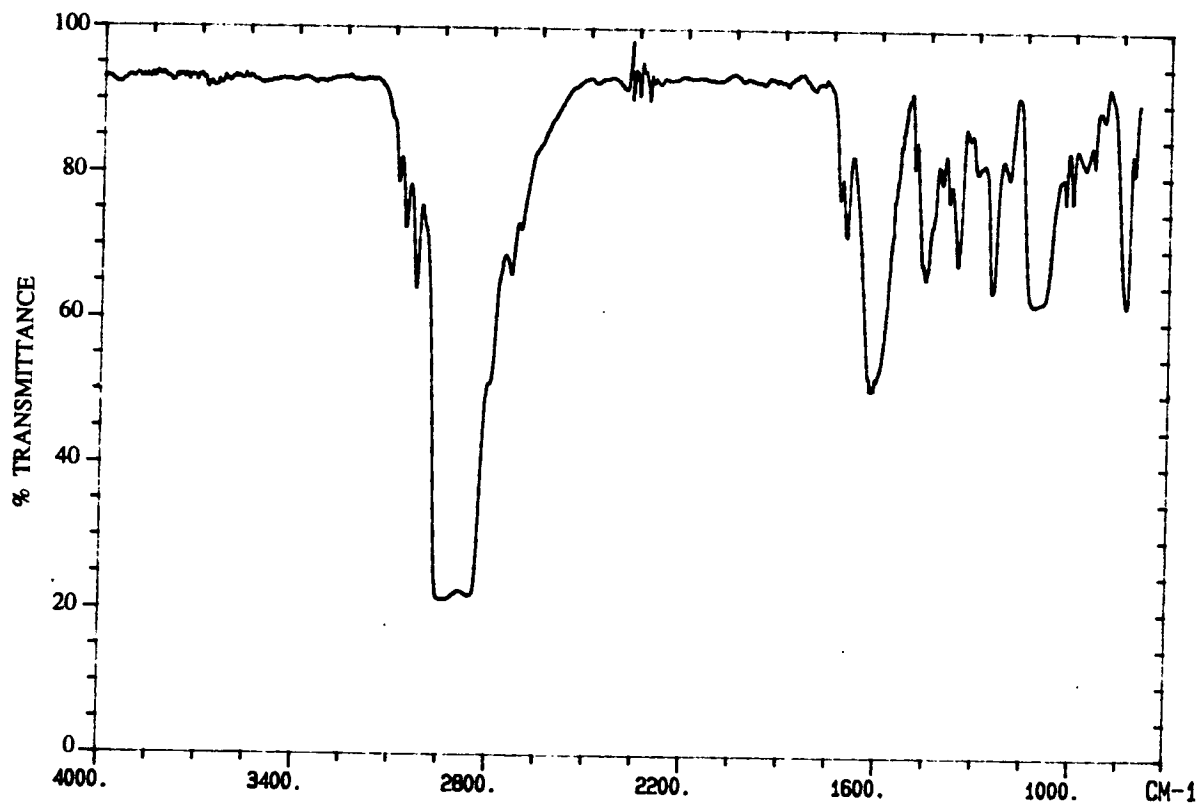
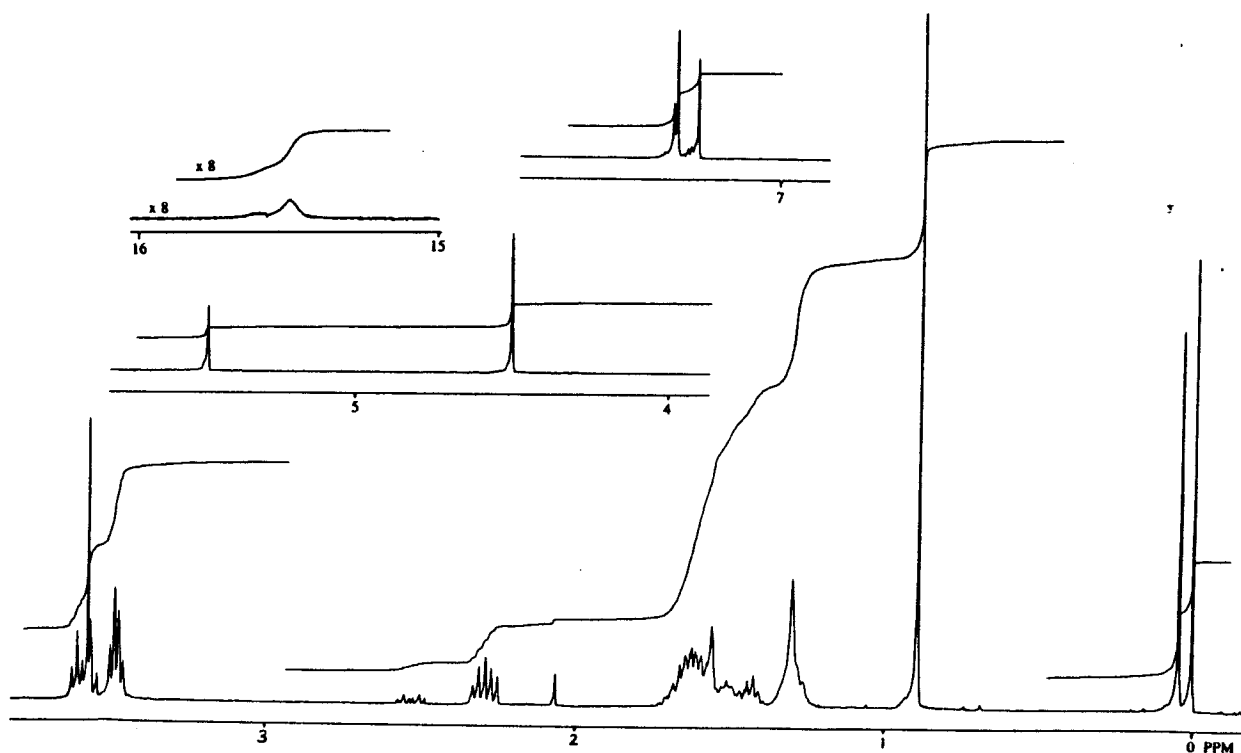
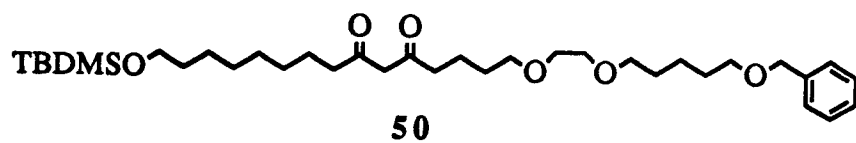


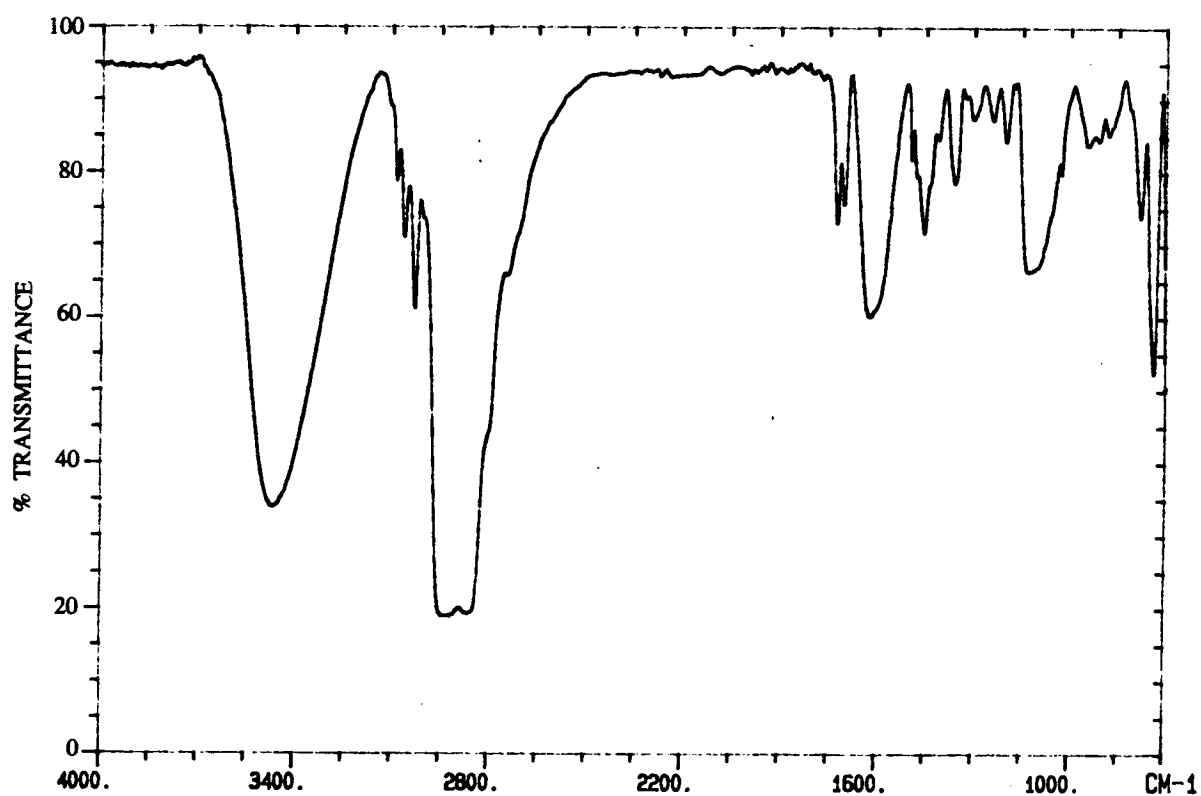
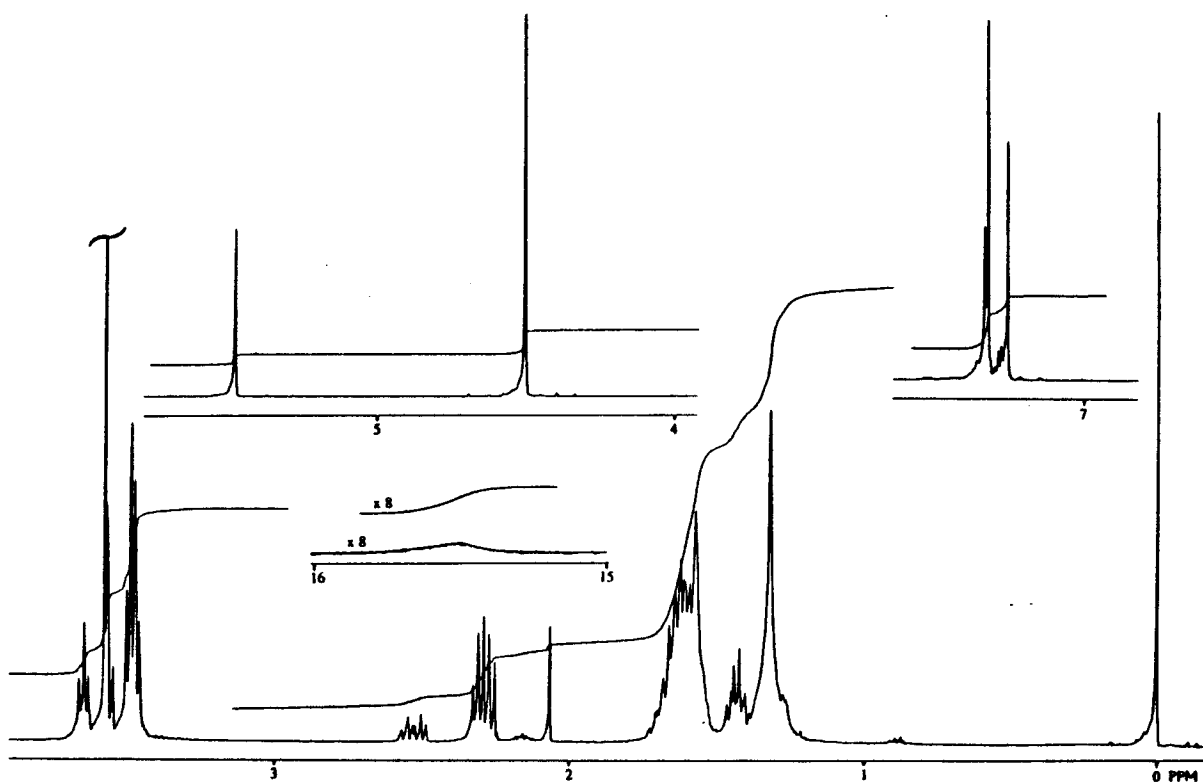
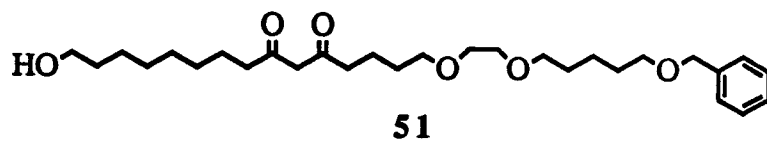


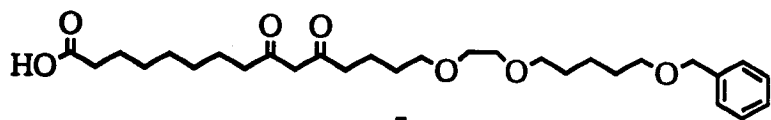




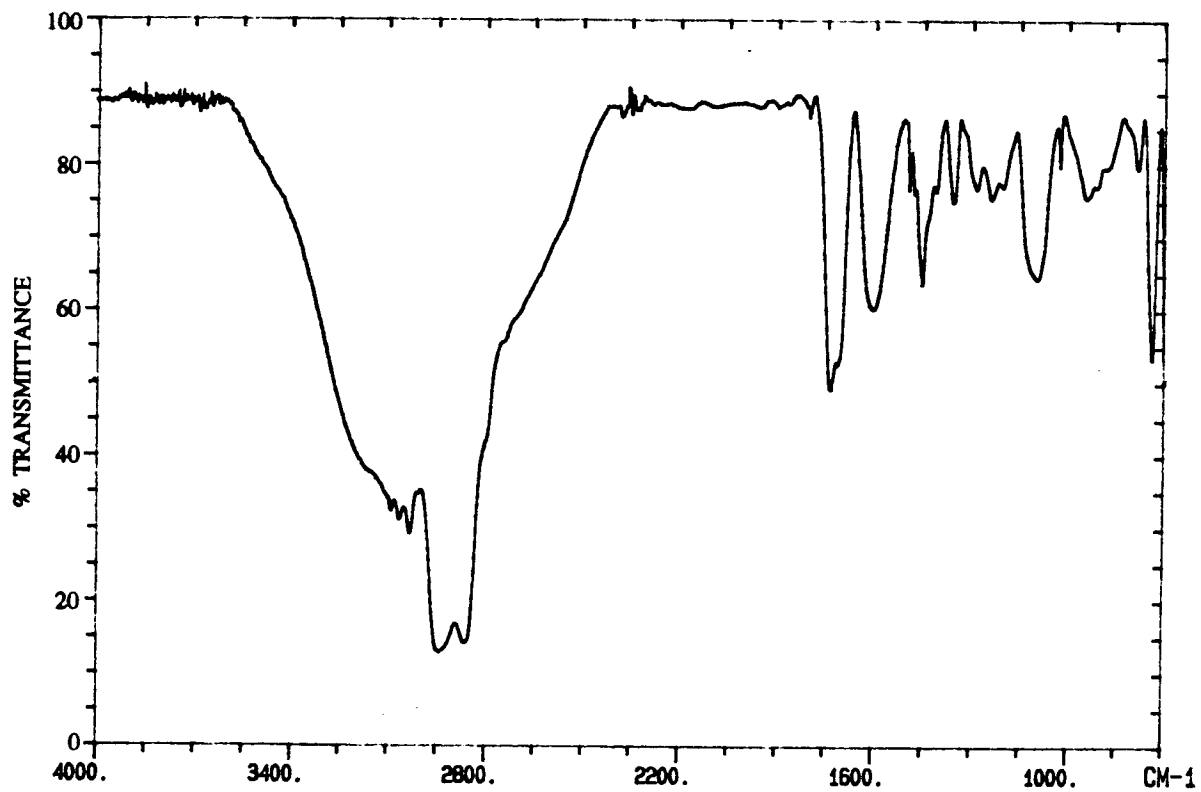
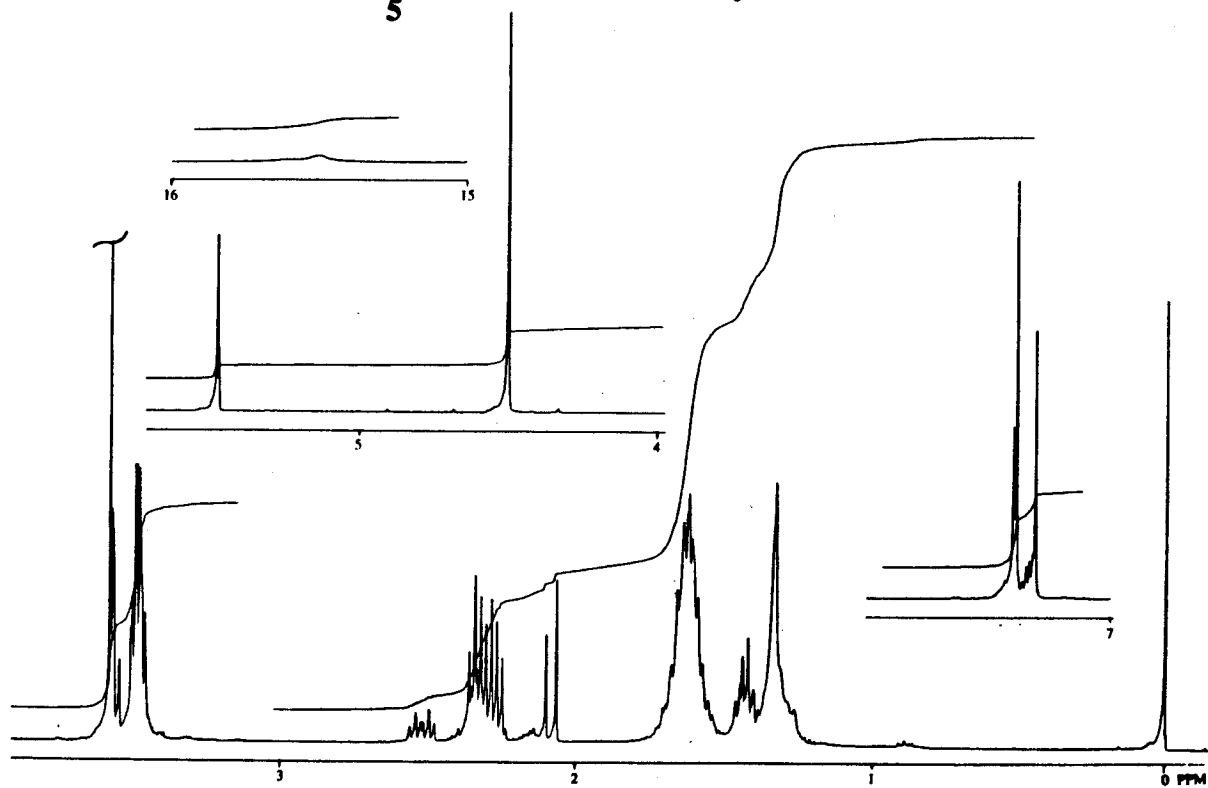




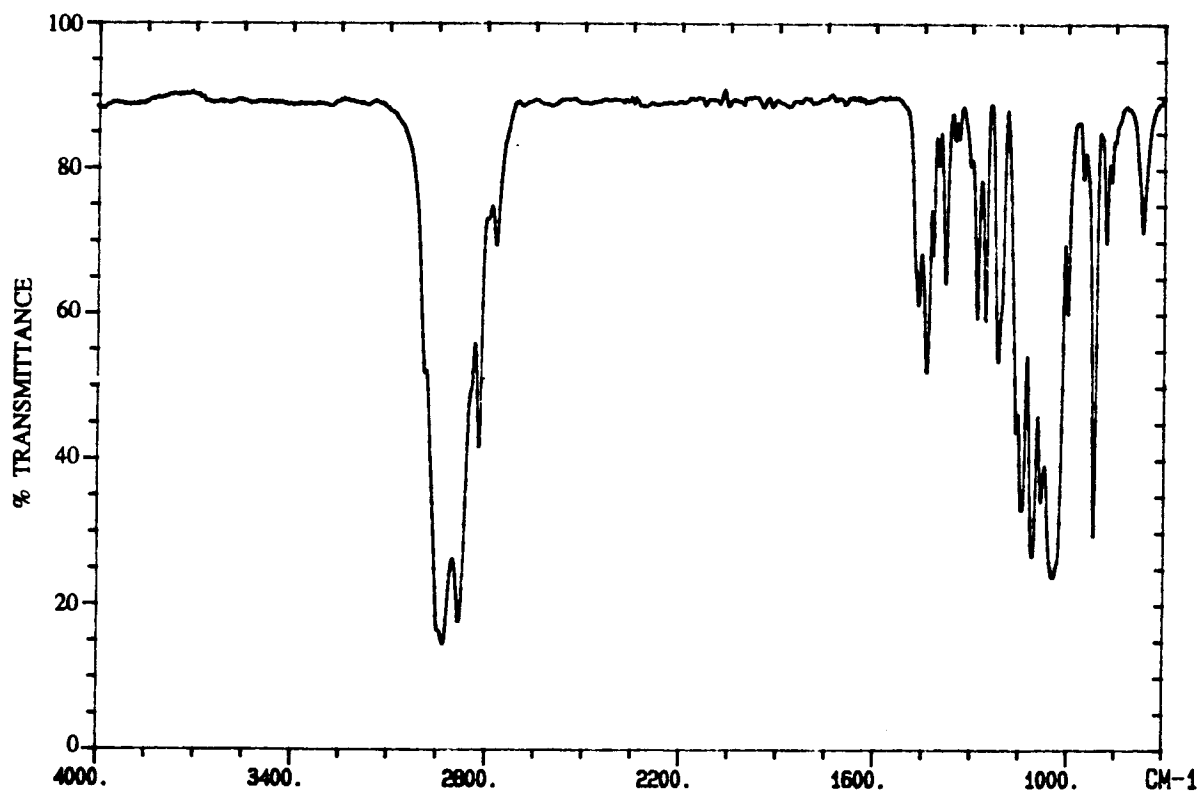
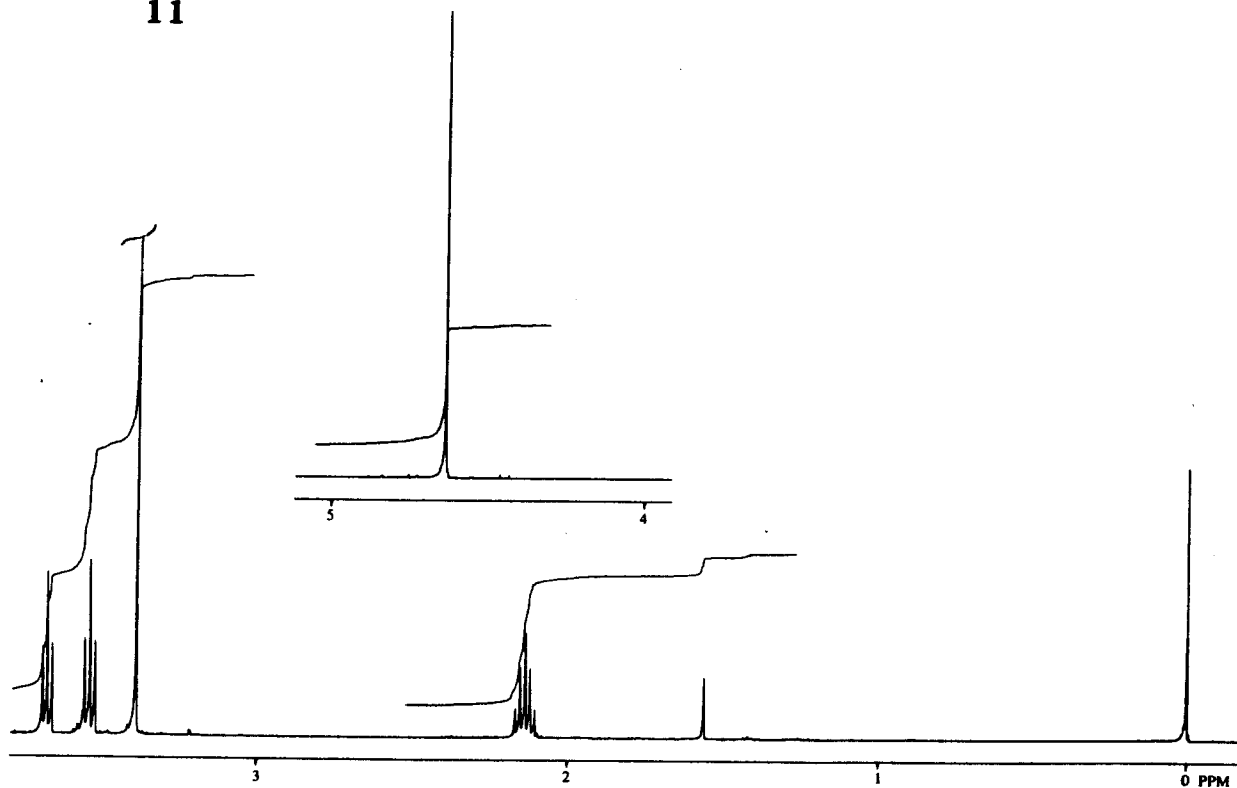
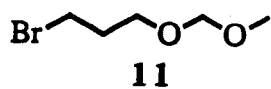


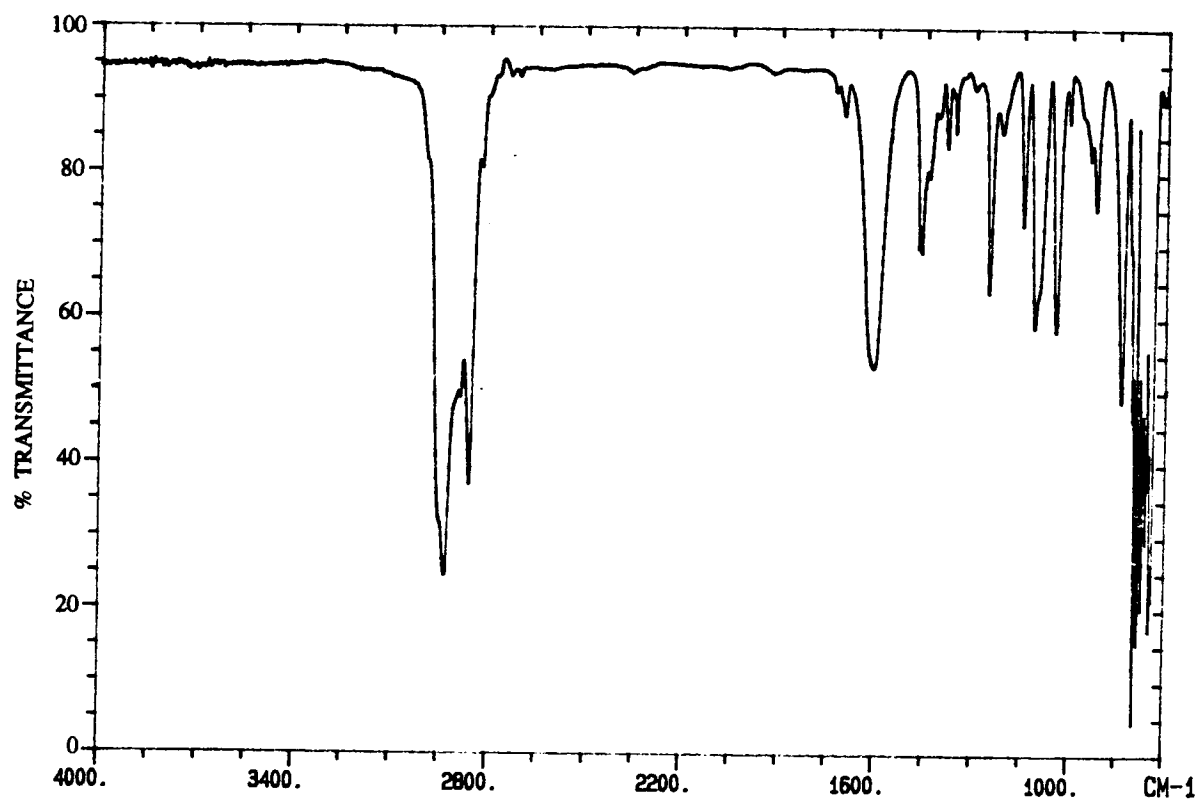
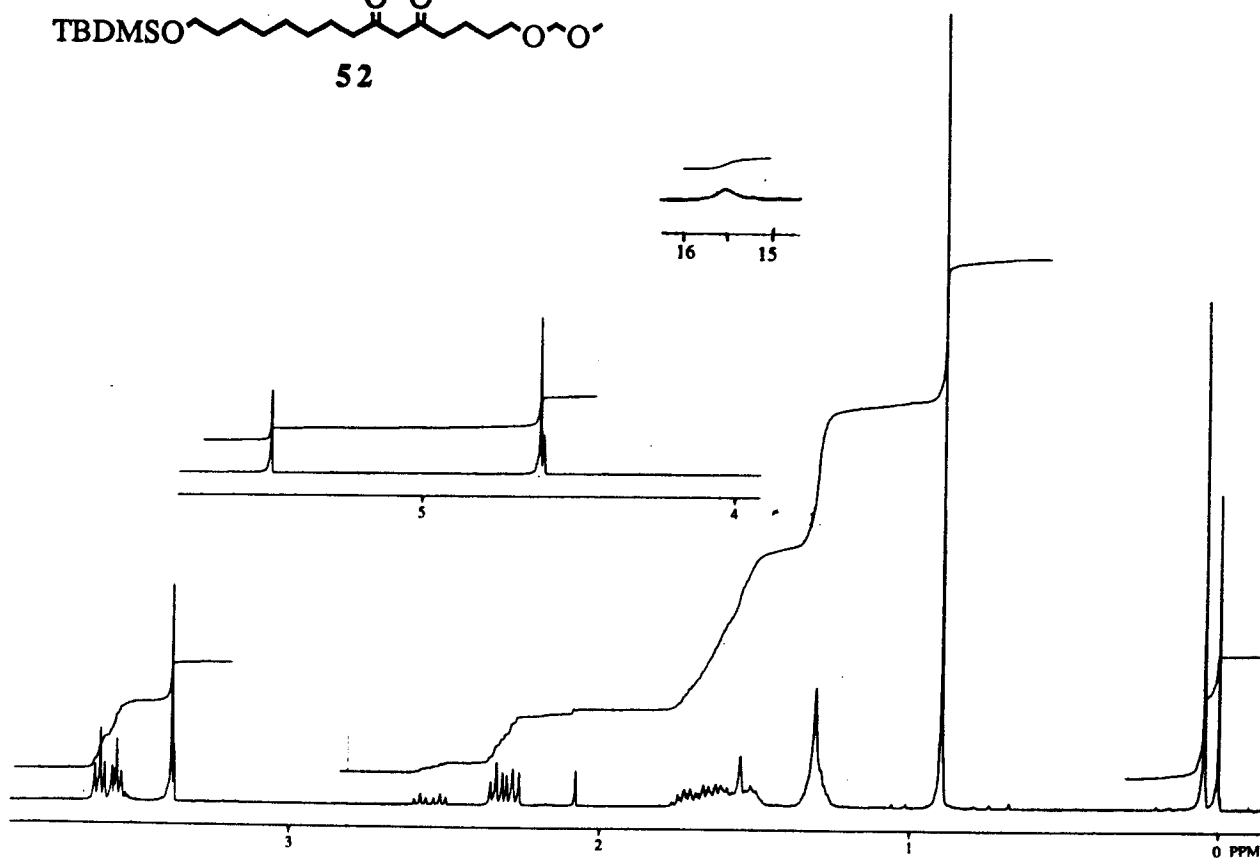
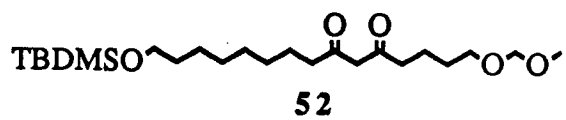


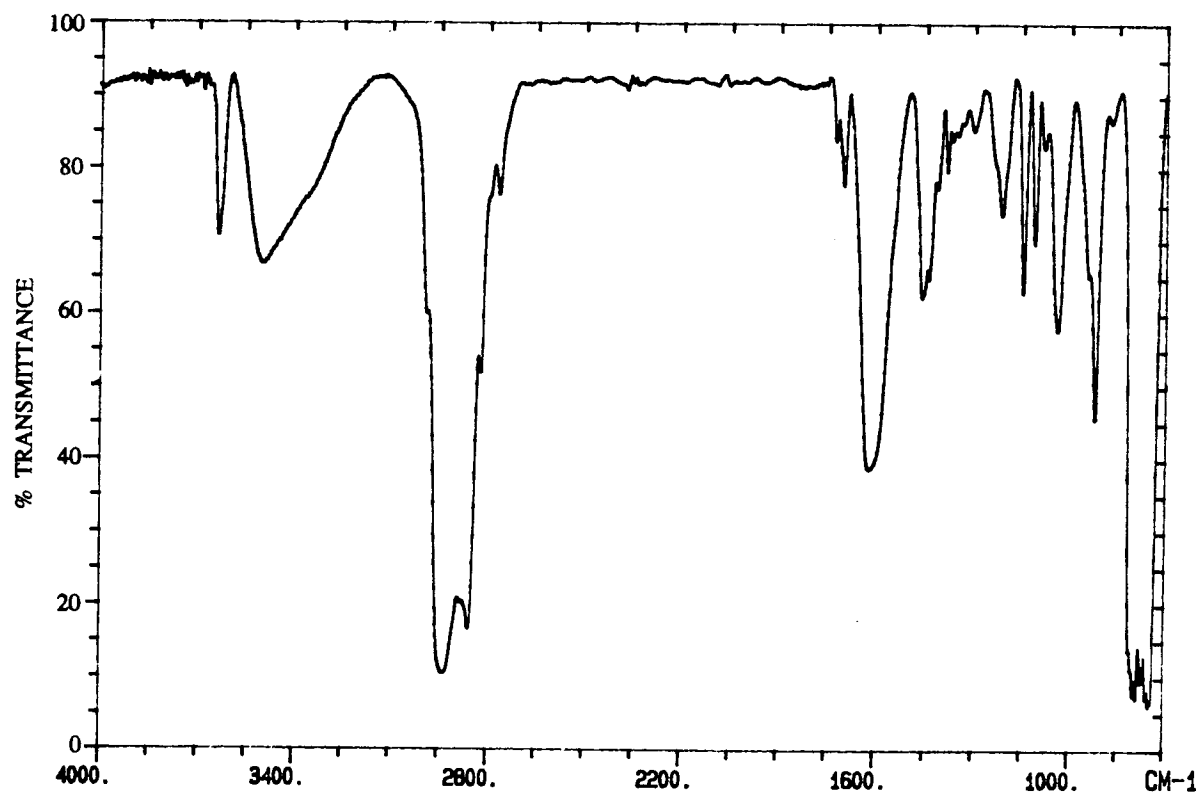
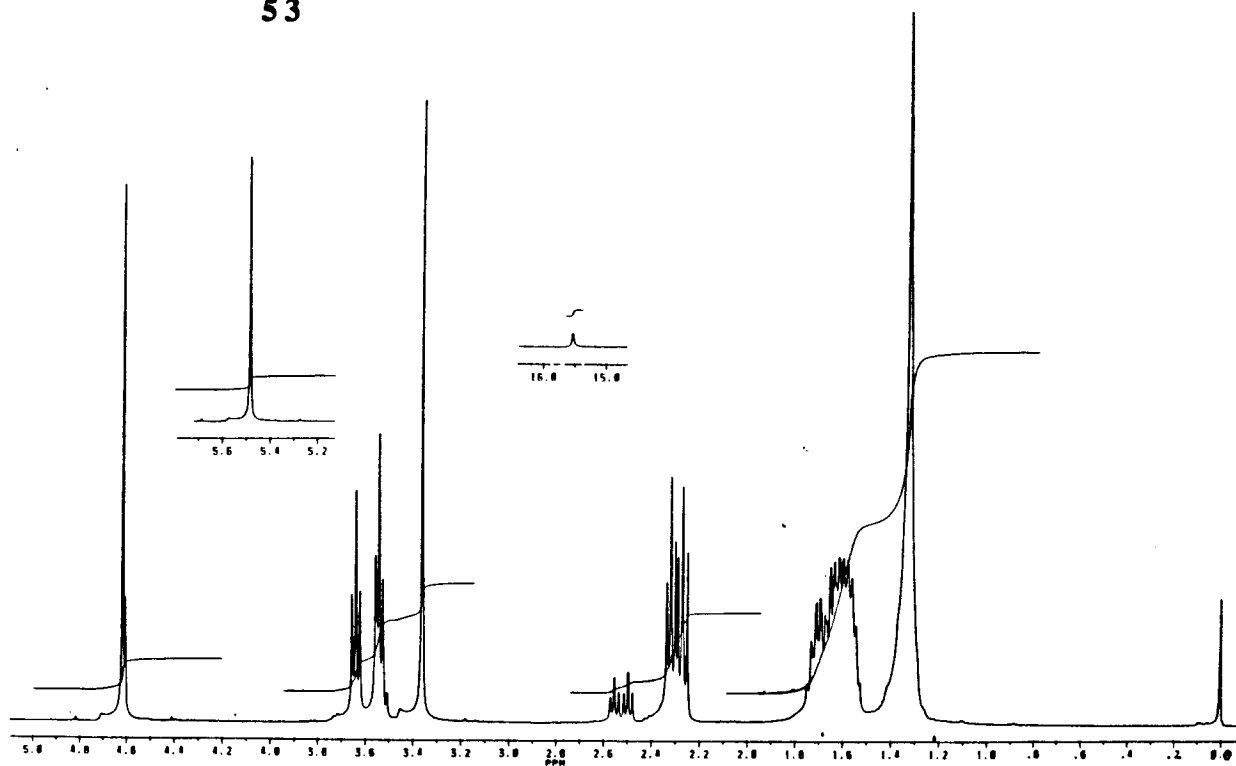
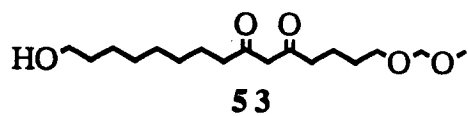
5

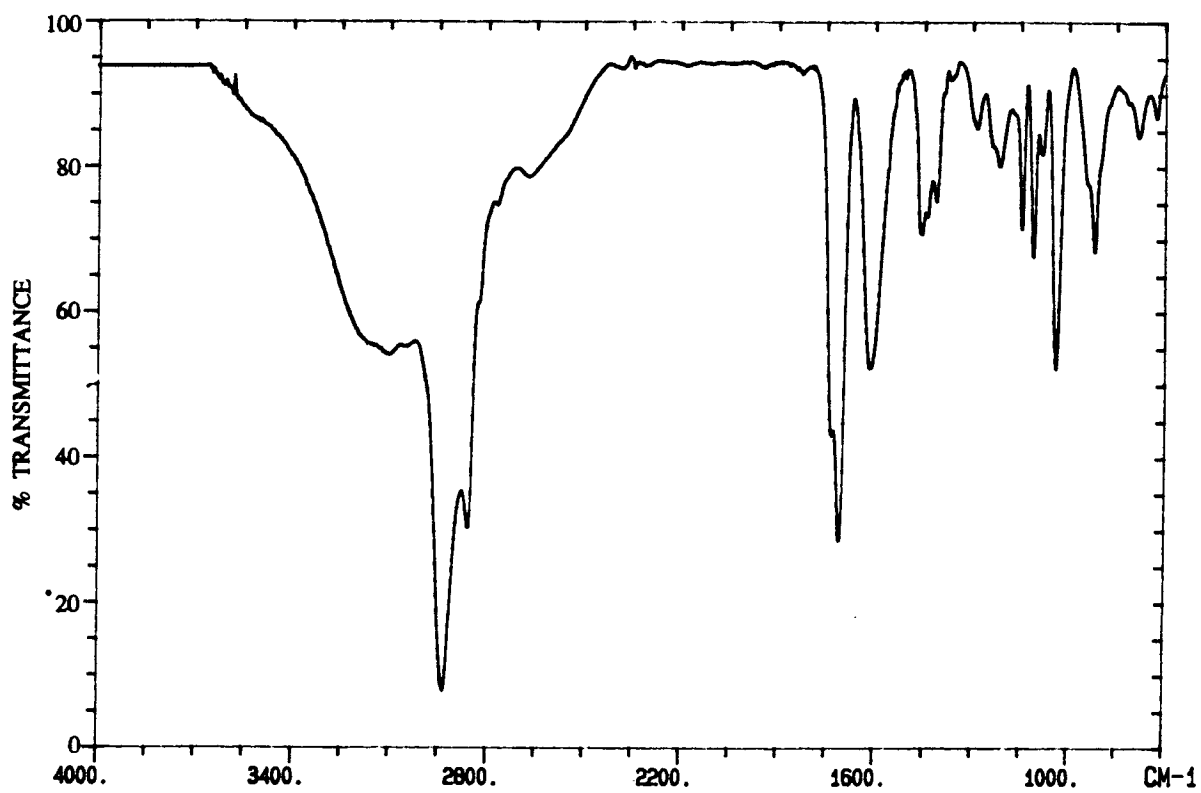
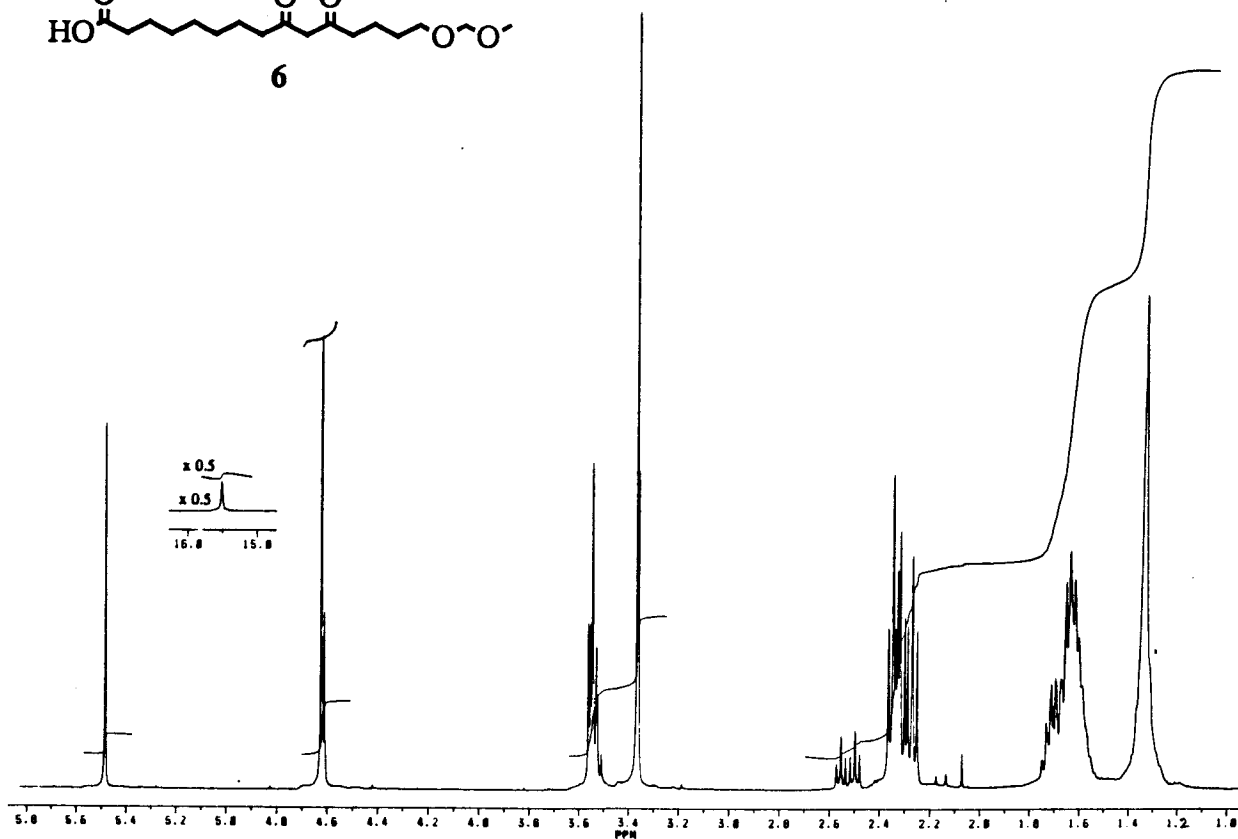
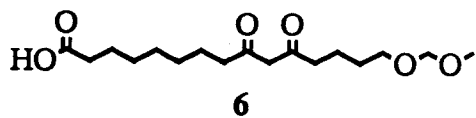


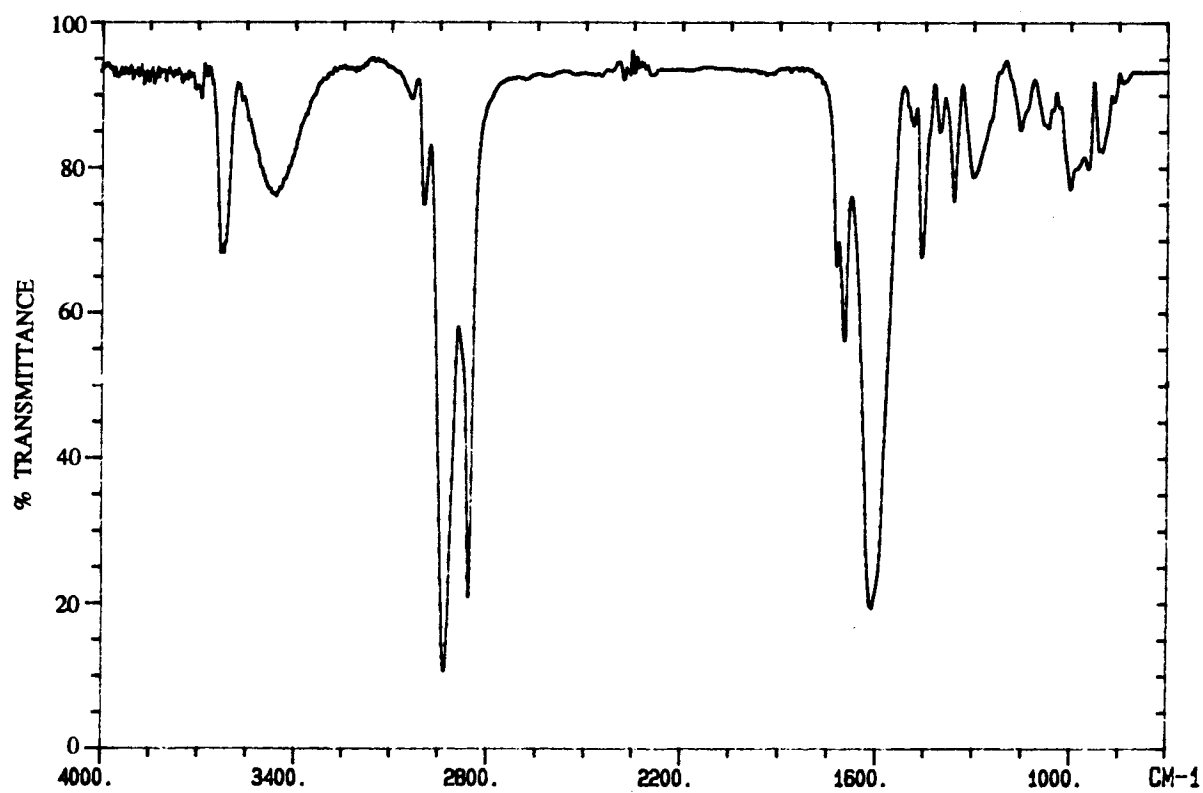
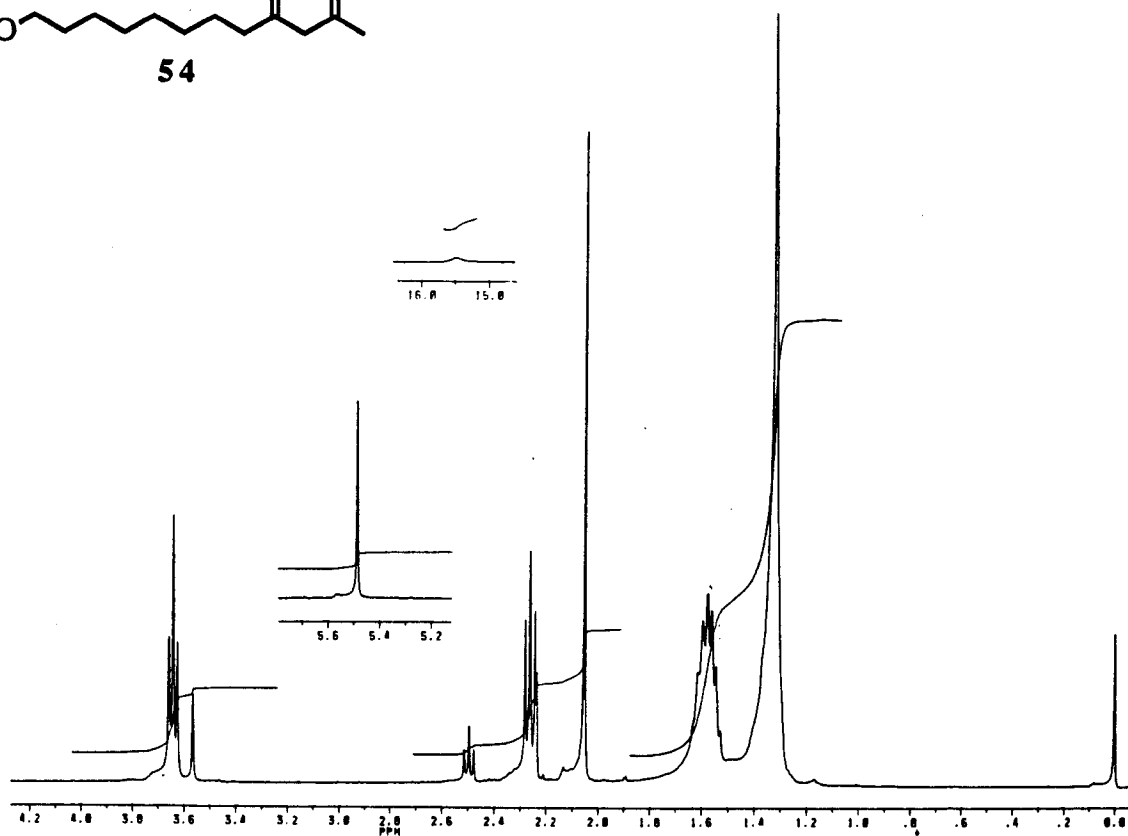
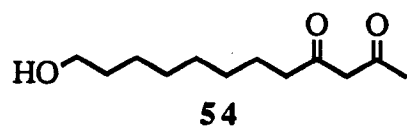


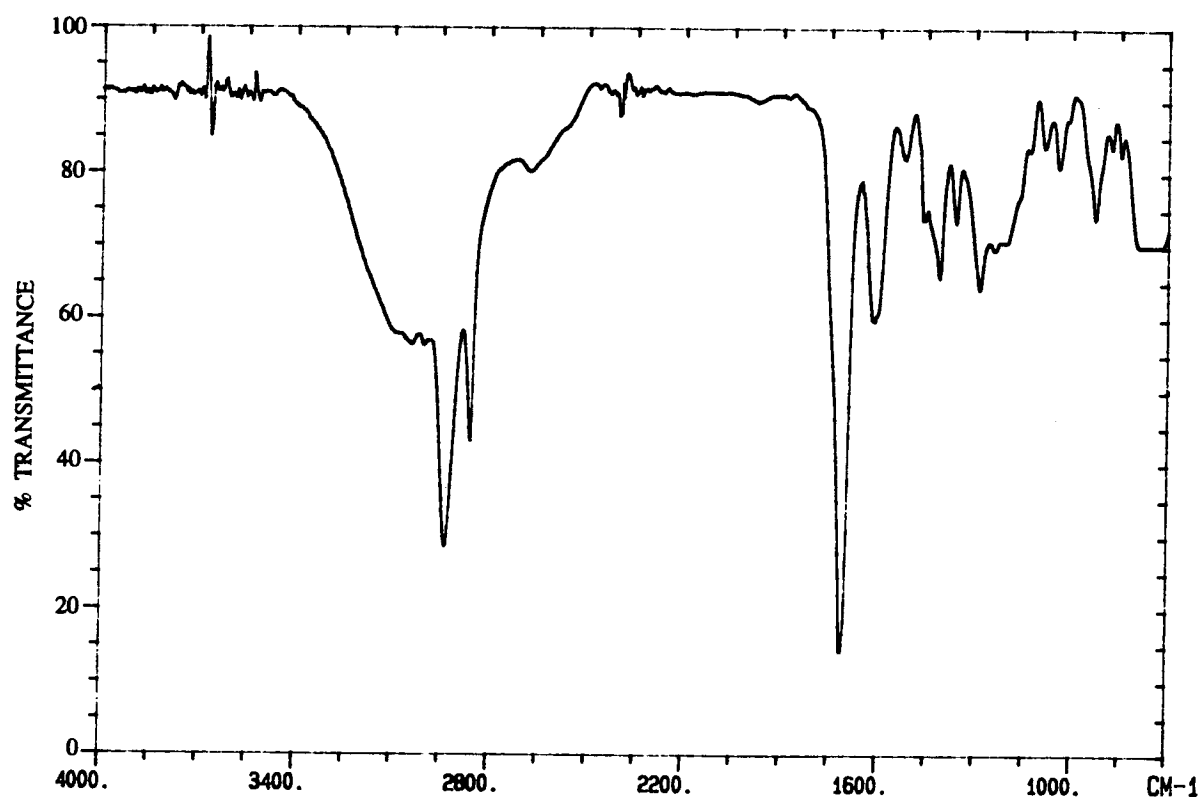
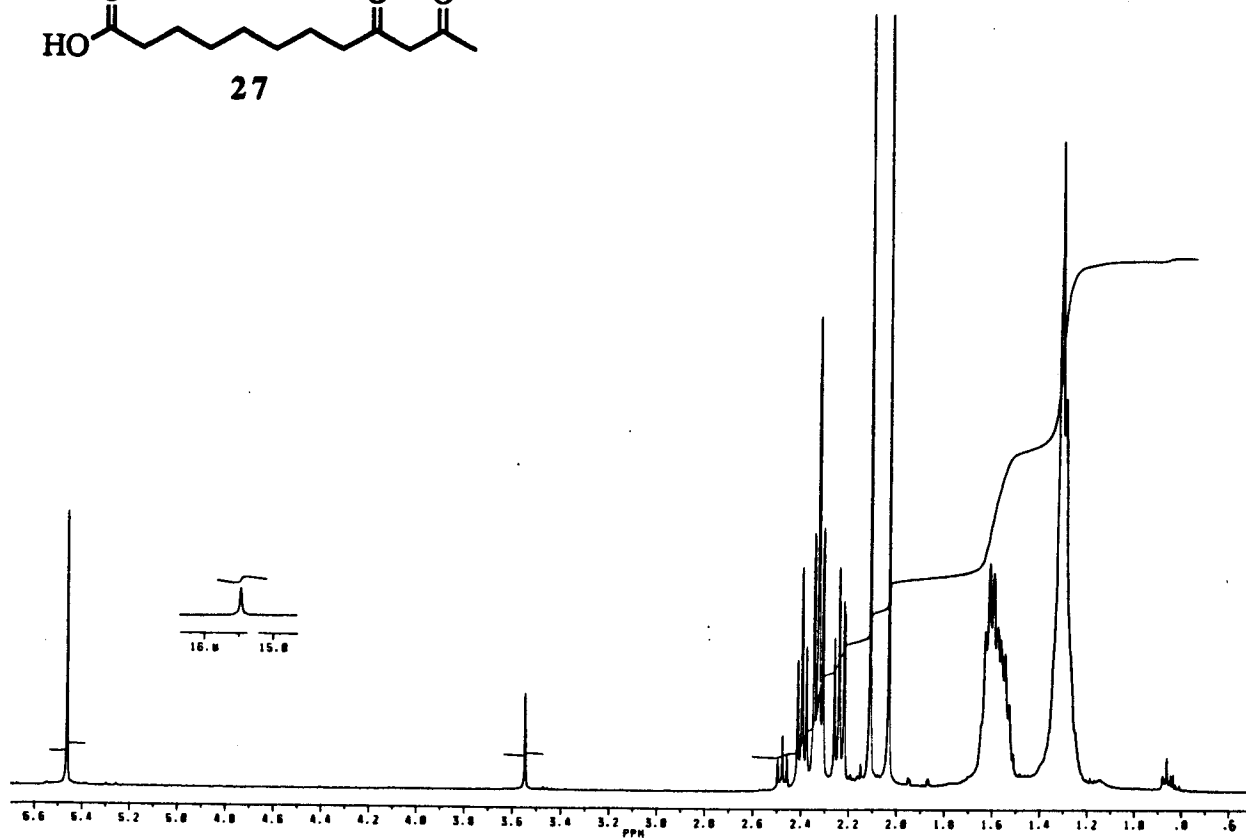
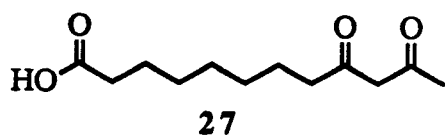


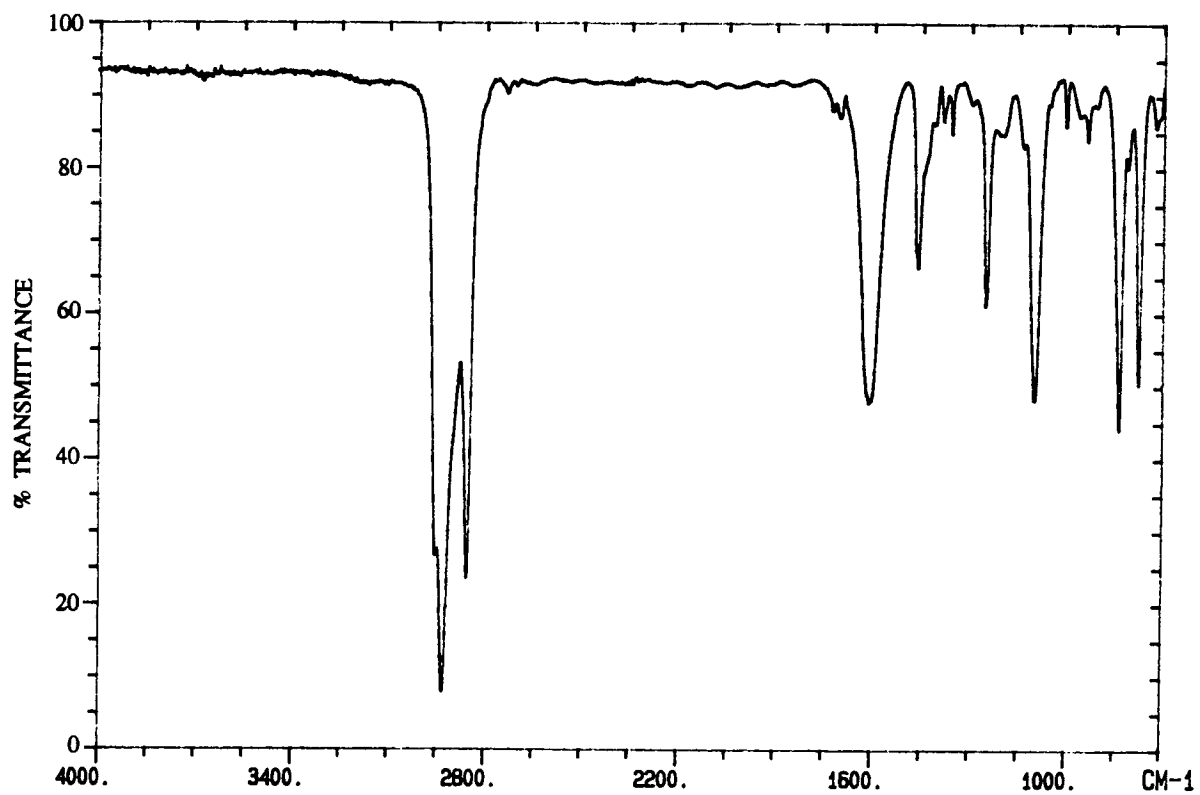
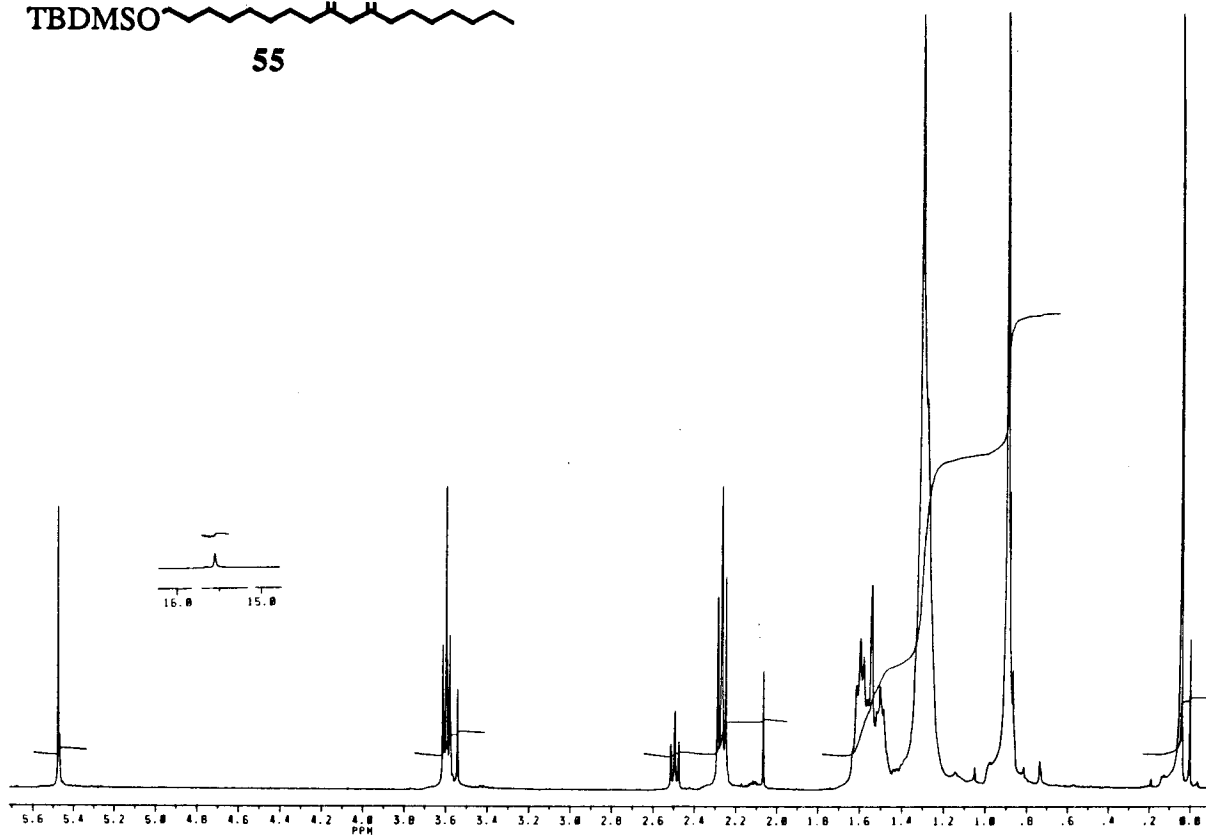
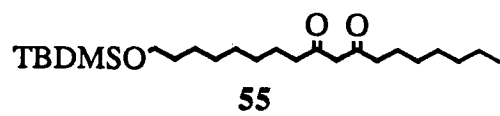


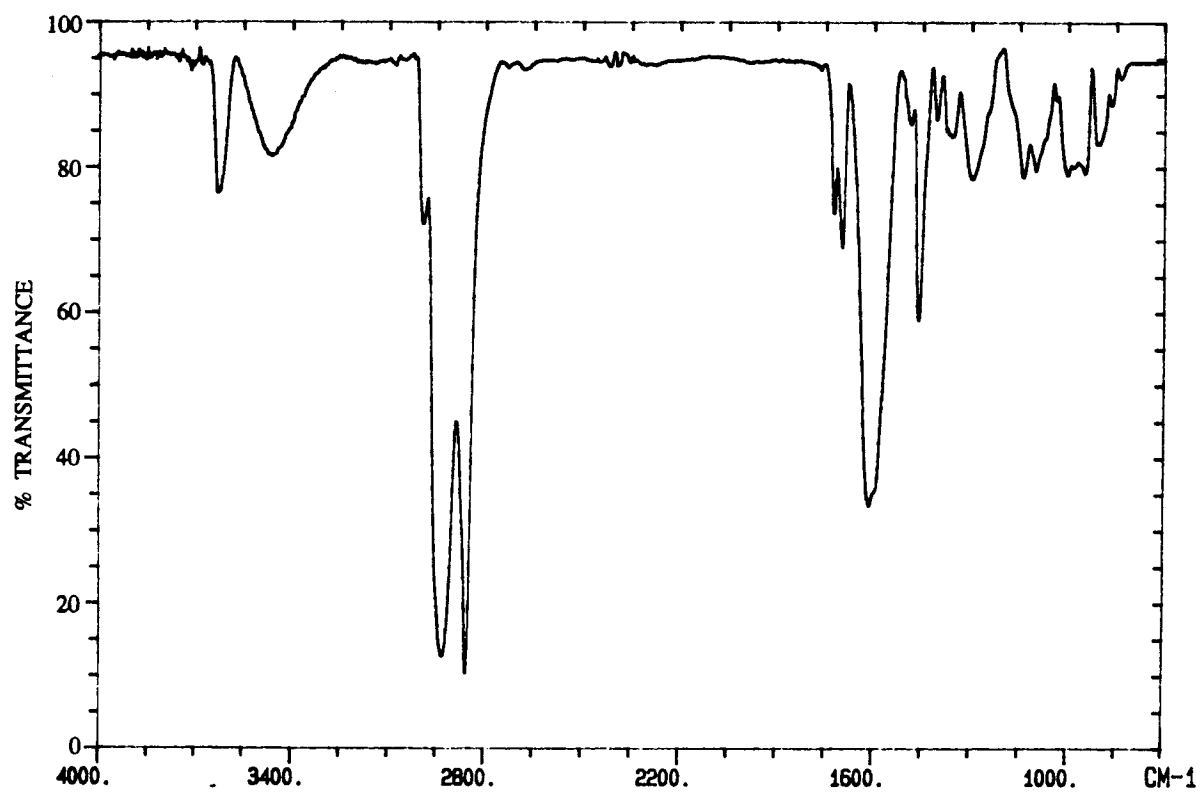
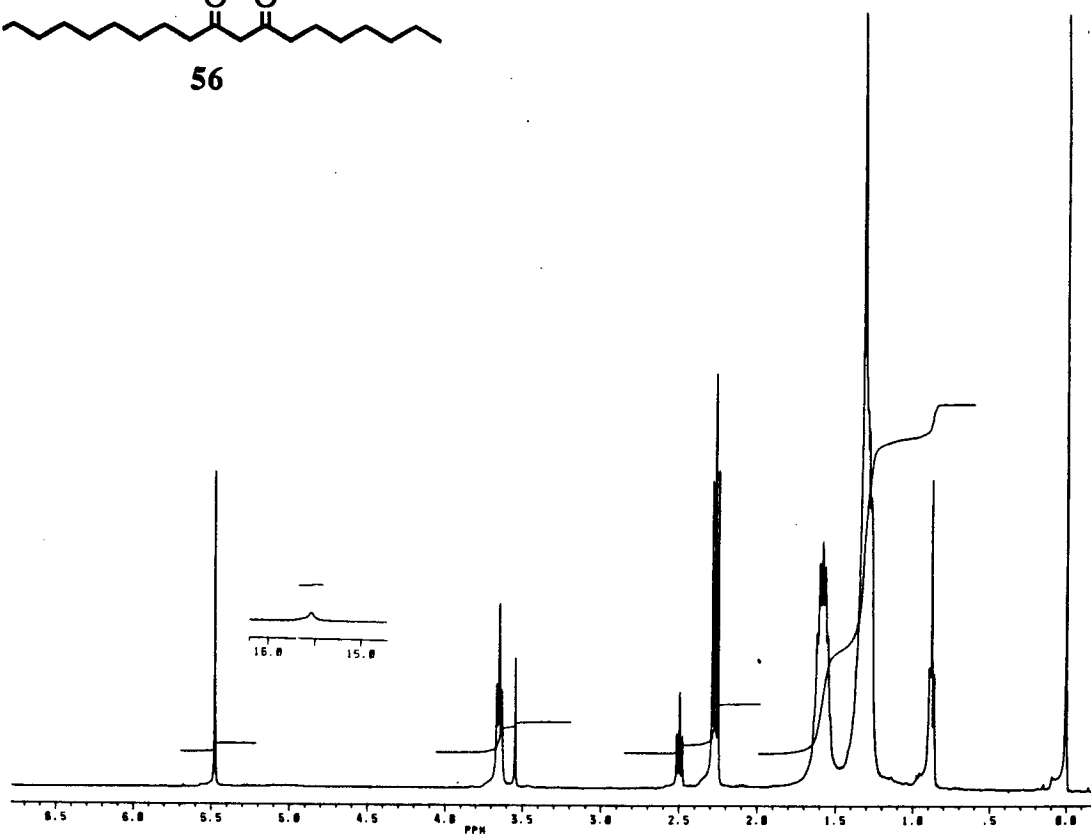
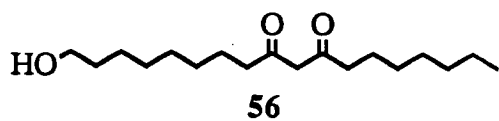




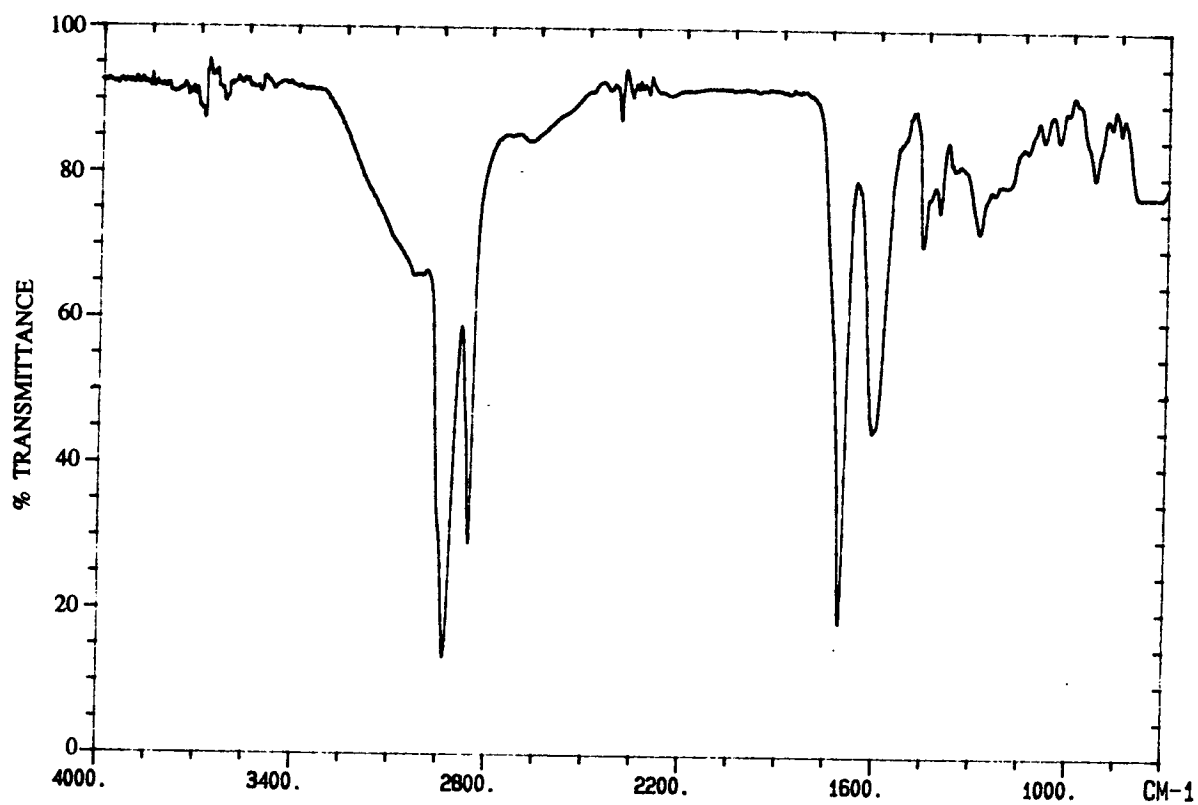
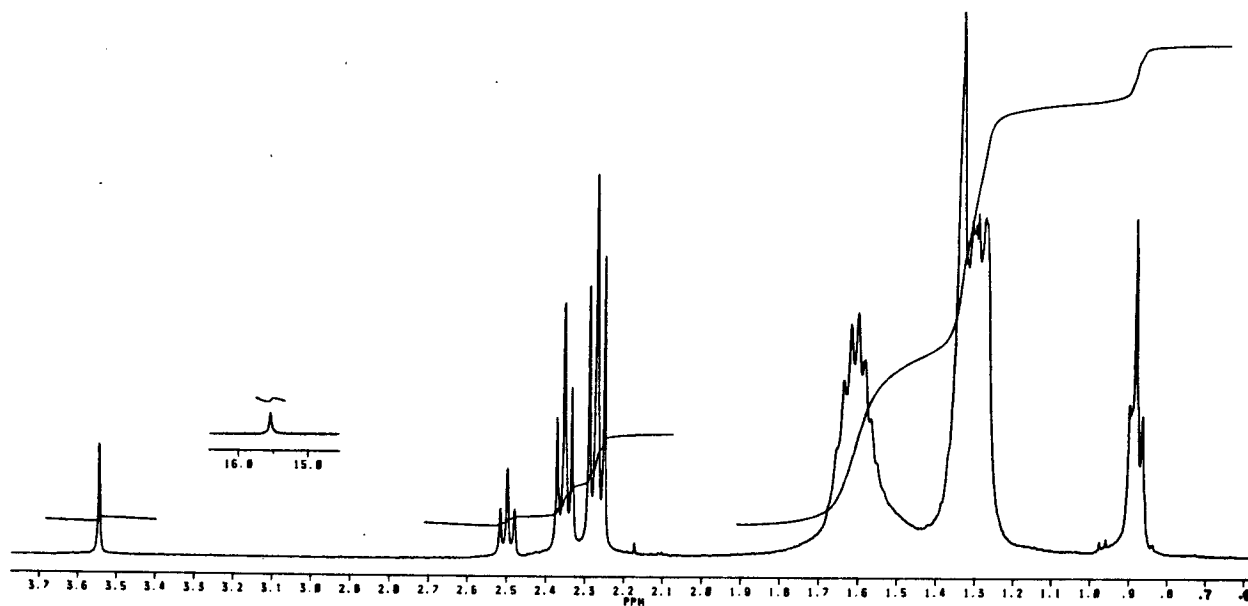
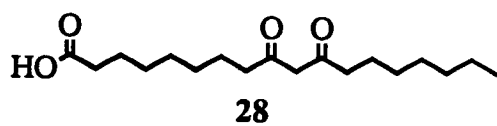


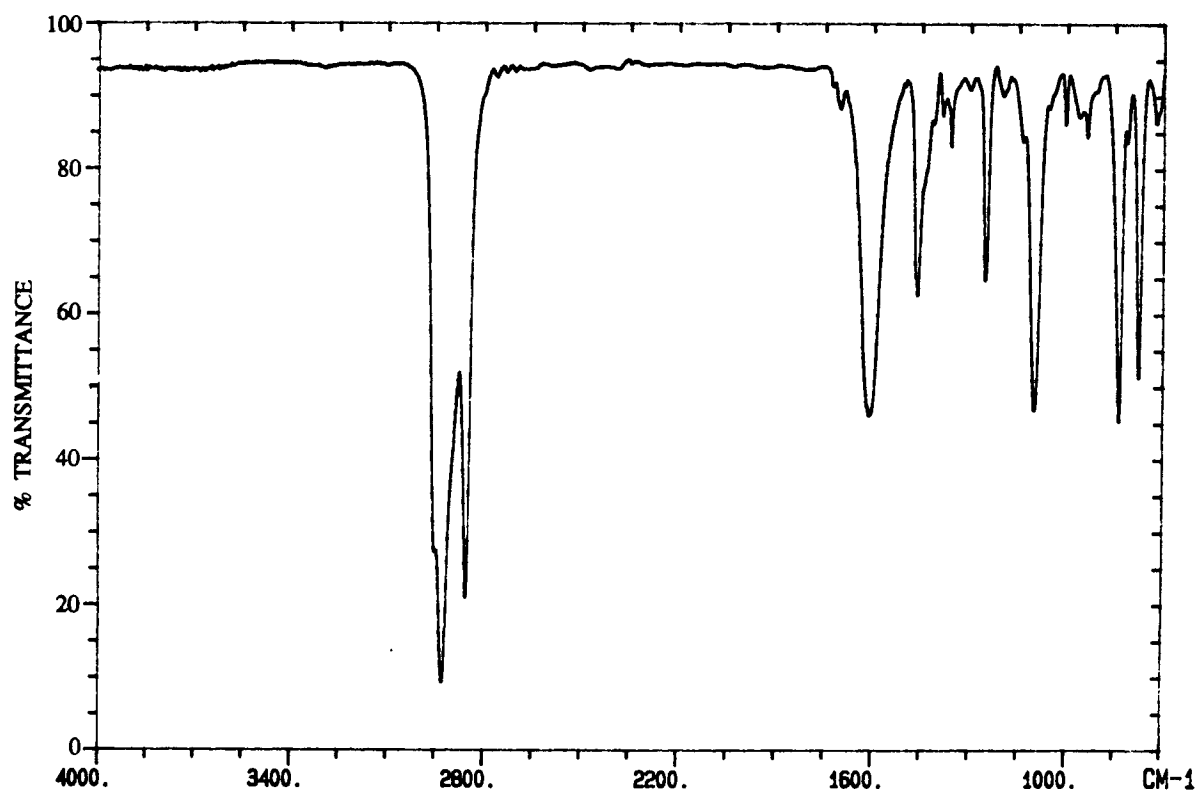
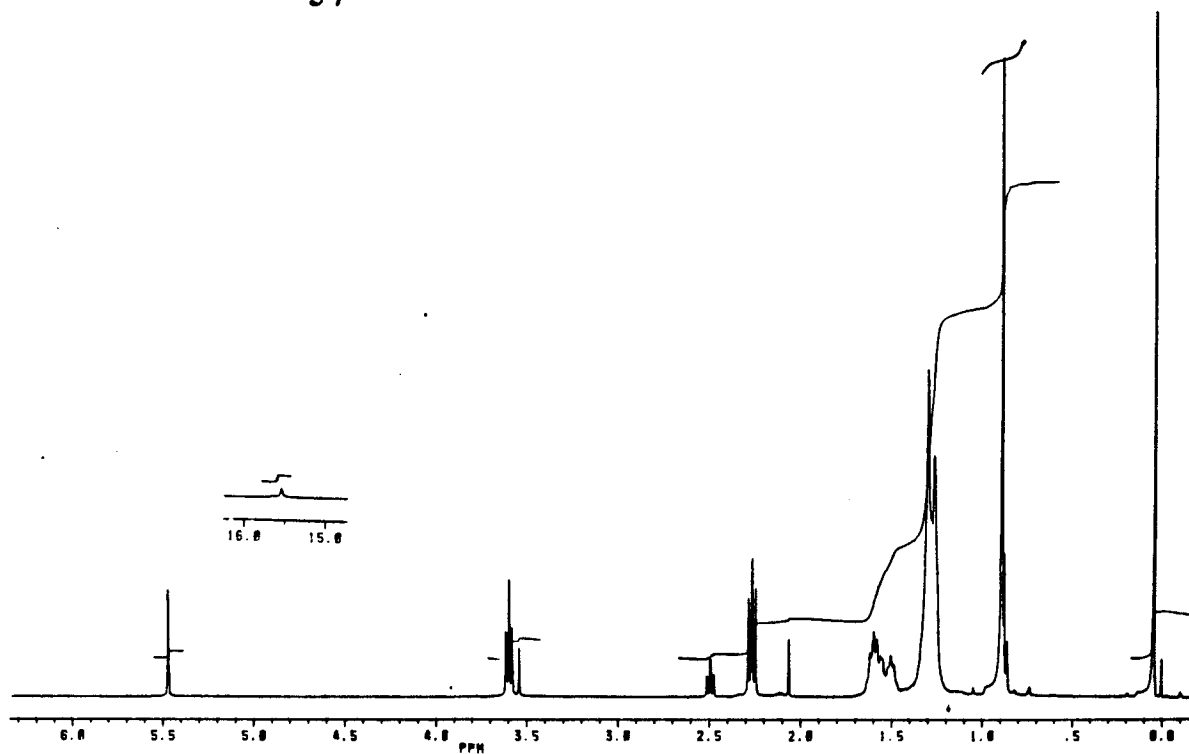
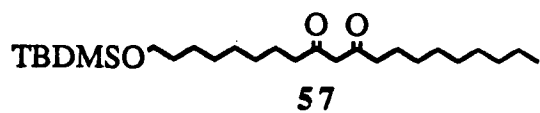


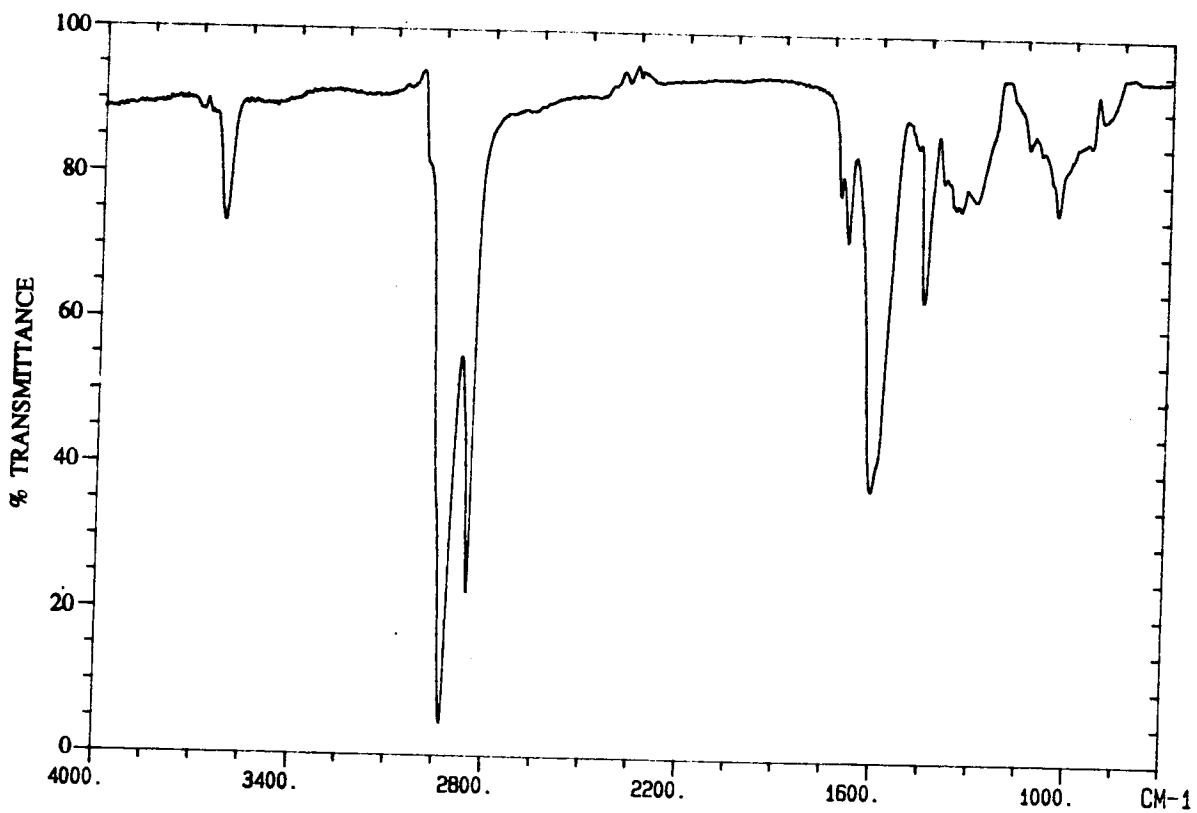
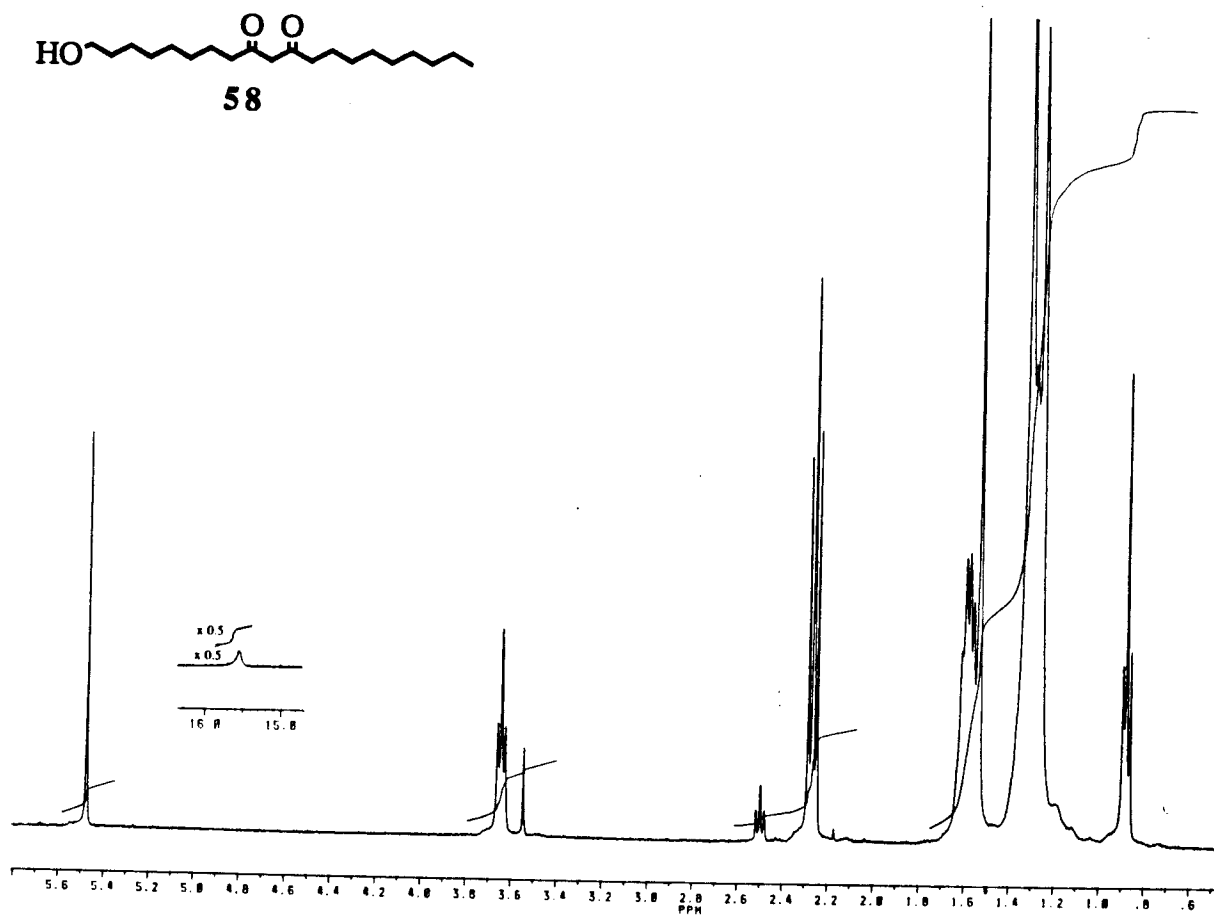


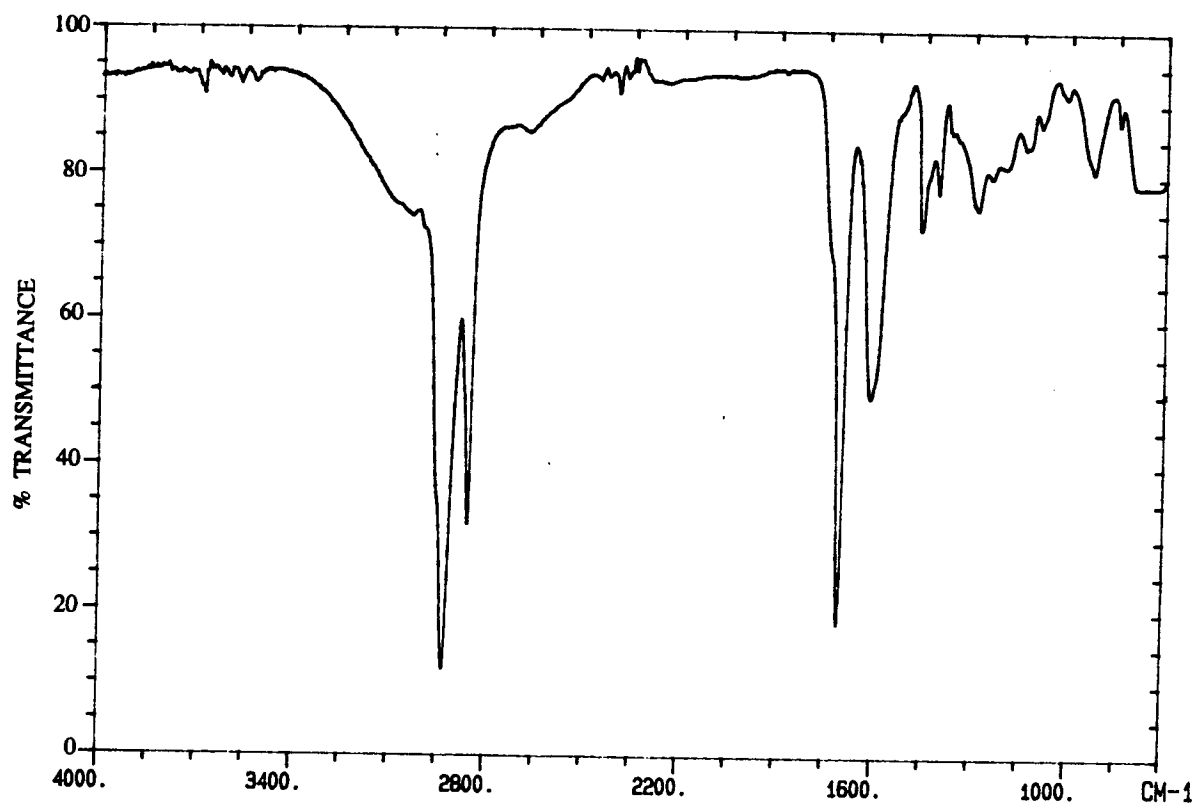
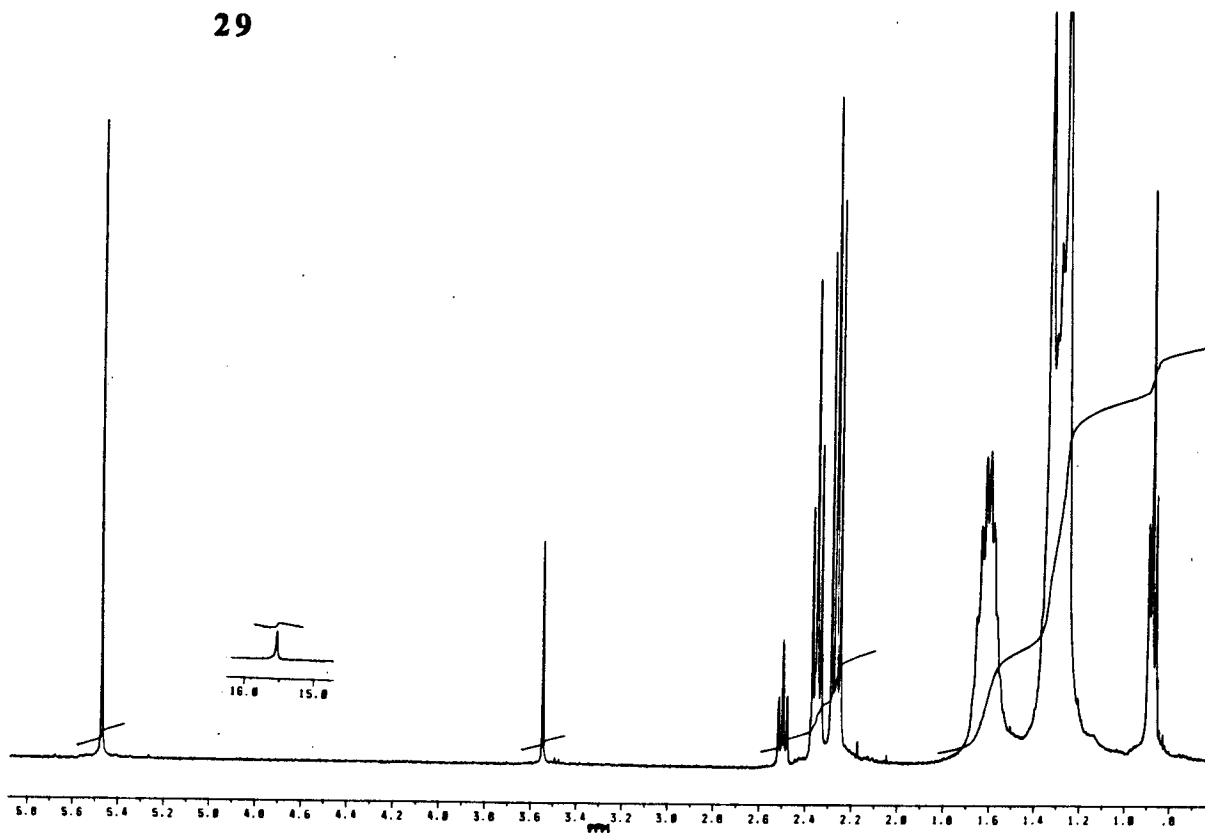
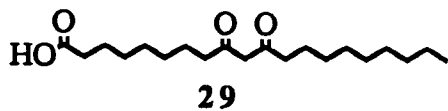


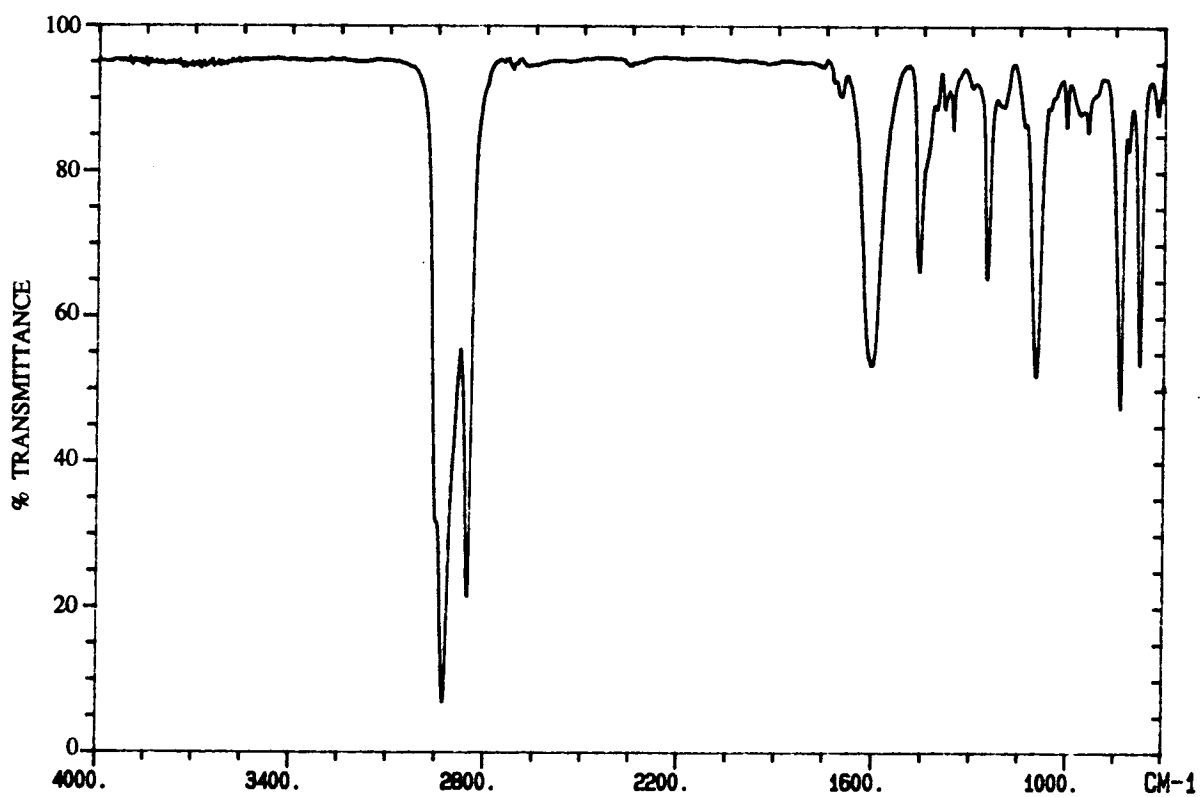
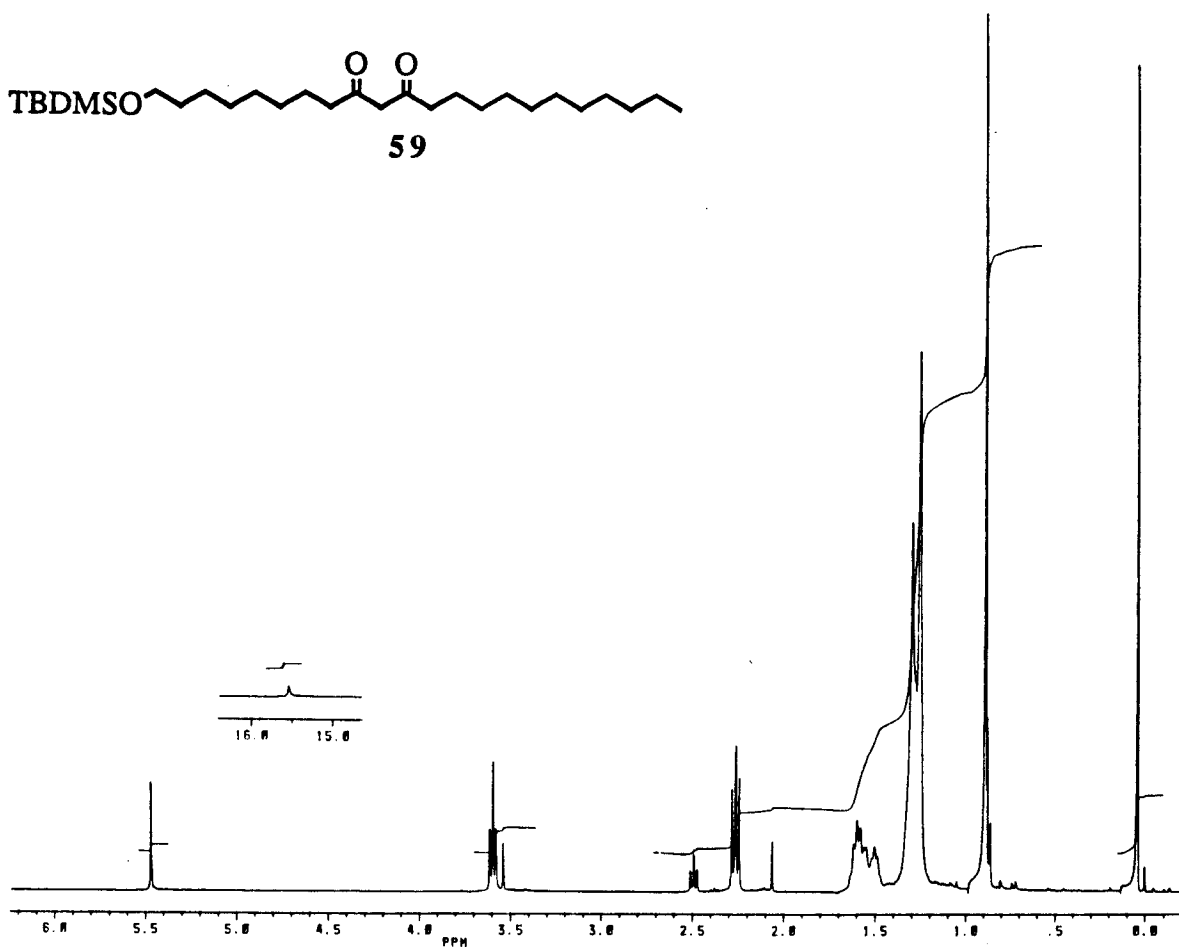
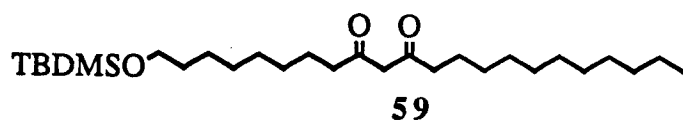


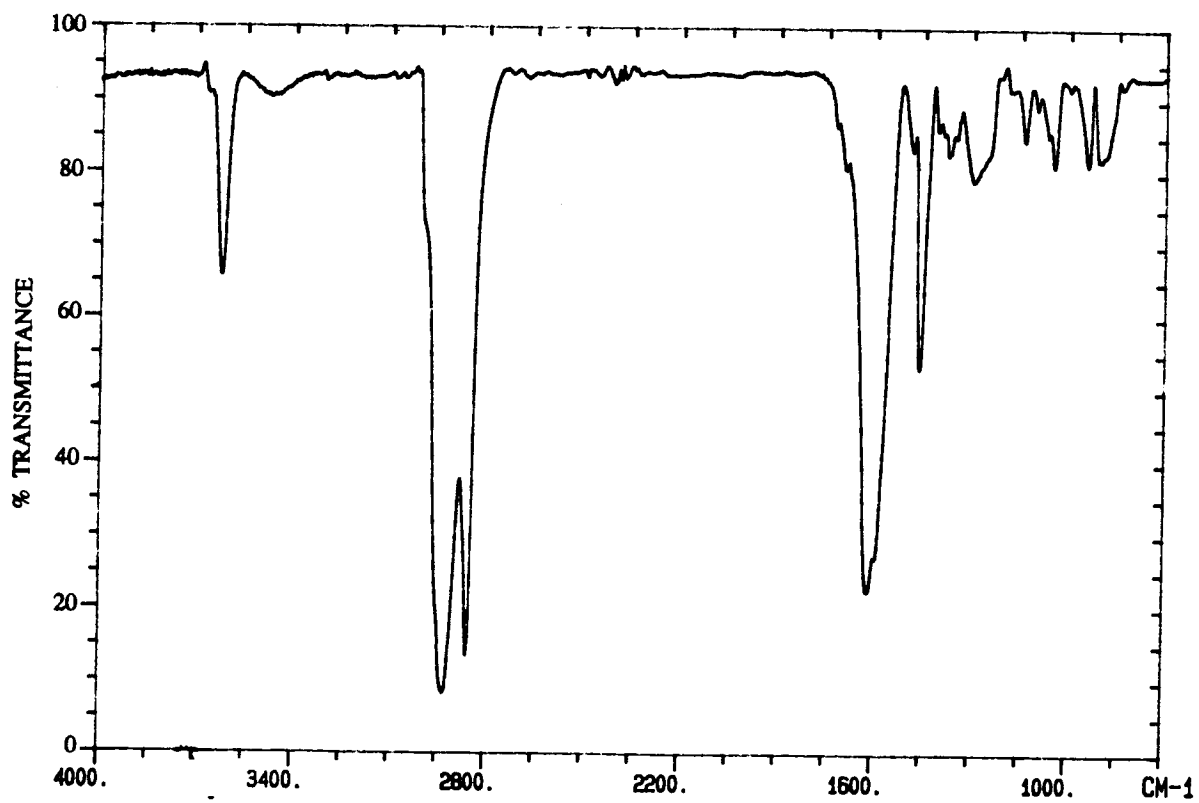
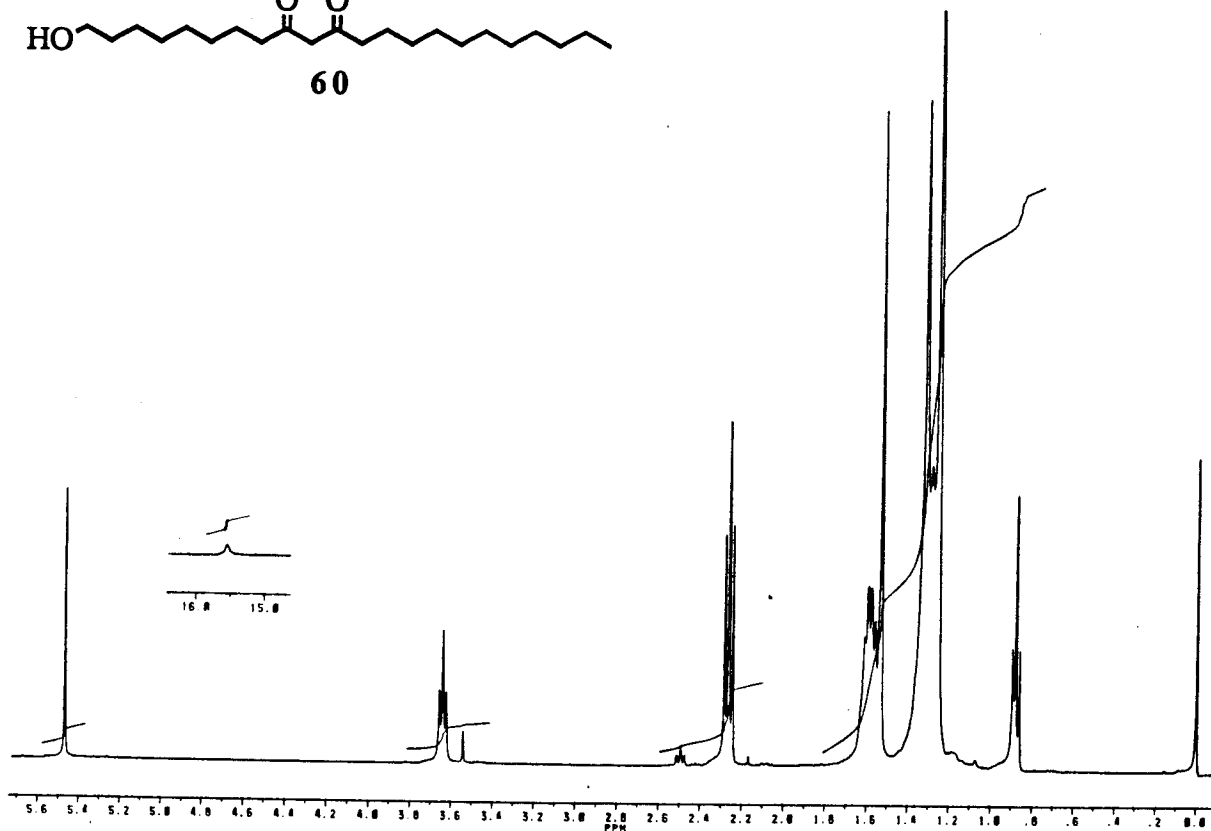
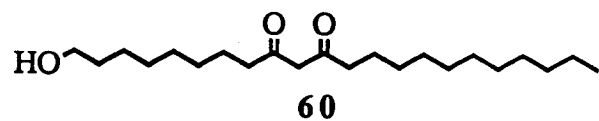


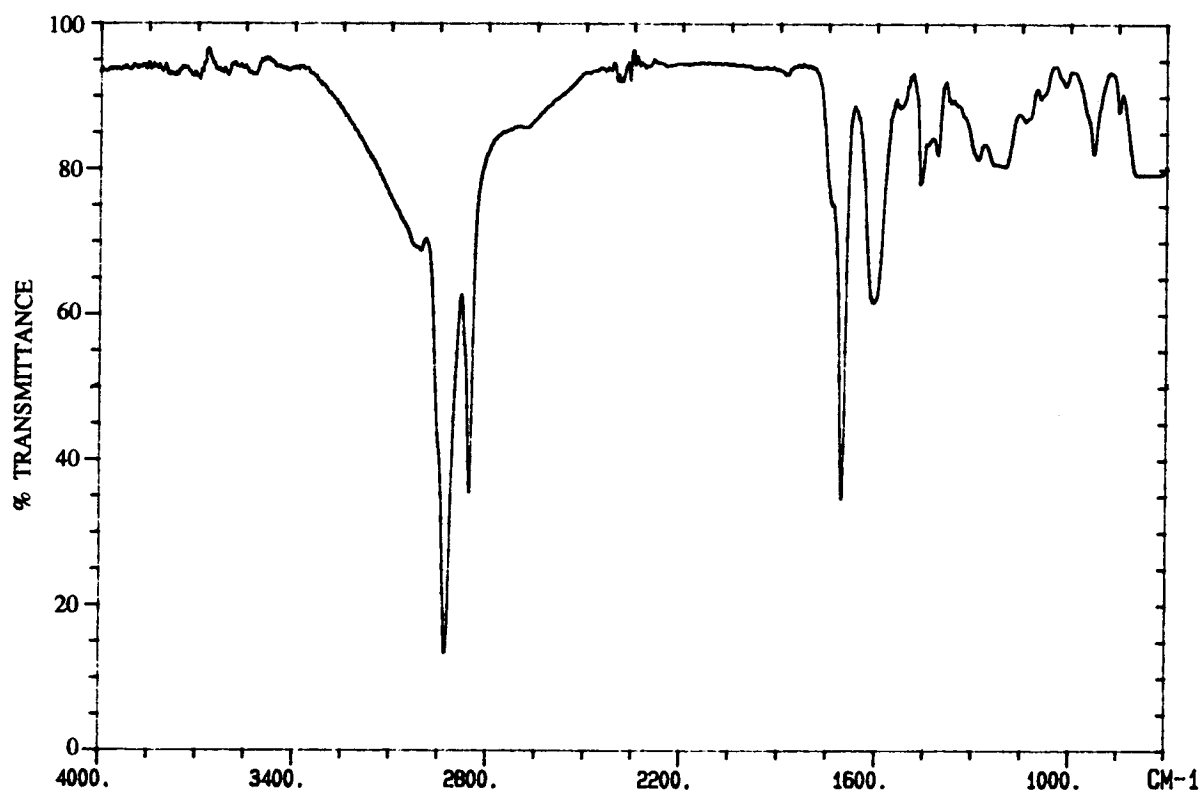
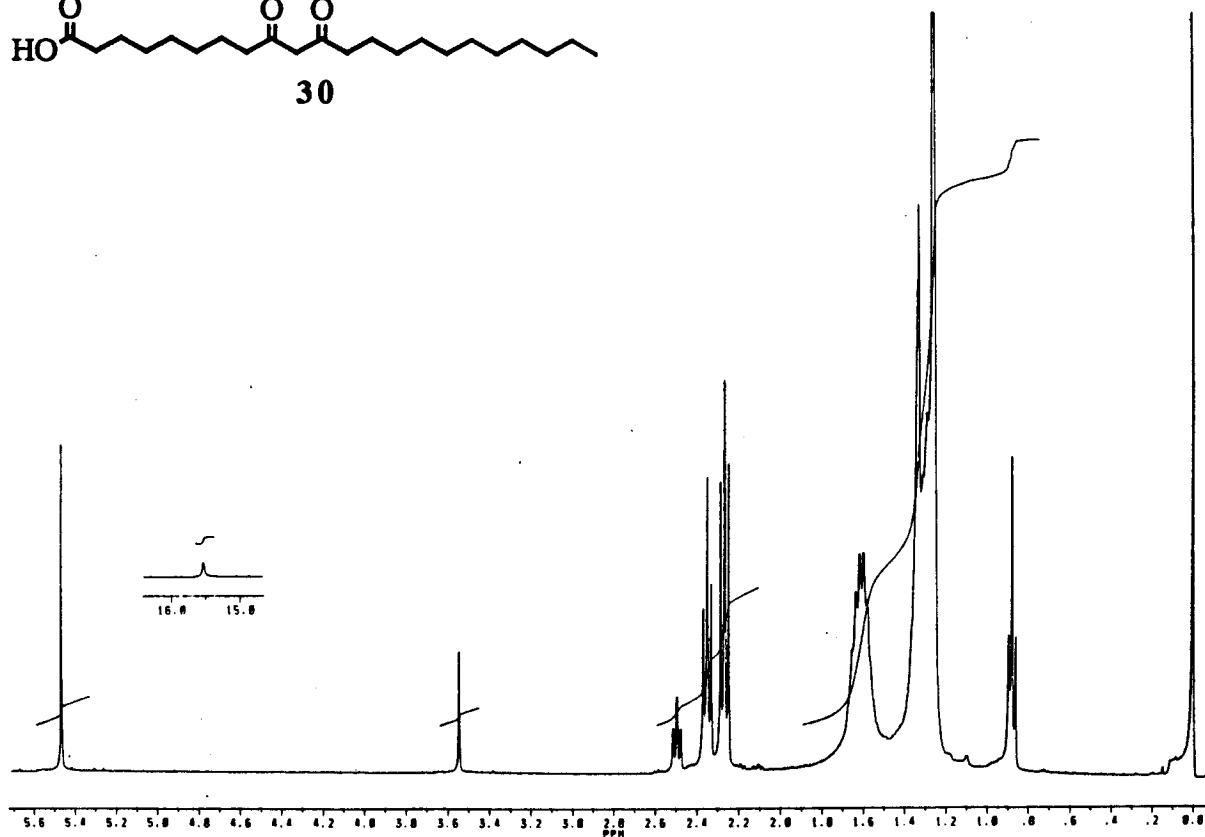
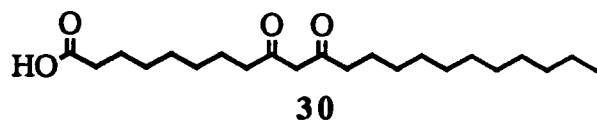


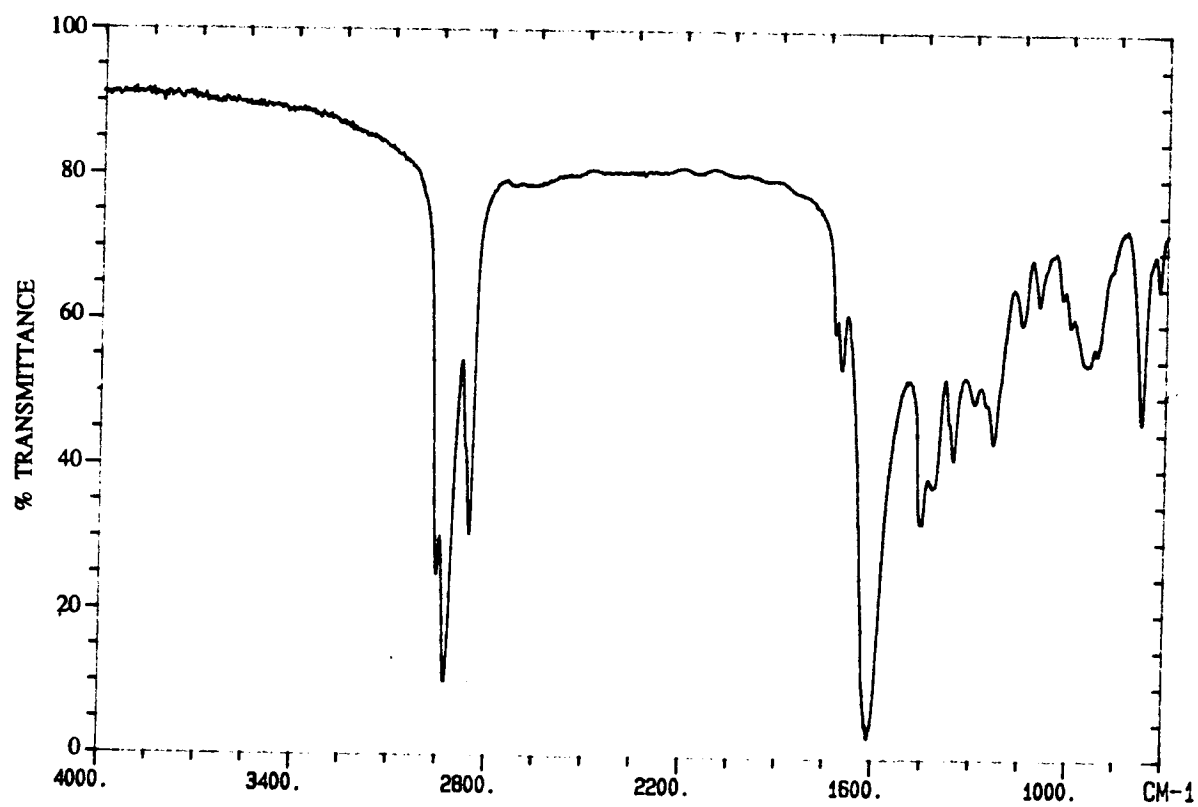
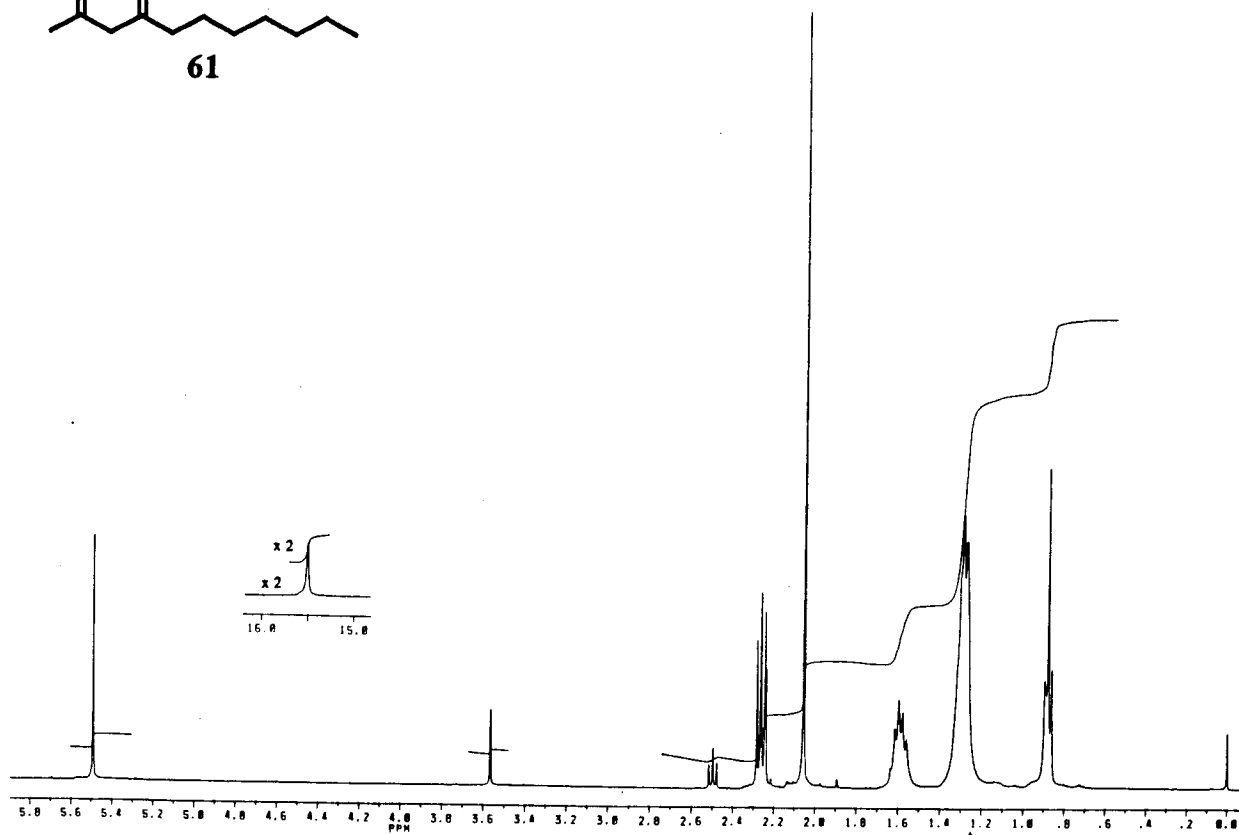
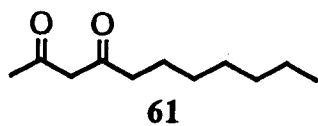




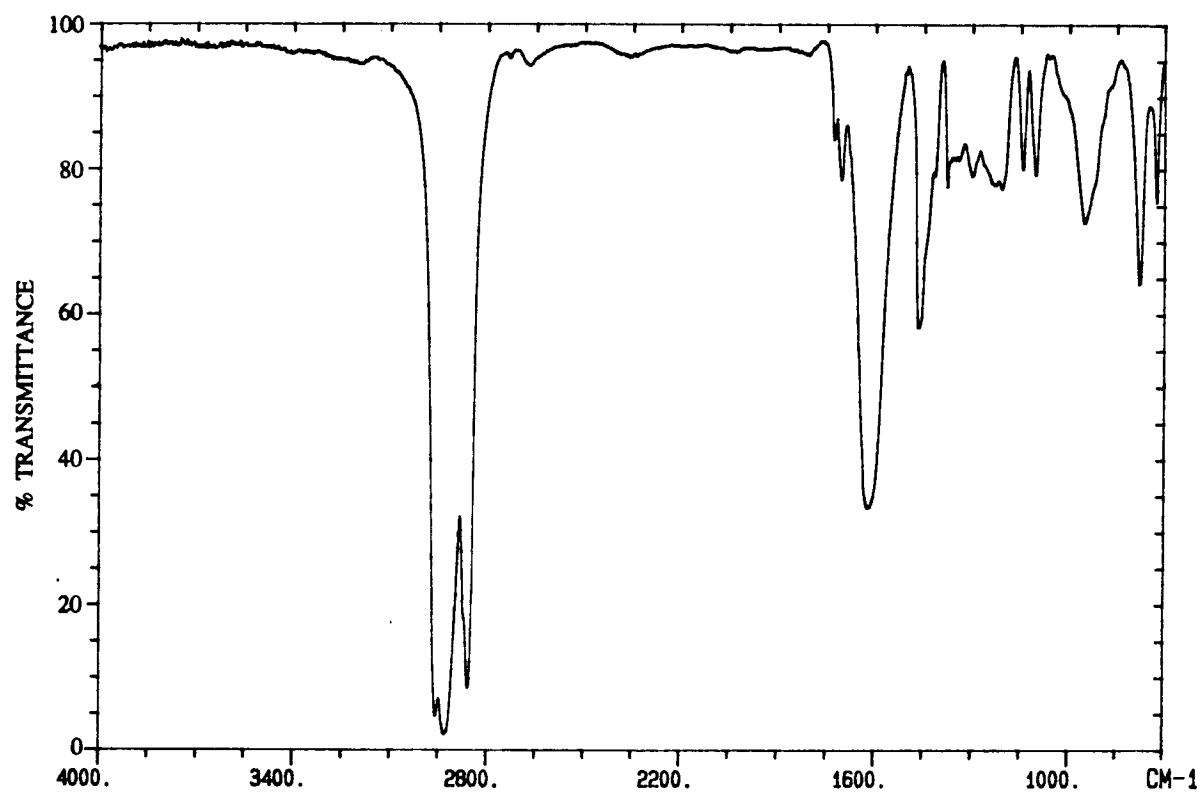
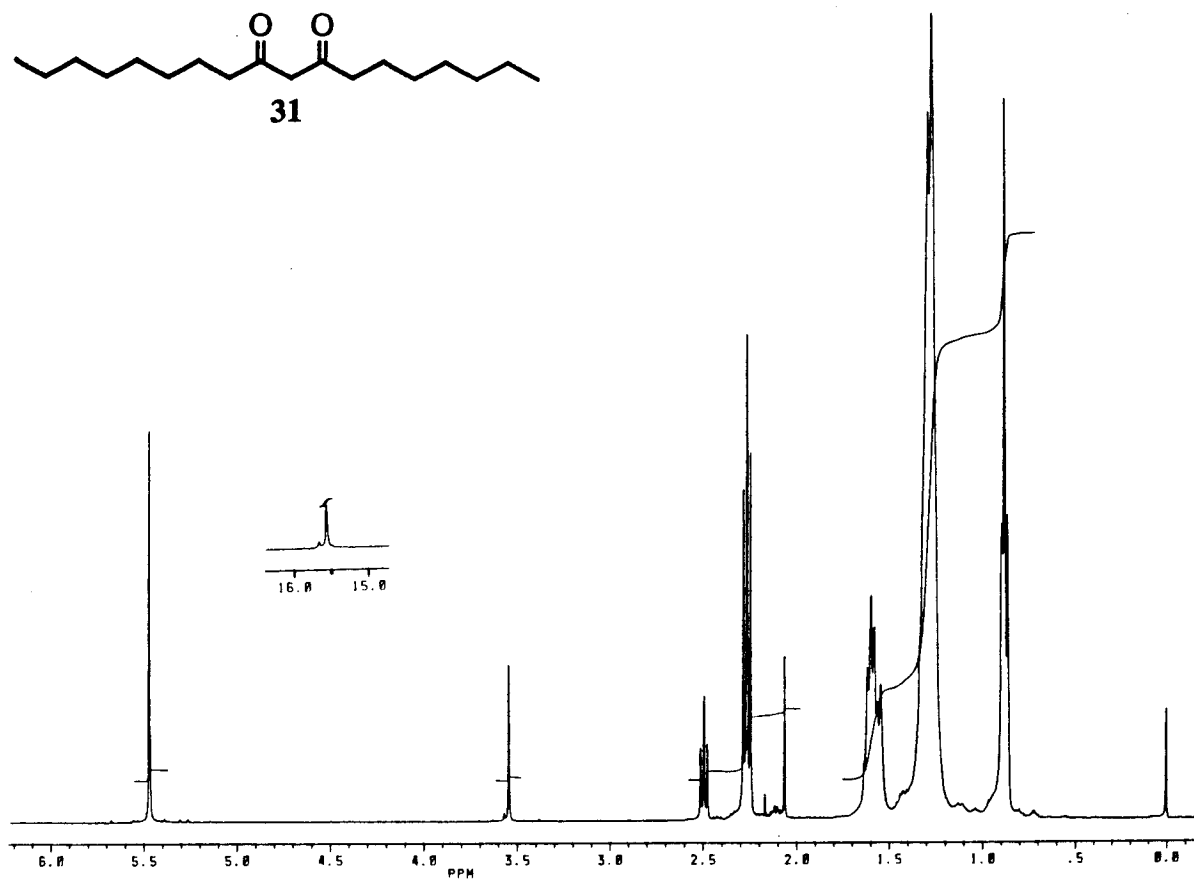
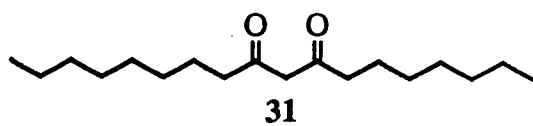


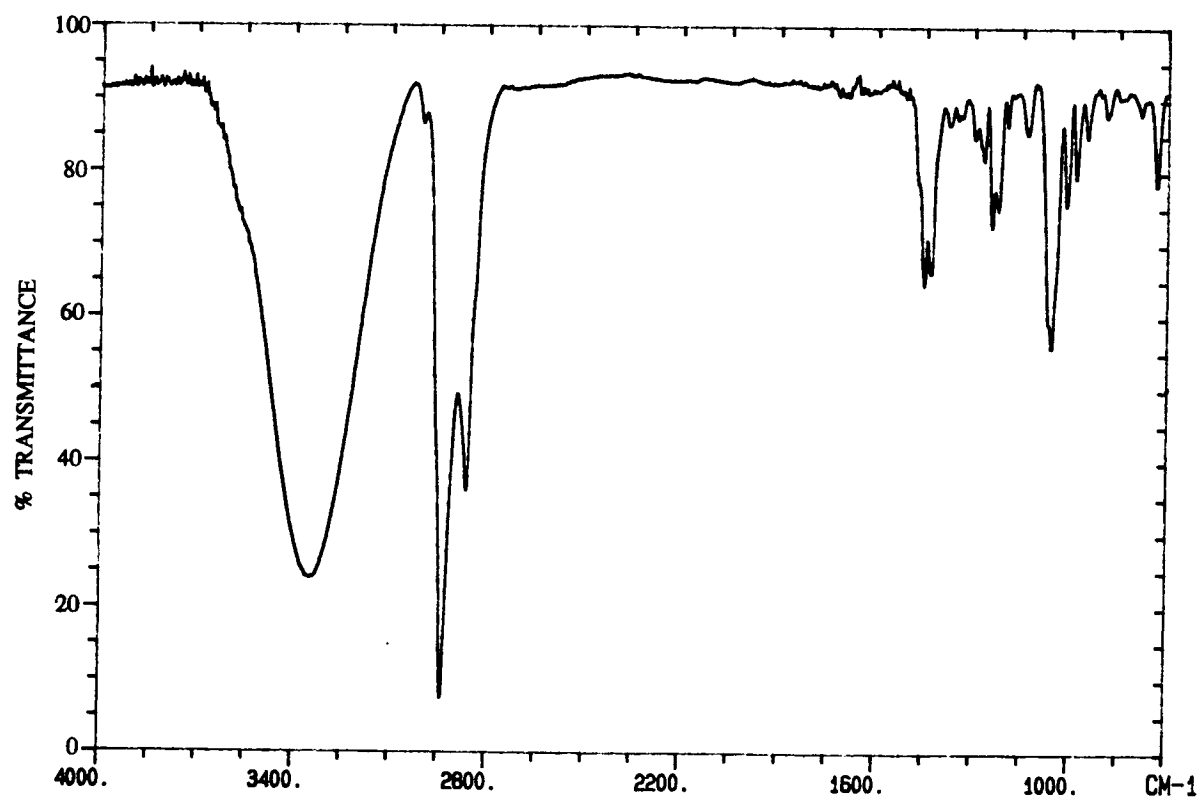
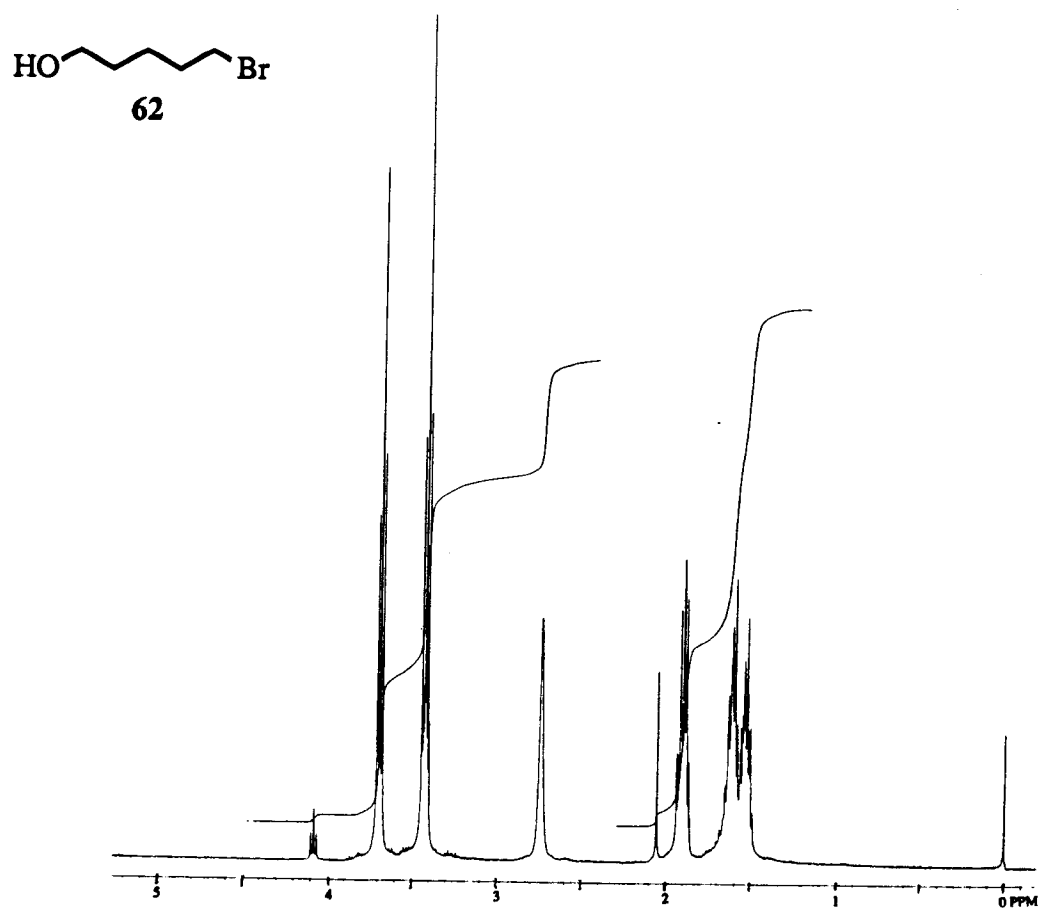


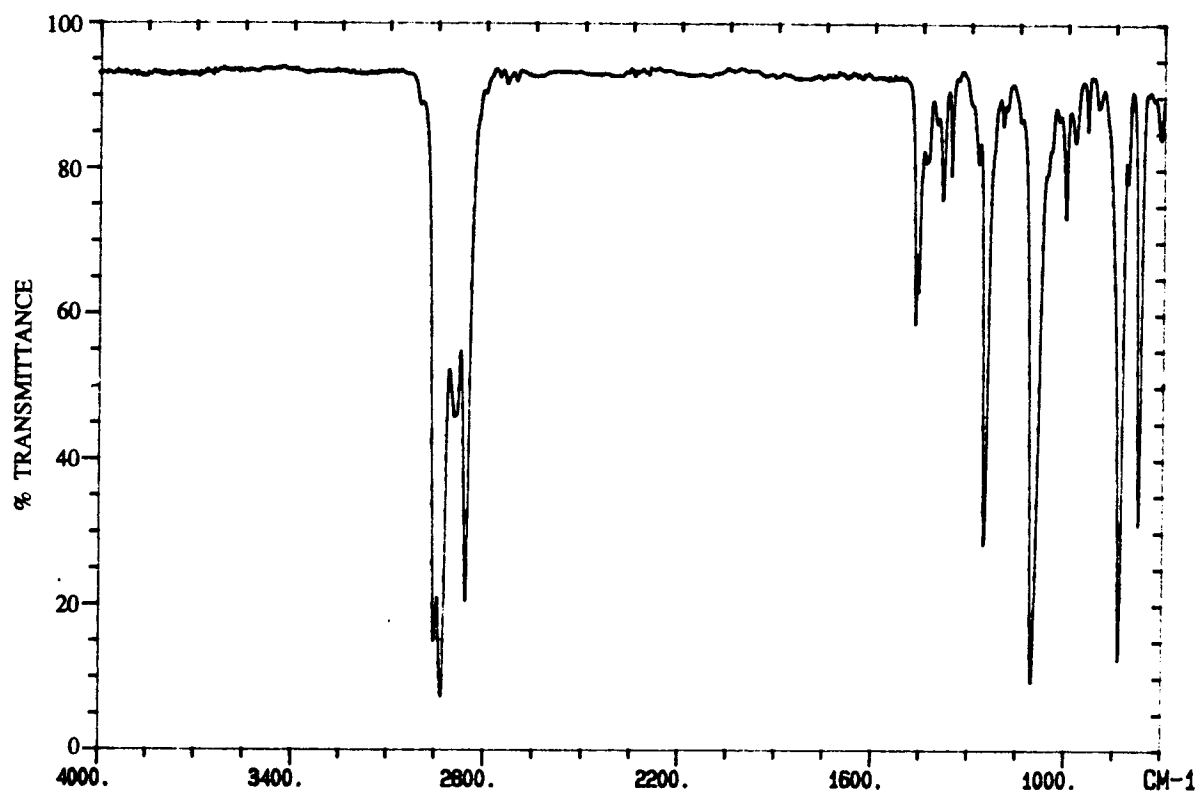
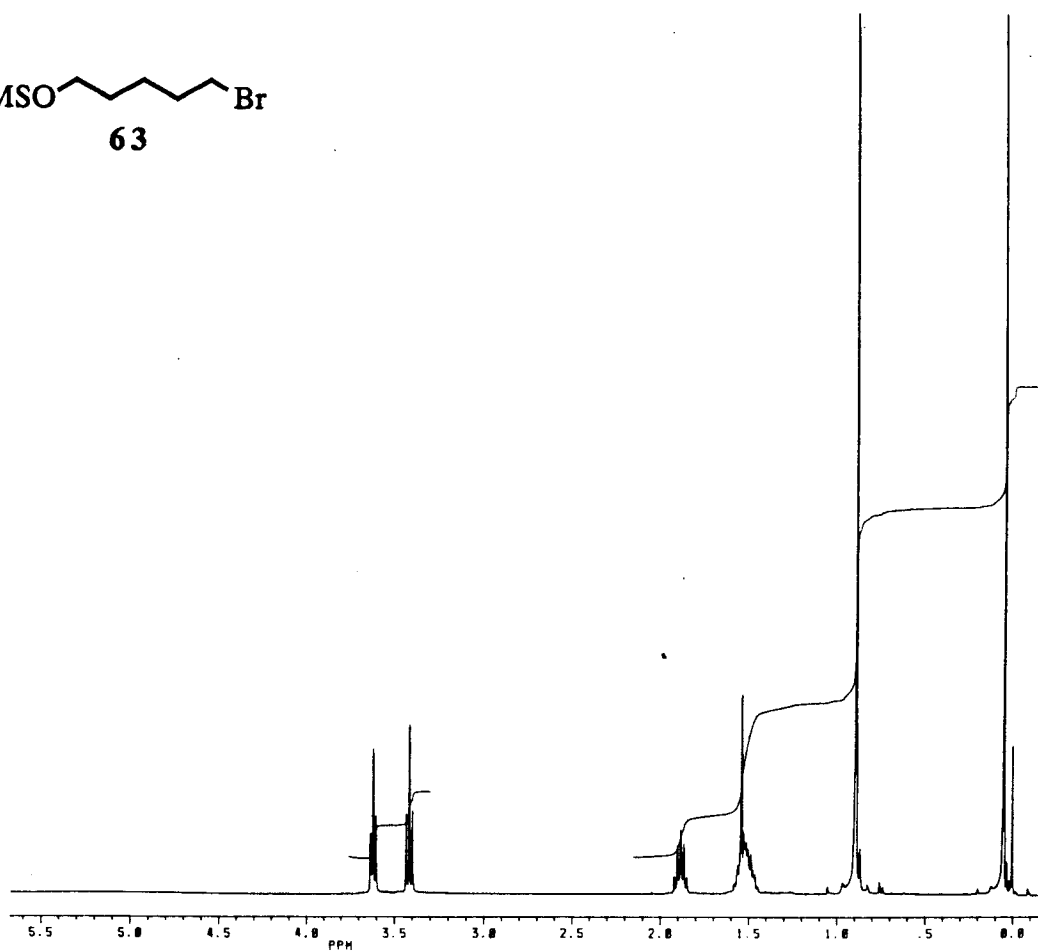
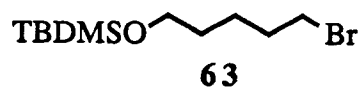


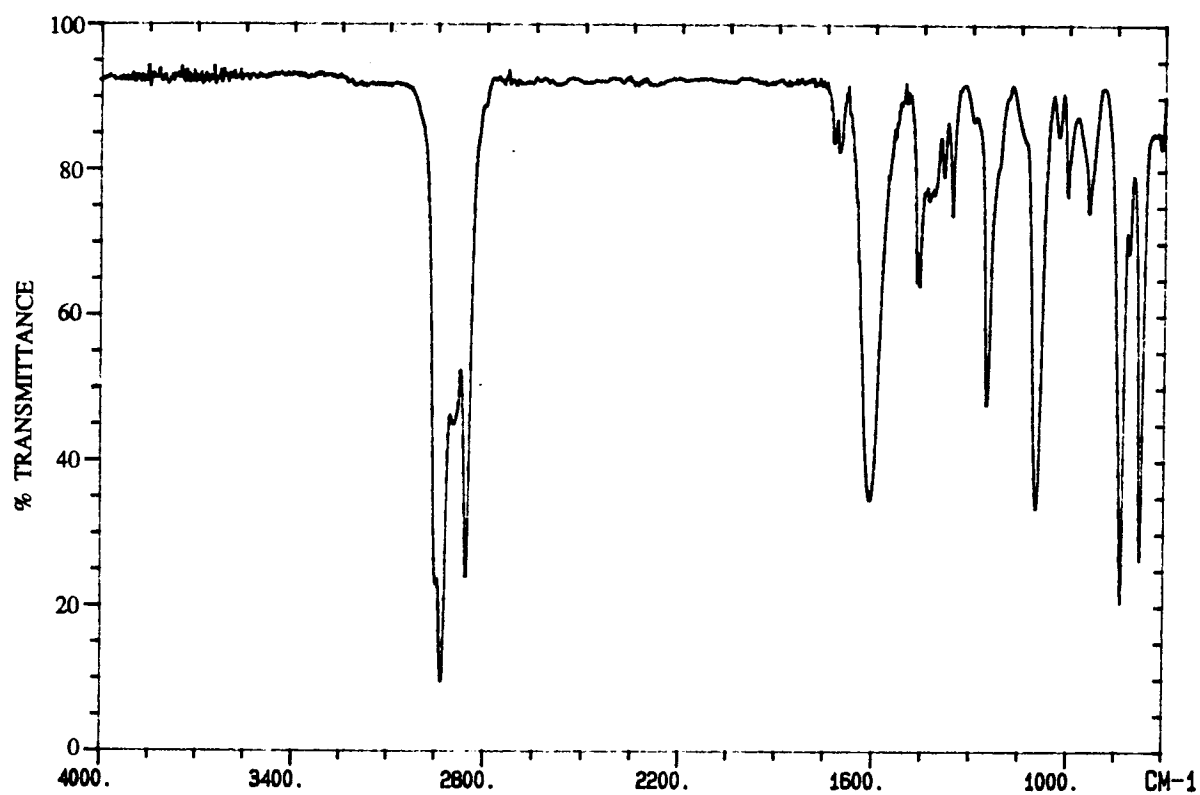
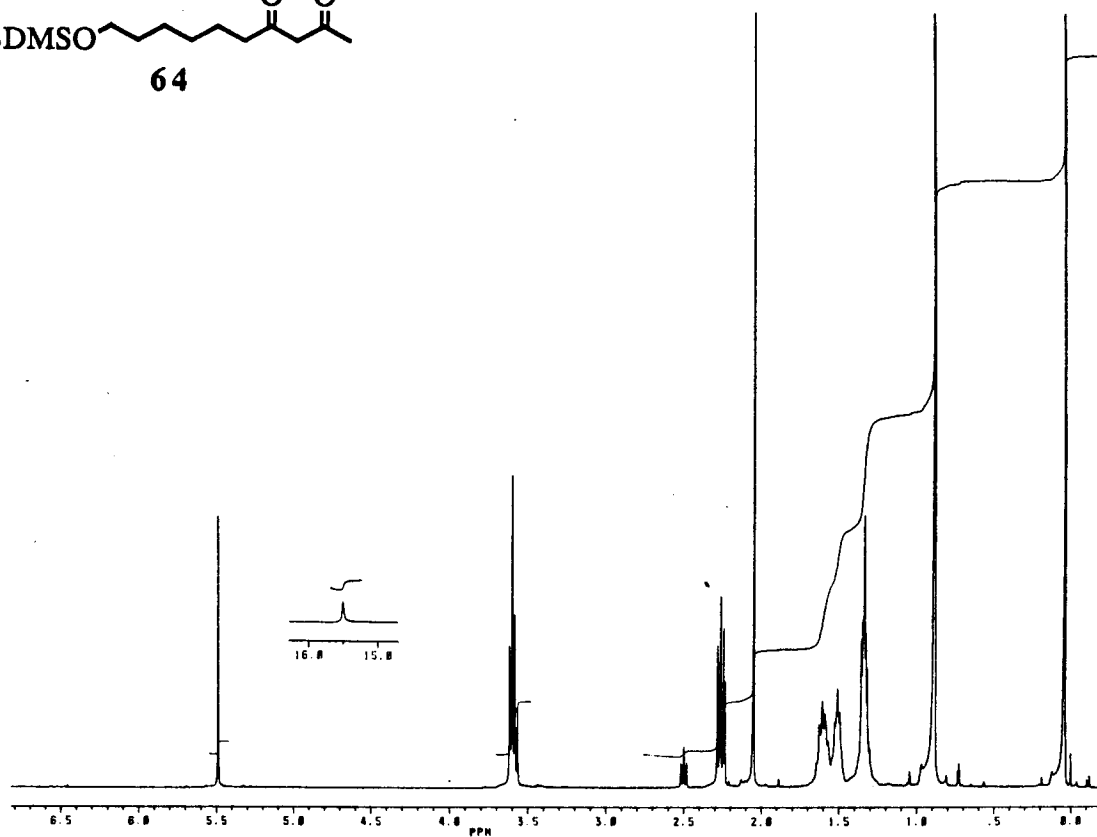
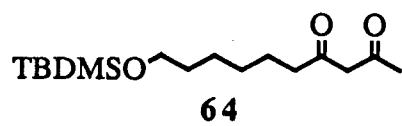


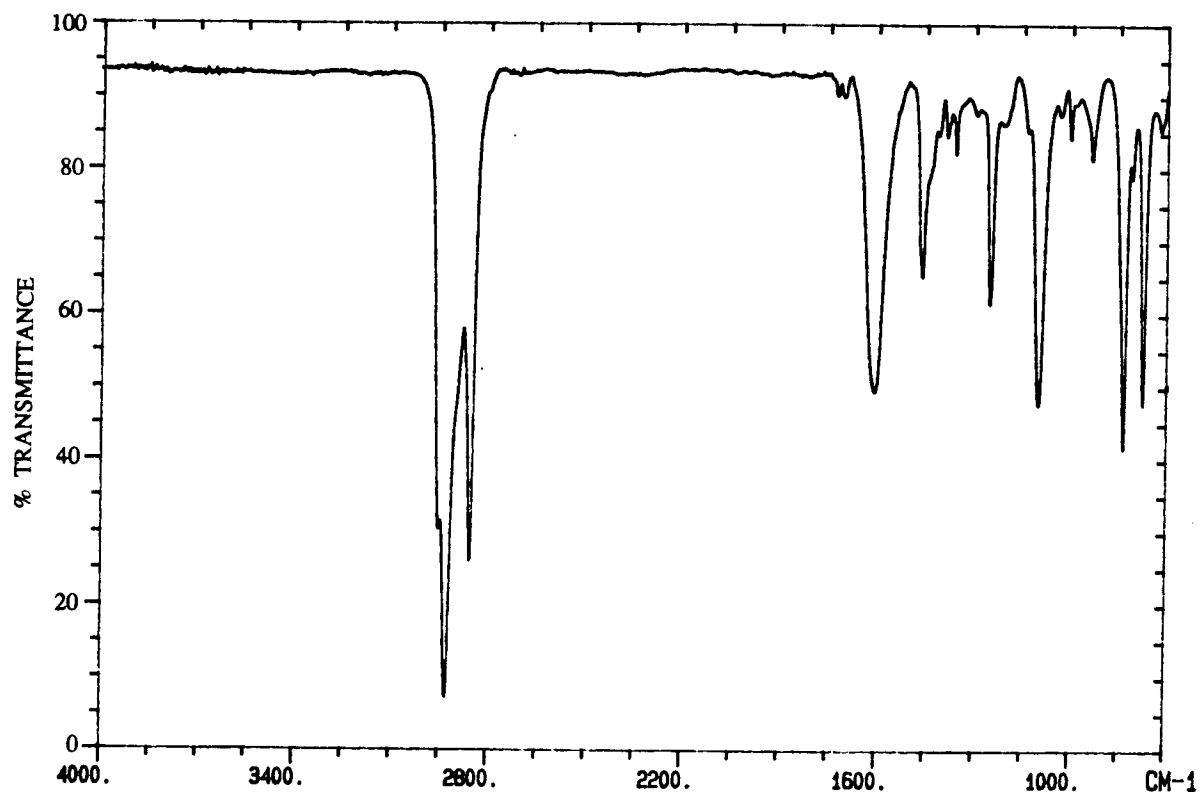
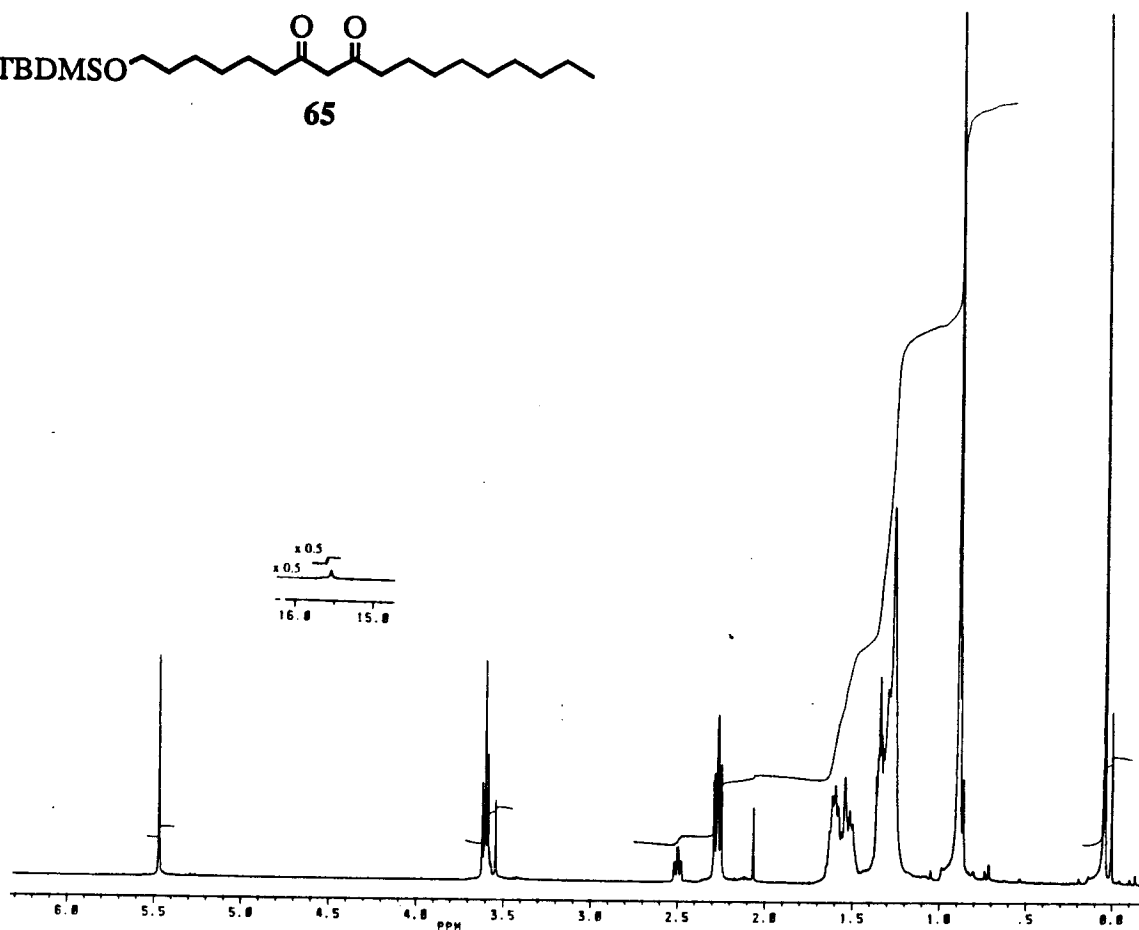
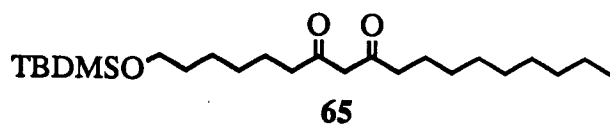


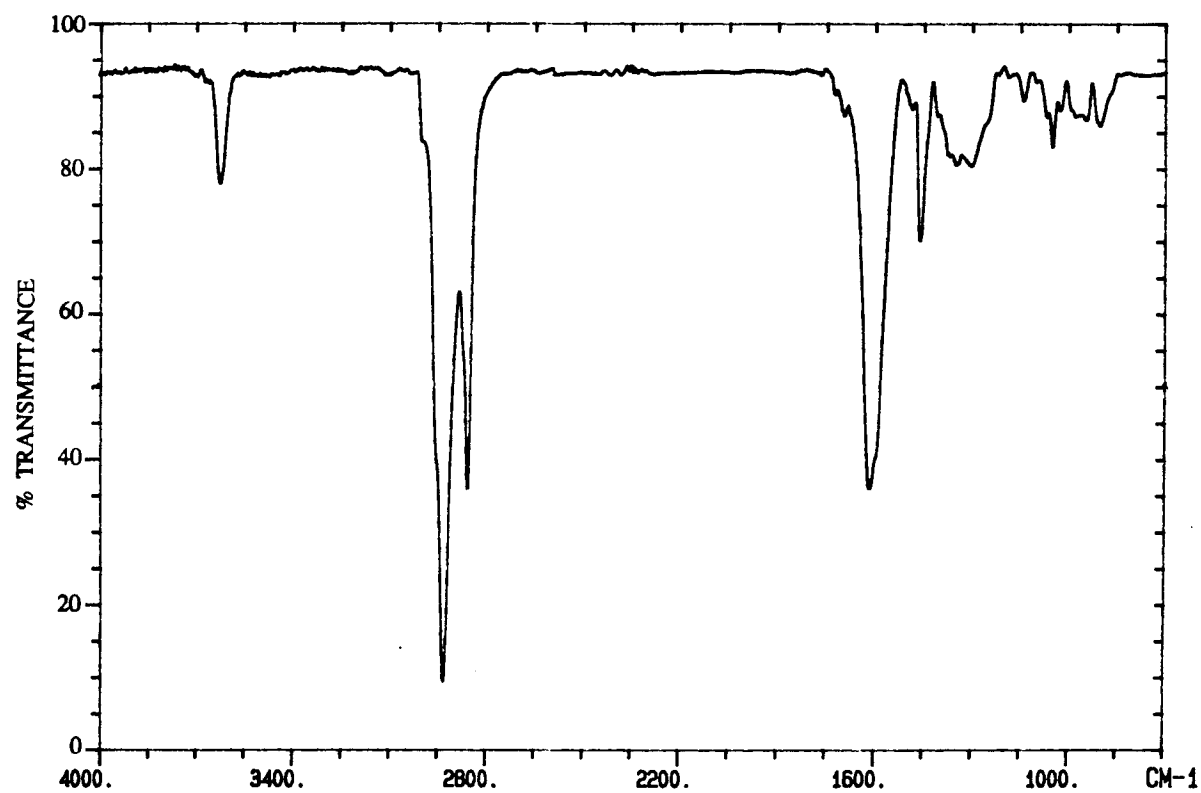
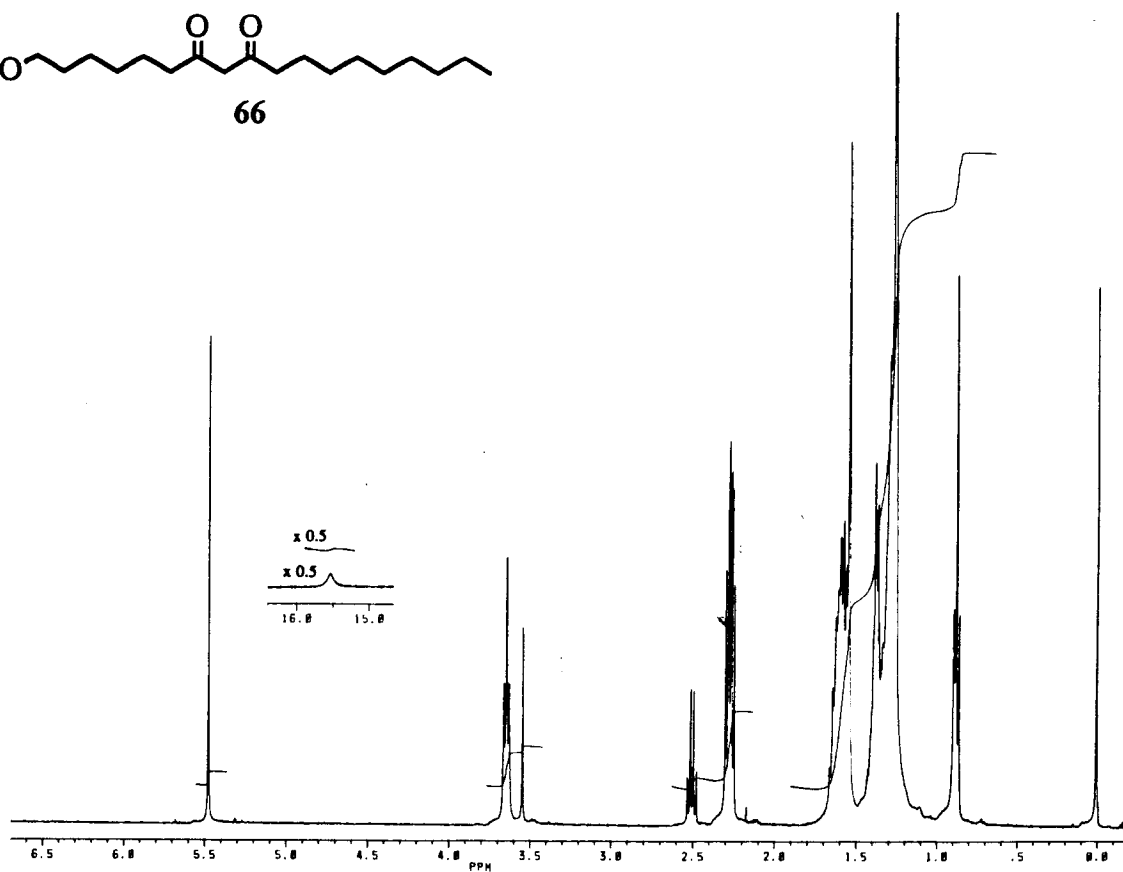
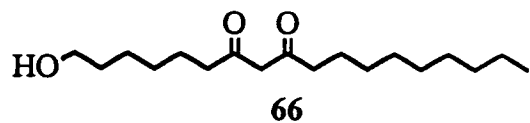


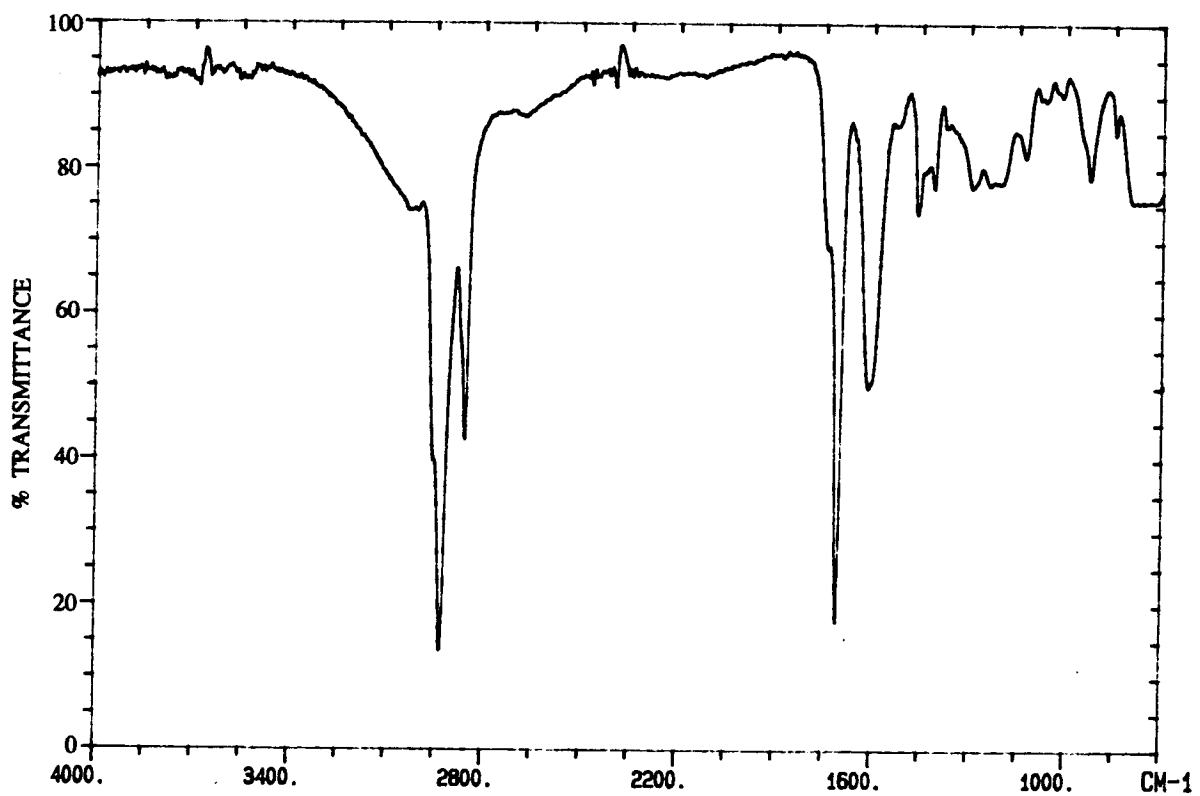
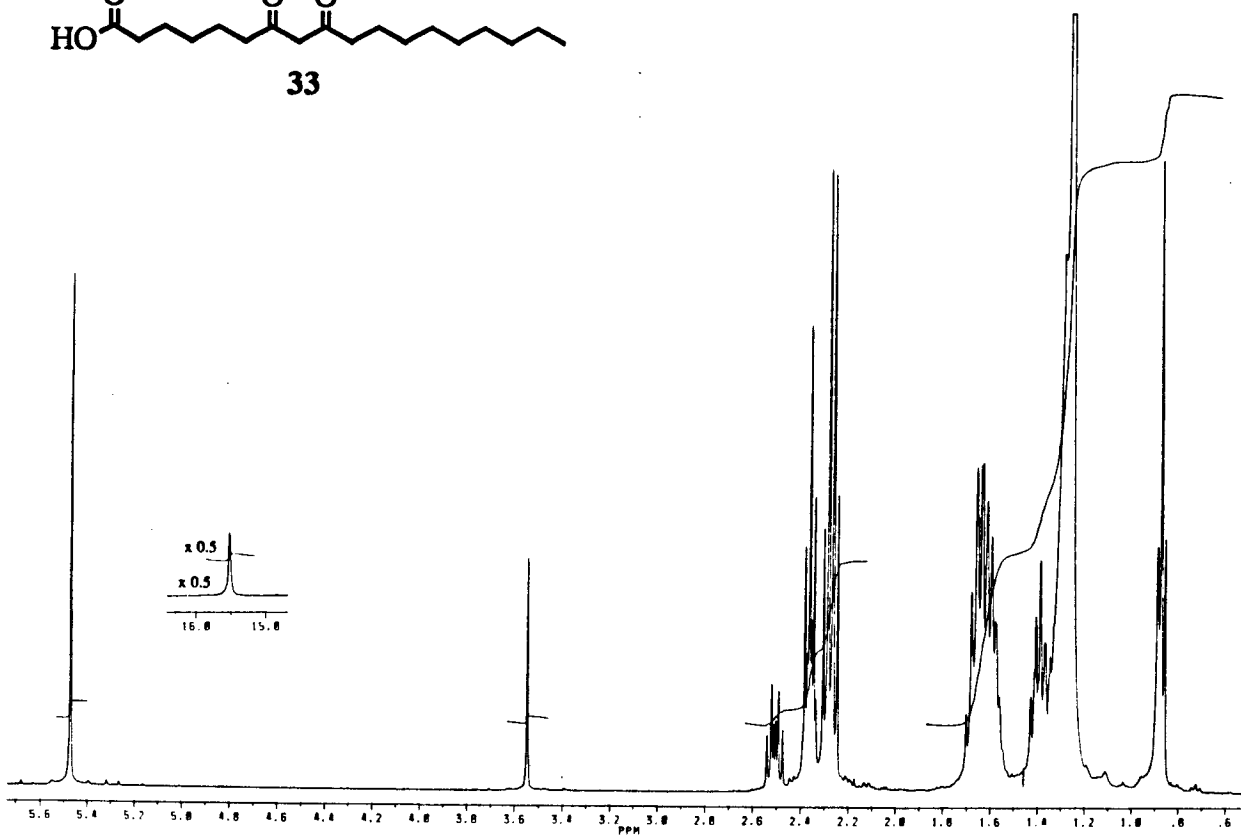
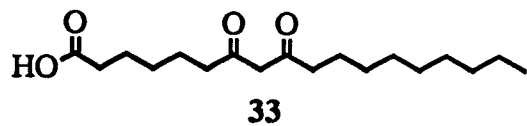


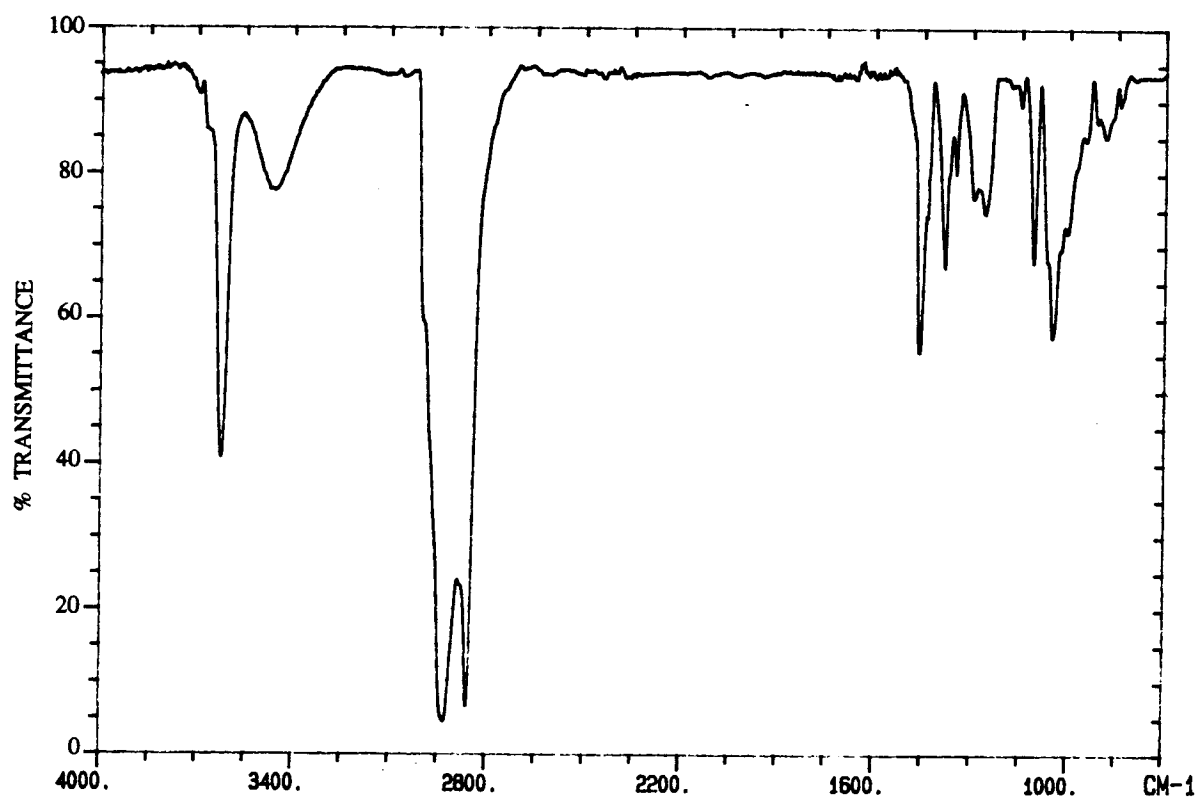
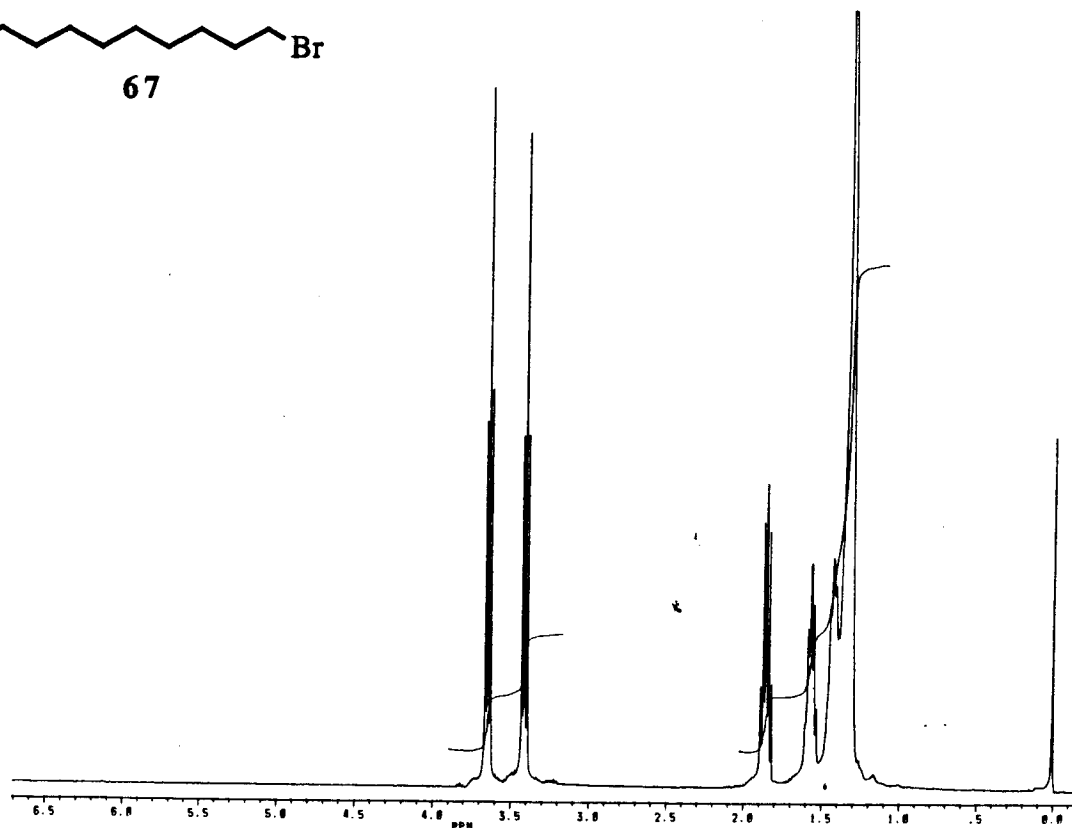
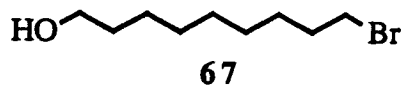




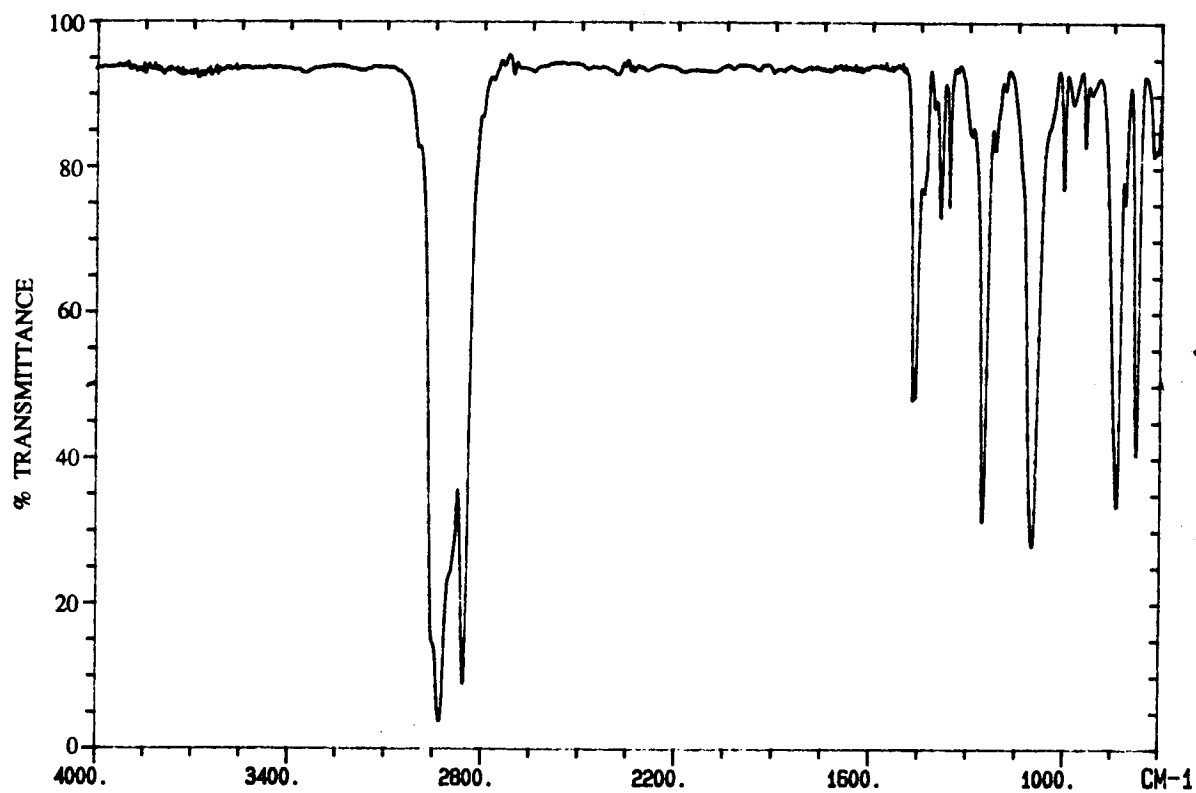
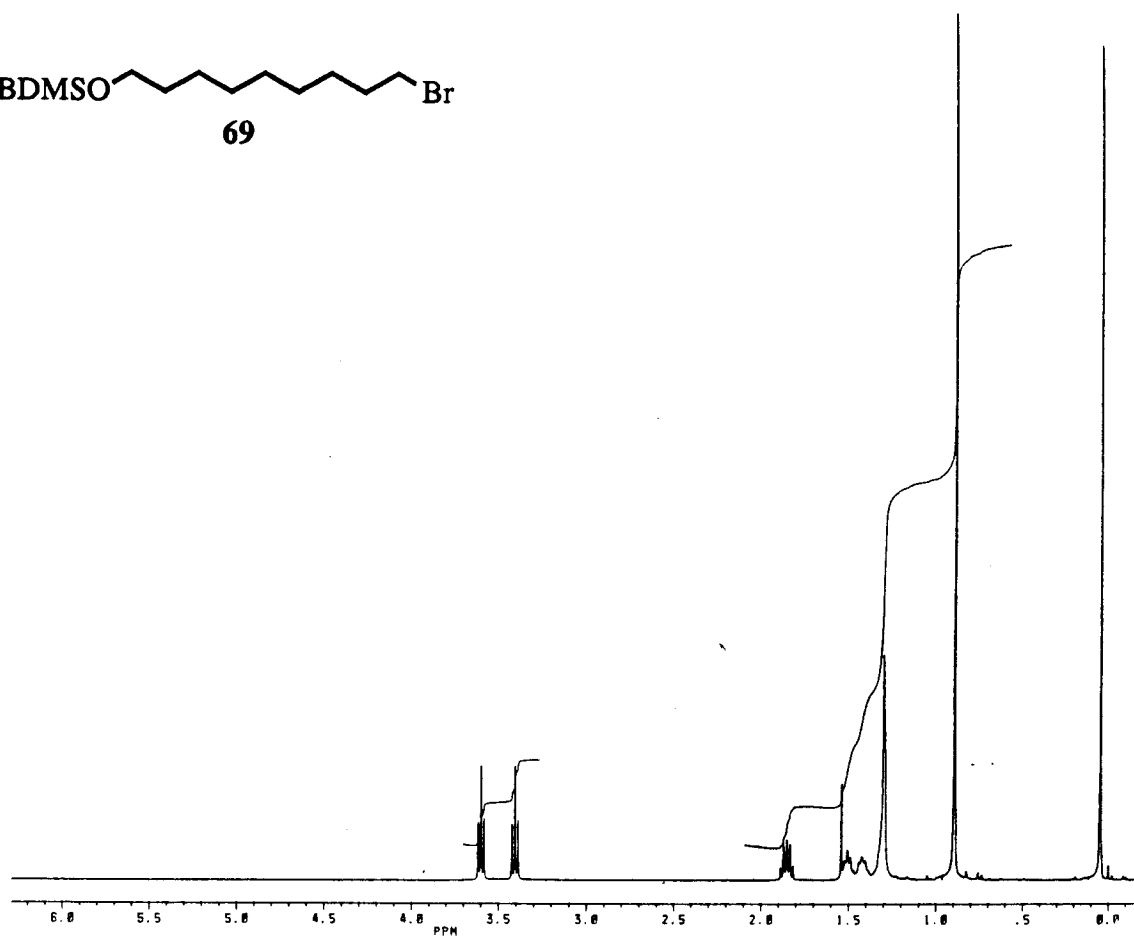
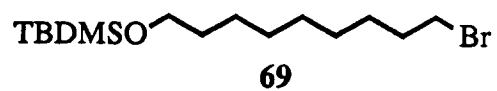


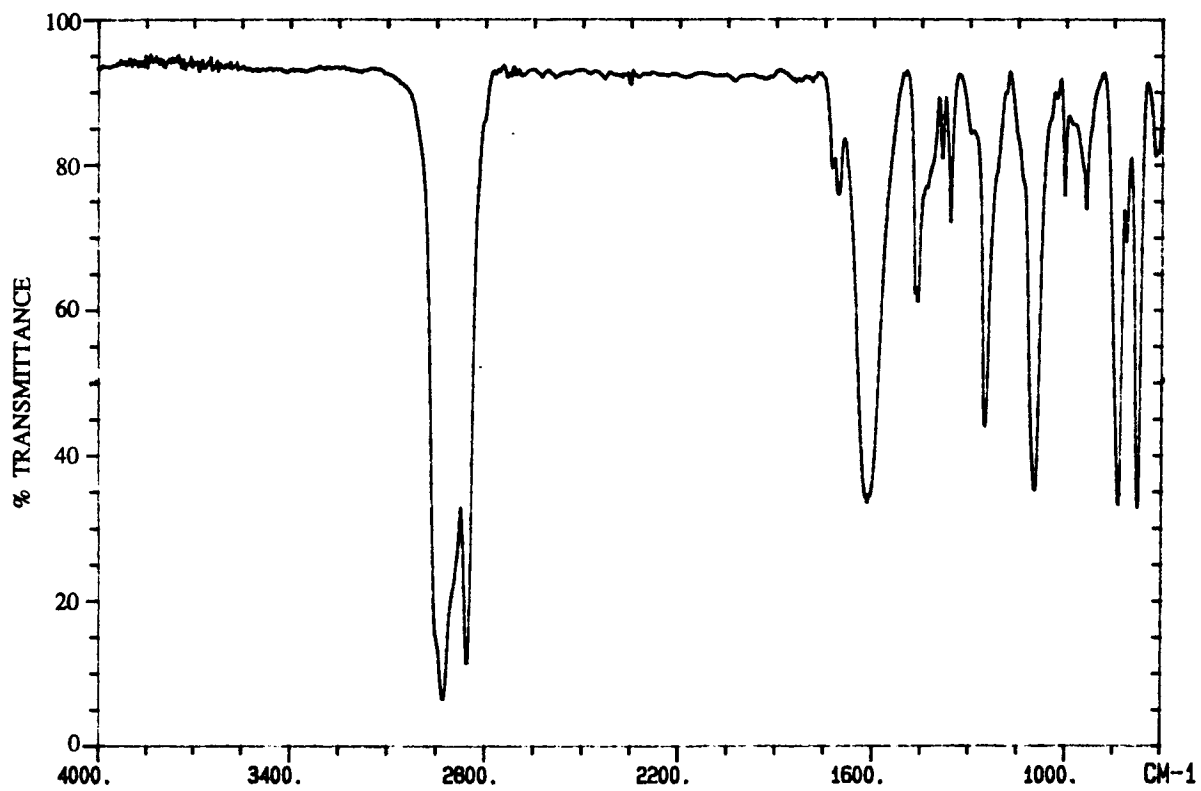
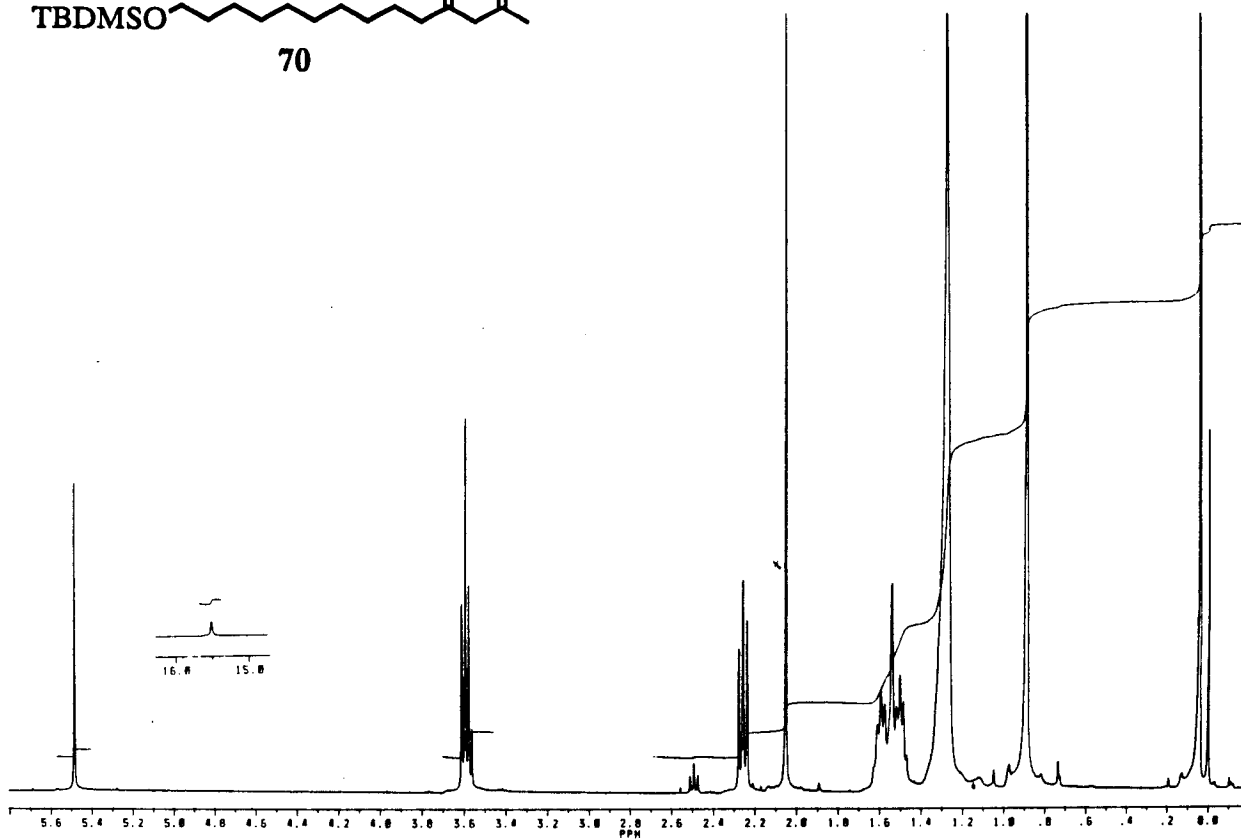
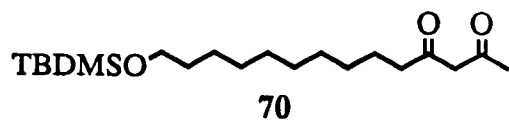


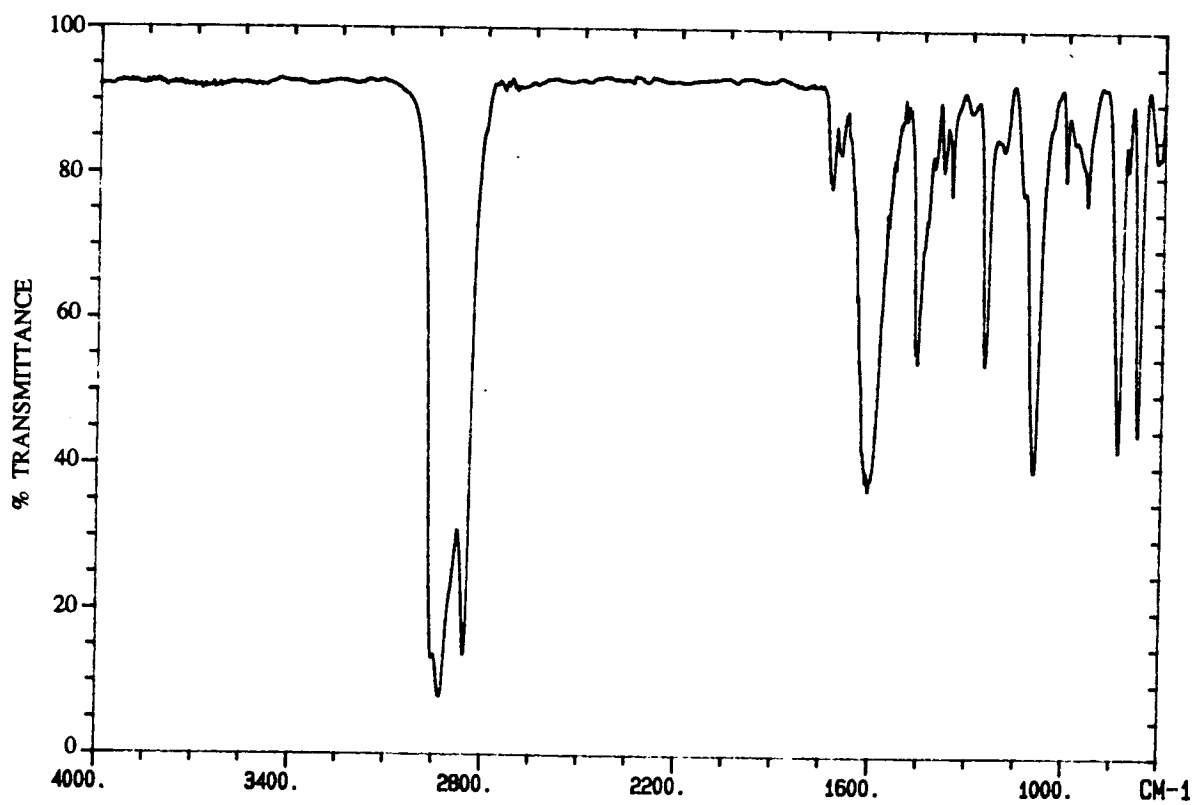
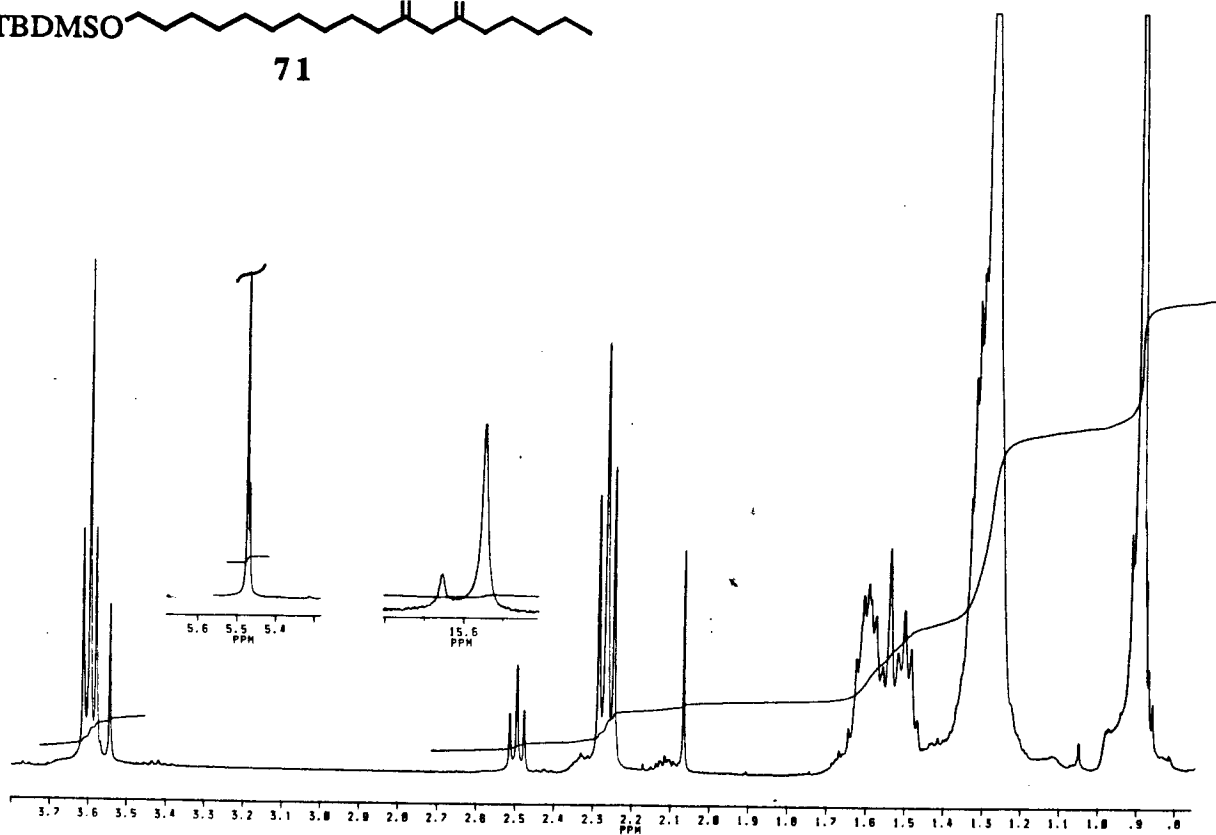
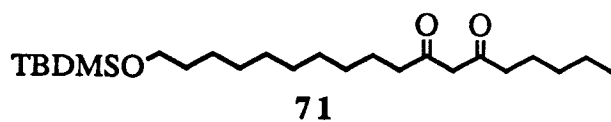


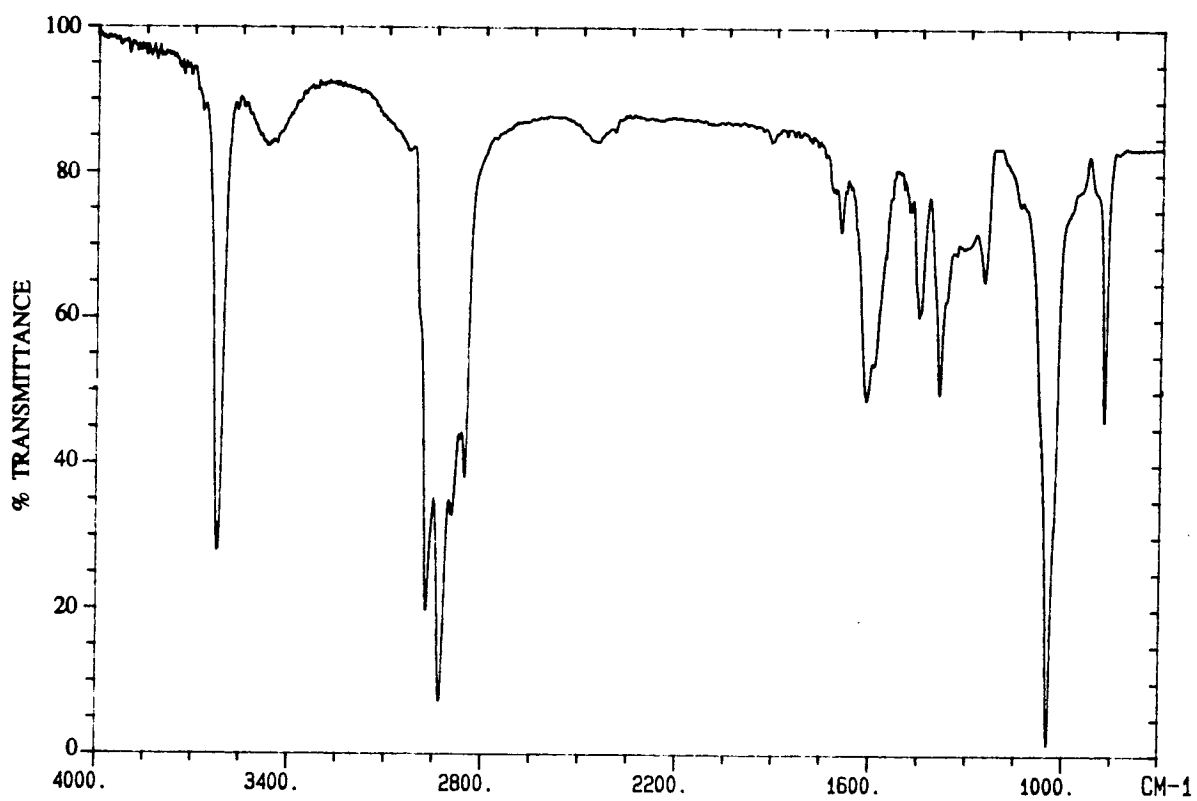
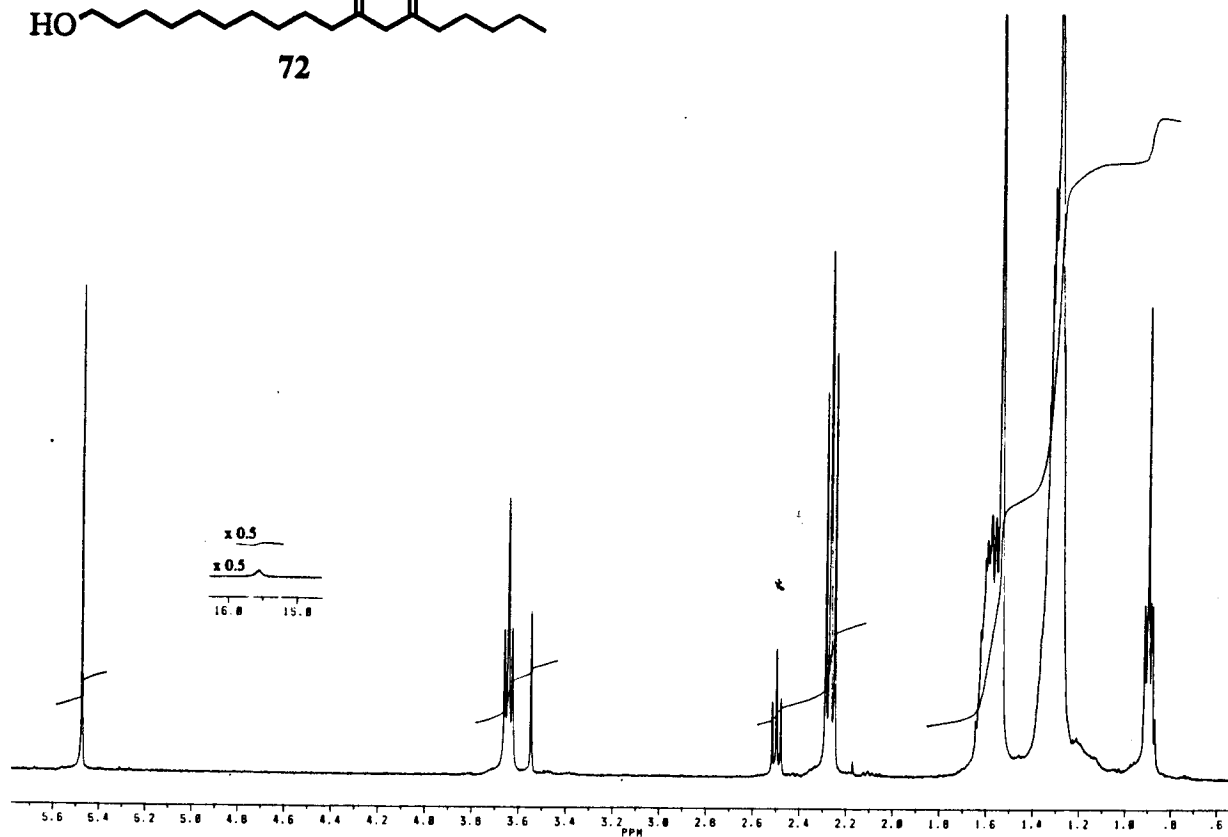
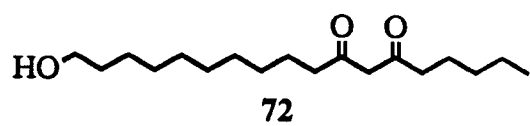


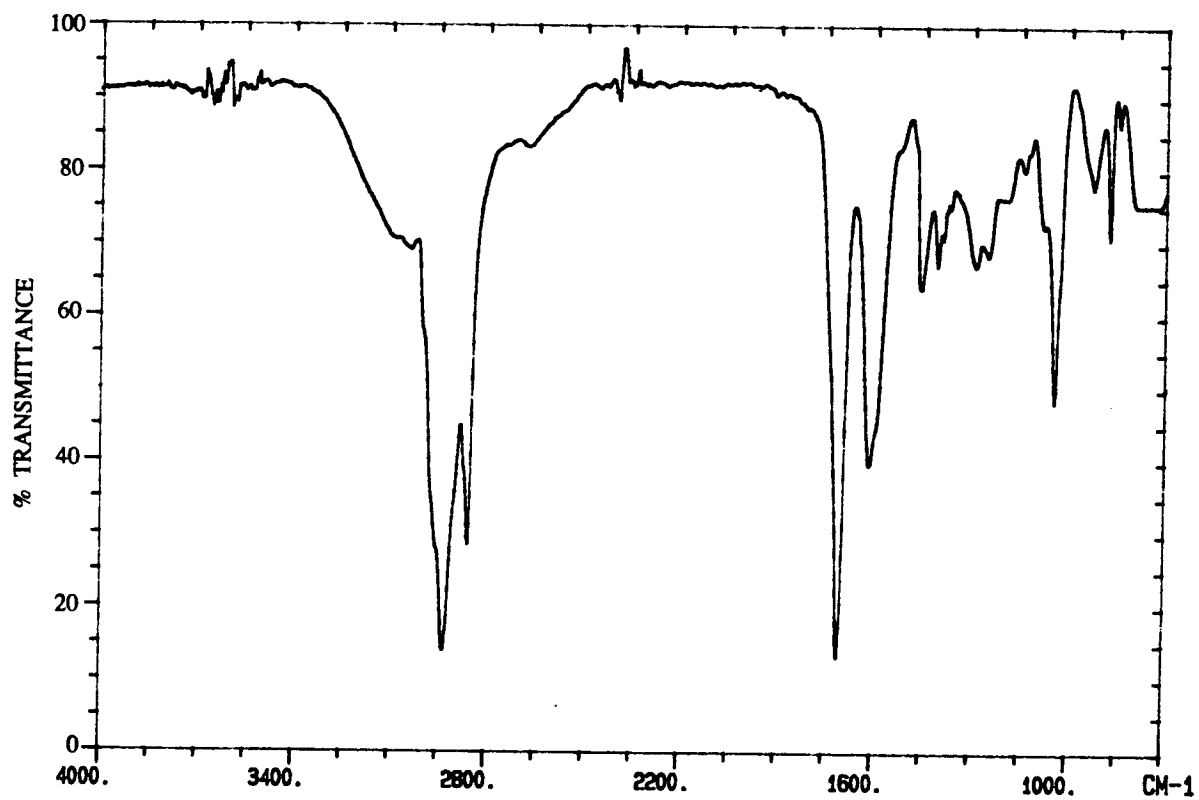
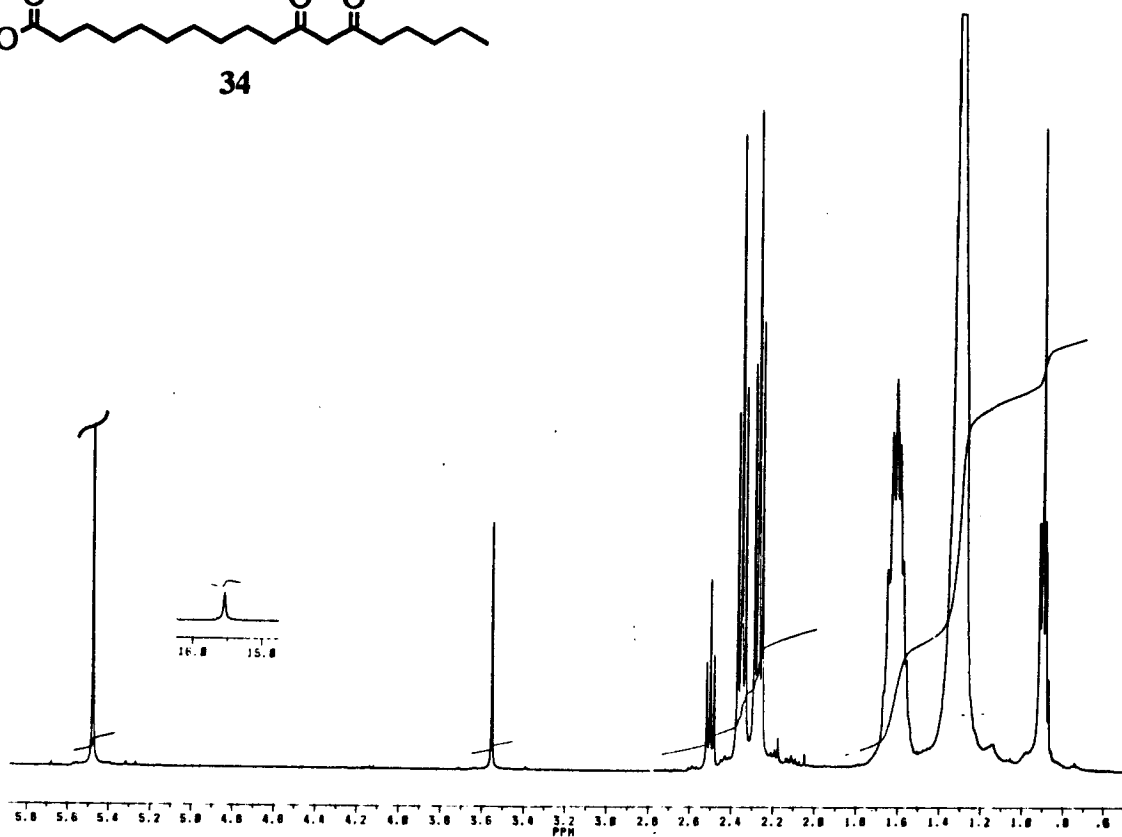
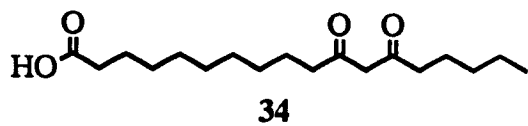


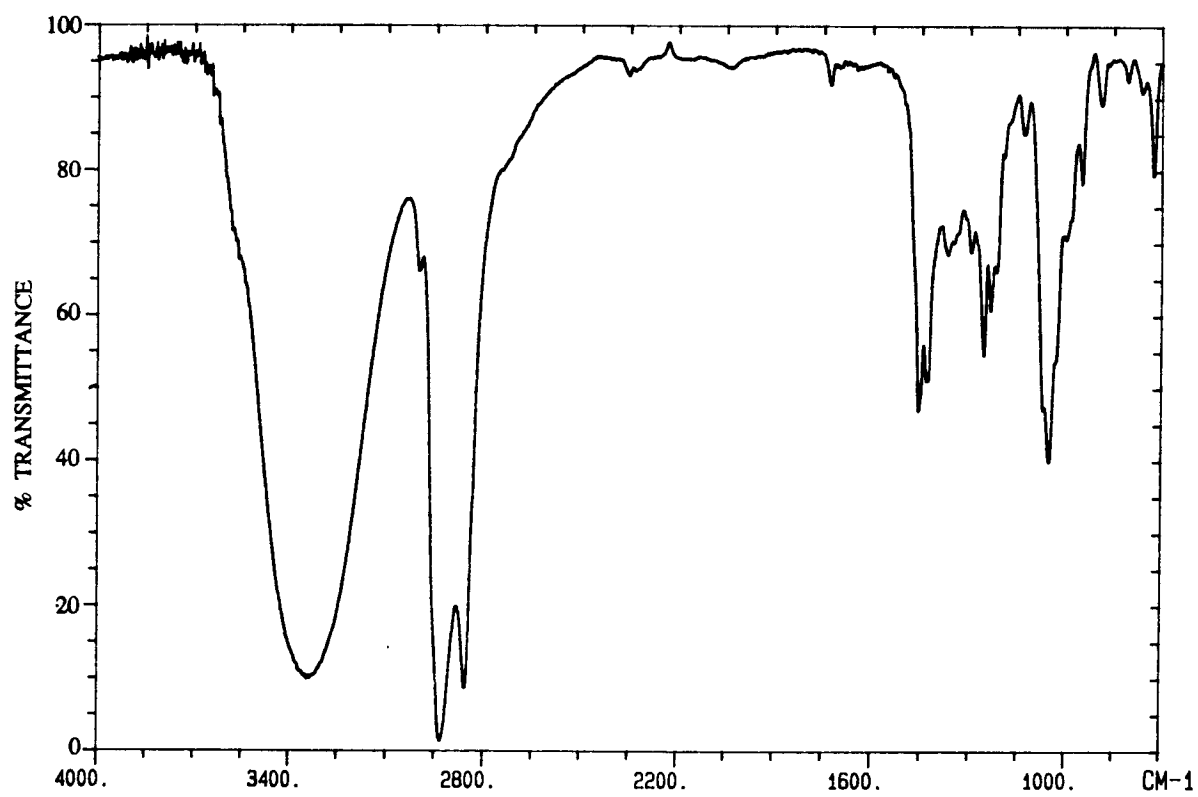
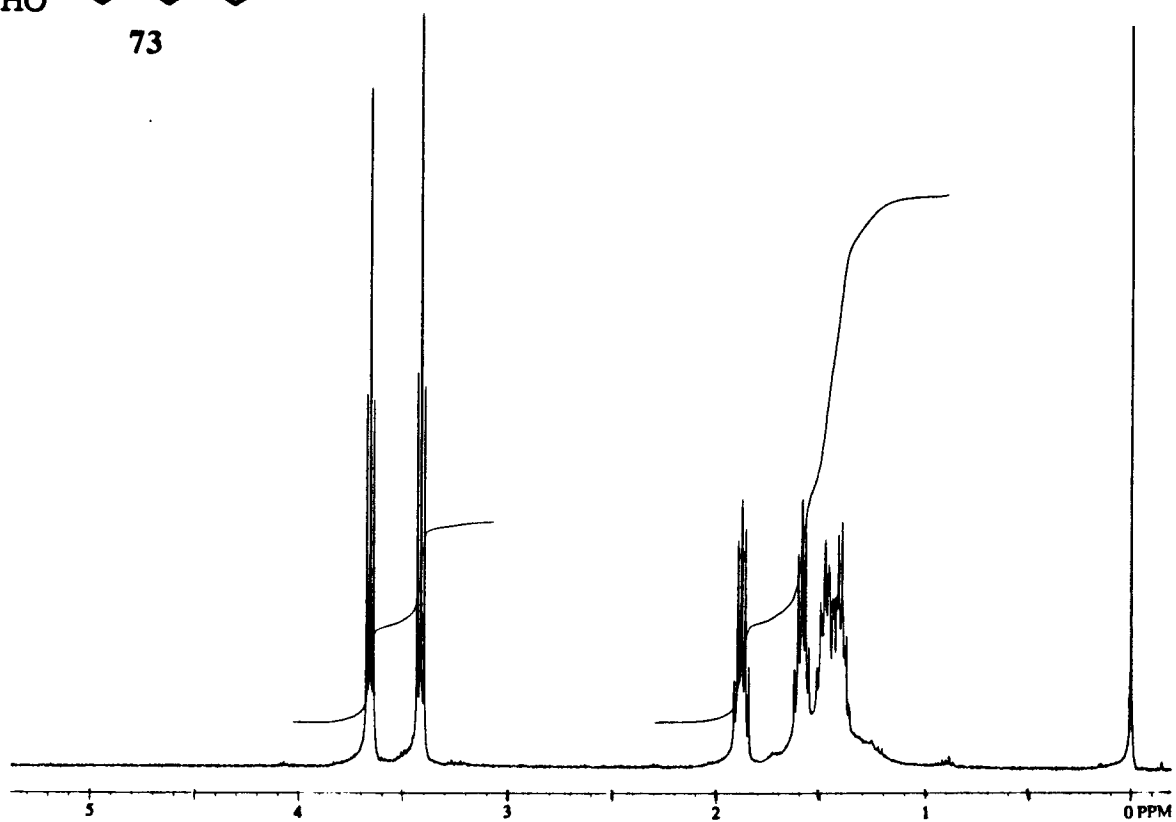
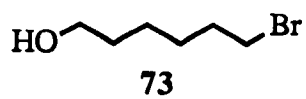


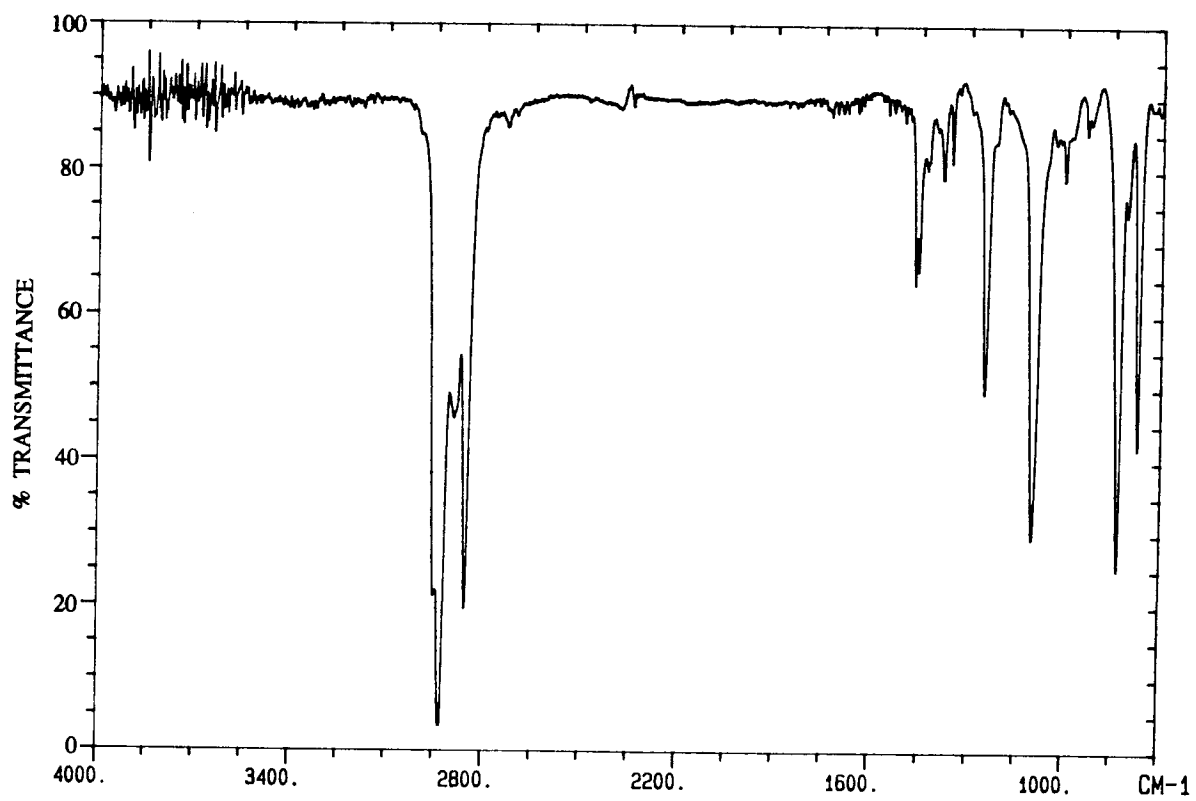
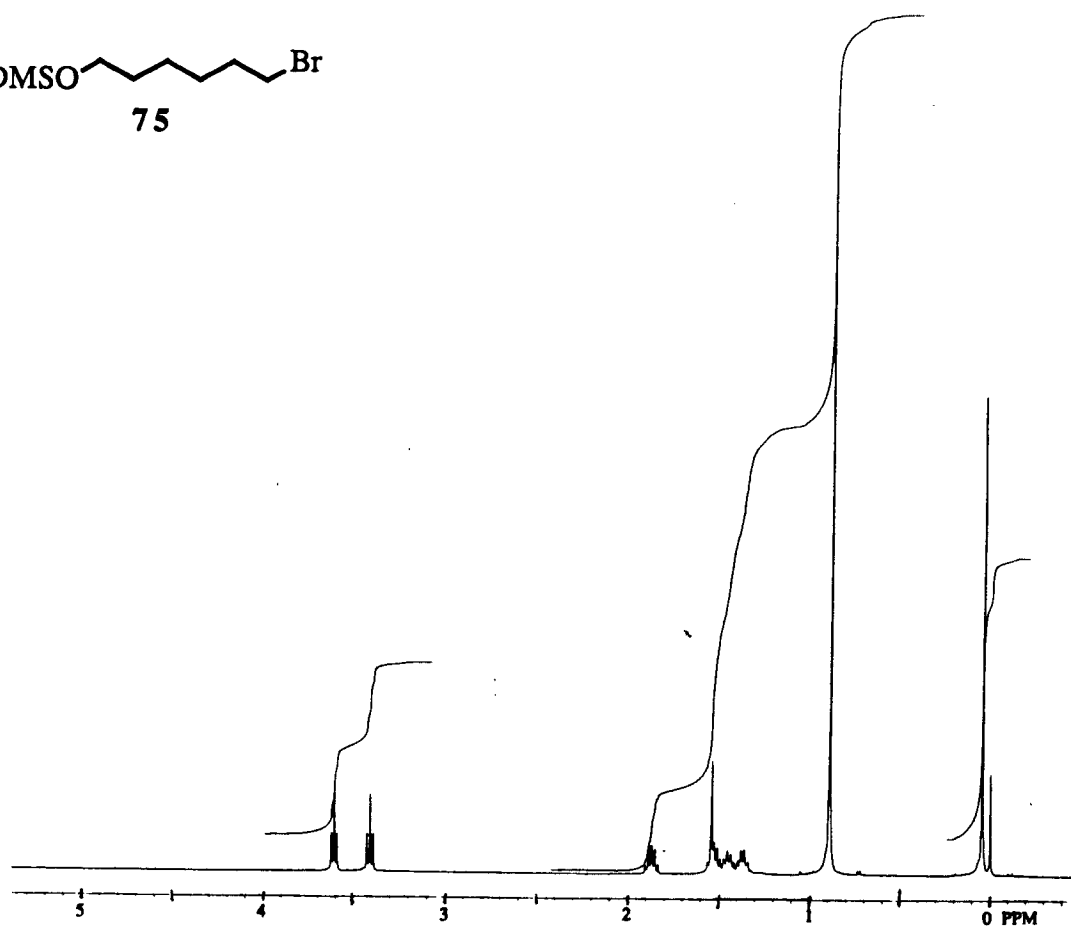
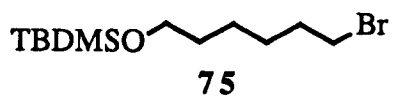


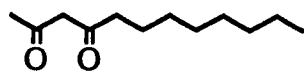




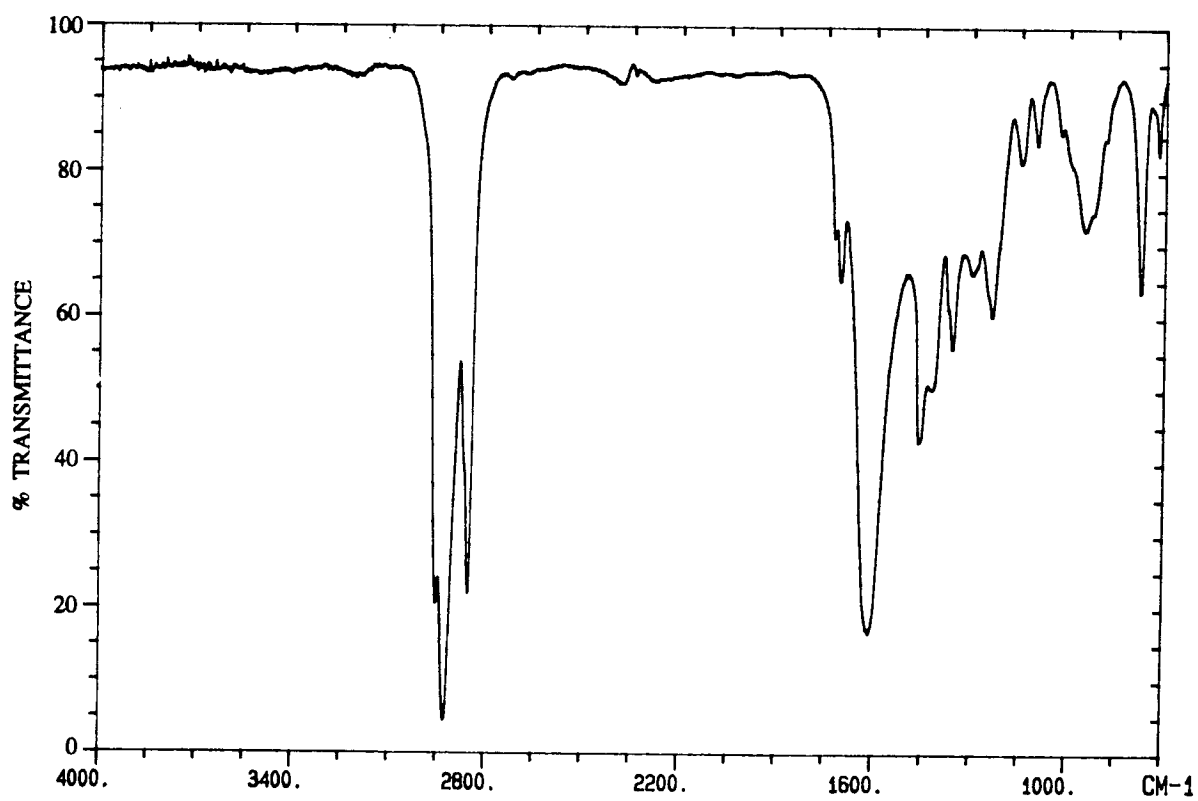
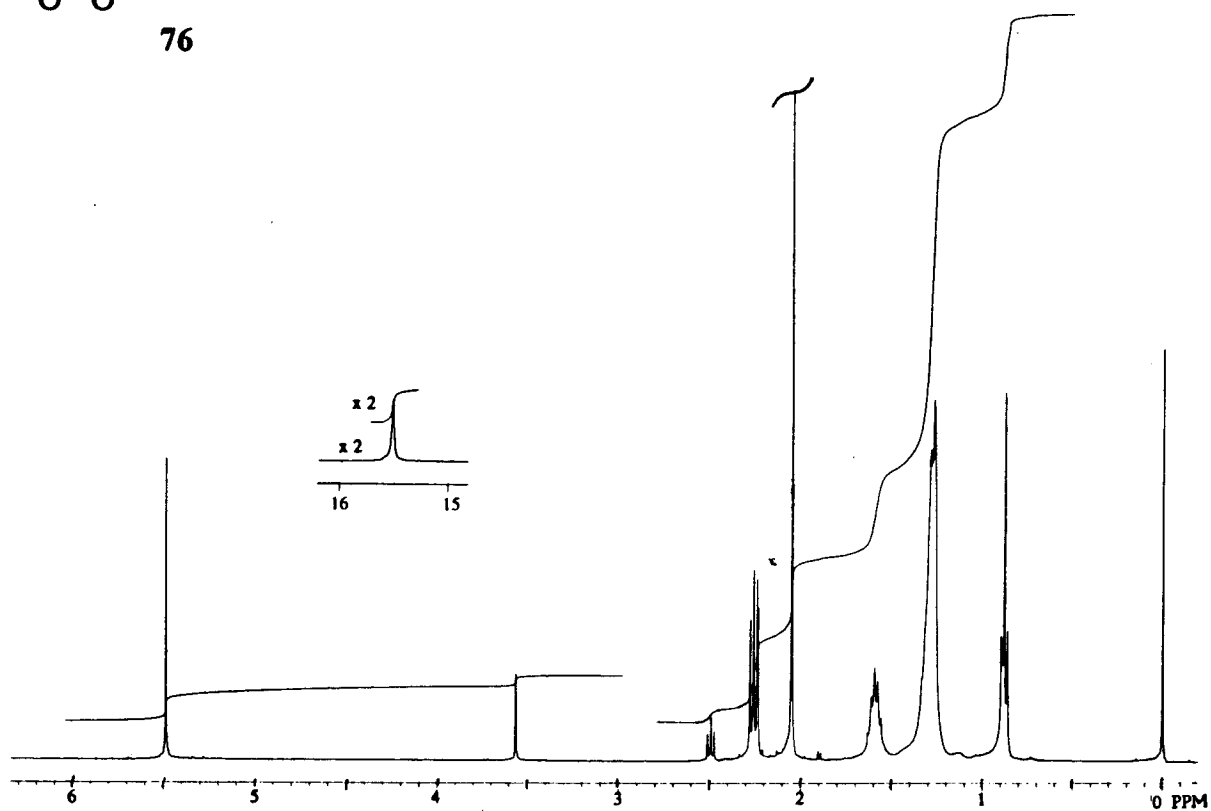




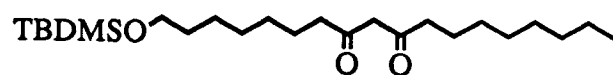




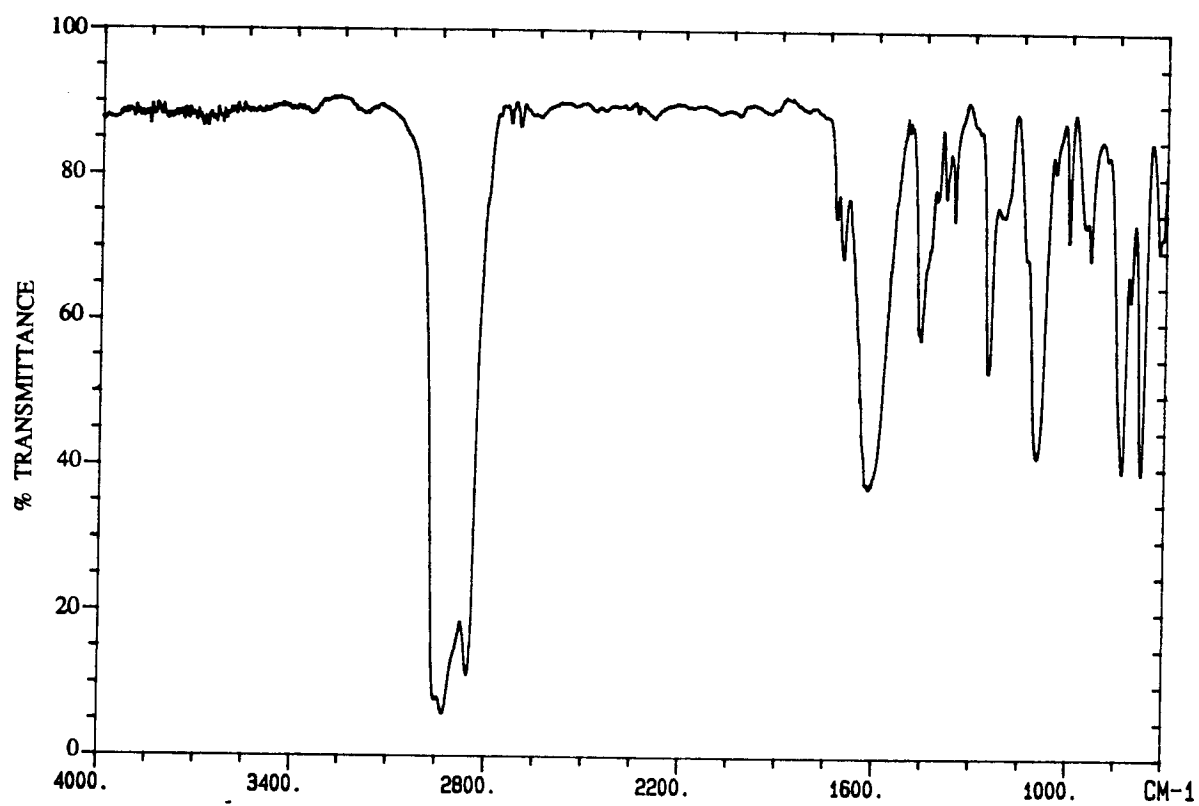
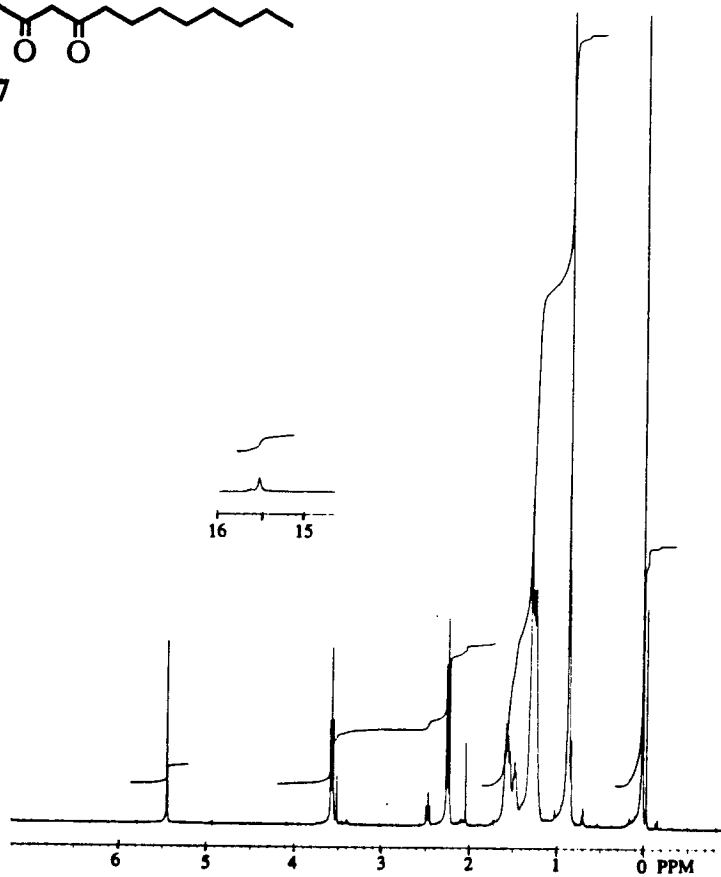
76

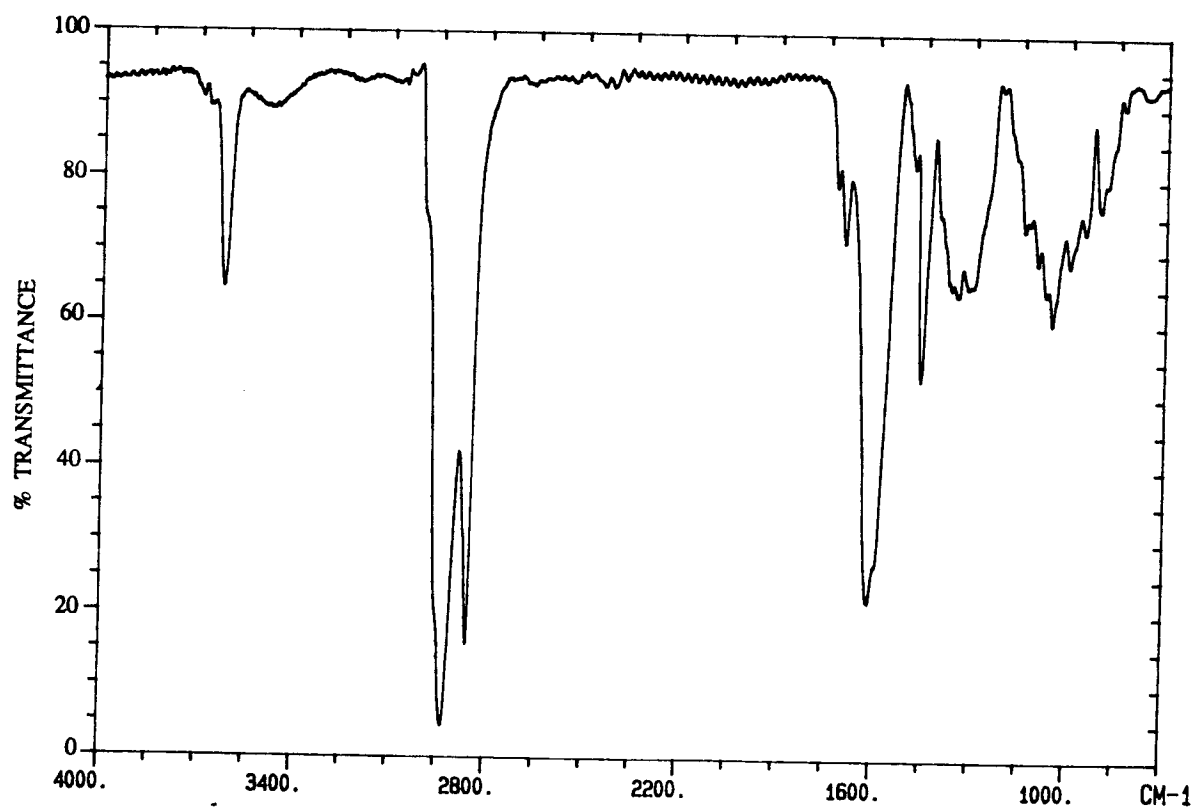
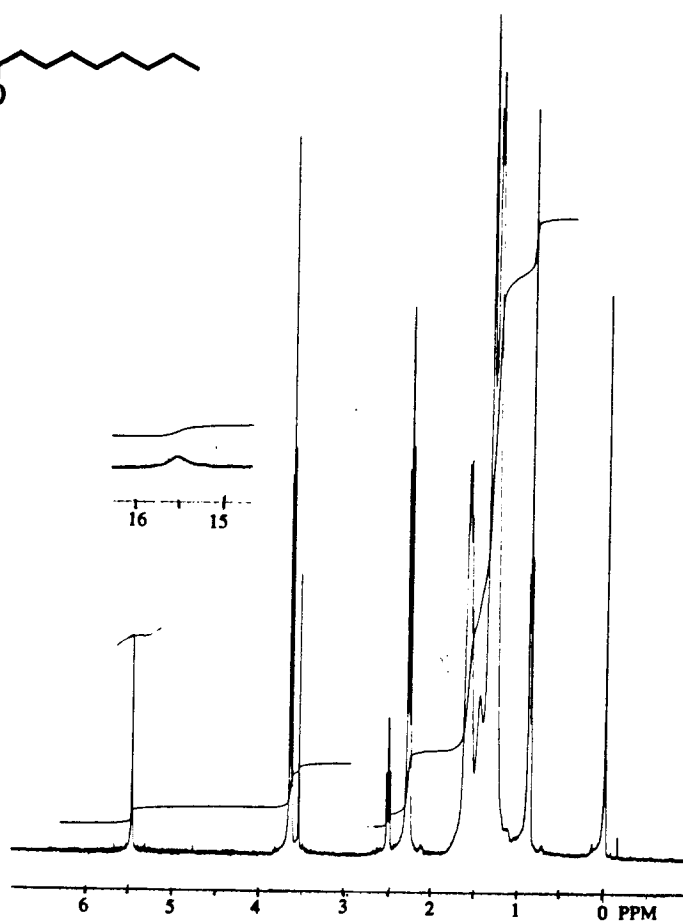
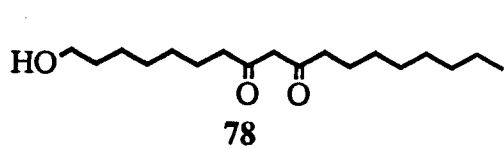


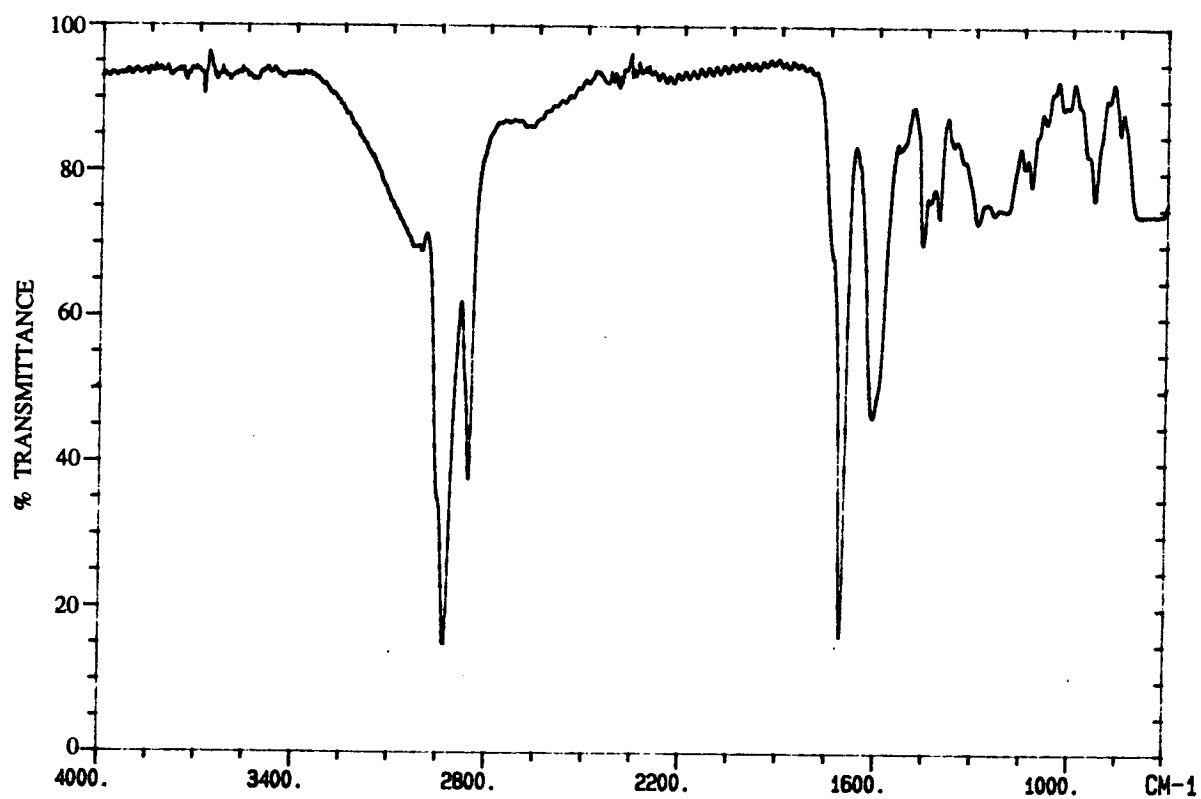
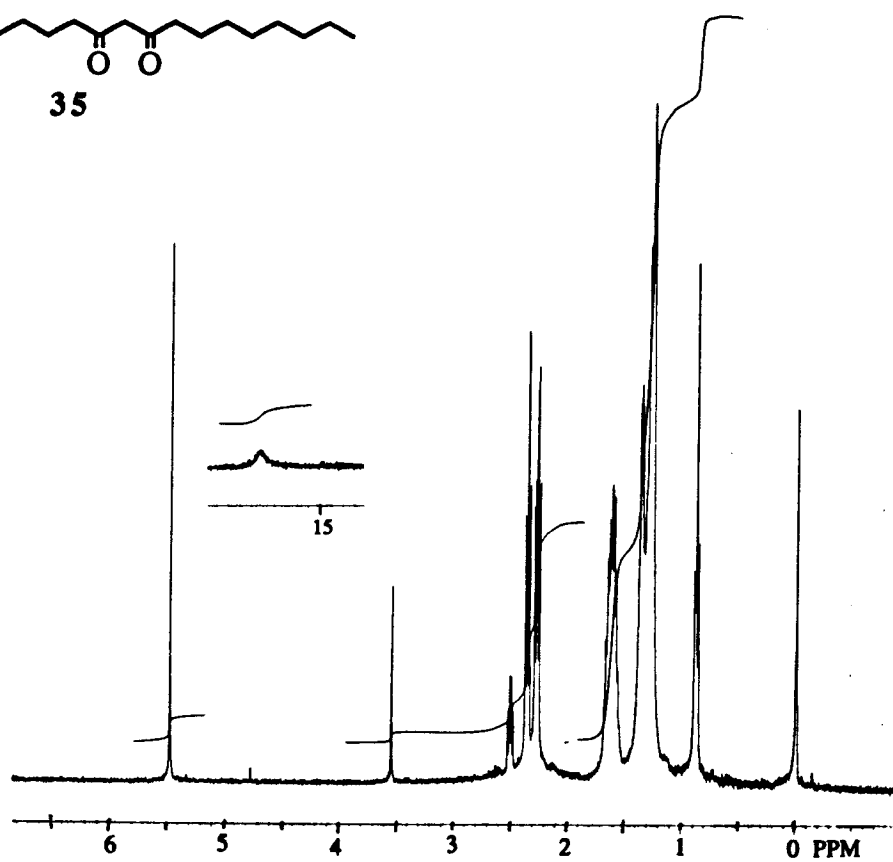
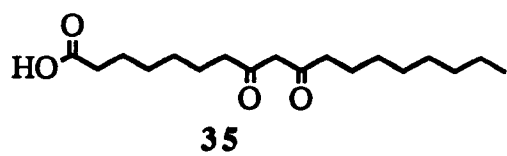


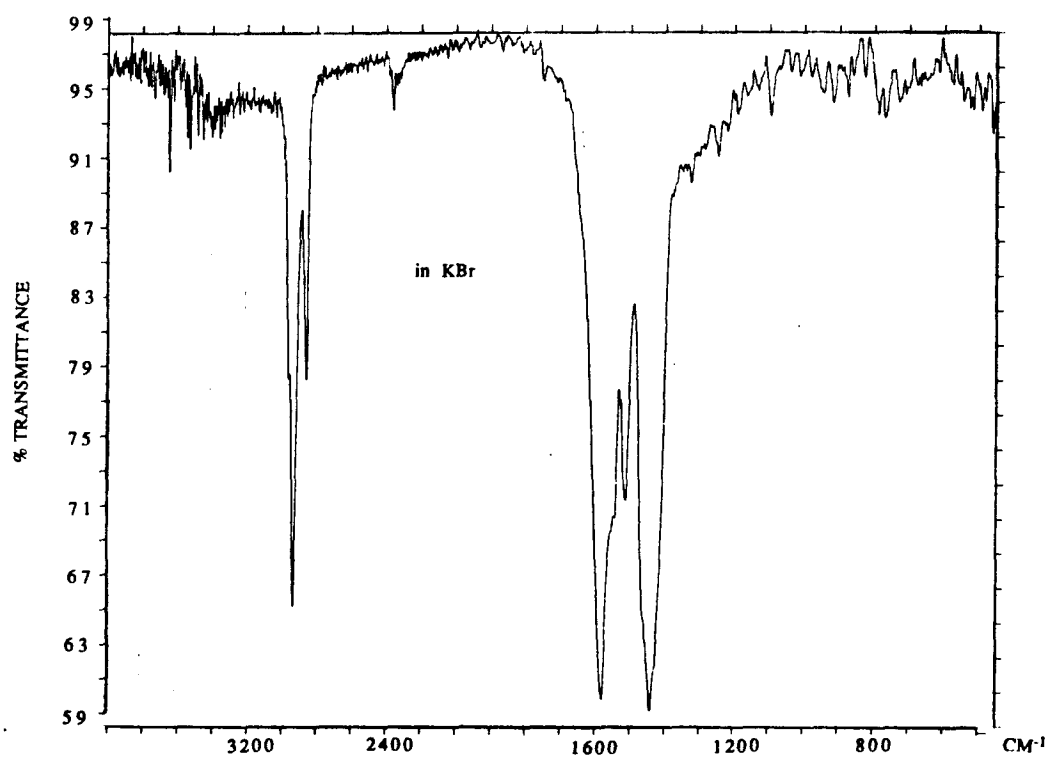
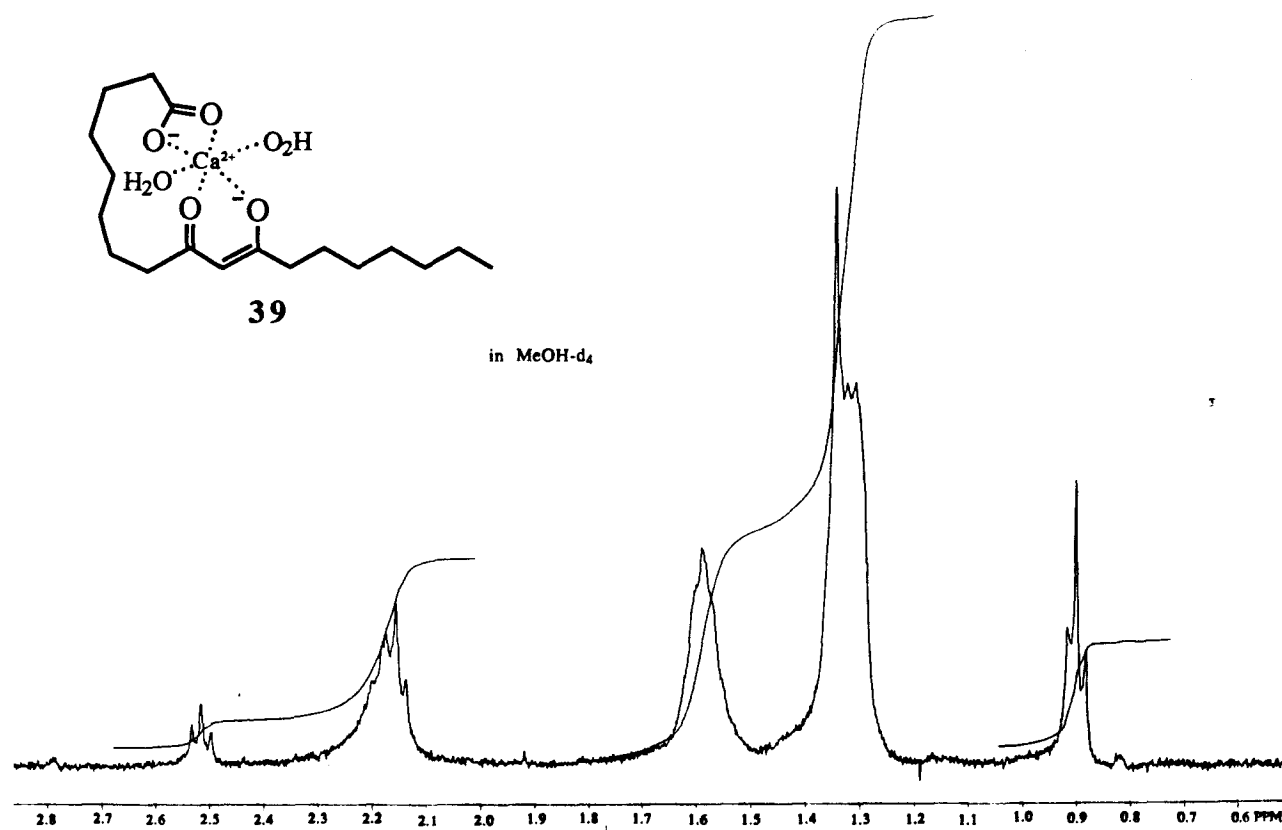


77

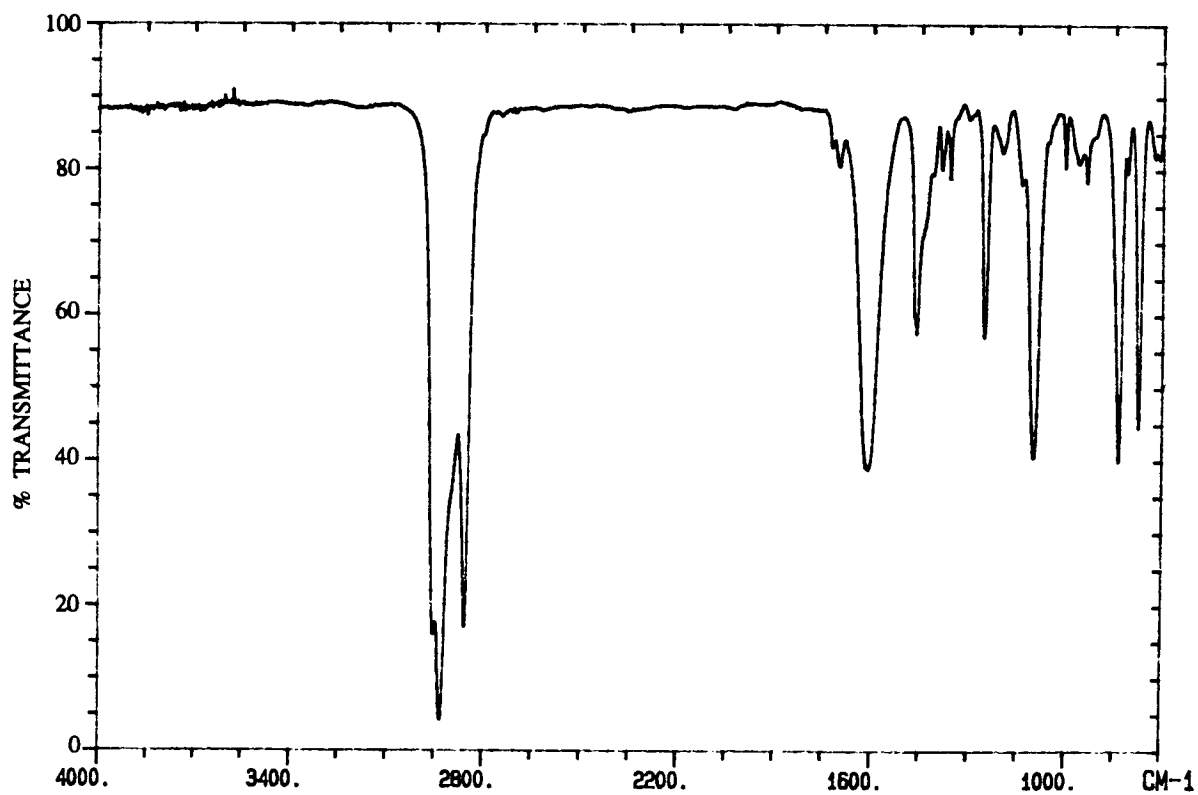
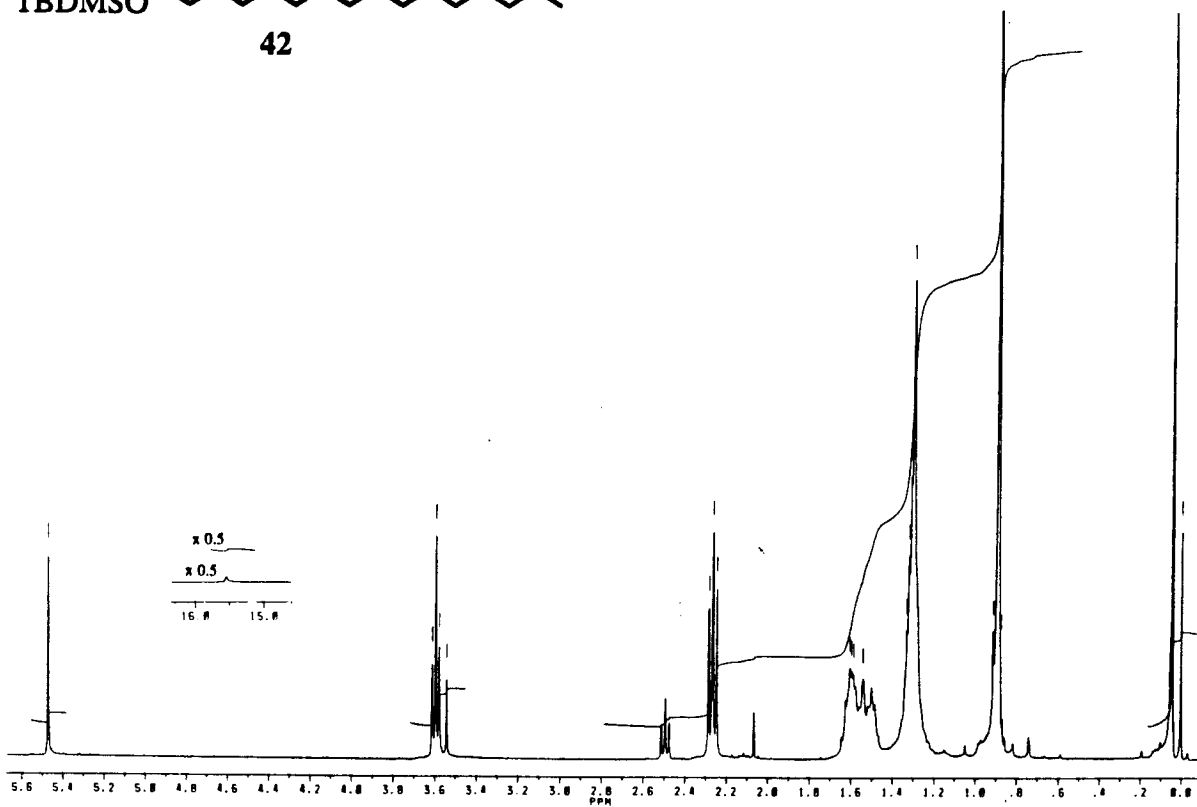
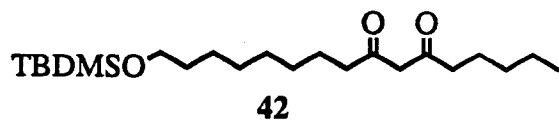


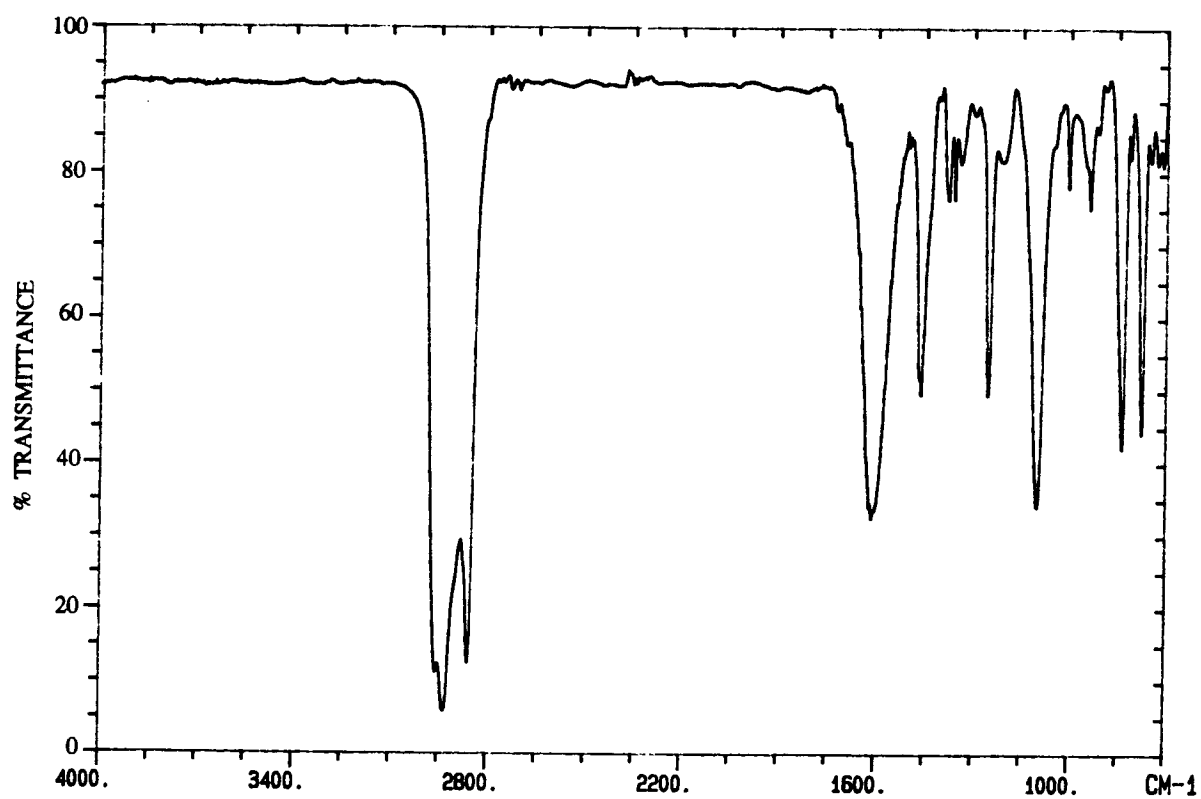
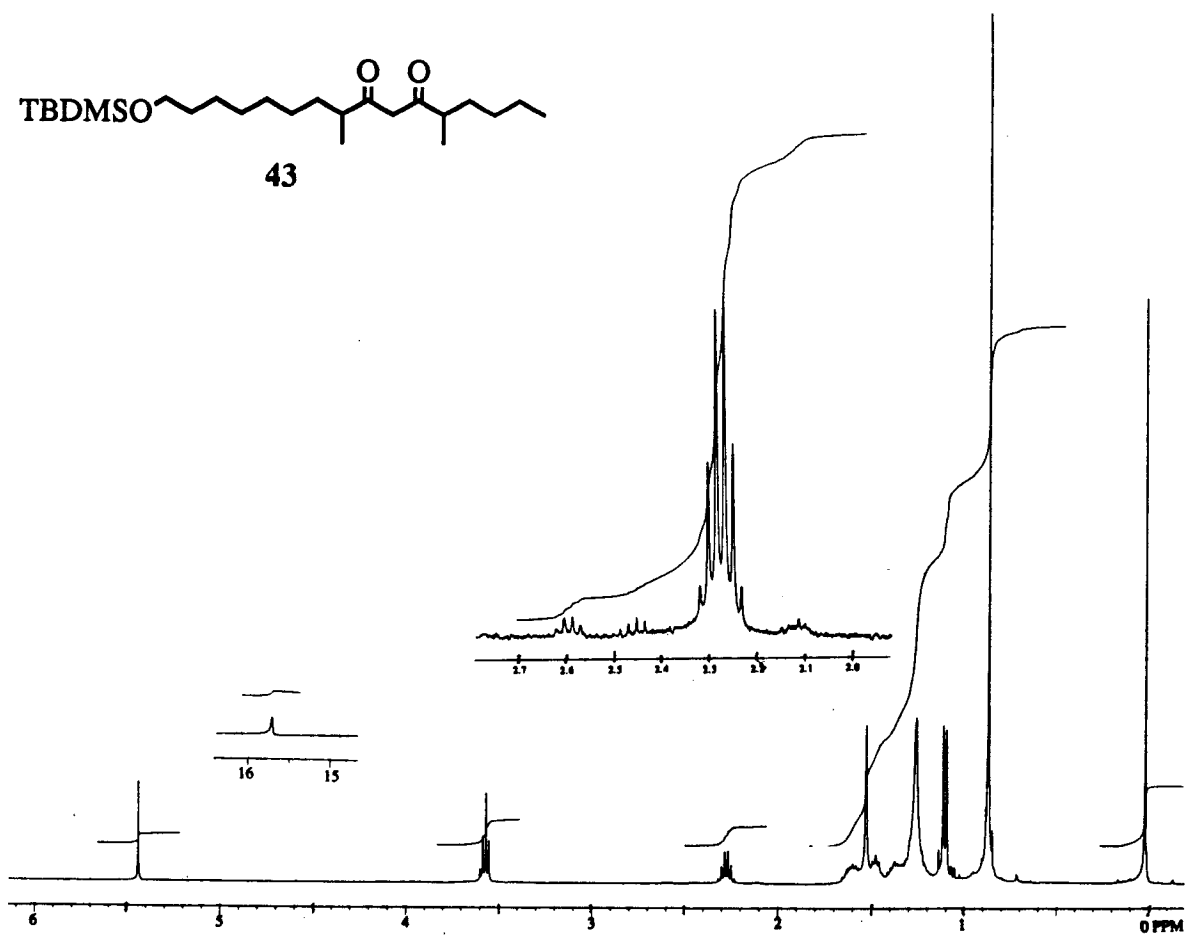
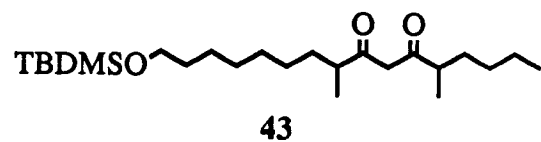


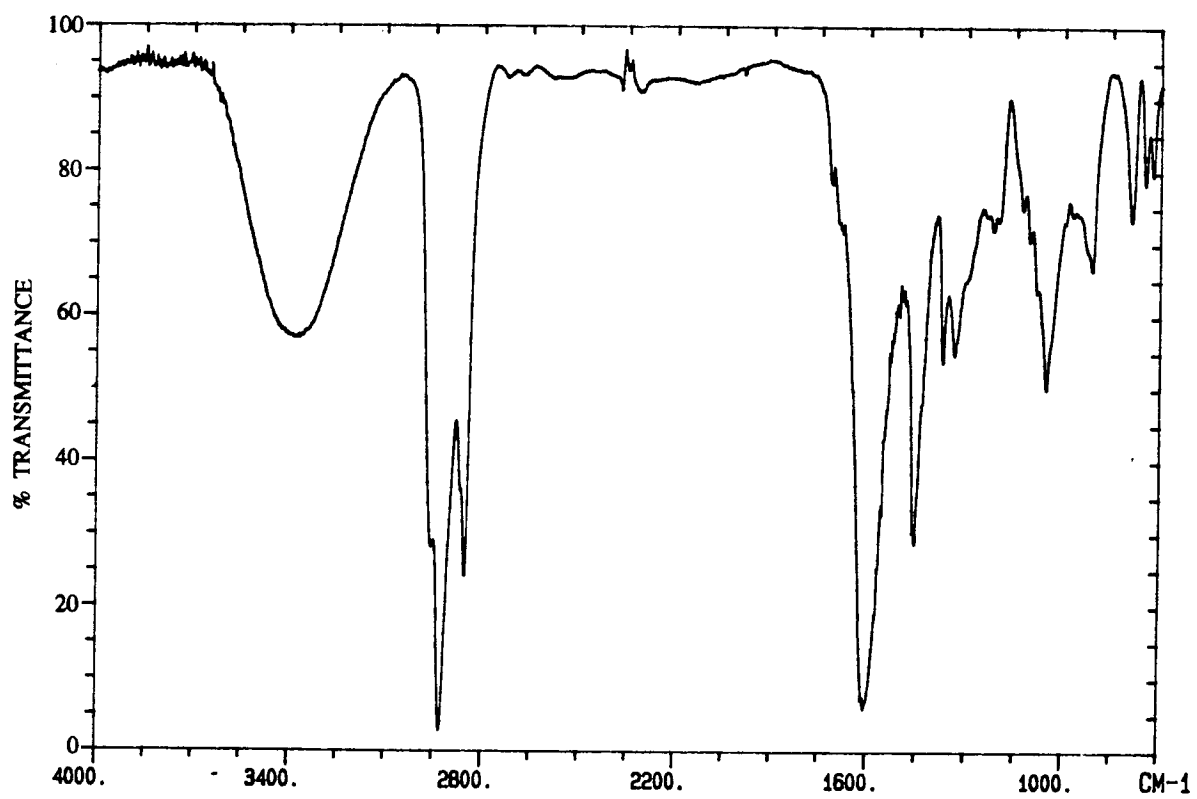
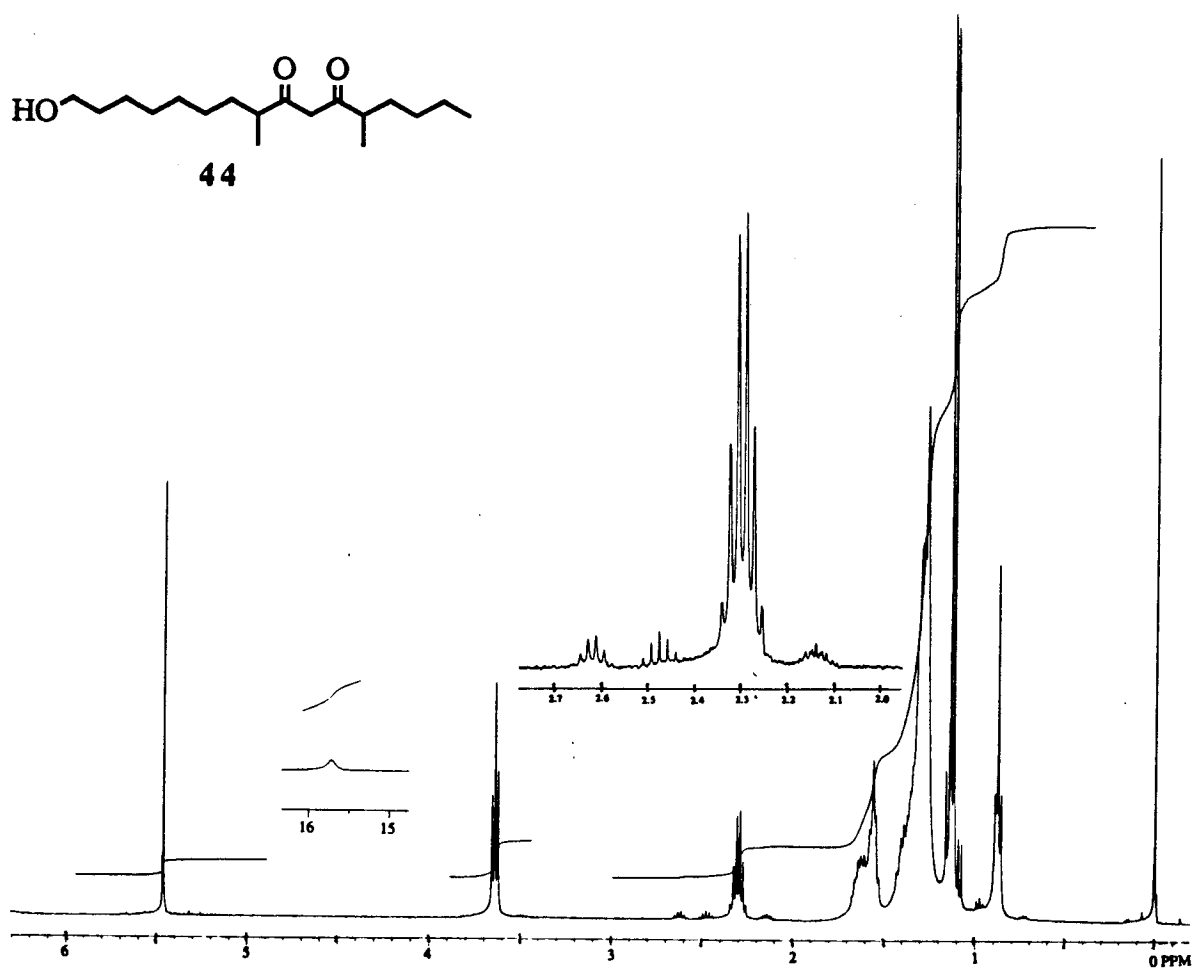
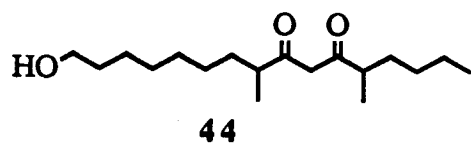


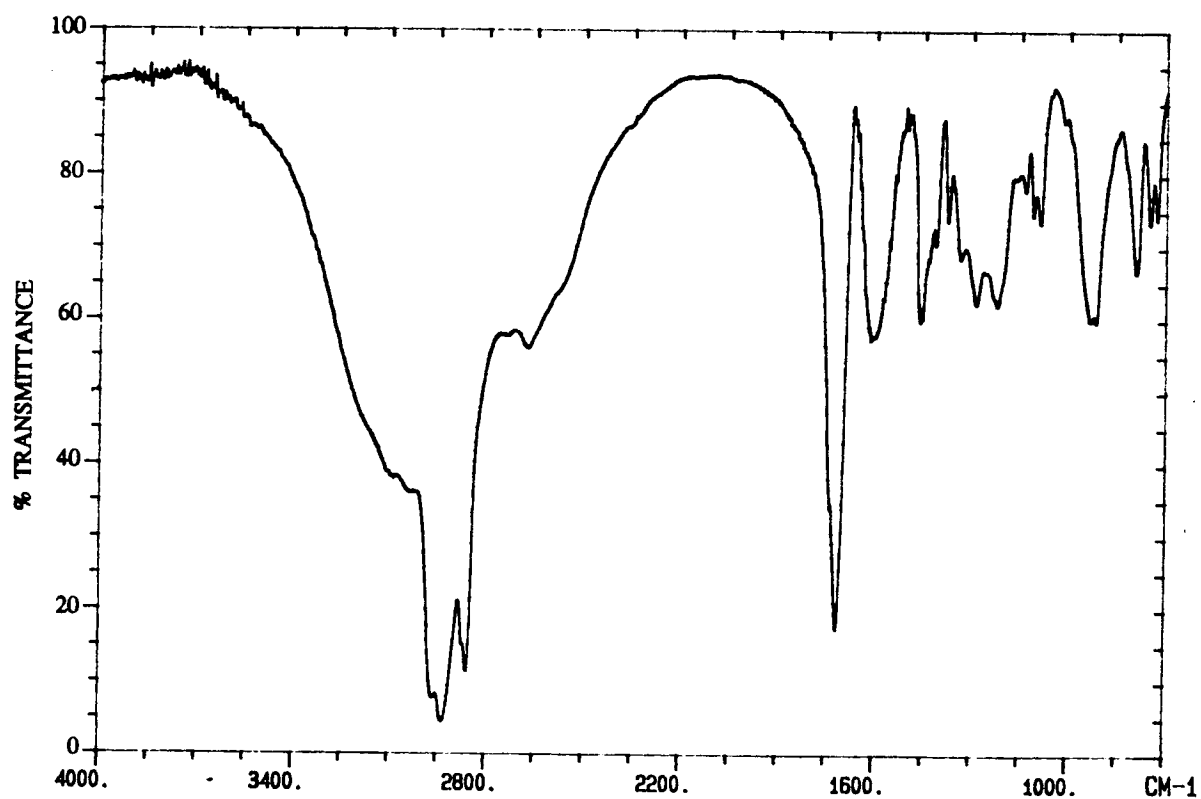
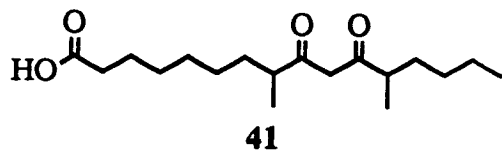


\* For IR spectrum of calcium complex **36** in the region of  $1000\text{--}400\text{ cm}^{-1}$ , see page 247.

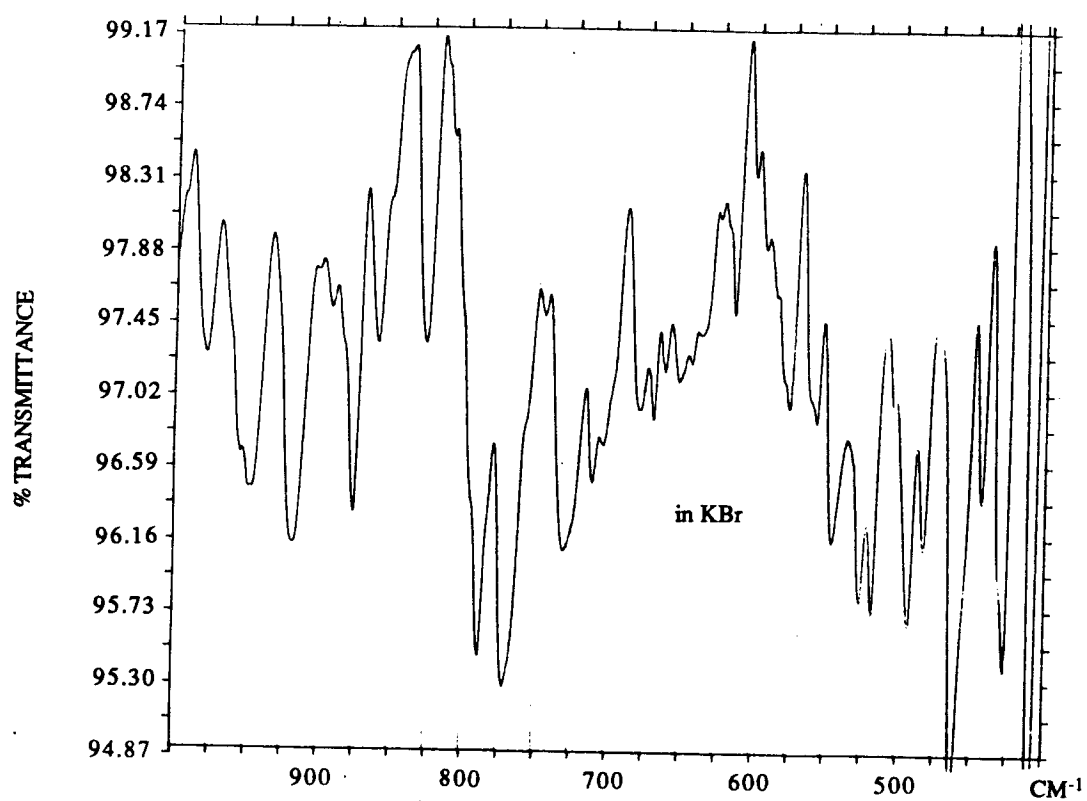
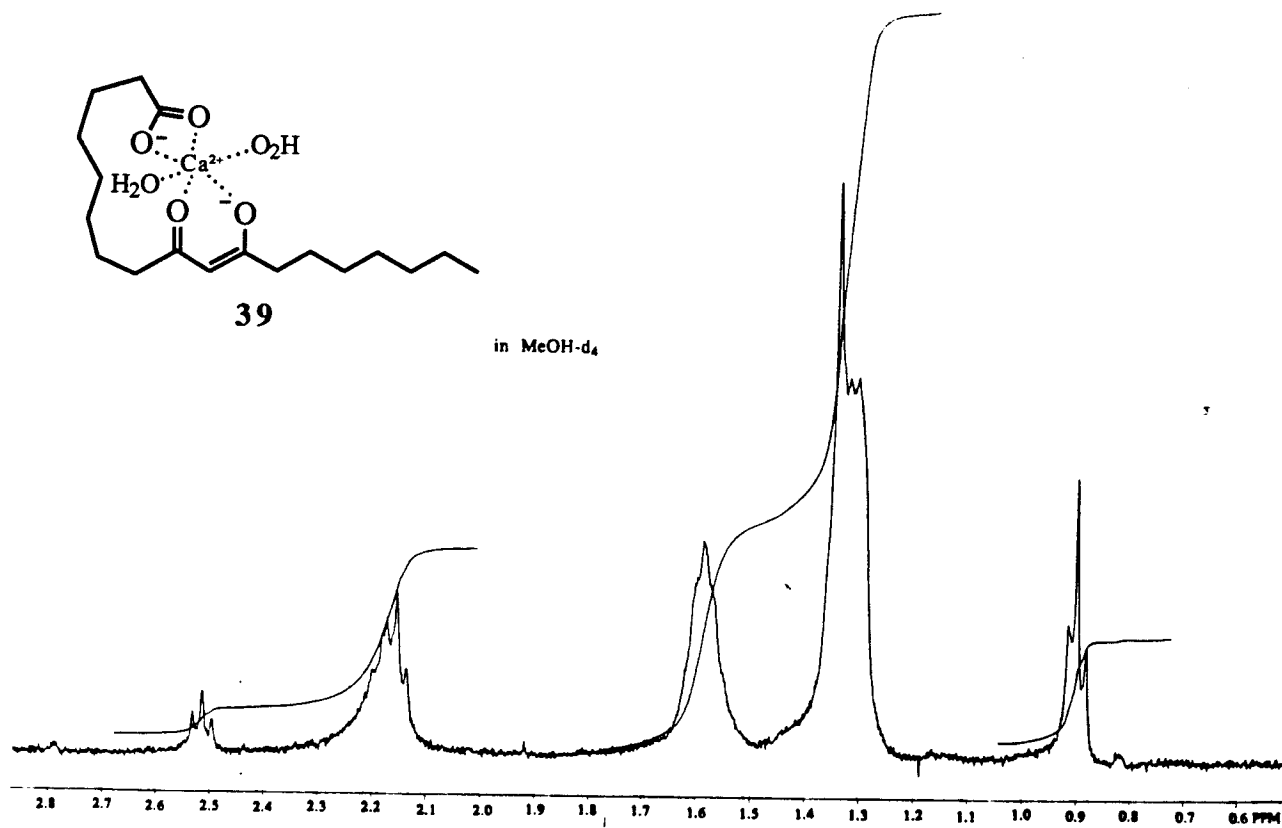












## APPENDIX 2

### PREPARATION OF BUFFERS

pH = 11.5	1.0 mL Me <sub>4</sub> NOH (10%) + 264 mg CAPS (pK <sub>a</sub> = 10.40) + 28.8 mL H <sub>2</sub> O
pH = 11.0	1.0 mL Me <sub>4</sub> NOH (10%) + 305 mg CAPS (pK <sub>a</sub> = 10.40) + 33.5 mL H <sub>2</sub> O
pH = 10.5	1.0 mL Me <sub>4</sub> NOH (10%) + 438 mg CAPS (pK <sub>a</sub> = 10.40) + 48.5 mL H <sub>2</sub> O
pH = 10.0	1.0 mL Me <sub>4</sub> NOH (10%) + 304 mg CHES (pK <sub>a</sub> = 9.50) + 35.2 mL H <sub>2</sub> O
pH = 9.5	1.0 mL Me <sub>4</sub> NOH (10%) + 462 mg CHES (pK <sub>a</sub> = 9.50) + 54.2 mL H <sub>2</sub> O
pH = 9.0	1.0 mL Me <sub>4</sub> NOH (10%) + 954 mg CHES (pK <sub>a</sub> = 9.50) + 113 mL H <sub>2</sub> O
pH = 8.5	1.0 mL Me <sub>4</sub> NOH (10%) + 365 mg HEPPS (pK <sub>a</sub> = 8.00) + 35.2 mL H <sub>2</sub> O
pH = 8.0	1.0 mL Me <sub>4</sub> NOH (10%) + 556 mg HEPPS (pK <sub>a</sub> = 8.00) + 54.2 mL H <sub>2</sub> O
pH = 7.5	1.0 mL Me <sub>4</sub> NOH (10%) + 347 mg MOPS (pK <sub>a</sub> = 7.20) + 40.4 mL H <sub>2</sub> O
pH = 7.0	1.0 mL Me <sub>4</sub> NOH (10%) + 600 mg MOPS (pK <sub>a</sub> = 7.20) + 70.4 mL H <sub>2</sub> O
pH = 6.0	1.0 mL Me <sub>4</sub> NOH (10%) + 520 mg MES (pK <sub>a</sub> = 6.15) + 65.6 mL H <sub>2</sub> O
pH = 5.0	1.0 mL Me <sub>4</sub> NOH (10%) + 108 mg S.A. (pK <sub>a2</sub> = 5.57) + 21.8 mL H <sub>2</sub> O
pH = 4.0	1.0 mL Me <sub>4</sub> NOH (10%) + 334 mg S.A. (pK <sub>a1</sub> = 4.19) + 69.8 mL H <sub>2</sub> O
pH = 3.0	1.0 mL Me <sub>4</sub> NOH (10%) + 456 mg C.A. (pK <sub>a1</sub> = 3.06) + 58.4 mL H <sub>2</sub> O